Vers l'utilisation rationnelle de biofilms positifs pour aider à maîtriser les microorganismes indésirables dans les bâtiments d'élevage

Virgile Guéneau

THESE DE DOCTORAT

NNT : 2023UPASB057

Vers l'utilisation rationnelle de biofilms positifs pour aider à maîtriser les microorganismes indésirables dans les bâtiments d'élevage

Towards the rational use of positive biofilms to aid in the management of undesirable microorganisms in livestock buildings

Thèse de doctorat de l'université Paris-Saclay

École Doctorale n°581 : Agriculture, Alimentation, Biologie, Environnement et Santé (ABIES)
Spécialité de doctorat : Microbiologie
Graduate School : Biosphera, Référent : AgroParisTech

Thèse préparée dans l'UMR **Micalis Institute** (Université Paris-Saclay, INRAE, AgroParisTech), sous la direction de **Romain BRIANDET**, Directeur de recherche, et le co-encadrement de **Mathieu CASTEX**, Directeur R&D de Lallemand Animal Nutrition

Thèse soutenue à Paris-Saclay, le 17 novembre 2023, par

Virgile GUÉNEAU

Composition du Jury

Membres du jury avec voix délibérative

Aurélie RIEU-GUIGON Professeure, Université de Bourgogne	Présidente
Philippe FRAVALO Professeur, CNAM	Rapporteur & Examinateur
Marie-France PILET Professeure, ONIRIS	Rapporteur & Examinatrice
Théodore BOUCHEZ ICPEF, INRAE (Université Paris-Saclay)	Examinateur
Alain DUFOUR Professeur, Université de Bretagne-Sud	Examinateur

université PARIS-SACLAY
ÉCOLE DOCTORALE
Agriculture, alimentation, biologie, environnement, santé (ABIES)

Titre: Vers l'utilisation rationnelle de biofilms positifs pour aider à maîtriser les microorganismes indésirables dans les bâtiments d'élevage

Mots clés: biofilms positifs, biosécurité, microorganismes indésirables, écologie microbienne dirigée, HCS-CLSM, analyse d'images

Résumé: La nécessité d'améliorer le bien-être animal, la durabilité et la sécurité microbiologique des systèmes de production entraîne des évolutions dans les itinéraires techniques des élevages. En accord avec le concept "One Health", des solutions préventives et complémentaires à l'utilisation d'intrants tels que les biocides chimiques et les antibiotiques sont en cours de développement. L'application de bactéries capables de former des biofilms positifs et de guider l'écologie microbienne de surface pour limiter l'installation de microorganismes indésirables est un procédé émergent pour aider à maintenir l'hygiène des bâtiments d'élevage. Bien que les bénéfices des biofilms positifs dans le contexte des exploitations agricoles soient de plus en plus établis, leur(s) mode(s) d'action ainsi que les techniques permettant de sélectionner de manière efficace les espèces et/ou souches appropriées pour composer ces solutions innovantes sont encore peu documentés. Dans l'optique d'aider à développer une nouvelle génération de produits, nous présentons une approche expérimentale adaptée à la sélection rationnelle d'espèces et de souches pour de telles applications. Ce processus repose sur l'analyse phénotypique des communautés constituants les biofilms par microscopie confocale à balayage laser (HCS-CLSM) et analyse d'images. Cette démarche a été utilisée pour cribler une collection de souches candidates pour leurs propriétés antagonistes vis-à-vis de microorganismes indésirables, ainsi que pour caractériser les mécanismes d'interaction au sein de différents modèles de biofilms mixtes. La capacité des souches candidates à coexister de manière stable au sein de biofilms mixtes a été étudiée en vue de créer des consortiums bénéfiques ayant une capacité accrue à coloniser les surfaces et à éviter/réduire le risque de colonisation par des communautés de microorganismes indésirables. En parallèle, une méthode d'échantillonnage basée sur le prélèvement de coupons de matériaux représentatifs des surfaces de bâtiments d'élevage a été mise en place pour caractériser les biofilms environnementaux, et étudier *in situ* les effets de l'application de biofilms positifs. A partir de ces résultats, nous engageons une discussion portant sur les opportunités d'amélioration en ce qui concerne la formulation de biofilms positifs de nouvelle génération. De plus, nous examinons les avantages et les bénéfices inhérents à ces produits en tant qu'éléments complémentaires aux méthodes de biosécurité traditionnellement employées dans les bâtiments d'élevage.

Title: Towards the rational use of positive biofilms to aid in the management of undesirable microorganisms in livestock buildings

Keywords: positive biofilms, biosecurity, undesirable microorganisms, guided microbial ecology, HCS-CLSM, image analysis

Abstract: The need to improve animal welfare, sustainability, and microbiological safety of livestock production systems is leading to changes in farm management. In line with the "One Health" concept, preventive and complementary solutions to the use of inputs such as chemical biocides and antibiotics are being developed. The application of bacteria capable of forming positive biofilms and guiding surface microbial ecology to limit the establishment of undesirable microorganisms is an emerging process to help maintain the hygiene of livestock buildings. Although the benefits of positive biofilms in the context of animal farming are increasingly established, their mode(s) of action as well as techniques to efficiently select appropriate species and/or strains to create these innovative solutions are still poorly documented. In order to contribute to the development of a new generation of products, we present an experimental approach adapted for the rational selection of species and strains for such applications. This process relies on the phenotypic analysis of the communities constituting the biofilms through confocal laser scanning microscopy (HCS-CLSM) and image analysis. This approach was used to screen a collection of candidate strains for their antagonistic properties against undesirable microorganisms, as well as to characterize interaction mechanisms within different models of mixed biofilms. The ability of candidate strains to stably coexist within mixed biofilms was studied with the aim of creating beneficial consortia with an increased capacity to colonize surfaces and to prevent/reduce the risk of colonization by undesirable microorganisms. In parallel, a sampling method based on the collection of representative material coupons from livestock building surfaces was established to characterize environmental biofilms and to study the *in situ* effects of applying positive biofilms. Based on these results, we initiate a discussion regarding opportunities for improvement in formulating next-generation positive biofilms. Furthermore, we examine the advantages and benefits inherent to these products as complementary elements to biosafety methods traditionally employed in livestock systems.

Remerciements

Merci à Philippe Fravalo, Marie-France Pilet, Théodore Bouchez, Alain Dufour et Aurélie Rieu d'avoir accepté de relire et évaluer mon travail. C'est un plaisir de vous compter parmi les membres de mon jury de thèse.

Romain, merci d'avoir été mon directeur de thèse. Cela fait maintenant plus de 4 ans que tu encadres mes projets depuis le master 2. Tu m'as soutenu et fait confiance. J'ai grandement apprécié nos échanges, souvent autour d'un café, tant sur des discussions scientifiques que personnelles. Tu m'as laissé une liberté de réflexion et d'expérimentation pour m'imprégner pleinement du projet et d'aller jusqu'au bout des choses. Je ressors de cette expérience encore plus passionné par mon projet et plus généralement par l'étude des biofilms. Je me réjouis de continuer ensemble cette belle histoire. J'ai été épanoui tout au long de ma thèse et c'est en partie grâce à toi, encore merci.

Mathieu, merci d'avoir été mon co-encadrant de thèse. Tu m'as beaucoup appris sur le métier de chercheur en R&D, et sur les attentes de l'industrie par rapport à notre recherche, avec une grande curiosité et un questionnement scientifique. J'ai grandement apprécié ces échanges et notre collaboration, et je suis ravi de la perspective de continuer à travailler avec toi. Mon expérience pendant ma thèse, au sein de cette interface entre l'équipe B3D et Lallemand, a été particulièrement enrichissante. Merci pour ta confiance.

Merci aux membres de mon comité de suivi de thèse, Laurent Guillier, Pascale Serror et Françoise Irlinger pour toutes les discussions et recommandations afin de mener à bien mon projet. Un merci particulier à Laurent qui m'a souvent accompagné dans mon projet et dans l'analyse de mes résultats.

Julia et Bastien, c'est toujours un plaisir d'interagir avec vous. Vous m'avez appris beaucoup sur le contexte applicatif des biofilms positifs. Les prélèvements sur le terrain, et les discussions avec les éleveurs en ta compagnie Bastien, m'ont permis de sortir de mon laboratoire et d'être confronté à la réalité du terrain. J'ai vraiment apprécié travailler avec vous, et je suis content que cela continue.

Merci à tout Micalis et surtout aux membres de l'équipe B3D. Merci à Marie-Françoise, Florence, Maud, Dominique, Julien, Marina, Jean-Christophe, Yasmine, Raphaël, Cécile… (j'en ai certainement oublié) pour toutes nos discussions, scientifiques ou pas. Julien, camarade de ferment'heure, merci pour toute ton aide pour la microscopie. Merci à tous les autres membres de l'équipe. Il y a eu beaucoup de roulement depuis mon arrivé mais cela a toujours été un plaisir de tous vous côtoyer. C'est en partie grâce à vous que j'arrive le matin au travail avec le sourire. Spéciale dédicace à Arthur et Alban, mes camarades musicos, enfin surtout sportifs, sauf quand il y a de la bière ou du saucisson.

Christophe, tu m'as appris ce qu'était un biofilm en Licence 1 (si je me souviens bien…). Nous avions alors prélevé des lames de microscope en verre que tu avais laissé plusieurs jours au fond d'une mare du campus d'Orsay. Nous avions observé au microscope ces communautés complexes et grouillantes de vie. Finalement, je n'ai pas arrêté depuis… Chacun des stages réalisés avec toi, d'abord sur les biofilms de *Bacillus subtilis*, puis ceux de *Shewanella oneidensis* m'ont conforté dans l'idée que je voulais faire de la recherche mon métier. Et pour ça, je t'en remercie.

Merci à toi Eric de m'avoir transmis ta passion pour la recherche. J'ai adoré la liberté d'expérimentation que j'avais en stage, me permettant m'exprimer et de tester tant de choses ! J'ai beaucoup apprécié cette première expérience sur un sujet transversal entre la physique, la chimie et la microbiologie et suis convaincu, depuis, de l'importance de créer ces interactions.

Un boxeur en thèse à quelques portes de mon bureau mais avant tout un ami… Merci Hugo BG, gant jaune, pour ces pauses café à parler de tout et de rien, c'était cool. Merci aussi pour tout ces bleues aux jambes, aux avant-bras, à la tête et j'en passe après les entrainements, ça aussi : trop cool.

Forcément, merci à tous mes amis d'être là pour me soutenir, me supporter et avoir permis de m'évader. Merci de m'avoir écouté, parfois longtemps, à faire un monologue, après la fameuse question «alors comment ça se passe la thèse ?».

A vous, mes parents et mes deux frères (le petit et le grand). Vous êtes un soutien fort pour moi sur lequel je pourrai toujours compter. Merci de m'écouter me plaindre alors, qu'avec du recul, il n'y avait très souvent aucune raison à cela.

Oh Marie, si tu savais… tout ce que je pourrais écrire pour décrire le soutien que tu as été pendant cette thèse, et dans ma vie en général. Toi qui es, toujours, plus heureuse que moi de mes propres accomplissements. Je ne vais pas te dire que je te dédie cette thèse : ça serait trop… mais saches que tu as été primordiale dans sa/ma réussite et mon bonheur.

TABLE DES MATIERES

1 INTRODUCTION

Ces dernières décennies, la production de volaille destinée à l'alimentation a connu une augmentation significative à l'échelle mondiale. Cette tendance est étroitement liée à la croissance démographique et à une hausse de la consommation, qui devrait selon les modèles se poursuivre dans les années à venir, principalement en raison des besoins croissants des pays en voie de développement [1]. Pour faire face à cette demande sociétale, une augmentation du nombre et de la taille des exploitations agricoles ainsi qu'une densification des animaux dans les bâtiments d'élevage sont envisagées. Cette densité d'animaux peut faciliter l'émergence de maladies transmises par des microorganismes pathogènes capables d'infecter directement les animaux et l'humain par l'intermédiaire des animaux, phénomène appelé zoonose [2]. Des moyens prophylactiques comme l'utilisation de la vaccination sont utilisés pour prévenir l'apparition de symptômes chez les animaux. D'autres pratiques curatives comme l'utilisation des antibiotiques et de biocides peuvent être employées afin de prévenir les contaminations par des microorganismes pathogènes. Cependant, l'utilisation d'antibiotiques est à l'origine de l'apparition de résistances génétiques pouvant être portées par les pathogènes [3,4]. Selon le rapport O'Neill (2016), plus de 10 millions de décès pourraient être causés par la résistance aux médicaments anti-infectieux en 2050. Ces résistances deviendraient la première cause de décès dans le monde d'ici 2050 si la situation actuelle ne change pas [5]. L'Organisation Mondiale de la Santé (OMS) pointe la résistance aux antimicrobiens comme un phénomène à l'origine d'une crise mondiale de santé publique qui doit être gérée de toute urgence [6]. Ainsi, il devient impératif de rechercher des solutions alternatives aux antibiotiques afin de réduire leur utilisation. Depuis plus de deux décennies l'industrie mondiale des productions animales a progressivement enclenché une mutation de ses pratiques vers une utilisation plus raisonnée des antibiotiques. La réglementation Européenne de 2006 sur l'interdiction de l'usage des antibiotiques facteurs de croissance chez les animaux d'élevage a été un point de départ et nous assistons dès lors à des évolutions réglementaires de ce type dans d'autres régions du monde. En 2022 l'Union Européenne a étendu cette interdiction par l'application du règlement (UE) 2019/6. Bien que plusieurs actes juridiques doivent encore compléter ce règlement, celui-ci prévoit une interdiction

de l'importation au sein de l'UE des produits animaux ayant été traités avec des antibiotiques facteurs de croissance.

Dans le contexte de mon projet de thèse, nous nous sommes intéressés aux élevages industriels hors-sols de poulets de chair. Les surfaces de ces bâtiments peuvent constituer des réservoirs de pathogènes microbiens en contact direct avec les animaux, agissant comme des vecteurs de maladies. Ainsi, des mesures de biosécurité agissant sur l'environnement des animaux sont appliquées afin de réduire cette charge microbienne, potentiellement indésirable. Des protocoles de nettoyage et de désinfection (N&D) des surfaces impliquant l'utilisation de molécules biocides sont appliqués entre deux lots successifs d'animaux. Les molécules alors utilisées sont polluantes, entraînent l'apparition de résistance et ne sont pas totalement efficaces [7]. Des réglementations de plus en plus restrictives concernant l'utilisation de ce type de molécules émergent afin de limiter une utilisation abusive, telles que la réglementation REACH en Europe (Regulation EC No. 1907/2006). L'efficacité réduite des procédures de N&D est directement liée à l'organisation des microorganismes sous forme de biofilms adhérents aux surfaces [8].

Les biofilms sont des communautés complexes de microorganismes spatialement organisées et intégrées dans une matrice extracellulaire sécrétée. Au sein de cette matrice qui structure la communauté, les microorganismes interagissent entre eux et avec leur environnement [9,10] (**Figure 1**).

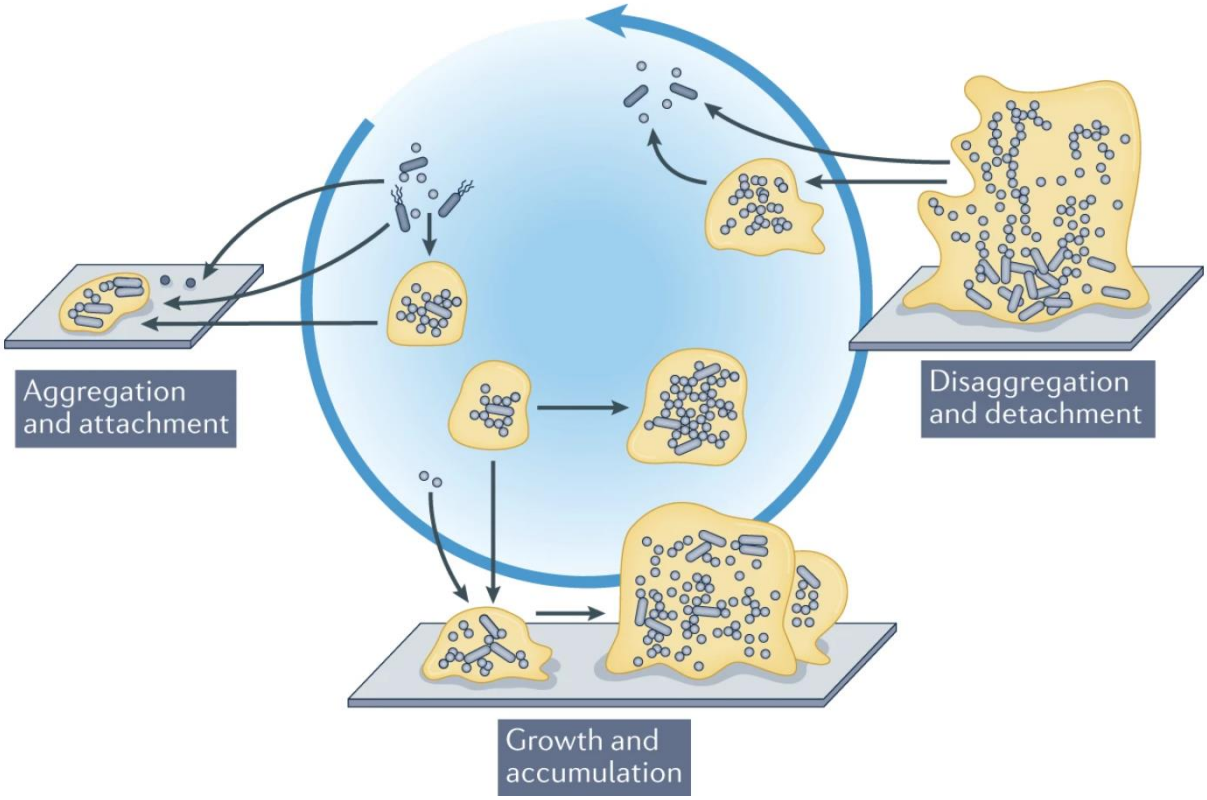

Figure 1: Le schéma présente le modèle de la formation des biofilms. Il inclut les trois principaux événements de la formation des biofilms indépendamment des surfaces et de l'initiation à partir de bactéries planctoniques unicellulaires, englobant ainsi les systèmes *in vitro*, *in situ* et *in vivo*. Le présent modèle prend en compte différents habitats, conditions et microenvironnements, ainsi que l'afflux possible de nouvelles cellules. En outre, le modèle englobe à la fois les biofilms attachés à la surface (anneau extérieur) et les biofilms non attachés à la surface (anneau intérieur), avec un échange possible entre les deux. Les bactéries peuvent entrer dans le modèle à n'importe quel moment. Agrégation et attachement : au cours de cet événement, les bactéries s'agrègent les unes aux autres ou s'attachent à des surfaces biotiques et abiotiques. Croissance et accumulation : au cours de cet événement, les colonies bactériennes agrégées et attachées s'étendent par la croissance et le recrutement des cellules environnantes. Désagrégation et détachement : au cours de cet événement, les bactéries peuvent quitter le biofilm sous forme d'agrégats ou de cellules individuelles, en fonction du mécanisme. Ces trois événements caractérisent et représentent la plupart, sinon la totalité, des scénarios de biofilms, indépendamment du temps et de la maturité. Adapté de Karin Sauer *et al.* [10].

Ces communautés polymicrobiennes sont ubiquitaires et colonisent tous les biotopes de notre planète. Selon une étude bibliographique, l'ensemble des biofilms qui recouvrent ces biotopes contiendraient jusqu'à 80% des microorganismes présents sur Terre [11]. La matrice extracellulaire des biofilms se compose principalement d'exopolysaccharides, de protéines, d'ADN extracellulaire (ADNe) et d’eau [12]. La présence de la matrice favorise une architecture

tridimensionnelle, au sein de laquelle se forment des gradients chimiques, gazeux et nutritionnels qui dépendent de la densité cellulaire ainsi que de la composition de la matrice [13]. Ces structures complexes peuvent héberger des bactéries et des archées [11], des virus [14], des champignons [15–17], ou encore des microalgues [18,19] et peuvent constituer des réservoirs de microorganismes pathogènes [20]. La disposition spatiale, l'hétérogénéité cellulaire des membres de la communauté microbienne, la diversité des composés de la matrice extracellulaire et des gradients physico-chimiques qui sont générés dans le biofilm, sont à l'origine de l'émergence de nouvelles propriétés au sein de ces communautés [12,13,21,22]. Contrairement au mode de vie planctonique, les bactéries au sein des biofilms sont capables d'une plus grande tolérance et adaptabilité vis à vis des stress environnementaux, tels que lors du passage dans le tractus digestif [23,24], ou lors de l'exposition à de fortes concentration de biocides, de désinfectants [8] ou d'antibiotiques [25].

Les biofilms ont jusqu'à présent été étudiés essentiellement pour leurs impacts négatifs sur la santé humaine [26,27], des animaux [28,29] et des plantes [17], dans le cadre de contamination dans les procédés industriels [30] ou encore sur l'intégrité des matériaux [31]. Le coût engendré par ces impacts des biofilms est évalué à près de 4 000 milliards de dollars par an à l'échelle mondiale, dont environ deux tiers sont dus à la bio-corrosion [32]. *The National Institutes of Health* (NIH) estime qu'environ 80% des infections humaines étaient associées à la formation de biofilms [27]. Cependant, au-delà de ces impacts négatifs, il faut rappeler que les biofilms représentent des intérêts majeurs au niveau environnemental et industriel. A l'échelle écologique, les biofilms sont essentiels au bon fonctionnement des écosystèmes. En industrie agroalimentaire, ils sont aussi largement impliqués dans la transformation d'aliments fermentés comme le fromage ou le *natto* [33]. Actuellement, il est reconnu que le mode de vie en biofilm est impliqué dans certains mécanismes de protection des cultures par des agents de biocontrôle microbiens [34].

En accord avec le concept "*One Health*", qui vise notamment à réduire l'utilisation de biocides et d'antibiotiques tout en améliorant le bien-être animal dans les

élevages, des moyens innovants de lutte et de prévention contre l'émergence de zoonoses sont développés. Une des approches novatrices consiste à appliquer des bactéries bénéfiques capables de former des biofilms positifs sur les surfaces en complément des procédures de N&D. Les biofilms positifs vont ainsi moduler le microbiote des surfaces dans les bâtiments d'élevage avec comme objectif de limiter l'implantation de microorganismes indésirables [35]. Ces biofilms positifs sont sélectionnés en fonction de leurs capacités à coloniser les surfaces et à exercer des activités compétitrices contre des microorganismes indésirables ciblés. Les produits disponibles actuellement sur le marché sont essentiellement composés d'assemblage de souches de *Bacillus* spp. et de bactéries lactiques (LAB). En effet, de nombreuses espèces de ces genres bactériens sont présentes sur la liste de présomption d'innocuité reconnue (QSP) de l'autorité européenne de sécurité des aliments (EFSA) [36] et possèdent le statut "généralement reconnu comme sans danger" (*Generally Recognized As Safe*, GRAS) de la *Food and Drug Administration* (FDA).

Actuellement, il existe sur le marché des biofilms positifs commerciaux utilisés par les éleveurs. Cependant, avant ce projet de thèse, aucune étude n'avait mis en évidence la possibilité de moduler les communautés de surfaces d'élevage par le développement des biofilms positifs. En effet, les méthodes couramment employées pour l'étude des communautés microbiennes de surface, telles que les écouvillonnages, boîtes de contact, chiffonnettes, et éponges, ne sont pas standardisées et sont fortement tributaires de l'expérimentateur [37]. Ces méthodes sont invasives, altèrent l'intégrité et modifient l'organisation spatiale du biofilm. L'examen des biofilms revêt une importance capitale en raison de leur rôle fondamental dans la tolérance des microorganismes, notamment face aux désinfectants [13].

De plus, les produits disponibles sur le marché sont des assemblages de souches dont l'effet augmenté des mélanges par rapport aux souches individuelles n'a pas été formellement démontré. Leur capacité à coloniser les surfaces sous forme de biofilm ou à exercer un effet antagoniste contre des microorganismes indésirables restent insuffisamment documentée. Cela s'explique par la présence de verrous

technologiques rendant difficile le suivi individuel des partenaires du biofilm au sein de la communauté. Cependant, l'accès à ces informations est essentiel pour décrypter les mécanismes d'interactions entre les différentes souches qui composent le biofilm.

Pour établir une base scientifique solide en vue de rationaliser l'utilisation de biofilms positifs dans l'élevage, deux objectifs majeurs ont été fixés.

Objectif i) **développer une méthodologie adaptée pour étudier de manière globale les communautés microbiennes associées aux surfaces des bâtiments d'élevages hors-sols, et la valider dans le contexte d'un élevage industriel**.

Objectif ii) **mettre en place une démarche expérimentale rationnelle visant à sélectionner et assembler des souches présentant des caractéristiques d'intérêt pour la formation des biofilms positifs**.

Pour répondre à ces objectifs, ce projet de thèse CIFRE a été mis en place. Il s'inscrit dans une collaboration entre l'équipe "Biofilms et Communautés Spatialement Organisées" (B3D) de l'Institut Micalis et l'entreprise Lallemand Animal Nutrition.

L'Institut Micalis est une unité mixte de recherche (UMR) associant l'INRAE, AgroParisTech et l'Université Paris-Saclay (UPSaclay). Les travaux de recherche menés portent sur la microbiologie de l'alimentation au service de la santé. Au sein de l'UMR Micalis, l'équipe "Biofilms et Communautés Spatialement Organisées (B3D) constitue l'une des dix équipes composant le pôle "Adaptation Bactérienne et Pathogenèse". Au sein de l'unité, l'équipe B3D occupe une position singulière en abordant la question de l'organisation spatiale des microorganismes dans un contexte de santé publique. Son objectif principal réside dans la caractérisation du comportement des agents pathogènes au sein de systèmes tridimensionnels complexes tout au long de la chaîne alimentaire. Les travaux visent à développer des approches innovantes pour maîtriser ces pathogènes en manipulant leur environnement local, en optimisant l'action d'agents antimicrobiens et en exploitant des microorganismes bénéfiques.

De son côté, Lallemand SAS fait partie du Groupe Lallemand, un groupe spécialisé dans la recherche, le développement et la production de microorganismes pour des applications dans divers domaines. L'un de ses domaines d'expertise de premier plan concerne le développement de solutions à base de microorganismes qui exercent une influence directe sur la stabilisation des microbiomes digestifs humain et animaux, ainsi que sur les fonctions de barrière et les mécanismes de régulation de la réponse immunitaire à l'échelle locale et systémique. Lallemand Animal Nutrition (LAN) est l'unité d'affaires dédiée au développement et à la commercialisation de solutions microbiennes à destination des animaux d'élevage et des animaux de compagnie. La société n'a cessé d'innover par le développement industriel de nouveaux produits et le développement de nouvelles applications des microorganismes en alimentation animale et plus récemment dans l'environnement des animaux d'élevages.

Cette thèse a été dirigée par Romain Briandet, directeur de recherche INRAE à l'Institut Micalis et responsable de l'équipe B3D et co-encadrée par Mathieu Castex, directeur R&D de Lallemand Animal Nutrition.

Le projet scientifique a été divisé en trois modules pour répondre aux objectifs énoncés, illustrés dans la **figure 2**, et décrits ci-dessous.

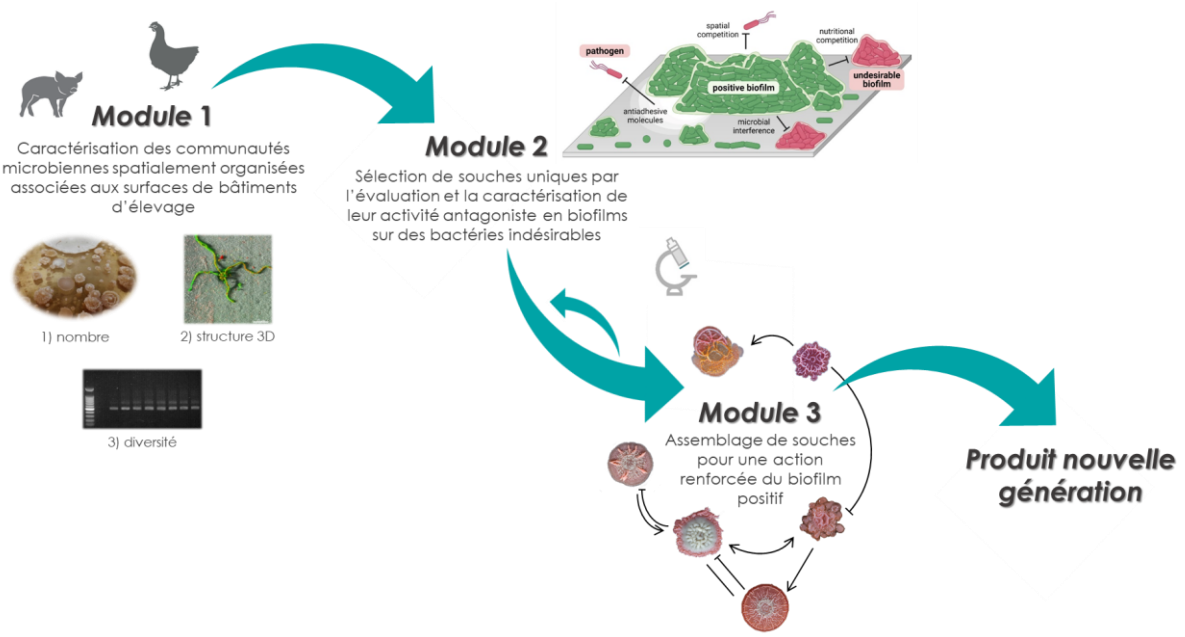

Figure 2: Schéma décrivant l'organisation des modules du projet scientifique.

Module 1: Caractérisation des communautés microbiennes spatialement organisées associées aux surfaces de bâtiments d'élevage. Une procédure d'échantillonnage *in-situ* utilisant des coupons de matériaux représentatifs des bâtiments d'élevage a été mise au point, associée à une analyse *ex-situ* en laboratoire. Cette technique d'échantillonnage permet de prélever la communauté microbienne sans perturber l'organisation spatiale du biofilm, étudiée par Microscopie Confocale à Balayage Laser (MCBL). Après détachement mécanique des biofilms développés sur les coupons, le nombre de bactéries a été déterminé par dénombrement sur différents milieux sélectifs. De plus, la diversité de ces communautés a été étudiée en séquençant le gène codant pour l'ARNr 16S. Cette approche a été mise au point sur un élevage expérimental de poulet de chair et un élevage commercial porcin. Étant donné que le système d'élevage de poulet de chair est plus facile à étudier par ces approches que celui des porcs, nous avons choisi de le considérer comme système modèle pour la suite du projet. Suite à cette phase de mise au point, notre méthode d'échantillonnage a été appliquée lors d'une étude visant à comprendre comment l'implantation d'un biofilm positif pouvait moduler les communautés microbiennes présentes sur les surfaces de bâtiments d'élevage de poulet de chair. Notre méthode de prélèvement des biofilms autochtones de l'élevage a également permis d'isoler certaines souches de *Bacillus* spp., caractérisées dans le cadre de ce projet.

Module 2: Sélection de souches uniques par l'évaluation et la caractérisation de leur activité antagoniste en biofilms sur des bactéries indésirables. Lors de ce module, des modèles *in-vitro* basés sur l'imagerie des biofilms permettant de quantifier et caractériser l'activité antagoniste en biofilm des souches candidates sur des bactéries indésirables ont été développés. Les meilleures souches candidates ont été sélectionnées en vue de concevoir un produit commercial de nouvelle génération. Des études approfondies ont également été menées pour comprendre les grandes familles de mécanismes impliquées dans l'activité antagoniste des souches sélectionnées.

Module 3: Assemblage de souches pour une action renforcée du biofilm positif. Dans le cadre de ce module, des consortiums de souches bénéfiques ont

été assemblés selon une approche innovante dans le domaine. Dans un premier temps, la capacité des souches candidates à former des biofilms multi-souches/espèces stables et compatibles a été vérifiée. Dans un second temps, les consortiums identifiés ont été évalués pour leur potentiel effet renforcé par rapport aux souches individuelles les composant. Dans le cas d'associations spécifiques, une activité antagoniste plus prononcée par rapport aux souches individuelles a été observée.

Le manuscrit de thèse présenté est organisé en trois parties :

La première partie constitue une étude bibliographique sous forme d'un article de revue et d'un chapitre de livre. Elle expose i) le contexte global du projet, en énonçant les avantages et limitations liés à l'utilisation des biofilms positifs dans des élevages hors sols, et ii) les différentes utilisations de la microscopie de fluorescence permettant l'analyse spatiale des biofilms bactériens multi-espèces, qui représente la principale méthode utilisée tout au long du projet.

La deuxième partie présente les résultats expérimentaux et est organisée en deux chapitres. Le premier chapitre se concentre sur la caractérisation des communautés microbiennes associées aux surfaces de bâtiments d'élevage et sur l'observation de leurs modulations suite à l'application d'un biofilm positif. Le deuxième décrit l'élaboration d'une stratégie innovante permettant la sélection et l'association de souches bénéfiques formant des biofilms capables de limiter l'implantation et la croissance des agents pathogènes.

La troisième partie conclut ce manuscrit par une discussion et décrit les perspectives scientifique et industrielle de l'étude. Elle met en avant les résultats obtenus, les enseignements tirés, et propose des orientations futures pour les recherches dans ce domaine, ainsi que des possibilités d'applications industrielles pour les produits de biofilm positif développés.

2 ETUDE BIBLIOGRAPHIQUE

2.1 ARTICLE 1: POSITIVE BIOFILMS TO GUIDE SURFACE MICROBIAL ECOLOGY IN LIVESTOCK BUILDING

Virgile Guéneau, Julia Plateau-Gonthier, Ludovic Arnaud, Jean-Christophe Piard, Mathieu Castex, Romain Briandet.

Biofilm, 2022, 4, pp.100075. 10.1016/j.bioflm.2022.100075.

Positive biofilms to guide surface microbial ecology in livestock buildings

Biofilm 4 (2022) 100075

Contents lists available at ScienceDirect

Biofilm

journal homepage: www.sciencedirect.com/journal/biofilm

Positive biofilms to guide surface microbial ecology in livestock buildings☆

Virgile Guéneau [a,b], Julia Plateau-Gonthier [b], Ludovic Arnaud [b], Jean-Christophe Piard [a], Mathieu Castex [b], Romain Briandet [a,*]

[a] Université Paris-Saclay, INRAE, AgroParisTech, Micalis Institute, 78350, Jouy-en-Josas, France
[b] Lallemand SAS, 31702, Blagnac, France

ARTICLE INFO

Keywords:
Positive biofilm
Livestock building
Microbial pathogens
Biosecurity
Microbial ecology

ABSTRACT

The increase in human consumption of animal proteins implies changes in the management of meat production. This is followed by increasingly restrictive regulations on antimicrobial products such as chemical biocides and antibiotics, used in particular to control pathogens that can spread zoonotic diseases. Aligned with the One Health concept, alternative biological solutions are under development and are starting to be used in animal production. Beneficial bacteria able to form positive biofilms and guide surface microbial ecology to limit microbial pathogen settlement are promising tools that could complement existing biosecurity practices to maintain the hygiene of livestock buildings. Although the benefits of positive biofilms have already been documented, the associated fundamental mechanisms and the rationale of the microbial composition of these new products are still sparce. This review provides an overview of the envisioned modes of action of positive biofilms used on livestock building surfaces and the resulting criteria for the selection of the appropriate microorganisms for this specific application. Limits and advantages of this biosecurity approach are discussed as well as the impact of such practices along the food chain, from farm to fork.

1. Introduction

Nowadays, a significant increase in the production of meat and fish is observed around the world [1]. This is linked to the growing consumer demand associated with the demographic and consumption increase in developing countries. To cope with this societal demand, an increase in the number and size of farms and a densification of animals in the buildings are envisioned. High animal density, particularly in confined buildings, can lead to the emergence of diseases, such as zoonosis. According to the World Organization for Animal Health, 60% of the 1400 human pathogens have an animal origin and 75% of emerging animal diseases can infect humans. Microbial pathogens in farms can trigger human diseases by direct contact with animals, but can also affect the whole food chain up to processed products such as meat or dairy products [2]. Characterizing pathogenic agents in livestock buildings and finding appropriate means to reduce their establishment and their propagation are therefore important challenges in the agrifood domain.

Prophylactic means of control such as vaccines to prevent the onset, spread and worsening of diseases or curative methods such as antibiotic therapy are mostly used to control these infectious diseases in animals. To limit animal contamination in farms, the surfaces of livestock buildings are cleaned and disinfected according to defined "biosecurity schemes" between each batch of animals. These protocols are aimed at limiting the microbial surface load that can be a reservoir of pathogens in livestock buildings before animals enter. However, these protocols may lack efficiency [3]. This variable effectiveness could be associated with the formation of spatially organized biofilms by the surface microbial communities. Biofilms are three-dimensional microbial structures adhering to a surface and buried in self-produced extracellular polymeric substances (EPS) [4]. They colonize all biotopes and are the most prevalent mode of life of microorganisms in nature [5]. The presence of an EPS matrix, the heterogeneity of cell types and the existence of specific intercellular communication phenomena such as the density-dependent intercellular communication system called *quorum sensing* give rise to emerging biofilm properties, including an extraordinary adaptation to environmental fluctuations. Microorganisms within a biofilm tolerate much more intense stresses than their planktonic counterparts, such as dehydration or the action of disinfectants

☆ Given his role as Editor, Romain Briandet had no involvement in the peer review of this article and has no access to information regarding its peer review. Full responsibility for the editorial process for this article was delegated to Ákos T. Kovács.

* Corresponding author.
E-mail address: romain.briandet@inrae.fr (R. Briandet).

https://doi.org/10.1016/j.biofilm.2022.100075
Received 14 February 2022; Received in revised form 7 April 2022; Accepted 10 April 2022
Available online 19 April 2022

[6]. Besides, these complex communities can harbor bacteria, viruses, yeasts, other fungi, microalgae, archaea, protists and can constitute reservoirs of pathogenic microorganisms [7,8]. The National Institutes of Health (NIH) have estimated that approximately 80% of human infections are associated with microbial biofilms [9]. These biostructures generate dramatic health issues and intensive efforts are used in the medical field to find new control strategies [10–13]. In farms, biofilms are found on walls, floors as well as in drinkers, feeders and even on the animals themselves. Biofilms are frequently associated with disinfection failure and pathogen persistency on surfaces [14–16].

Currently, there is strong pressure from consumers and legislators to reduce chemical disinfectant inputs in livestock farming to limit environmental impact and improve animal welfare and human health [17,18]. To ensure both farming sustainability and biosafety management, innovative solutions based on guided microbial ecology approaches have emerged recently in livestock production. The use of beneficial microorganisms to protect surfaces is applied under different usage names depending on the sector [7]: *e.g.* biocontrol for plants [19], biopreservation for food [20,21] or bioremediation for environmental issues [22]. In livestock buildings the term "positive biofilms" is now widespread for biosafety issues [23]. In this review, "positive biofilms" refers to the application of defined mixtures of bacteria in livestock buildings, selected for their capacity to colonize this environment and generate biofilms able to outcompete undesirable microorganisms. This review describes the concept, functioning and current use of positive biofilms and how they can complement conventional antimicrobial interventions. Because of their action to limit pathogens in animal production systems, the use of positive biofilms fits well in the One Health concept [17]. This is intended to limit the use of antimicrobials in farms and to propose additional solutions to prevent zoonoses.

2. Biosafety tools for the livestock sector

2.1. Direct actions on animals to limit diseases

2.1.1. Vaccines: successes and limitations

Vaccines are considered one of the greatest public health successes, along with the discovery of antibiotics. Vaccination aims to induce protective immunity to a targeted pathogen, thereby limiting the risk of developing the disease and reducing its potential impact on health. The principle is to inject a live attenuated pathogen, inactivated pathogen or part of a pathogen into a host [24]. These can be cellular debris, surface proteins or other molecules specific to the presence of the pathogen such as RNA molecules that will be used by the host cell to produce a pathogenic protein. Vaccines allow the body to obtain a long-lasting immune memory against the injected product. Typically, the active agent of a vaccine is recognized by cells of the immune system, which will produce large quantities of antibodies specifically directed against the pathogen. When the virulent pathogen infects the host, it will be immediately taken care of by a large number of cells secreting antibodies against it. Vaccines can have beneficial effects against pathogens other than the one initially targeted [25]. The use of vaccines helps to prevent the proliferation of pathogens in farms. It is a prophylactic action performed under the prescription of veterinarians. Because a vaccination plan is preventive, a strategy linked to a global prevention and control plan must be undertaken. The latter comprises local and global health recommendations [26]. The price of global vaccination in one farm is high, but the cost of diseases is higher [27,28]. One limit of the utilization of vaccines is silent infection [29]. Administration protocols may also be a limitation for some species and vaccines are not available for all infectious diseases in farms.

2.1.2. Antibiotic use for animals

Antibiotics are molecules that kill or inhibit the growth of susceptible bacteria. They are naturally secreted by fungi or other microorganisms and can be produced synthetically or by large-scale fermentation. The use of such molecules has saved countless lives, both human and animal, but their use is subject to worrying abuses [17]. Antibiotic sales increase in proportion to population growth. In some countries, they can be purchased without a medical prescription and in others they are used as growth promoters for livestock and aquaculture productions [30]. Antibiotic consumption may increase by 67% between 2010 and 2030 worldwide [31].

Careless use of antibiotics leads to the emergence of resistance in bacteria that may be transmitted to human microbiota. Antibiotic resistance is a genetically encoded mechanism in bacteria that allows a change in the target of the antibiotic or a reduction in the concentration of the antibiotic in the cell, preventing destruction [32,33]. The World Health Organization characterizes antimicrobial resistance (AMR) as a global public health crisis that must be managed with the utmost urgency [34]. Due to poor absorption by the body, 30–90% of antibiotics used in the animal food-producing industry are released into the environment [35,36]. The intensive exposure of environmental microbial communities to antibiotics can promote the emergence of intrinsic resistance and the transfer of resistance genes between bacteria (acquired resistance genes). Hence, animal carcasses can be contaminated in slaughterhouses with antibiotic-resistant pathogens [37]. As a consequence, food can contain bacteria harboring acquired antibiotic resistance genes that can be transmitted horizontally to bacteria from our gut microbiota [32]. The major health issue related to AMR is linked to the acquisition of resistance genes by bacteria capable of zoonosis. Some pathogenic bacteria such as *S. aureus* and *Escherichia coli* can become resistant to a very large spectrum of antibiotics [38,39].

According to the O'Neill report, more than 10 million deaths could have been caused by resistance to anti-infective drugs in 2016 which may become the leading cause of death in the world by 2050 if the situation does not change [40]. The economic cost could reach US $ 100 billion in this case [40]. To address this risk, the European Union implemented a regulation to ban antibiotics as growth promoters in animal feed in 2003 (Regulation 1831/2003/EC) and in June 2022 a new regulation will ban the use of therapeutic dose of zinc oxide, which is known to contribute to the emergence of bacterial resistance. The goal is not to ban their curative usage but to foster more reasonable use to limit the spread of antibiotic-resistant bacteria in the food chain. This is of particular interest as antibiotics used in veterinary medicine are often the same molecules as in human medicine. In the European Union, legislation will oblige member states to transmit sales and usage data of antimicrobials by species, before January 28, 2024, for cattle (including cattle of less than a year in age), pigs, poultry (chickens and turkeys).

2.1.3. Probiotics to maintain animals in good health

Probiotics are defined by the World Health Organization and the Food and Agriculture Organization of the United Nations as live strains of strictly selected microorganisms which, when administered in adequate amounts, confer a health benefit on the host [41,42]. Probiotics are given to animals or humans in aqueous solution, feed or in lyophilized form. They can be used to confer benefits such as promoting a beneficial microbiota and result in growth-promoting effects and morbidity reduction. The main microorganisms used as probiotics are *Saccharomyces* spp., *Bifidobacterium* spp., *Pediococcus* spp., *Lactobacillus* spp., *Lactococcus* spp., *Bacillus* spp., *Streptococcus* spp. *Enterococcus* spp. and *Escherichia coli* [43,44]. Research is under way to find new candidates as live biotherapeutics with specific probiotic properties such as *Faecalibacterium prausnitzii*, which has shown anti-inflammatory activity in the gut [45,46]. Probiotics can have positive effects on animal welfare, for instance by alleviating the stress of farming animals transitioning to a different production stage (such as the weaning phase in piglets). Probiotics can also stabilize animal intestinal flora and reduce the need for antibiotic treatments and associated propagation of AMR strains [47]. Probiotics are usually administrated to the host in "planktonic" form and are typically freeze-dried or spray dried. Recent reports have explored the possibility of formulating probiotics in a

Table 1
Major microbial pathogens isolated from biofilms in animal farms.

Zoonosis rank[a]	Pathogens	Place	Surface of development	Sources
1	*Campylobacter* spp.	poultry, slaughterhouse	stainless steel, surface-water isolates, human epithelial cells	[68–70]
2	*Salmonella* spp.	pig farm, poultry	eggshells, glass, broiler bedding material, polystyrene	[15, 71–74]
3	*Escherichia coli*	broiler material	broiler bedding material, air-handling system, water	[75]
4	*Yersinia enterocolitica*	mammals	flea intestine (vector of disease), polystyrene	[76,77]
5	*Listeria monocytogenes*	pork processing industry, floor drain and drain water, poultry meat	stainless steel, glass	[78–82]
	Staphylococcus aureus	bovines	bovine magpie	[83]
	Enterococcus faecalis	cattle farm	intestine	[84]
	Mycoplasma hyopneumoniae	pig farm	tracheal epithelium from pigs, glass	[85]
	Pseudomonas aeruginosa	drinking water of broiler houses, floor drain	stainless steel, glass	[86]
	Clostridium perfringens	poultry	livestock building (water supply lines, wall, feed)	[87,88]
	Pasteurella multocida	pigs and poultry	glass, calf trachea	[89]
	Streptococcus suis	pigs	endothelial cells	[90,91]
	Mycobacterium spp.	cattle	lung, liquid/air interface	[92,93]
	Vibrio spp.	aquaculture	glass, surface of the digestive tract of shrimp	[94,95]

[a] The European Union One Health 2019 Zoonoses Report [67].

biofilm form, allowing better tolerance to stressors encountered in the digestive tract and to boost the beneficial effect [48–50].

2.2. Management of undesirable microbes in the holobiont environment

2.2.1. Microbial flows in the farm influence the equilibrium of the holobiont

The holobiont is a biological organization composed of the host and the microbial communities associated with it, including viruses, and prokaryotic and eukaryotic organisms [51]. The whole genome of the holobiont is called a hologenome. If there is a disorder in the organization of the hologenome, it can affect the phenotype of the host and its microbiota. Comprehension of the relation between the host, its microbiota, and the environment is essential to understand how the addition of positive bacteria on farms can have beneficial effects on the host [52]. To safeguard animal health and holobiont balance, a set of biosecurity measures can be taken. Biosecurity is defined by the Food and Agriculture Organization as a strategic and integrated approach to the analysis and management of risks to the life and health of people, animals, plants and associated risks to the environment [53]. Good farming practices and effective biosecurity measures are essential, as they are the first barrier to the entry of pathogens into farms. External biosecurity measures designate strategies used to reduce disease introduction like fencing, quarantine, movement restriction, cleaning and disinfection procedures, and transport. Internal biosecurity measures are strategies used to reduce disease spread with, for example, the isolation of sick animals, and the control of rodents and insects. Biosecurity management is complex but first involves daily animal monitoring. Humans and animals present in the farm (*e.g.* cats, dogs, insects, rodents) can be vectors of contamination and may be responsible for transmitting them [54]. For example, flies are carriers of Enterobacteria, which are possibly pathogenic *e.g. Salmonella* spp. [55]. For 20 flies caught in pig farms, 10^4 to 10^6 *E. coli* were quantified [56]. To control these vectors, semi-containment measures are used in certain farms, along with airlocks that limit the risk of external contamination. Next comes hygienic practices such as the use of overshoes, hand cleaning, taking a shower, or the management of inputs including water, feed, litter and effluents such as manure. Indeed, water and feed can also transmit diseases to animals, which can lead to zoonoses [57,58]. Biosecurity management measures must be taken until the end of the chain and not only during breeding. Organic waste from livestock can be used as fertilizer for crops and thus disseminate pathogens in the environment [59].

Among internal biosecurity measures to limit the persistence and proliferation of pathogenic bacteria in livestock buildings, cleaning and disinfection (C&D) protocols are applied between each breeding cycle. In addition to environmental and safety concerns associated with their use, several studies have shown that these chemical biocides are poorly effective on biofilms and only allow the elimination of a small fraction of the microbiota present on surfaces [3,60,61]. Hence, it has been shown in avian farms that C&D protocols are not totally effective in eradicating residual pathogens responsible for cross-contamination between different batches of animals such as *Salmonella* spp., *Campylobacter jejuni, Enterococcus* spp. and *Escherichia coli* [62–66]. This decrease in efficiency of C&D is directly associated with the formation of biofilms by these surface-associated communities. As shown in Table 1, microbial pathogens of major public health interest that can trigger zoonoses are able to form biofilms on surfaces typically encountered in livestock buildings [67].

2.2.2. Towards innovative biosecurity approaches in livestock buildings

For more than two decades, the international scientific community has been searching for alternative strategies to chemical biocides to control unwanted microorganisms. While physical processes (*e.g.* pulsed-light or plasma gas decontamination devices) are promising for specific industrial applications, their high demand in energy and cost limit large-scale use [96]. Most of the alternative processes considered nowadays for livestock building applications are based on biological systems. For instance, enzyme-based detergents improve the cleaning and disinfection process [97]. Different enzymes can be used such as proteases, cellulases, polysaccharide depolymerases, alginate lyase, dispersin B, or DNAse [98,99]. In industrial environments, numerous microbial species can grow within the same biofilm, thus increasing the biochemical heterogeneity of the matrix composition. Therefore, formulations used to destroy biofilm organization are generally composed of mixtures of enzymes with different substrate spectra. Novel anti-biofilm approaches targeting *quorum sensing* systems are emerging [100]. Several *quorum sensing* inhibitors, such as brominated furanones, interfering with biofilm formation in lab conditions [101,102]. Similarly, cyclic-di-GMP pathways that are involved in many biofilm formation processes could be promising drug targets [102–104]. Antimicrobial molecules extracted from natural compounds are also considered for use in livestock buildings. These are screened for having a high antagonistic effect against undesirable microorganisms while having a very low environmental impact. Honey bee products (bee venom, propolis or honey), plant essential oils and microorganism metabolites have shown antibacterial and antibiofilm activities [105–107]. A wide variety of organisms such as insects and amphibians can also secrete antimicrobial peptides with anti-biofilm activities against pathogenic bacteria [108–110]. The use of phages (viruses that infect

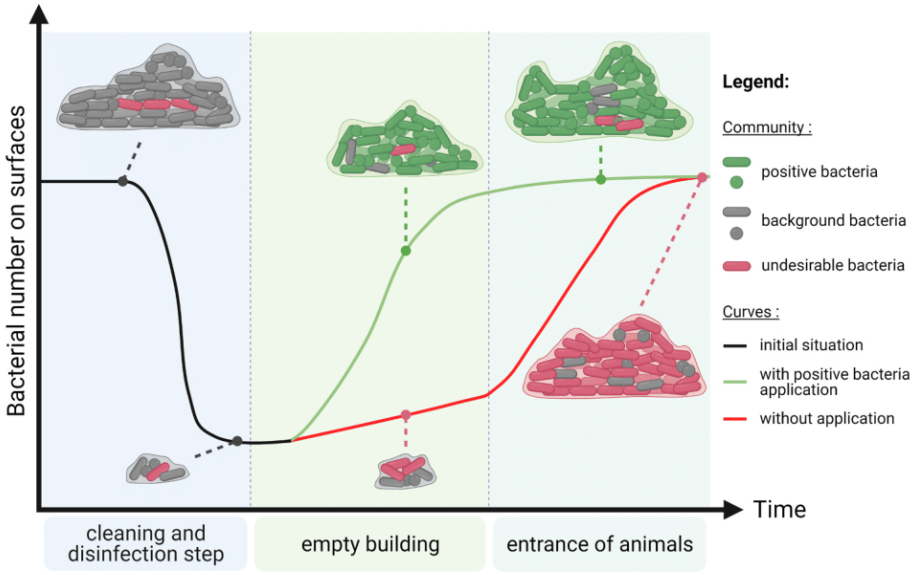

Fig. 1. Schematic representation of the concept of positive biofilms to guide the microbial ecology on the surface of livestock buildings. Biofilm communities that colonize livestock buildings are composed of background microorganisms that may contain undesirable bacteria. When animals leave the building, the microbial density on the surface is at its highest level. C&D protocols are used to reduce microbial load on surfaces (black curve). After the C&D procedures, two situations are possible: *i)* a positive biofilm is applied to the surface (green curve), *ii)* no application (red curve). In the first situation, the bacteria that are sprayed in large quantity adhere to surface to initiate a positive biofilm. This biofilm has an antagonistic effect on pathogens and prevents their proliferation. The objective is to have a mature positive biofilm before the entrance of animals in the building. In the second situation symbolized by the red curve, only the residual community that persisted after C&D is initiating a biofilm from a very low contamination level. Organic matter including feces or food projection is brought into surfaces when animals come into the livestock building. At that time, some undesirable bacteria that have survived the C&D protocols and that are competitive can proliferate with low competitive pressure. Figure created with https://biorender.com/. (For interpretation of the references to colour in this figure legend, the reader is referred to the Web version of this article.)

bacteria) to attack target pathogens is a promising solution that is already used in different sectors in some countries [111]. Phages can diffuse through the biofilm matrix [112] and are active on established biofilms [113]. They are already used in livestock buildings in poultry farms [114,115], and increasing research is being carried out to find new candidates [116]. Bacteria themselves can be used to sensitize unwanted biofilms to antimicrobial action. In a proof of concept study, Houry et al. [117] demonstrated that selected bacilli were able to swim inside exogenic biofilm matrix of pathogens such as *S. aureus*. Their infiltration generated a network of transient pores vascularizing the biofilm and increasing the efficacy of biocides. The authors also demonstrated that swimming bacilli that produce antimicrobial compounds could eradicate unwanted target biofilm [117].

None of these agents proved to be universal anti-biofilm molecules and combined approaches appear of value in limiting the emergence of resistance mechanisms [118]. Another way to use microorganisms in biosecurity applications is to guide the ecology of a surface by settling positive biofilms that will colonize and protect the surface from pathogen multiplication.

3. Positive biofilms to protect surfaces

3.1. Lessons from nature

Multispecies biofilms colonize most ecological niches. Antagonistic but also synergistic interactions can take place between species in these natural communities. A disorder of host microbial diversity (dysbiosis) can lead to the emergence of pathogens and associated diseases. This phenomenon is described with *Clostridium difficile* gastrointestinal infection which occurs essentially after antibiotic treatment alters competitive microbiota [119]. Similar situations can occur on the surface of livestock buildings after C&D protocols that leave free habitats on the surface for microbial pathogen settlement.

Many examples of natural positive biofilms illustrate competition with microbial pathogens. Indeed, selected bacteria, such as some strains of *Bacillus*, can act as plant growth-promoting rhizobacteria with the capacity to form a biofilm on the root [120–122]. In this case, bacteria can actively migrate by chemotaxis directed by root exudate. There it will form a biofilm preventing pathogen settlement by a set of complementary mechanisms of competition and interference. Similarly, some lactic acid bacteria (LAB) can naturally colonize amphibian skin and form biofilms that exclude the fungal pathogen *Batrachochytrium dendrobatidis* [123]. *Lactobacillus* spp. and *Bifidobacterium* spp. can form biofilms on the wall of honey crops with beneficial effects on beehive health through antimicrobial secretion [124]. Bacterial biofilms are also able to colonize coastal reefs and attract or repulse opportunistic algae [125]. These few examples of complex synergic and antagonist interactions inside a microbial community and its associated hosts are the subject of numerous mechanistic studies designed to decipher the mode of action of these positive biofilms against undesirable microorganisms.

3.2. Practical use of positive biofilms

3.2.1. Positive biofilms are already used in many sectors

Natural properties of positive biofilms have been used for centuries for many applications, particularly in fermented food production [126–129]. Biopreservation of food can use positive microorganisms, fermentation processes, metabolites or purified molecules to preserve food against pathogens. For example, *Lactococcus piscium*, a bacterium isolated from rainbow trout, has shown anti-*Listeria monocytogenes* activity in diverse foods [130]. Several products are commercialized as biocontrol agents for plants [131,132]. Bacteria from the rhizosphere used as biocontrol agents in plant culture have shown the capability to combat pathogens [133]. *Pseudomonas* spp. has shown anti-*Phytophthora infestans* activity in a potato model [134]. With the same principle, *Bacillus velezensis* QST713 can form biofilm on *Agaricus bisporus* compost excluding the green mold pathogen *Trichoderma aggressivum* [135,136]. Using microbial solutions to maintain the microbiological quality of inert surfaces is also envisioned in specific sectors. Some *Bacillus* spp. strains used as cleaning products on hard surfaces in hospitals can reduce by 50–89% healthcare-associated infections in comparison with conventional cleaning protocols [137]. The application of positive bacteria on building surfaces is an innovative solution already used in several sectors to control the establishment of microbial pathogens and limit the spread of AMR while reducing the use of toxic chemicals [138, 139].

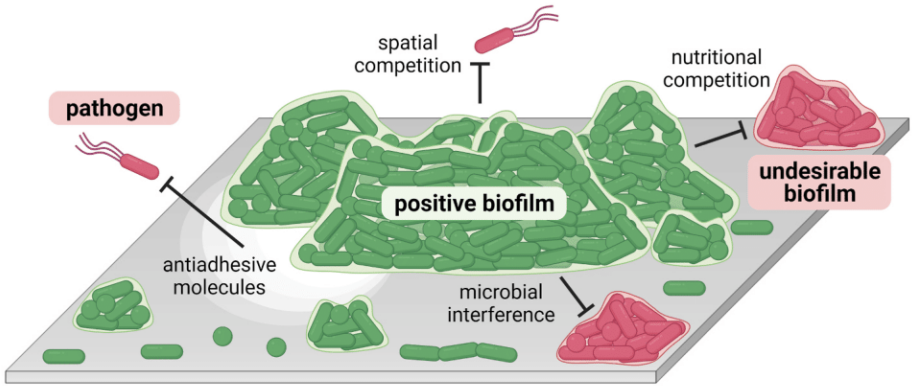

Fig. 2. Schematic representation of the mechanisms triggering exclusion of undesirable microorganisms by the settlement of positive biofilms. A positive biofilm can reduce the implantation of undesirable bacteria by several complementary mechanisms. *i)* An antiadhesive effect: the presence of the positive biofilm itself, or surface-active molecules it produces, can limit the initial adhesion of free planktonic pathogens on the surface. *ii)* A spatial and nutritional competition; by occupying the space and consuming available nutritional resources, the positive biofilm can limit the proliferation of pathogens recruited on the surface. *iii)* Microbial interference: through the secretion of specific effectors such as organic acids or antagonistic molecules, positive biofilm can reduce the presence of undesirable microorganisms on the surface. Figure created with https://biorender.com/.

3.2.2. *The case of positive biofilms in livestock buildings*

Selected bacteria can be applied to building surfaces to guide the microbial ecology of biofilm after cleaning and disinfection procedures. As described previously, biosecurity is crucial for livestock production. Current C&D protocols have shown their limits due to the development of negative biofilms on surfaces *e.g.* biofilm with microbial pathogens. These biofilms can persist between two production batches despite the application of biosecurity measures [3,60,61]. After C&D protocols and before the entry of animals, positive bacteria can be sprayed on the building surface and material to colonize the "empty" biotope and help to prevent the settlement of undesirable microorganisms. This concept is illustrated in Fig. 1.

This concept has already turned into practical products and applications. The products currently available on the market are composed of selected bacteria and form a biofilm on the surface of livestock buildings after application of the required C&D protocols. These positive biofilms limit the proliferation of undesirable microorganisms in the buildings through nutritional and spatial competition. Most products are composed of LAB, such as Lactococcus spp, Lactobacillus spp. or Pediococcus spp., often in combination with Bacillus spp. [140]. Large-scale evaluation of those products in field is still sparce due to experimental limitations in livestock buildings, and demonstrations toward pathogens are still mainly performed at lab scale [141].

3.3. *How does it work?*

Several mechanisms of exclusion of undesirable microorganisms by positive biofilms can be invoked. They are detailed in Fig. 2 and in the next sections.

3.3.1. *Competition for substrate*

Within a microbial community, bacteria with competitive advantages to access and consume nutrients essential for their growth will be favored. Nutrients essential for pathogen growth can be consumed by the bacteria within the positive biofilm and thus prevent pathogen proliferation, a phenomenon called the *Jamson effect* [142]. Enzymes can be secreted to metabolize specific substrates in the environment and other secreted proteins can bind to the product before being recognized by the bacteria for transport into the cell [143,144]. Cheating bacteria that can produce cellular receptors homologous to other enzyme-producer bacteria to incorporate specific substrates through proteins will then have an advantage [145]. Substrate availability with coevolution of different species exerts selection pressure to find the most economical way to use substrates in the environment. Interactions like cooperation, competition, or cheating drive the diversity profile of bacteria in the natural environment, which is modified by the availability of the substrate [144].

3.3.2. *Spatial competition*

Motility gives bacteria the capacity to find a favorable place to settle and multiply [146]. The ability to sense food gradients and orientate the cell movement along this gradient is a phenomenon called chemotaxis. It uses two-component systems that detect a molecule by specific chemoreceptors on the membrane allowing the cell to move in the right direction. For planktonic cells, swimming using flagella is the most widespread process of movement. Surface-associated bacteria can migrate through several mechanisms and use flagella to migrate in groups in a highly regulated process named swarming. Secretion of biosurfactants like cyclic lipopeptides can help bacteria to migrate on the surface by reducing the surface tension [147–149], preventing also the adhesion of other species. The most studied molecule is surfactin which can be secreted by *Bacillus* spp. and has been described in a biocontrol effect on plants [150,151]. Another example is *Lysinibacillus fusiformis* S9 which produces a biosurfactant that inhibits biofilm formation and adhesion of other bacteria without any bactericidal activity [152]. Bacteria can also "twitch" on surfaces by anchoring and retraction of dedicated pili [153,154] or colonized surfaces only by cell division [155].

Two-dimensional spatial competition on a surface is transformed into three-dimensional nutritional competition within biofilms; nutrients are consumed faster than they can diffuse through the biofilm matrix, thus generating sharp nutrient gradients [156,157]. These gradients, which influence the competition in biofilms, are influenced by their three-dimensional structures [158]. Flagella and pili participate in the adhesion step inherent in biofilm formation, as well as in biofilm structuration. For example, it has been reported that *Lactococcus lactis* has pili implicated in the structuring of the biofilm [159]. The apparent volume of the cell with a polysaccharide capsule is an advantage in space competition because it allows the bacteria to occupy a larger volume and increase cell fitness and this is implicated in biofilm formation [160]. For the same number of bacteria of the same size, those that will produce a capsule will take up more space and will therefore have access to more nutrients. Bacteria that are able to grow faster will have an advantage in the mixed biofilm because they will colonize surfaces faster, preventing other community members from accessing nutrients [155].

3.3.3. *Interspecies interference*

Interference includes all negative specific interactions other than those of bacterial cells of a given strain with themselves [161,162]. One of the best-known examples of microbial interference is the secretion of antimicrobials by bacteria [163,164]. *Bacillus* strains used as plant biocontrol agents typically contain between 5 and 8% of their total genome dedicated to the biosynthesis of antimicrobials [165]. LAB frequently used in the food industry produce a wide variety of antimicrobials such as bacteriocins [166] or organic acid preventing in particular fungal food spoilage [167]. Similarly, some LAB can inhibit

biofilm formation of food-borne pathogens on abiotic surfaces by secretion of bacteriocins or hydrogen peroxide [168–170]. Some of these mechanisms require physical contact between the two cells as shown for a bacteriocin of *Lactococcus piscium* inhibiting *Listeria monocytogenes* [171,172]. *Lactococcus lactis* used in cheesemaking can secrete nisin with strong anti-*Listeria monocytogenes* activity in milk [173].

All bacteria have a growth/no-growth interface in relation to environmental physicochemical parameters (temperatures, pH and a_w (water activity)). LAB can secrete organic acid such as lactic acid that lowers the pH value of their microenvironment thus limiting the growth of pathogens [174,175]. pH fluctuation can be modulated by gradients in biofilms or EPS secretion [176]. The activity of organic acids involves the pH, but also the effects of undissociated acids. For example, for a given pH, the growth of *S. aureus* is more affected if the acidification of the medium is due to the addition of lactic acid rather than HCl [177].

Another example of interspecies interference involves intercellular communication systems. Most virulence factors of *Staphylococcus aureus* are under the control of the *agr quorum sensing* system. *Staphylococcus simulans,* a commensal coagulase-negative *Staphylococcus*, can secrete a peptide that interferes with the *agr* system of *S. aureus* [178]. Similarly *Bacillus licheniformis* DAHB1 shows biofilm-inhibitory activity against the shrimp pathogen *Vibrio parahaemolyticus* by this mechanism [179], as described in several interspecies mechanisms [180,181].

All these competition phenomena can be involved in pathogen exclusion by positive biofilms on the surfaces of livestock buildings.

4. Bottlenecks and trends for positive biofilms in livestock

4.1. Regulatory positions on positive biofilms

As microbial-based products used in animal surroundings can be in contact with the animals, it is appropriate in Europe to refer to the General Food Law (*i.e.* Regulation (EC) No 178/2002, as amended) as regards to the safety of those products. The Classification, Labelling, Packaging (CLP) regulation, the directive on safety of microorganisms as well as other elements such as those of the QSP (Qualified Presumption of Safety) list of the EFSA (European Food Safety Authority) guidance or the GRAS (generally recognized as safe) criteria of the FDA (U.S. Food and Drug Administration (*i.e.* qualified presumption of safety list) on the characterization of microorganisms used as feed additives or as production organisms may also be taken into consideration [182]. Today, C&D in livestock buildings mainly involves chemical products based on detergents and disinfectants. The Biocidal Product Regulation (BPR) (*i.e.* Regulation (EC) no. 528/212) establishes the legal framework for placing on the market new C&D molecules. The chemically oriented requirements of the BPR are, however, not adapted to microbial solutions such as positive biofilms.

4.2. Point of vigilance with the use of positive biofilm

The development of positive biofilm in livestock buildings has some limitations and points of vigilance to consider. The biosafety of the strains used as positive agents must be documented and must comply with national and international regulations (*e.g.* on the list of authorized strains, without AMR genes). Despite biosecurity efforts, bioprotective products can be spread outside the farm environment by water, insects, wind, manure, or humans, making it important to evaluate their safety with standards similar to those for food use. For example, the use of the biocontrol agent *B. thuringiensis*, which has been used for many years in the field, has recently raised questions in the scientific community on their possible involvement in human foodborne infections [183]. In addition, in some conditions, biofilms can protect microbial pathogens from C&D. It has been shown for example that the strain *Bacillus subtilis* NDmed isolated in an endoscope washer disinfector was able to protect *S. aureus* from biocide action in a mixed community [184]. A recent bioinformatics study highlighted the presence of acquired and potentially mobile AMR genes in commercial probiotic strains [185]. The demonstration of intrinsic versus acquired resistance is a complex topic with regulatory agencies around the world having different requirements [185–187]. The identification and monitoring of these genetic elements and the AMR genes are to be considered during the development of the products.

4.3. Rational selection of strains able to form positive biofilms

Environmental conditions on surface livestock buildings are far different from synthetic biofilms grown in laboratories. These synthetic ecosystems are of prime importance to simplify, control and model microbial interactions [188], but on-site field analyses are also required to identify and validate rational screening criteria for strain selection. Data describing natural biofilm structures and composition in livestock buildings are very scarce, due to the lack of adapted tools. Sampling methodology such as scrubbing, rinsing, sonication, scraping and grinding destroys the 3D structure of the biofilm, but is very dependent on the experimenter and leads to only limited community recovery [189]. *In-situ* sampling methodologies on coupons are emerging strategies to capture the whole community with preserved spatial organization [190]. Diversity studies using metabarcoding, metagenomics or other molecular methods such as PCR or qPCR are also interesting to pinpoint community members associated with pathogen prevalence [191–194]. Dynamic models of interaction networks such as the generalized Lotka-Volterra model can be used in an experiment of community dynamics to identify the species involved in a coexistence or species exclusion effect [195]. For example, it has been shown using the Lotka-Volterra model that the resistance of pathogen infection of *Clostridium difficile* was associated with *Clostridium scindens*, a bile acid 7-dehydroxylating intestinal bacterium [196]. One application of these models is to understand the relationship between surface-attached microbial communities and animal disease by studying the microbial communities of healthy livestock buildings and comparing them with buildings where pathogenic bacteria are reported to be present. If there are differences between the two, a selection of positive bacteria from "healthy" livestock buildings identified by the model as barrier effect bacteria against pathogens can be used to guide the microbial ecology in other buildings.

One important criterion for selecting candidate strains for use in positive biofilms is their fitness in the farm environment. Bacterial strain selection is mainly done using laboratory conditions, which is optimal for growth. The physico-chemical and biological parameters of the farm environment, such as temperature, humidity, pH, composition of the culture medium, indigenous microbiota and material, must be taken into consideration to develop a more rational and field-like model [197].

Most current commercial products are mixtures of LAB and *Bacillus* spp., but there are few scientific studies demonstrating synergistic mechanisms between these species. *Bacillus subtilis* biofilm can protect LAB from desiccation and there is a synergy between them against *S. aureus* proliferation in laboratory models [198]. Multispecies positive biofilms can have enhanced properties in comparison to strains cultivated alone [199–201] and new methodologies are emerging to screen strains alone and in combination. High-throughput methods like kChip screening have been developed to screen around 100,000 different communities per day using droplet assay and different optical growth assays. In this case, the communities can be screened quickly for their capacity to inhibit pathogen growth [202].

The application methodology like spraying or atomizing of the agents has also to be carefully adapted to the strains and the environment of application. Nutrients can be added to the formulation to initiate the growth of the positive bacteria. Other molecules like surfactants and sugars can also help to enhance the initial adhesion or surface colonization. Recently, it has been shown that sucrose enhances root colonization by *Bacillus subtilis* by increasing surfactin secretion [203]. One other important parameter is that the selected strains must

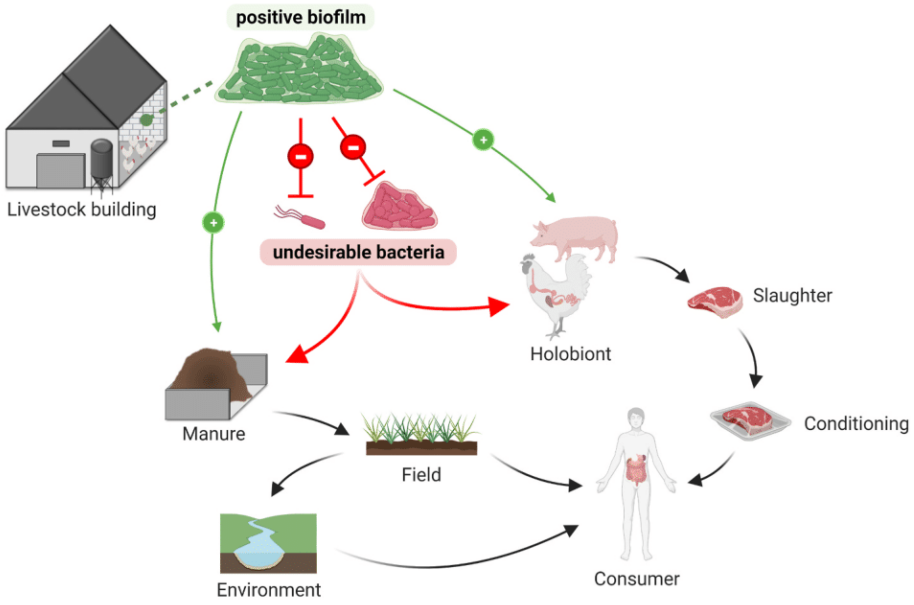

Fig. 3. Potential impact of the addition of positive biofilm in livestock buildings on the spread of undesirable bacteria from farm to fork. Positive bacteria that are applied to livestock building surfaces and that form positive biofilms have an antagonistic effect on undesirable bacteria that can be present as harmful bacteria reservoirs. By limiting the establishment of these undesirable bacteria, animal diseases are directly reduced, as is the abundance of undesirable bacteria in manure used to fertilize the soil (red arrow). Overall, positive biofilm establishment limits proliferation of undesirable bacteria at the beginning of the food chain. This leads to a reduction of spread from animals to consumers via slaughter and the conditioning steps, but also to a reduction of spread via manure to the environment and to fields that finally reach the consumer (black arrow). Finally, the positive biofilm can have a direct positive impact on the fermentation process of manure. Likewise, the positive bacteria that enter in direct contact with animals can also have a positive effect on the holobiont with, for example, a positive effect on the gut like probiotics (green arrow). Figure created with https://biorender.com/. (For interpretation of the references to colour in this figure legend, the reader is referred to the Web version of this article.)

be easy to produce on an industrial scale. For example, *Bacillus* can form spores that are less costly energetically to produce than the lyophilization process used for LAB.

4.4. Beyond excluding pathogens on livestock surfaces

Positive biofilms used in livestock buildings prevent the settlement of undesirable microorganisms on the surfaces. Microorganisms from the positive biofilm may also have side effects outside the farm, *e.g.* by reducing the spreading of pathogenic organisms and by seeding beneficial bacteria in the food chain (Fig. 3). In close contact with animals, especially in early life stages, they can modulate their microbiota and be beneficial for their health. In this regard, it has been demonstrated that a probiotic-based cleaning product applied to poultry farm litter can modify the litter's microbial diversity, but also the chicken caeca microbiota compared with an un-exposed control group [204].

Natural surface communities in livestock buildings can harbor bacteria containing genes of antibiotic resistance [205]. The application of a positive biofilm with selected strains dilutes those organisms and limits the spread of antibiotic resistance genes in the food chain.

The organic matter left at the end of a cycle in a livestock building (bedding, manure, slurry) can contain microbial pathogens and is frequently used as fertilizer in crop fields. Bacteria used in the formulation of positive biofilms can enrich the population of strains able to ferment these products (*e.g.* LAB) and prevent the development of pathogens before spreading [206,207]. Bacteria from positive biofilms such as *Bacillus* spp. have also been shown to have beneficial effects on plants by producing growth-promoting factors or by excluding pathogens from the roots [131,165,208].

5. Conclusion

Political and societal demand to reduce the use of chemical products and antibiotics in farms has triggered the development of alternative biosecurity approaches, including the use of microbial positive biofilms to protect surfaces. This biological approach has shifted from labs to farms in recent years with various commercial products now on the market in several countries. However, these promising approaches need a deeper understanding of the associated microbial interactions and their variability in different breeding contexts to be used successfully. Research is also needed to further assess their benefits from the farm to the fork, in particular by limiting the spread of undesirable bacteria in the food chain and the environment. Finally, national and international regulations should adapt to these innovative sustainable solutions to encourage research, development and their use on farms.

Declaration of competing interest

The authors declare that they have no known competing financial interests or personal relationships that could have appeared to influence the work reported in this paper.

Acknowledgments

The authors acknowledge Pascale Serror (INRAE) for stimulating discussions about livestock microbiology. This work was funded by INRAE, LALLEMAND SAS and the "Association Nationale de la Recherche et de la Technologie", France (contract 2020/0548). All figures were created with https://biorender.com/. David Marsh, professional English translator, corrected syntax and language.

References

[1] OECD, Food and Agriculture Organization of the United Nations. OECD-FAO agricultural outlook 2021-2030. OECD; 2021. https://doi.org/10.1787/19428846-en.
[2] Antunes P, Novais C, Peixe L. Food-to-Humans bacterial transmission. Microbiol Spectr 2020;8. https://doi.org/10.1128/microbiolspec.MTBP-0019-2016.
[3] Luyckx KY, Van Weyenberg S, Dewulf J, Herman L, Zoons J, Vervaet E, et al. On-farm comparisons of different cleaning protocols in broiler houses. Poultry Sci 2015;94:1986. https://doi.org/10.3382/ps/pev143. –93.
[4] Flemming H-C. The perfect slime. Colloids Surf B Biointerfaces 2011;86:251–9. https://doi.org/10.1016/j.colsurfb.2011.04.025.
[5] Flemming H-C, Wuertz S. Bacteria and archaea on Earth and their abundance in biofilms. Nat Rev Microbiol 2019;17:247–60. https://doi.org/10.1038/s41579-019-0158-9.
[6] Bridier A, Briandet R, Thomas V, Dubois-Brissonnet F. Resistance of bacterial biofilms to disinfectants: a review. Biofouling 2011;27:1017–32. https://doi.org/10.1080/08927014.2011.626899.
[7] Flemming H-C. Biofouling and me: my Stockholm syndrome with biofilms. Water Res 2020;173:115576. https://doi.org/10.1016/j.watres.2020.115576.
[8] Vishwakarma V. Impact of environmental biofilms: industrial components and its remediation. J Basic Microbiol 2020;60:198–206. https://doi.org/10.1002/jobm.201900569.
[9] Anonymous NIH. Research ON microbial biofilms. 2002. https://grants.nih.gov/grants/guide/pa-files/pa-03-047.html. [Accessed 20 December 2021].

[10] Clutterbuck AL, Woods EJ, Knottenbelt DC, Clegg PD, Cochrane CA, Percival SL. Biofilms and their relevance to veterinary medicine. Vet Microbiol 2007;121:1–17. https://doi.org/10.1016/j.vetmic.2006.12.029.

[11] Costerton JW, Stewart PS, Greenberg EP. Bacterial biofilms: a common cause of persistent infections. Science 1999;284:1318–22. https://doi.org/10.1126/science.284.5418.1318.

[12] Jacques M, Aragon V, Tremblay YDN. Biofilm formation in bacterial pathogens of veterinary importance. Anim Health Res Rev 2010;11:97–121. https://doi.org/10.1017/S1466252310000149.

[13] Abdullahi UF, Igwenagu E, Mu'azu A, Aliyu S, Umar MI. Intrigues of biofilm: a perspective in veterinary medicine. Vet World 2016;9:12–8. https://doi.org/10.14202/vetworld.2016.12-18.

[14] Larsen MH, Dalmasso M, Ingmer H, Langsrud S, Malakauskas M, Mader A, et al. Persistence of foodborne pathogens and their control in primary and secondary food production chains. Food Control 2014;44:92–109. https://doi.org/10.1016/j.foodcont.2014.03.039.

[15] Tassinari E, Duffy G, Bawn M, Burgess CM, McCabe EM, Lawlor PG, et al. Microevolution of antimicrobial resistance and biofilm formation of *Salmonella Typhimurium* during persistence on pig farms. Sci Rep 2019;9:8832. https://doi.org/10.1038/s41598-019-45216-w.

[16] Abdallah M, Benoliel C, Drider D, Dhulster P, Chihib N-E. Biofilm formation and persistence on abiotic surfaces in the context of food and medical environments. Arch Microbiol 2014;196:453–72. https://doi.org/10.1007/s00203-014-0983-1.

[17] McEwen SA, Collignon PJ. Antimicrobial resistance: a one health perspective. Microbiol Spectr 2018;6. https://doi.org/10.1128/microbiolspec.ARBA-0009-2017.

[18] Durso LM, Cook KL. One health and antibiotic resistance in agroecosystems. EcoHealth 2019;16:414–9. https://doi.org/10.1007/s10393-018-1324-7.

[19] Legein M, Smets W, Vandenheuvel D, Eilers T, Muyshondt B, Prinsen E, et al. Modes of action of microbial biocontrol in the phyllosphere. Front Microbiol 2020;11:1619. https://doi.org/10.3389/fmicb.2020.01619.

[20] Leyva Salas M, Mounier J, Valence F, Coton M, Thierry A, Coton E. Antifungal microbial agents for food biopreservation-A review. Microorganisms 2017;5:E37. https://doi.org/10.3390/microorganisms5030037.

[21] Sundh I, Melin P. Safety and regulation of yeasts used for biocontrol or biopreservation in the food or feed chain. Antonie Leeuwenhoek 2011;99:113–9. https://doi.org/10.1007/s10482-010-9528-z.

[22] Azubuike CC, Chikere CB, Okpokwasili GC. Bioremediation techniques-classification based on site of application: principles, advantages, limitations and prospects. World J Microbiol Biotechnol 2016;32:180. https://doi.org/10.1007/s11274-016-2137-x.

[23] Berry ED, Wells JE. Reducing foodborne pathogen persistence and transmission in animal production environments: challenges and opportunities. Microbiol Spectr 2016;4. https://doi.org/10.1128/microbiolspec.PFS-0006-2014.

[24] Vetter V, Denizer G, Friedland LR, Krishnan J, Shapiro M. Understanding modern-day vaccines: what you need to know. Ann Med 2018;50:110–20. https://doi.org/10.1080/07853890.2017.1407035.

[25] Messina NL, Zimmermann P, Curtis N. The impact of vaccines on heterologous adaptive immunity. Clin Microbiol Infect 2019;25:1484–93. https://doi.org/10.1016/j.cmi.2019.02.016.

[26] Marangon S, Busani L. The use of vaccination in poultry production. Rev Sci Tech 2007;26:265–74.

[27] McLeod A, Rushton J. Economics of animal vaccination. Rev Sci Tech 2007;26:313–26.

[28] Thomann B, Rushton J, Schuepbach-Regula G, Nathues H. Modeling economic effects of vaccination against porcine reproductive and respiratory syndrome: impact of vaccination effectiveness, vaccine price, and vaccination coverage. Front Vet Sci 2020;7:500. https://doi.org/10.3389/fvets.2020.00500.

[29] Gulbudak H, Martcheva M. A structured avian influenza model with imperfect vaccination and vaccine-induced asymptomatic infection. Bull Math Biol 2014;76:2389–425. https://doi.org/10.1007/s11538-014-0012-1.

[30] Lillehoj H, Liu Y, Calsamiglia S, Fernandez-Miyakawa ME, Chi F, Cravens RL, et al. Phytochemicals as antibiotic alternatives to promote growth and enhance host health. Vet Res 2018;49. https://doi.org/10.1186/s13567-018-0562-6.

[31] Van Boeckel TP, Brower C, Gilbert M, Grenfell BT, Levin SA, Robinson TP, et al. Global trends in antimicrobial use in food animals. Proc Natl Acad Sci USA 2015;112:5649–54. https://doi.org/10.1073/pnas.1503141112.

[32] Bengtsson-Palme J, Kristiansson E, Larsson DGJ. Environmental factors influencing the development and spread of antibiotic resistance. FEMS Microbiol Rev 2018;42. https://doi.org/10.1093/femsre/fux053.

[33] Blair JMA, Webber MA, Baylay AJ, Ogbolu DO, Piddock LJV. Molecular mechanisms of antibiotic resistance. Nat Rev Microbiol 2015;13:42–51. https://doi.org/10.1038/nrmicro3380.

[34] Who. Global action plan on antimicrobial resistance. 2015. https://www.who.int/publications/i/item/9789241509763.

[35] Sarmah AK, Meyer MT, Boxall ABA. A global perspective on the use, sales, exposure pathways, occurrence, fate and effects of veterinary antibiotics (VAs) in the environment. Chemosphere 2006;65:725–59. https://doi.org/10.1016/j.chemosphere.2006.03.026.

[36] Vieno NM, Härkki H, Tuhkanen T, Kronberg L. Occurrence of pharmaceuticals in river water and their elimination in a pilot-scale drinking water treatment plant. Environ Sci Technol 2007;41:5077–84. https://doi.org/10.1021/es062720x.

[37] Bridier A, Le Grandois P, Moreau M-H, Prénom C, Le Roux A, Feurer C, et al. Impact of cleaning and disinfection procedures on microbial ecology and *Salmonella* antimicrobial resistance in a pig slaughterhouse. Sci Rep 2019;9. https://doi.org/10.1038/s41598-019-49464-8.

[38] Vestergaard M, Frees D, Ingmer H. Antibiotic resistance and the MRSA problem. Microbiol Spectr 2019;7. https://doi.org/10.1128/microbiolspec.GPP3-0057-2018.

[39] Bacci C, Barilli E, Frascolla V, Rega M, Torreggiani C, Vismarra A. Antibiotic treatment administered to pigs and antibiotic resistance of *Escherichia coli* isolated from their feces and carcasses. Microb Drug Resist 2020. https://doi.org/10.1089/mdr.2019.0247.

[40] O'Neill J. Tackling drug-resistant infections globally: final report and recommendations. Government of the United Kingdom; 2016. https://amr-review.org/sites/default/files/160518_Final%20paper_with%20cover.pdf.

[41] Syngai GG, Gopi R, Bharali R, Dey S, Lakshmanan GMA, Ahmed G. Probiotics - the versatile functional food ingredients. J Food Sci Technol 2016;53:921–33. https://doi.org/10.1007/s13197-015-2011-0.

[42] Hill C, Guarner F, Reid G, Gibson GR, Merenstein DJ, Pot B, et al. Expert consensus document. The International Scientific Association for Probiotics and Prebiotics consensus statement on the scope and appropriate use of the term probiotic. Nat Rev Gastroenterol Hepatol 2014;11:506–14. https://doi.org/10.1038/nrgastro.2014.66.

[43] Gadde U, Kim WH, Oh ST, Lillehoj HS. Alternatives to antibiotics for maximizing growth performance and feed efficiency in poultry: a review. Anim Health Res Rev 2017;18:26–45. https://doi.org/10.1017/S1466252316000207.

[44] Markowiak P, Śliżewska K. The role of probiotics, prebiotics and synbiotics in animal nutrition. Gut Pathog 2018;10:21. https://doi.org/10.1186/s13099-018-0250-0.

[45] Sokol H, Pigneur B, Watterlot L, Lakhdari O, Bermúdez-Humarán LG, Gratadoux J-J, et al. *Faecalibacterium prausnitzii* is an anti-inflammatory commensal bacterium identified by gut microbiota analysis of Crohn disease patients. Proc Natl Acad Sci U S A 2008;105:16731–6. https://doi.org/10.1073/pnas.0804812105.

[46] Miquel S, Martín R, Rossi O, Bermúdez-Humarán LG, Chatel JM, Sokol H, et al. *Faecalibacterium prausnitzii* and human intestinal health. Curr Opin Microbiol 2013;16:255–61. https://doi.org/10.1016/j.mib.2013.06.003.

[47] Goldenberg JZ, Yap C, Lytvyn L, Lo CK-F, Beardsley J, Mertz D, et al. Probiotics for the prevention of *Clostridium difficile*-associated diarrhea in adults and children. Cochrane Database Syst Rev 2017;12:CD006095. https://doi.org/10.1002/14651858.CD006095.pub4.

[48] Chamignon C, Guéneau V, Medina S, Deschamps J, Gil-Izquierdo A, Briandet R, et al. Evaluation of the probiotic properties and the capacity to form biofilms of various *Lactobacillus* strains. Microorganisms 2020;8:E1053. https://doi.org/10.3390/microorganisms8071053.

[49] Cheow WS, Hadinoto K. Biofilm-like *Lactobacillus rhamnosus* probiotics encapsulated in alginate and carrageenan microcapsules exhibiting enhanced thermotolerance and freeze-drying resistance. Biomacromolecules 2013;14:3214–22. https://doi.org/10.1021/bm400853d.

[50] Cheow WS, Kiew TY, Hadinoto K. Controlled release of *Lactobacillus rhamnosus* biofilm probiotics from alginate-locust bean gum microcapsules. Carbohydr Polym 2014;103:587–95. https://doi.org/10.1016/j.carbpol.2014.01.036.

[51] Bordenstein SR, Theis KR. Host biology in light of the microbiome: ten principles of holobionts and hologenomes. PLoS Biol 2015;13:e1002226. https://doi.org/10.1371/journal.pbio.1002226.

[52] Chen X, Xu J, Ren E, Su Y, Zhu W. Co-occurrence of early gut colonization in neonatal piglets with microbiota in the maternal and surrounding delivery environments. Anaerobe 2018;49:30–40. https://doi.org/10.1016/j.anaerobe.2017.12.002.

[53] FAO. The biosecurity approach: a review and evaluation of its application by FAO, internationally and in various countries. Rome, Italy: FAO; 2016. https://www.fao.org/3/ca9040en/CA9040EN.pdf.

[54] Zurek L, Ghosh A. Insects represent a link between food animal farms and the urban environment for antibiotic resistance traits. Appl Environ Microbiol 2014;80:3562–7. https://doi.org/10.1128/AEM.00600-14.

[55] Donoso A, Paredes N, Retamal P. Detection of antimicrobial resistant *Salmonella enterica* strains in larval and adult forms of lesser mealworm (*Alphitobius diaperinus*) from industrial poultry farms. Front Vet Sci 2020;7:577848. https://doi.org/10.3389/fvets.2020.577848.

[56] Cervelin V, Fongaro G, Pastore JB, Engel F, Reimers MA, Viancelli A. Enterobacteria associated with houseflies (*Musca domestica*) as an infection risk indicator in swine production farms. Acta Trop 2018;185:13–7. https://doi.org/10.1016/j.actatropica.2018.04.024.

[57] Castells M, Schild C, Caffarena D, Bok M, Giannitti F, Armendano J, et al. Prevalence and viability of group A rotavirus in dairy farm water sources. J Appl Microbiol 2018;124:922–9. https://doi.org/10.1111/jam.13691.

[58] Ximenes E, Hoagland L, Ku S, Li X, Ladisch M. Human pathogens in plant biofilms: formation, physiology, and detection. Biotechnol Bioeng 2017;114:1403–18. https://doi.org/10.1002/bit.26247.

[59] Schierstaedt J, Grosch R, Schikora A. Agricultural production systems can serve as reservoir for human pathogens. FEMS Microbiol Lett 2019;366. https://doi.org/10.1093/femsle/fnaa016.

[60] Mannion C, Leonard FC, Lynch PB, Egan J. Efficacy of cleaning and disinfection on pig farms in Ireland. Vet Rec 2007;161:371–5. https://doi.org/10.1136/vr.161.11.371.

[61] Misra S, van Middelaar CE, Jordan K, Upton J, Quinn AJ, de Boer IJM, et al. Effect of different cleaning procedures on water use and bacterial levels in weaner pig pens. PLoS One 2020;15:e0242495. https://doi.org/10.1371/journal.pone.0242495.

[62] Marin C, Hernandiz A, Lainez M. Biofilm development capacity of *Salmonella* strains isolated in poultry risk factors and their resistance against disinfectants. Poultry Sci 2009;88:424–31. https://doi.org/10.3382/ps.2008-00241.

[63] Wales A, Breslin M, Davies R. Assessment of cleaning and disinfection in *Salmonella*-contaminated poultry layer houses using qualitative and semi-quantitative culture techniques. Vet Microbiol 2006;116:283–93. https://doi.org/10.1016/j.vetmic.2006.04.026.

[64] Martelli F, Gosling RJ, Callaby R, Davies R. Observations on *Salmonella* contamination of commercial duck farms before and after cleaning and disinfection. Avian Pathol 2017;46:131–7. https://doi.org/10.1080/03079457.2016.1223835.

[65] Marin C, Balasch S, Vega S, Lainez M. Sources of *Salmonella* contamination during broiler production in Eastern Spain. Prev Vet Med 2011;98:39–45. https://doi.org/10.1016/j.prevetmed.2010.09.006.

[66] Peyrat MB, Soumet C, Maris P, Sanders P. Recovery of *Campylobacter jejuni* from surfaces of poultry slaughterhouses after cleaning and disinfection procedures: analysis of a potential source of carcass contamination. Int J Food Microbiol 2008;124:188–94. https://doi.org/10.1016/j.ijfoodmicro.2008.03.030.

[67] European Food Safety Authority, European Centre for Disease Prevention and Control. The European union one health 2019 zoonoses report. EFSA J 2021;19:e06406. https://doi.org/10.2903/j.efsa.2021.6406.

[68] García-Sánchez L, Melero B, Jaime I, Rossi M, Ortega I, Rovira J. Biofilm formation, virulence and antimicrobial resistance of different *Campylobacter jejuni* isolates from a poultry slaughterhouse. Food Microbiol 2019;83:193–9. https://doi.org/10.1016/j.fm.2019.05.016.

[69] Bronnec V, Turoňová H, Bouju A, Cruveiller S, Rodrigues R, Demnerova K, et al. Adhesion, biofilm formation, and genomic features of *Campylobacter jejuni* bf, an atypical strain able to grow under aerobic conditions. Front Microbiol 2016;7:1002. https://doi.org/10.3389/fmicb.2016.01002.

[70] Šimunović K, Zajkoska S, Bezek K, Klančnik A, Barlič Maganja D, Smole Možina S. Comparison of *Campylobacter jejuni* slaughterhouse and surface-water isolates indicates better adaptation of slaughterhouse isolates to the chicken host environment. Microorganisms 2020;8:E1693. https://doi.org/10.3390/microorganisms8111693.

[71] Chylkova T, Cadena M, Ferreiro A, Pitesky M. Susceptibility of *Salmonella* biofilm and planktonic bacteria to common disinfectant agents used in poultry processing. J Food Protect 2017;80:1072–9. https://doi.org/10.4315/0362-028X.JFP-16-393.

[72] Silva PLAPA, Goulart LR, Reis TFM, Mendonça EP, Melo RT, Penha VAS, et al. biofilm formation in different *Salmonella* serotypes isolated from poultry. Curr Microbiol 2019;76:124–9. https://doi.org/10.1007/s00284-018-1599-5.

[73] Ćwiek K, Korzekwa K, Tabiś A, Bania J, Bugla-Płoskońska G, Wieliczko A. Antimicrobial resistance and biofilm formation capacity of *Salmonella enterica* serovar *enteritidis* strains isolated from poultry and humans in Poland. Pathogens 2020;9:E643. https://doi.org/10.3390/pathogens9080643.

[74] Vestby LK, Møretrø T, Langsrud S, Heir E, Nesse LL. Biofilm forming abilities of *Salmonella* are correlated with persistence in fish meal- and feed factories. BMC Vet Res 2009;5:20. https://doi.org/10.1186/1746-6148-5-20.

[75] Rodrigues SV, Laviniki V, Borges KA, Furian TQ, Moraes HLS, Nascimento VP, et al. biofilm formation by avian pathogenic *Escherichia coli* is not related to in vivo pathogenicity. Curr Microbiol 2019;76:194–9. https://doi.org/10.1007/s00284-018-1608-8.

[76] Hinnebusch BJ, Jarrett CO, Bland DM. Molecular and genetic mechanisms that mediate transmission of *Yersinia pestis* by fleas. Biomolecules 2021;11:210. https://doi.org/10.3390/biom11020210.

[77] Di Marco NI, Pungitore CR, Lucero-Estrada CSM. Aporphinoid alkaloids inhibit biofilm formation of *Yersinia enterocolitica* isolated from sausages. J Appl Microbiol 2020;129:1029–42. https://doi.org/10.1111/jam.14664.

[78] Dzieciol M, Schornsteiner E, Muhterem-Uyar M, Stessl B, Wagner M, Schmitz-Esser S. Bacterial diversity of floor drain biofilms and drain waters in a *Listeria monocytogenes* contaminated food processing environment. Int J Food Microbiol 2016;223:33–40. https://doi.org/10.1016/j.ijfoodmicro.2016.02.004.

[79] Alonso-Calleja C, Gómez-Fernández S, Carballo J, Capita R. Prevalence, molecular typing, and determination of the biofilm-forming ability of *Listeria monocytogenes* serotypes from poultry meat and poultry preparations in Spain. Microorganisms 2019;7:E529. https://doi.org/10.3390/microorganisms7110529.

[80] Di Bonaventura G, Piccolomini R, Paludi D, D'Orio V, Vergara A, Conter M, et al. Influence of temperature on biofilm formation by *Listeria monocytogenes* on various food-contact surfaces: relationship with motility and cell surface hydrophobicity. J Appl Microbiol 2008;104:1552–61. https://doi.org/10.1111/j.1365-2672.2007.03688.x.

[81] Mazaheri T, Cervantes-Huamán BRH, Bermúdez-Capdevila M, Ripolles-Avila C, Rodríguez-Jerez JJ. *Listeria monocytogenes* biofilms in the food industry: is the current hygiene program sufficient to combat the persistence of the pathogen? Microorganisms 2021;9:181. https://doi.org/10.3390/microorganisms9010181.

[82] Sereno MJ, Viana C, Pegoraro K, da Silva DAL, Yamatogi RS, Nero LA, et al. Distribution, adhesion, virulence and antibiotic resistance of persistent *Listeria monocytogenes* in a pig slaughterhouse in Brazil. Food Microbiol 2019;84:103234. https://doi.org/10.1016/j.fm.2019.05.018.

[83] Grunert T, Stessl B, Wolf F, Sordelli DO, Buzzola FR, Ehling-Schulz M. Distinct phenotypic traits of *Staphylococcus aureus* are associated with persistent, contagious bovine intramammary infections. Sci Rep 2018;8:15968. https://doi.org/10.1038/s41598-018-34371-1.

[84] Zischka M, Künne CT, Blom J, Wobser D, Sakinc T, Schmidt-Hohagen K, et al. Comprehensive molecular, genomic and phenotypic analysis of a major clone of *Enterococcus faecalis* MLST ST40. BMC Genom 2015;16:175. https://doi.org/10.1186/s12864-015-1367-x.

[85] Raymond BBA, Jenkins C, Turnbull L, Whitchurch CB, Djordjevic SP. Extracellular DNA release from the genome-reduced pathogen *Mycoplasma hyopneumoniae* is essential for biofilm formation on abiotic surfaces. Sci Rep 2018;8:10373. https://doi.org/10.1038/s41598-018-28678-2.

[86] Maes S, Vackier T, Nguyen Huu S, Heyndrickx M, Steenackers H, Sampers I, et al. Occurrence and characterisation of biofilms in drinking water systems of broiler houses. BMC Microbiol 2019;19:77. https://doi.org/10.1186/s12866-019-1451-5.

[87] Lepp D, Zhou Y, Ojha S, Mehdizadeh Gohari I, Carere J, Yang C, et al. *Clostridium perfringens* produces an adhesive pilus required for the pathogenesis of necrotic enteritis in poultry. J Bacteriol 2021;203:e00578. https://doi.org/10.1128/JB.00578-20. 20.

[88] Charlebois A, Parent E, Létourneau-Montminy M-P, Boulianne M. Persistence of a *Clostridium perfringens* strain in a broiler chicken farm over a three-year period. Avian Dis 2020;64:415–20. https://doi.org/10.1637/aviandiseases-D-19-00112.

[89] Turni C, Singh R, Blackall PJ. Genotypic diversity of *Pasteurella multocida* isolates from pigs and poultry in Australia. Aust Vet J 2018;96:390–4. https://doi.org/10.1111/avj.12748.

[90] Wang Y, Wang Y, Sun L, Grenier D, Yi L. *Streptococcus suis* biofilm: regulation, drug-resistance mechanisms, and disinfection strategies. Appl Microbiol Biotechnol 2018;102:9121–9. https://doi.org/10.1007/s00253-018-9356-z.

[91] Waack U, Nicholson TL. Subinhibitory concentrations of amoxicillin, lincomycin, and oxytetracycline commonly used to treat swine increase *Streptococcus suis* biofilm formation. Front Microbiol 2018;9:2707. https://doi.org/10.3389/fmicb.2018.02707.

[92] Chakraborty P, Bajeli S, Kaushal D, Radotra BD, Kumar A. Biofilm formation in the lung contributes to virulence and drug tolerance of *Mycobacterium tuberculosis*. Nat Commun 2021;12:1606. https://doi.org/10.1038/s41467-021-21748-6.

[93] Ojha AK, Baughn AD, Sambandan D, Hsu T, Trivelli X, Guerardel Y, et al. Growth of *Mycobacterium tuberculosis* biofilms containing free mycolic acids and harbouring drug-tolerant bacteria. Mol Microbiol 2008;69:164–74. https://doi.org/10.1111/j.1365-2958.2008.06274.x.

[94] Srinivasan R, Santhakumari S, Ravi AV. In vitro antibiofilm efficacy of Piper betle against quorum sensing mediated biofilm formation of luminescent *Vibrio harveyi*. Microb Pathog 2017;110:232–9. https://doi.org/10.1016/j.micpath.2017.07.001.

[95] Soonthornchai W, Chaiyapechara S, Jarayabhand P, Söderhäll K, Jiravanichpaisal P. Interaction of *Vibrio* spp. with the inner surface of the digestive tract of *Penaeus monodon*. PLoS One 2015;10:e0135783. https://doi.org/10.1371/journal.pone.0135783.

[96] Kramer B, Wunderlich J, Muranyi P. Recent findings in pulsed light disinfection. J Appl Microbiol 2017;122:830–56. https://doi.org/10.1111/jam.13389.

[97] Delhalle L, Taminiau B, Fastrez S, Fall A, Ballesteros M, Burteau S, et al. Evaluation of enzymatic cleaning on food processing installations and food products bacterial microflora. Front Microbiol 2020;11:1827. https://doi.org/10.3389/fmicb.2020.01827.

[98] Jabbouri S, Sadovskaya I. Characteristics of the biofilm matrix and its role as a possible target for the detection and eradication of *Staphylococcus epidermidis* associated with medical implant infections. FEMS Immunol Med Microbiol 2010;59:280–91. https://doi.org/10.1111/j.1574-695X.2010.00695.x.

[99] Orgaz B, Neufeld RJ, SanJose C. Single-step biofilm removal with delayed release encapsulated Pronase mixed with soluble enzymes. Enzym Microb Technol 2007;40:1045–51. https://doi.org/10.1016/j.enzmictec.2006.08.003.

[100] Hassan YI, Lahaye L, Gong MM, Peng J, Gong J, Liu S, et al. Innovative drugs, chemicals, and enzymes within the animal production chain. Vet Res 2018;49:71. https://doi.org/10.1186/s13567-018-0559-1.

[101] Ni N, Li M, Wang J, Wang B. Inhibitors and antagonists of bacterial quorum sensing. Med Res Rev 2009;29:65–124. https://doi.org/10.1002/med.20145.

[102] Sintim HO, Smith JAI, Wang J, Nakayama S, Yan L. Paradigm shift in discovering next-generation anti-infective agents: targeting quorum sensing, c-di-GMP signaling and biofilm formation in bacteria with small molecules. Future Med Chem 2010;2:1005–35. https://doi.org/10.4155/fmc.10.185.

[103] Römling U, Amikam D. Cyclic di-GMP as a second messenger. Curr Opin Microbiol 2006;9:218–28. https://doi.org/10.1016/j.mib.2006.02.010.

[104] Caly DL, Bellini D, Walsh MA, Dow JM, Ryan RP. Targeting cyclic di-GMP signalling: a strategy to control biofilm formation? Curr Pharmaceut Des 2015;21:12–24. https://doi.org/10.2174/1381612820666140905124701.

[105] Ratajczak M, Kaminska D, Matuszewska E, Hołderna-Kedzia E, Rogacki J, Matysiak J. Promising antimicrobial properties of bioactive compounds from different honeybee products. Molecules 2021;26:4007. https://doi.org/10.3390/molecules26134007.

[106] Karpiński TM, Ożarowski M, Seremak-Mrozikiewicz A, Wolski H, Adamczak A. Plant preparations and compounds with activities against biofilms formed by *Candida* spp. J Fungi (Basel) 2021;7:360. https://doi.org/10.3390/jof7050360.

[107] Pusparajah P, Letchumanan V, Law JW-F, Ab Mutalib N-S, Ong YS, Goh B-H, et al. *Streptomyces* sp.-A treasure trove of weapons to combat methicillin-resistant *Staphylococcus aureus* biofilm associated with biomedical devices. Int J Mol Sci 2021;22:9360. https://doi.org/10.3390/ijms22179360.

[108] Chung PY, Khanum R. Antimicrobial peptides as potential anti-biofilm agents against multidrug-resistant bacteria. J Microbiol Immunol Infect 2017;50:405–10. https://doi.org/10.1016/j.jmii.2016.12.005.

[109] Casciaro B, Loffredo MR, Cappiello F, Fabiano G, Torrini L, Mangoni ML. The antimicrobial peptide temporin G: anti-biofilm, anti-persister activities, and

potentiator effect of tobramycin efficacy against *Staphylococcus aureus*. Int J Mol Sci 2020;21:E9410. https://doi.org/10.3390/ijms21249410.
[110] Yi H-Y, Chowdhury M, Huang Y-D, Yu X-Q. Insect antimicrobial peptides and their applications. Appl Microbiol Biotechnol 2014;98:5807–22. https://doi.org/10.1007/s00253-014-5792-6.
[111] Salmond GPC, Fineran PC. A century of the phage: past, present and future. Nat Rev Microbiol 2015;13:777–86. https://doi.org/10.1038/nrmicro3564.
[112] Briandet R, Lacroix-Gueu P, Renault M, Lecart S, Meylheuc T, Bidnenko E, et al. Fluorescence correlation spectroscopy to study diffusion and reaction of bacteriophages inside biofilms. Appl Environ Microbiol 2008;74:2135–43. https://doi.org/10.1128/AEM.02304-07.
[113] Gutiérrez D, Rodríguez-Rubio L, Martínez B, Rodríguez A, García P. Bacteriophages as weapons against bacterial biofilms in the food industry. Front Microbiol 2016;7:825. https://doi.org/10.3389/fmicb.2016.00825.
[114] Żbikowska K, Michalczuk M, Dolka B. The use of bacteriophages in the poultry industry. Animals (Basel) 2020;10:E872. https://doi.org/10.3390/ani10050872.
[115] Clavijo V, Baquero D, Hernandez S, Farfan JC, Arias J, Arévalo A, et al. Phage cocktail SalmoFREE® reduces *Salmonella* on a commercial broiler farm. Poultry Sci 2019;98:5054–63. https://doi.org/10.3382/ps/pez251.
[116] Wang Z, Xue Y, Gao Y, Guo M, Liu Y, Zou X, et al. Phage vB_PaeS-PAJD-1 rescues murine mastitis infected with multidrug-resistant *Pseudomonas aeruginosa*. Front Cell Infect Microbiol 2021;11:689770. https://doi.org/10.3389/fcimb.2021.689770.
[117] Houry A, Gohar M, Deschamps J, Tischenko E, Aymerich S, Gruss A, et al. Bacterial swimmers that infiltrate and take over the biofilm matrix. Proc Natl Acad Sci U S A 2012;109:13088–93. https://doi.org/10.1073/pnas.1200791109.
[118] Alvarez-Ordóñez A, Coughlan LM, Briandet R, Cotter PD. Biofilms in food processing environments: challenges and opportunities. Annu Rev Food Sci Technol 2019;10:173–95. https://doi.org/10.1146/annurev-food-032818-121805.
[119] Pakpour S, Bhanvadia A, Zhu R, Amarnani A, Gibbons SM, Gurry T, et al. Identifying predictive features of *Clostridium difficile* infection recurrence before, during, and after primary antibiotic treatment. Microbiome 2017;5:148. https://doi.org/10.1186/s40168-017-0368-1.
[120] Zhang N, Yang D, Wang D, Miao Y, Shao J, Zhou X, et al. Whole transcriptomic analysis of the plant-beneficial rhizobacterium *Bacillus amyloliquefaciens* SQR9 during enhanced biofilm formation regulated by maize root exudates. BMC Genom 2015;16:685. https://doi.org/10.1186/s12864-015-1825-5.
[121] Townsley L, Yannarell SM, Huynh TN, Woodward JJ, Shank EA. Cyclic di-AMP acts as an extracellular signal that impacts *Bacillus subtilis* biofilm formation and plant attachment. mBio 2018;9. https://doi.org/10.1128/mBio.00341-18.
[122] Li Q, Li Z, Li X, Xia L, Zhou X, Xu Z, et al. FtsEX-CwlO regulates biofilm formation by a plant-beneficial rhizobacterium Bacillus velezensis SQR9. Res Microbiol 2018;169:166–76. https://doi.org/10.1016/j.resmic.2018.01.004.
[123] Niederle MV, Bosch J, Ale CE, Nader-Macías ME, Aristimuño Ficoseco C, Toledo LF, et al. Skin-associated lactic acid bacteria from North American bullfrogs as potential control agents of *Batrachochytrium dendrobatidis*. PLoS One 2019;14:e0223020. https://doi.org/10.1371/journal.pone.0223020.
[124] Vásquez A, Forsgren E, Fries I, Paxton RJ, Flaberg E, Szekely L, et al. Symbionts as major modulators of insect health: lactic acid bacteria and honeybees. PLoS One 2012;7:e33188. https://doi.org/10.1371/journal.pone.0033188.
[125] Li J, Wang T, Yu S, Bai J, Qin S. Community characteristics and ecological roles of bacterial biofilms associated with various algal settlements on coastal reefs. J Environ Manag 2019;250:109459. https://doi.org/10.1016/j.jenvman.2019.109459.
[126] Mariani C, Briandet R, Chamba J-F, Notz E, Carnet-Pantiez A, Eyoug RN, et al. Biofilm ecology of wooden shelves used in ripening the French raw milk smear cheese Reblochon de Savoie. J Dairy Sci 2007;90:1653–61. https://doi.org/10.3168/jds.2006-190.
[127] Marin-Menguiano M, Romero-Sanchez S, Barrales RR, Ibeas JI. Population analysis of biofilm yeasts during fino sherry wine aging in the Montilla-Moriles D. O. region. Int J Food Microbiol 2017;244:67–73. https://doi.org/10.1016/j.ijfoodmicro.2016.12.019.
[128] Abid Y, Casillo A, Gharsallah H, Joulak I, Lanzetta R, Corsaro MM, et al. Production and structural characterization of exopolysaccharides from newly isolated probiotic lactic acid bacteria. Int J Biol Macromol 2018;108:719–28. https://doi.org/10.1016/j.ijbiomac.2017.10.155.
[129] Bourdichon F, Casaregola S, Farrokh C, Frisvad JC, Gerds ML, Hammes WP, et al. Food fermentations: microorganisms with technological beneficial use. Int J Food Microbiol 2012;154:87–97. https://doi.org/10.1016/j.ijfoodmicro.2011.12.030.
[130] Saraoui T, Leroi F, Björkroth J, Pilet MF. *Lactococcus piscium*: a psychrotrophic lactic acid bacterium with bioprotective or spoilage activity in food-a review. J Appl Microbiol 2016;121:907–18. https://doi.org/10.1111/jam.13179.
[131] Wang XQ, Zhao DL, Shen LL, Jing CL, Zhang CS. Application and mechanisms of *Bacillus subtilis* in biological control of plant disease. In: Meena VS, editor. Role of rhizospheric microbes in soil: volume 1: stress management and agricultural sustainability. Singapore: Springer; 2018. p. 225–50. https://doi.org/10.1007/978-981-10-8402-7_9.
[132] Huang T-P, Tzeng DD-S, Wong ACL, Chen C-H, Lu K-M, Lee Y-H, et al. DNA polymorphisms and biocontrol of *Bacillus* antagonistic to citrus bacterial canker with indication of the interference of phyllosphere biofilms. PLoS One 2012;7:e42124. https://doi.org/10.1371/journal.pone.0042124.
[133] Sharma R, Gal L, Garmyn D, Bisaria VS, Sharma S, Piveteau P. Evidence of biocontrol activity of bioinoculants against a human pathogen, *Listeria monocytogenes*. Front Microbiol 2020;11:350. https://doi.org/10.3389/fmicb.2020.00350.
[134] De Vrieze M, Gloor R, Massana Codina J, Torriani S, Gindro K, L'Haridon F, et al. Biocontrol activity of three *Pseudomonas* in a newly assembled collection of *Phytophthora infestans* isolates. Phytopathology 2019;109:1555–65. https://doi.org/10.1094/PHYTO-12-18-0487-R.
[135] Pandin C, Darsonval M, Mayeur C, Le Coq D, Aymerich S, Briandet R. biofilm formation and synthesis of antimicrobial compounds by the biocontrol agent *Bacillus velezensis* QST713 in an *Agaricus bisporus* compost micromodel. Appl Environ Microbiol 2019;85:e00327. https://doi.org/10.1128/AEM.00327-19. 19.
[136] Pandin C, Le Coq D, Deschamps J, Védie R, Rousseau T, Aymerich S, et al. Complete genome sequence of *Bacillus velezensis* QST713: a biocontrol agent that protects *Agaricus bisporus* crops against the green mould disease. J Biotechnol 2018;278:10–9. https://doi.org/10.1016/j.jbiotec.2018.04.014.
[137] Vandini A, Temmerman R, Frabetti A, Caselli E, Antonioli P, Balboni PG, et al. Hard surface biocontrol in hospitals using microbial-based cleaning products. PLoS One 2014;9:e108598. https://doi.org/10.1371/journal.pone.0108598.
[138] Stone W, Tolmay J, Tucker K, Wolfaardt GM. Disinfectant, soap or probiotic cleaning? Surface microbiome diversity and biofilm competitive exclusion. Microorganisms 2020;8:E1726. https://doi.org/10.3390/microorganisms8111726.
[139] D'Accolti M, Soffritti I, Bini F, Mazziga E, Mazzacane S, Caselli E. Pathogen control in the built environment: a probiotic-based system as a remedy for the spread of antibiotic resistance. Microorganisms 2022;10:225. https://doi.org/10.3390/microorganisms10020225.
[140] Merino L, Procura F, Trejo FM, Bueno DJ, Golowczyc MA. Biofilm formation by *Salmonella* sp. in the poultry industry: detection, control and eradication strategies. Food Res Int 2019;119:530–40. https://doi.org/10.1016/j.foodres.2017.11.024.
[141] Monteiro GP, Rossi DA, Valadares Jr EC, Peres P, Braz RF, Notário FO, et al. Lactic bacterium and *Bacillus* sp. Biofilms can decrease the viability of *Salmonella gallinarum, Salmonella heidelberg, Campylobacter jejuni* and methicillin resistant *Staphylococcus aureus* on different substrates. Braz J Poult Sci 2021;23. https://doi.org/10.1590/1806-9061-2020-1408.
[142] Guillier L, Stahl V, Hezard B, Notz E, Briandet R. Modelling the competitive growth between *Listeria monocytogenes* and biofilm microflora of smear cheese wooden shelves. Int J Food Microbiol 2008;128:51–7. https://doi.org/10.1016/j.ijfoodmicro.2008.06.028.
[143] Briggs JA, Grondin JM, Brumer H. Communal living: glycan utilization by the human gut microbiota. Environ Microbiol 2021;23:15–35. https://doi.org/10.1111/1462-2920.15317.
[144] Kramer J, Özkaya Ö, Kümmerli R. Bacterial siderophores in community and host interactions. Nat Rev Microbiol 2020;18:152–63. https://doi.org/10.1038/s41579-019-0284-4.
[145] Hibbing ME, Fuqua C, Parsek MR, Peterson SB. Bacterial competition: surviving and thriving in the microbial jungle. Nat Rev Microbiol 2010;8:15–25. https://doi.org/10.1038/nrmicro2259.
[146] Moens S, Vanderleyden J. Functions of bacterial flagella. Crit Rev Microbiol 1996;22:67–100. https://doi.org/10.3109/10408419609106456.
[147] Ke W-J, Hsueh Y-H, Cheng Y-C, Wu C-C, Liu S-T. Water surface tension modulates the swarming mechanics of *Bacillus subtilis*. Front Microbiol 2015;6:1017. https://doi.org/10.3389/fmicb.2015.01017.
[148] Singh AK, Dhanjal S, Cameotra SS. Surfactin restores and enhances swarming motility under heavy metal stress. Colloids Surf B Biointerfaces 2014;116:26–31. https://doi.org/10.1016/j.colsurfb.2013.12.035.
[149] Aleti G, Lehner S, Bacher M, Compant S, Nikolic B, Plesko M, et al. Surfactin variants mediate species-specific biofilm formation and root colonization in Bacillus. Environ Microbiol 2016;18:2634–45. https://doi.org/10.1111/1462-2920.13405.
[150] Sarwar A, Hassan MN, Imran M, Iqbal M, Majeed S, Brader G, et al. Biocontrol activity of surfactin A purified from Bacillus NH-100 and NH-217 against rice bakanae disease. Microbiol Res 2018;209:1–13. https://doi.org/10.1016/j.micres.2018.01.006.
[151] Sarwar A, Brader G, Corretto E, Aleti G, Ullah MA, Sessitsch A, et al. Qualitative analysis of biosurfactants from *Bacillus* species exhibiting antifungal activity. PLoS One 2018;13:e0198107. https://doi.org/10.1371/journal.pone.0198107.
[152] Pradhan AK, Pradhan N, Sukla LB, Panda PK, Mishra BK. Inhibition of pathogenic bacterial biofilm by biosurfactant produced by *Lysinibacillus fusiformis* S9. Bioproc Biosyst Eng 2014;37:139–49. https://doi.org/10.1007/s00449-013-0976-5.
[153] Oliveira NM, Foster KR, Durham WM. Single-cell twitching chemotaxis in developing biofilms. Proc Natl Acad Sci U S A 2016;113:6532–7. https://doi.org/10.1073/pnas.1600760113.
[154] Sampedro I, Parales RE, Krell T, Hill JE. *Pseudomonas* chemotaxis. FEMS Microbiol Rev 2015;39:17–46. https://doi.org/10.1111/1574-6976.12081.
[155] Habimana O, Guillier L, Kulakauskas S, Briandet R. Spatial competition with *Lactococcus lactis* in mixed-species continuous-flow biofilms inhibits *Listeria monocytogenes* growth. Biofouling 2011;27:1065–72. https://doi.org/10.1080/08927014.2011.626124.
[156] Bridier A, Piard J-C, Pandin C, Labarthe S, Dubois-Brissonnet F, Briandet R. Spatial organization plasticity as an adaptive driver of surface microbial communities. Front Microbiol 2017;8:1364. https://doi.org/10.3389/fmicb.2017.01364.
[157] Liu J, Prindle A, Humphries J, Gabalda-Sagarra M, Asally M, Lee DD, et al. Metabolic co-dependence gives rise to collective oscillations within biofilms. Nature 2015;523:550–4. https://doi.org/10.1038/nature14660.
[158] Flemming H-C, Wingender J, Szewzyk U, Steinberg P, Rice SA, Kjelleberg S. Biofilms: an emergent form of bacterial life. Nat Rev Microbiol 2016;14:563–75. https://doi.org/10.1038/nrmicro.2016.94.

[159] Oxaran V, Ledue-Clier F, Dieye Y, Herry J-M, Péchoux C, Meylheuc T, et al. Pilus biogenesis in *Lactococcus lactis*: molecular characterization and role in aggregation and biofilm formation. PLoS One 2012;7:e50989. https://doi.org/10.1371/journal.pone.0050989.
[160] Limoli DH, Jones CJ, Wozniak DJ. Bacterial extracellular polysaccharides in biofilm formation and function. Microbiol Spectr 2015;3. https://doi.org/10.1128/microbiolspec.MB-0011-2014.
[161] Ghoul M, Mitri S. The ecology and evolution of microbial competition. Trends Microbiol 2016;24:833–45. https://doi.org/10.1016/j.tim.2016.06.011.
[162] Bridier A, Briandet R, Bouchez T, Jabot F. A model-based approach to detect interspecific interactions during biofilm development. Biofouling 2014;30:761–71. https://doi.org/10.1080/08927014.2014.923409.
[163] Liu G, Chater KF, Chandra G, Niu G, Tan H. Molecular regulation of antibiotic biosynthesis in *streptomyces*. Microbiol Mol Biol Rev 2013;77:112–43. https://doi.org/10.1128/MMBR.00054-12.
[164] Procópio RE de L, Silva IR da, Martins MK, Azevedo JL de, Araújo JM de. Antibiotics produced by *streptomyces*. Braz J Infect Dis 2012;16:466–71. https://doi.org/10.1016/j.bjid.2012.08.014.
[165] Fira D, Dimkić I, Berić T, Lozo J, Stanković S. Biological control of plant pathogens by *Bacillus* species. J Biotechnol 2018;285:44–55. https://doi.org/10.1016/j.jbiotec.2018.07.044.
[166] Alvarez-Sieiro P, Montalbán-López M, Mu D, Kuipers OP. Bacteriocins of lactic acid bacteria: extending the family. Appl Microbiol Biotechnol 2016;100:2939–51. https://doi.org/10.1007/s00253-016-7343-9.
[167] Siedler S, Balti R, Neves AR. Bioprotective mechanisms of lactic acid bacteria against fungal spoilage of food. Curr Opin Biotechnol 2019;56:138–46. https://doi.org/10.1016/j.copbio.2018.11.015.
[168] Lee D-H, Kim BS, Kang S-S. Bacteriocin of *Pediococcus acidilactici* HW01 inhibits biofilm formation and virulence factor production by *Pseudomonas aeruginosa*. Probiotics Antimicrob Proteins 2020;12:73–81. https://doi.org/10.1007/s12602-019-09623-9.
[169] Diguță CF, Nițoi GD, Matei F, Luță G, Cornea CP. The biotechnological potential of *Pediococcus* spp. isolated from Kombucha microbial consortium. Foods 2020;9:E1780. https://doi.org/10.3390/foods9121780.
[170] Santos CMA, Pires MCV, Leão TL, Hernández ZP, Rodriguez ML, Martins AKS, et al. Selection of *Lactobacillus strains* as potential probiotics for vaginitis treatment. Microbiology (Reading, Engl) 2016;162:1195–207. https://doi.org/10.1099/mic.0.000302.
[171] Saraoui T, Fall PA, Leroi F, Antignac J-P, Chéreau S, Pilet MF. Inhibition mechanism of *Listeria monocytogenes* by a bioprotective bacteria *Lactococcus piscium* CNCM I-4031. Food Microbiol 2016;53:70–8. https://doi.org/10.1016/j.fm.2015.01.002.
[172] El Kheir SM, Cherrat L, Awussi AA, Ramia NE, Taha S, Rahman A, et al. High-throughput identification of candidate strains for biopreservation by using bioluminescent *Listeria monocytogenes*. Front Microbiol 2018;9:1883. https://doi.org/10.3389/fmicb.2018.01883.
[173] Bukvicki D, Siroli L, D'Alessandro M, Cosentino S, Fliss I, Said LB, et al. Unravelling the potential of *Lactococcus lactis* strains to Be used in cheesemaking production as biocontrol agents. Foods 2020;9:E1815. https://doi.org/10.3390/foods9121815.
[174] Canon F, Nidelet T, Guédon E, Thierry A, Gagnaire V. Understanding the mechanisms of positive microbial interactions that benefit lactic acid bacteria Co-cultures. Front Microbiol 2020;11:2088. https://doi.org/10.3389/fmicb.2020.02088.
[175] Betesho Babrud R, Kasra Kermanshahi R, Motamedi Sede F, Moosavinejad SZ. The effect of *Lactobacillus reuteri* cell free supernatant on growth and biofilm formation of *Paenibacillus larvae*. Iran J Vet Res 2019;20:192–8.
[176] Sengupta D, Datta S, Biswas D. Towards a better production of bacterial exopolysaccharides by controlling genetic as well as physico-chemical parameters. Appl Microbiol Biotechnol 2018;102:1587–98. https://doi.org/10.1007/s00253-018-8745-7.
[177] Zhou C, Fey PD. The acid response network of *Staphylococcus aureus*. Curr Opin Microbiol 2020;55:67–73. https://doi.org/10.1016/j.mib.2020.03.006.
[178] Brown MM, Kwiecinski JM, Cruz LM, Shahbandi A, Todd DA, Cech NB, et al. Novel peptide from commensal *Staphylococcus simulans* blocks methicillin-resistant *Staphylococcus aureus* quorum sensing and protects host skin from damage. Antimicrob Agents Chemother 2020;64:e00172. https://doi.org/10.1128/AAC.00172-20. 20.
[179] Vinoj G, Vaseeharan B, Thomas S, Spiers AJ, Shanthi S. Quorum-quenching activity of the AHL-lactonase from *Bacillus licheniformis* DAHB1 inhibits *Vibrio* biofilm formation in vitro and reduces shrimp intestinal colonisation and mortality. Mar Biotechnol 2014;16:707–15. https://doi.org/10.1007/s10126-014-9585-9.
[180] Zhao J, Quan C, Jin L, Chen M. Production, detection and application perspectives of quorum sensing autoinducer-2 in bacteria. J Biotechnol 2018;268:53–60. https://doi.org/10.1016/j.jbiotec.2018.01.009.
[181] Wu S, Liu J, Liu C, Yang A, Qiao J. Quorum sensing for population-level control of bacteria and potential therapeutic applications. Cell Mol Life Sci 2020;77:1319–43. https://doi.org/10.1007/s00018-019-03326-8.
[182] EFSA Panel on Biological Hazards (BIOHAZ), Koutsoumanis K, Allende A, Alvarez-Ordóñez A, Bolton D, Bover-Cid S, et al. Update of the list of QPS-recommended biological agents intentionally added to food or feed as notified to EFSA 13: suitability of taxonomic units notified to EFSA until September 2020. EFSA J 2021;19:e06377. https://doi.org/10.2903/j.efsa.2021.6377.
[183] Bonis M, Felten A, Pairaud S, Dijoux A, Maladen V, Mallet L, et al. Comparative phenotypic, genotypic and genomic analyses of *Bacillus thuringiensis* associated with foodborne outbreaks in France. PLoS One 2021;16:e0246885. https://doi.org/10.1371/journal.pone.0246885.
[184] Sanchez-Vizuete P, Le Coq D, Bridier A, Herry J-M, Aymerich S, Briandet R. Identification of ypqP as a New *Bacillus subtilis* biofilm determinant that mediates the protection of *Staphylococcus aureus* against antimicrobial agents in mixed-species communities. Appl Environ Microbiol 2015;81:109–18. https://doi.org/10.1128/AEM.02473-14.
[185] Tóth AG, Csabai I, Judge MF, Maróti G, Á Becsei, Spisák S, et al. Mobile antimicrobial resistance genes in probiotics. Antibiotics (Basel) 2021;10:1287. https://doi.org/10.3390/antibiotics10111287.
[186] Glenwright H, Pohl S, Navarro F, Miro E, Jiménez G, Blanch AR, et al. The identification of intrinsic chloramphenicol and tetracycline resistance genes in members of the *Bacillus cereus* group (sensu lato). Front Microbiol 2016;7:2122. https://doi.org/10.3389/fmicb.2016.02122.
[187] EFSA Panel on Additives and Products or Substances used in Animal Feed (FEEDAP), Rychen G, Aquilina G, Azimonti G, Bampidis V, Bastos M de L, et al. Guidance on the characterisation of microorganisms used as feed additives or as production organisms. EFSA J 2018;16:e05206. https://doi.org/10.2903/j.efsa.2018.5206.
[188] De Roy K, Marzorati M, Van den Abbeele P, Van de Wiele T, Boon N. Synthetic microbial ecosystems: an exciting tool to understand and apply microbial communities. Environ Microbiol 2014;16:1472–81. https://doi.org/10.1111/1462-2920.12343.
[189] Ismaïl R, Aviat F, Michel V, Le Bayon I, Gay-Perret P, Kutnik M, et al. Methods for recovering microorganisms from solid surfaces used in the food industry: a review of the literature. Int J Environ Res Publ Health 2013;10:6169–83. https://doi.org/10.3390/ijerph10116169.
[190] Guéneau V, Rodiles A, Piard J-C, Frayssinet B, Castex M, Plateau-Gonthier J, et al. Capture and ex-situ analysis of environmental biofilms in livestock buildings. Microorganisms 2022;10:2. https://doi.org/10.3390/microorganisms10010002.
[191] Whiley H, Taylor M. Legionella detection by culture and qPCR: comparing apples and oranges. Crit Rev Microbiol 2016;42:65–74. https://doi.org/10.3109/1040841X.2014.885930.
[192] Pui CF, Wong WC, Chai LC, Lee HY, Noorlis A, Zainazor TCT, et al. Multiplex PCR for the concurrent detection and differentiation of *Salmonella* spp., *Salmonella Typhi* and *Salmonella Typhimurium*. Trop Med Health 2011;39:9–15. https://doi.org/10.2149/tmh.2010-20.
[193] Kerdsin A, Dejsirilert S, Akeda Y, Sekizaki T, Hamada S, Gottschalk M, et al. Fifteen *Streptococcus suis* serotypes identified by multiplex PCR. J Med Microbiol 2012;61:1669–72. https://doi.org/10.1099/jmm.0.048587-0.
[194] Li B, Liu H, Wang W. Multiplex real-time PCR assay for detection of *Escherichia coli* O157:H7 and screening for non-O157 Shiga toxin-producing *E. coli*. BMC Microbiol 2017;17:215. https://doi.org/10.1186/s12866-017-1123-2.
[195] Stein RR, Bucci V, Toussaint NC, Buffie CG, Rätsch G, Pamer EG, et al. Ecological modeling from time-series inference: insight into dynamics and stability of intestinal microbiota. PLoS Comput Biol 2013;9:e1003388. https://doi.org/10.1371/journal.pcbi.1003388.
[196] Buffie CG, Bucci V, Stein RR, McKenney PT, Ling L, Gobourne A, et al. Precision microbiome reconstitution restores bile acid mediated resistance to *Clostridium difficile*. Nature 2015;517:205–8. https://doi.org/10.1038/nature13828.
[197] Fong W, Li Q, Yu J. Gut microbiota modulation: a novel strategy for prevention and treatment of colorectal cancer. Oncogene 2020;39:4925–43. https://doi.org/10.1038/s41388-020-1341-1.
[198] Kimelman H, Shemesh M. Probiotic bifunctionality of *Bacillus subtilis*-rescuing lactic acid bacteria from desiccation and antagonizing pathogenic *Staphylococcus aureus*. Microorganisms 2019;7. https://doi.org/10.3390/microorganisms7100407.
[199] Burmølle M, Webb JS, Rao D, Hansen LH, Sørensen SJ, Kjelleberg S. Enhanced biofilm formation and increased resistance to antimicrobial agents and bacterial invasion are caused by synergistic interactions in multispecies biofilms. Appl Environ Microbiol 2006;72:3916–23. https://doi.org/10.1128/AEM.03022-05.
[200] Liu W, Jacquiod S, Brejnrod A, Russel J, Burmølle M, Sørensen SJ. Deciphering links between bacterial interactions and spatial organization in multispecies biofilms. ISME J 2019;13:3054–66. https://doi.org/10.1038/s41396-019-0494-9.
[201] Andersson S, Kuttuva Rajarao G, Land CJ, Dalhammar G. Biofilm formation and interactions of bacterial strains found in wastewater treatment systems. FEMS Microbiol Lett 2008;283:83–90. https://doi.org/10.1111/j.1574-6968.2008.01149.x.
[202] Kehe J, Kulesa A, Ortiz A, Ackerman CM, Thakku SG, Sellers D, et al. Massively parallel screening of synthetic microbial communities. Proc Natl Acad Sci USA 2019;116:12804–9. https://doi.org/10.1073/pnas.1900102116.
[203] Tian T, Sun B, Shi H, Gao T, He Y, Li Y, et al. Sucrose triggers a novel signaling cascade promoting *Bacillus subtilis* rhizosphere colonization. ISME J 2021;15:2723–37. https://doi.org/10.1038/s41396-021-00966-2.
[204] De Cesare A, Caselli E, Lucchi A, Sala C, Parisi A, Manfreda G, et al. Impact of a probiotic-based cleaning product on the microbiological profile of broiler litters and chicken caeca microbiota. Poultry Sci 2019;98:3602–10. https://doi.org/10.3382/ps/pez148.
[205] Woolhouse M, Ward M, van Bunnik B, Farrar J. Antimicrobial resistance in humans, livestock and the wider environment. Philos Trans R Soc Lond B Biol Sci 2015;370:20140083. https://doi.org/10.1098/rstb.2014.0083.

[206] Cheong D-Y, Harvey JT, Kim J, Lee C. Improving biomethanation of chicken manure by Co-digestion with ethanol plant effluent. Int J Environ Res Publ Health 2019;16:E5023. https://doi.org/10.3390/ijerph16245023.
[207] Scheinemann HA, Dittmar K, Stöckel FS, Müller H, Krüger ME. Hygienisation and nutrient conservation of sewage sludge or cattle manure by lactic acid fermentation. PLoS One 2015;10:e0118230. https://doi.org/10.1371/journal.pone.0118230.
[208] Strafella S, Simpson DJ, Yaghoubi Khanghahi M, De Angelis M, Gänzle M, Minervini F, et al. Comparative genomics and in vitro plant growth promotion and biocontrol traits of lactic acid bacteria from the wheat rhizosphere. Microorganisms 2020;9:E78. https://doi.org/10.3390/microorganisms9010078.

2.2 ARTICLE 2 : SPATIAL ANALYSIS OF MULTISPECIES BACTERIAL BIOFILMS

Virgile Guéneau, Raphaël Charron, Vlad Costache, Arnaud Bridier, Romain Briandet.

MIM 53: Biofilms, Elsevier, 2023, Methods in Microbiology, 10.1016/bs.mim.2023.03.002.

Spatial analysis of multispecies bacterial biofilms

Virgile Guéneau[a,b,†], Raphaël Charron[a,c,†], Vlad Costache[a,d], Arnaud Bridier[c,*], and Romain Briandet[a,*]

[a]*Université Paris-Saclay, INRAE, AgroParisTech, Micalis Institute, Jouy-en-Josas, France*

[b]*Lallemand SAS, Blagnac, France*

[c]*Antibiotics, Biocides, Residues and Resistance Unit, Fougères Laboratory, French Agency for Food, Environmental and Occupational Health & Safety (ANSES), Fougères, France*

[d]*MIMA2 Imaging Facility, Microscopie et Imagerie des Microorganismes, Animaux et Aliments, INRAE, Jouy-en-Josas, France*

**Corresponding authors: e-mail address: arnaud.bridier@anses.fr; romain.briandet@inrae.fr*

1 Introduction

Life in sessile communities known as biofilms constitutes the main microbial state over the earth. Biofilms profoundly affect our everyday life through their involvement in natural and ecological processes as well as through their deleterious impact on health or industrial productivity. In such biological structures, bacteria are close to each other and embedded in a complex 3D polymeric matrix, which shapes the specific features of the biofilm and is composed of diverse polysaccharides, proteins, nucleic acids and lipids (Karygianni, Ren, Koo, & Thurnheer, 2020). This communal lifestyle greatly influences the emergence of functional properties, which directly result from the biofilm spatial organization, phenotypic heterogeneity and social interactions of individuals in the community (Arnaouteli, Bamford, Stanley-Wall, & Kovács, 2021; Jo, Price-Whelan, & Dietrich, 2022; Sadiq et al., 2021). Recently, Díaz-Pascual et al. (2021) demonstrated that alanine metabolism is spatially and temporally heterogeneous and determines local growth dynamics in *E. coli* colonies. They highlighted an interplay between the anoxic base of the colony close to nutritive agar where alanine was secreted and the oxic nutrient-deprived region at the top of the colony where alanine was then used as a carbon source. This resulted in the metabolic specialization of subpopulations according to their spatial location and governed the shaping of the colony architecture and functions. Likewise, focusing on dental caries Kim et al. (2020) revealed a corona-like 3D

[†]These authors contributed equally.

Methods in Microbiology, ISSN 0580-9517, https://doi.org/10.1016/bs.mim.2023.03.002

architecture of polymicrobial biofilm with the pathogen *Streptococcus mutans* in the inner core. They observed that such specific micron-scale spatial organization modulated pathogen virulence potential and interactions with the host. Such findings illustrate the close relationships between spatial organization and functions in multicellular bacterial communities. Reciprocally, the plasticity of biofilm architecture constitutes a collective way to adapt to the dynamics of such internal subpopulation interactions and to face the environmental fluctuations that finally affect the survival of biofilm-dwelling cells (Bridier et al., 2017). Several studies reported, for instance, the effective protection against antibiotic or biocidal stresses of bacteria living in a biofilm in comparison to their planktonic counterparts (Bowler, Murphy, & Wolcott, 2020; Bridier, Briandet, Thomas, & Dubois-Brissonnet, 2011; Høiby, Bjarnsholt, Givskov, Molin, & Ciofu, 2010).

In industrial and natural environments, biofilms are mostly complex associations of different bacterial strains or species rather than pure cultures. Such ecological heterogeneity reinforces the complexity of social relationships within the biofilm 3D structure depending on the cooperative or competitive nature of social phenotypes and their dynamics, and greatly affects bacterial phenotype and fitness (Elias & Banin, 2012). Along the food chain, in certain conditions, some bacteria are poor biofilm formers alone, but benefit from the association with other species in mixed communities. It has been reported that biofilms of various foodborne pathogens including *Listeria monocytogenes*, *E. coli,* or *Salmonella enterica* may thus be promoted by the presence of other bacteria in mixed communities (Giaouris et al., 2015; Xu, Hu, Han, & Chen, 2022). Moreover, interactions in multispecies biofilms can also lead to a better tolerance of bacterial subpopulations to disinfectants (Li et al., 2021). Phenomena of pathogen protection by resident flora against the effect of biocides, especially due to spatial organization and matrix components sharing was indeed described as reviewed earlier (Sanchez-Vizuete, Orgaz, Aymerich, Le Coq, & Briandet, 2015). Recent work performed on meat processing plant microcosms showed, for instance, that resident microflora may affect the colonization and the subsequent sanitizer tolerance of the pathogen *E. coli* O157:H7 (Chitlapilly Dass et al., 2020). Observations indicated a link between the degree of species diversity of resident biofilm and the level of protection provided. Conversely, the presence of resident microbiota can limit the colonization of surfaces by pathogenic bacteria due to nutrient and spatial competition. Relations between the composition and diversity of the resident microflora and the presence of specific bacterial species have also been associated with a lower prevalence of *L. monocytogenes* in mixed communities (Fagerlund, Langsrud, & Møretrø, 2021). A better deciphering of these ecological interactions and their impact on biofilm emergent properties is therefore of prime importance from a health perspective and constitutes a scientific challenge.

In this perspective, the analysis of species spatial organization gives crucial information on the nature of interactions in 3D multicellular communities since specific architectural patterns reflect the way individual bacterial strains interplay through deleterious, neutral or beneficial processes (Liu et al., 2016). Different studies using synthetic communities and/or computational approaches indeed demonstrated

that the analysis of spatiotemporal community structures enabled a comprehensive understanding of the roles of pairwise social interactions in the structuration of dual-species agar colonies (Blanchard & Lu, 2015; Bonicoli, Angelini, Riela, & Taiani, 1987). In previous work, we proposed an approach relying on the comparison of 4D confocal image series of biofilm development in flow-cells with a simple mathematical null model of biofilm growth to detect non-trivial interspecific interactions between pairs of *Pseudomonas* species expressing distinct fluorescent proteins (Bridier, Briandet, Bouchez, & Jabot, 2014). Such a structure-based approach has proven to be successful to identify how bacterial interactions vary depending on bacterial strains.

These last years, dramatic improvements in biofilm imaging methods were achieved, through the development of microscopy techniques, fluorescence-associated tools, genetic engineering, computing and artificial intelligence for image processing, and their integration, which provide an unprecedented opportunity to dive deep into our understanding of bacterial interactions in biofilms (Bridier & Briandet, 2022). The possibility of differentially tagged distinct species in biofilm structure using specific fluorescent genetic constructs makes it possible to monitor independently each subpopulation at the single-cell resolution during biofilm development.

2 General workflow for biofilms spatial analysis

The experimental process for biofilm spatial analysis is composed of four major steps: the biofilm model choice, the fluorescent probe choice and labelling, the image vizualisation and the data treatment. All these steps are summarized in Fig. 1.

2.1 Generating and capturing biofilms for spatial analysis

2.1.1 In vitro *biofilms*

Many setups with different geometries and hydrodynamics have been developed to study biofilms *in vitro* (Azeredo et al., 2017). The choice of the assay will deeply impact the observed effects on biofilm formation as illustrated in Yarwood, Bartels, Volper, and Greenberg (2004). Historically, the first setups allowed axenic biofilms to grow reproducibly in the lab compatibly with Confocal Laser Scanning Microscopy (CLSM) were based on millifluidic flowcells mounted on microscopic grade glass slides (Habimana, Guillier, Kulakauskas, & Briandet, 2011; Pamp, Sternberg, & Tolker-Nielsen, 2009; Tolker-Nielsen & Sternberg, 2011, 2014). The main drawback of these millifluidic systems was the low throughput of experiments (typically only a few flowcells every week). To overcome this limitation, protocols of biofilm formation based on microscopic grade microtiter plates were combined with High-Content-Screening CLSM, both in static (Bridier, Dubois-Brissonnet, Boubetra, Thomas, & Briandet, 2010) or dynamic microfluidic systems (Pouget et al., 2021). These high-throughput approaches allowed the exploration of

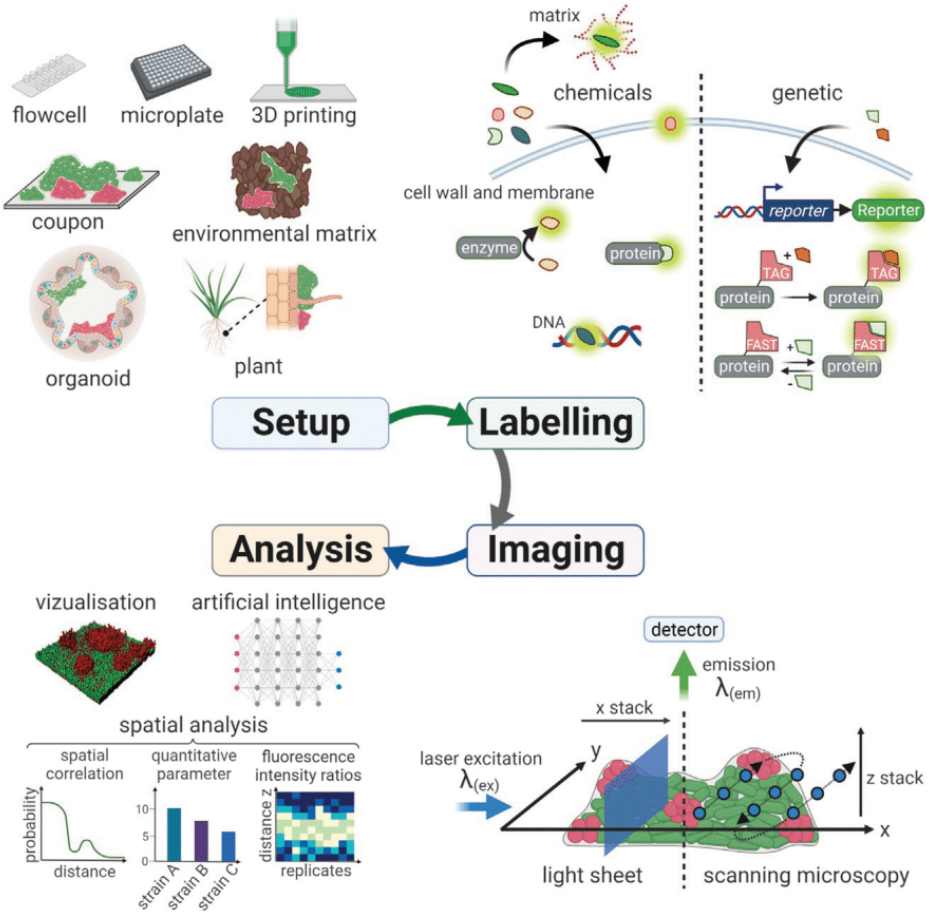

FIG. 1

Workflow to study mixed biofilms using fluorescence microscopy. First, the biofilm type of growth must be chosen from a large list of *in vitro*, *ex situ* and *in vivo* methods available. Then, genetic and chemical fluorescent markers are used to stain bacterial cells inside the biofilm. Consequently, excitation of these markers allows for the observation of the biofilms under fluorescence microscopy. Finally, images can be processed using various softwares to perform 3D reconstruction, spatial quantitative analysis or more in-depth analysis using artificial intelligence. Figure created with https://biorender.com/.

interspecies diversity of biofilms formation and to pinpoint genetic determinants and their regulations, but also to access dynamic processes at different time scales (Béchon et al., 2022; Canette, Deschamps, & Briandet, 2019; Guilbaud, Piveteau, Desvaux, Brisse, & Briandet, 2015; Sanchez-Vizuete et al., 2022).

Polymeric 3D printing was recently used to generate a large variety of device geometries to grow biofilms *in vitro* under various hydrodynamic regimes (Hall, Palmer, Ji, Ehrlich, & Król, 2021; Kristensen, Leonhardt, Neland, & Schlafer, 2020; Zaborskytė, Wistrand-Yuen, Hjort, Andersson, & Sandegren, 2021).

To study the impact of the local microenvironment on biofilm formation, bacteria can be loaded on hydrogels with specific compositions (Heumann et al., 2020; Saint Martin et al., 2022). Depending on the texture of the gel and its physicochemical properties, different morphologies of biofilms can emerge and affect microbial behaviour (van Tatenhove-Pel et al., 2021). 3D bioprinting of simplified structured matrixes with patterned microbial ecosystems allows the exploration of cellular diversification and modelling of interaction between species within structured communities (Connell, Ritschdorff, Whiteley, & Shear, 2013; Huang, Xia, Yang, & Jin, 2018; Krishna Kumar et al., 2021; Ning et al., 2019). An illustrative example of these 3D polymicrobial structures is the formation of autoreplicative kefir granules used in fermented beverages with reported beneficial effects on health. These granule starters that can measure up to a couple of centimetres in diameter are symbiotic communities (often described as functional superorganisms) including lactic acid bacteria and yeasts embedded in a dense extracellular polymeric matrix (Lu et al., 2014). Nowadays, no report has described sucessful initiation of kefir grain from assembled planktonic communities and 3D bioprinting is envisioned to nucleate such communities in synthetic ecology approaches.

2.1.2 Environmental samples

Numerous techniques using swabs, wipes or sponges are used to collect environmental biofilms for studying their composition using DNA sequencing or enumeration on agar. However, these techniques can at best recover <90% of the biofilm community (Grand et al., 2011). In addition, these approaches are based on biofilm disruption for their collection and hence are not compatible with microscopic exploration (Guéneau et al., 2021). As it has been demonstrated that biofilm spatial organization is an important trait of biofilm properties, microscopy has been applied on environmental samples that could be transferred to a lab, or on coupons of relevant materials previously deposited on the surface and sampled *in situ* after biofilms developed in the local ecosystem (Douterelo, Jackson, Solomon, & Boxall, 2016; Guéneau et al., 2021; O'Donnell, Young, Rushton, Shirley, & Crawford, 2007; Romani, Carrion, Fernandez, Lebaron, & Lami, 2021; Shank et al., 2011; Silva et al., 2018).

2.1.3 Biofilms associated with host cells

Tissues and associated biofilms removed from the host (biopsies) can be analysed under the microscope to visualize patterns of the microbial–host interaction. As an example, dental plaque can be sampled and marked with a genus-specific fluorescent label to show the highly complex stratification of surface communities attached to teeth (Mark Welch, Rossetti, Rieken, Dewhirst, & Borisy, 2016; Zijnge et al., 2010). Microscopic observations of histological sections of mouse gastrointestinal tract tissues pinpointed *in vivo* biofilm formation by bacterial pathobionts (Barnes et al., 2017). Organoid 3D models of cell cultures are increasingly being developed. The advantage of these models is that they mimic the organization of organs using human cells, sometimes taken directly from patients (Clevers, 2016). Interaction studies between organoids and microorganisms can be done using

fluorescence microscopy (Dekkers et al., 2019; Han et al., 2021). A human epidermis organoid model was developed to study the development of methicillin-resistant *Staphylococcus aureus* and *P. aeruginosa* biofilms (Wu et al., 2021). Organoids can also mimic the natural environment of the pathogen (*Helicobacter pylori*) responsible for gastric cancer, increasing the knowledge about this bacterium (Amieva & Peek, 2016). Gut-on-chips that mimic the organization of digestive tract tissues are also used to study biofilm formation on epithelial tissue cells (Yuan et al., 2020).

Plant–microbe interactions are also intensively explored by imaging technologies: plants are, for example, used as laboratory models to study bacterial colonization on roots. *P. fluorescens* and *B. subtilis* biofilm formation on *Populus tremuloides* roots were studied using microfluidic chips coupled with confocal microscopy (Noirot-Gros et al., 2020). Exclusion of the fungal pathogen *Trichoderma aggressivum* by *B. velezensis* that developed on hyphae of *Agaricus bisporus* was also deciphered with fluorescent tools (Pandin et al., 2019). Interactions between microalgae and bacteria can be studied in polymicrobial biofilms taking advantage of the autofluorescence of photosynthetic organisms to discriminate the different species in the community (Doiron et al., 2012).

2.2 Biofilm labelling for fluorescence microscopy

2.2.1 Chemical fluorophores

2.2.1.1 Geolocation of cells and matrix components

Fluorophores that specifically target cell compounds can be used to label biofilms. Probes able to penetrate cells and intercalate into the nucleic acids such as 4′,6-diamidino-2-phenylindole (DAPI) or SYTO fluorescently label the entire microbial population (Johnson & Criss, 2013). These treatments do not destructure the biofilm organization but are toxic to the bacteria and they can not be used for live dynamic experiments. In contrast, cell membrane-intercalating markers such as FM4-64 or matrix contrasting EbbaBiolight can be used to perform real-time kinetics of biofilm formation when used at an appropriate concentration (Bassères et al., 2021; Choong et al., 2021; Sanchez-Vizuete et al., 2022). Immunofluorescence can be used to pinpoint a specific organism within the community by using antibodies targeting specific surface antigens. Primary antibodies targeting several pathogenic microorganisms such as *Staphylococcus aureus* and *Listeria monocytogenes* are commercially available (Kühbacher, Cossart, & Pizarro-Cerdá, 2021). Antibodies can be directly coupled with a fluorophore, or a second fluorescent antibody directed towards antibodies produced by a specific animal species can be used in a second reaction (Deshmukh, Joshi, Bhand, & Roy, 2016).

Fluorescent *In Situ* Hybridization (FISH) is based on fluorescent oligonucleotides able to fix a strain-specific sequence of the genome allowing the visualization of specific members in the microbial community (Frickmann et al., 2017). Biofilms must be chemically fixed and cells permeabilized to allow the probes to penetrate the cells, thus altering the native biofilm architecture. The coupling of several

species-specific oligonucleotides tagged with different fluorophores allowed the visualization of the very specific and stratified spatial organization of environmental multispecies biofilms (Mark Welch et al., 2016).

A biofilm matrix is a complex mixture of extracellular biomolecules. It is often described as the biofilm *dark matter* as it is complex to visualize (Flemming, Neu, & Wingender, 2017). No universal matrix dyes exist and it is often necessary to use a combination of probes to obtain only partial contrast of this biofilm component. Exopolysaccharides can be contrasted by fluorescent lectins such as concanavalin A or wheat germ agglutinin (WGA) (Farasin et al., 2017; Neu & Lawrence, 1999). However, a biofilm matrix is often a mixture of several polysaccharides and often there is no other choice than to screen different lectins to find the ones reacting with the sample being studied. Around 80 fluorescent lectins are commercially available and some suppliers provide kits with small aliquots of dozen of lectins to screen them. Another important component of the biofilm matrix is extracellular DNA (eDNA). It can be targeted by several nucleic acid binding fluorophores, but the preferred molecules would be cell impermeant so they do not label intracellular DNA. This is the case for SYTOX green or TOTO1 (Béchon et al., 2022). Dyes labelling proteins (Sypro Ruby, DyLight) or amyloid plaque core proteins (Thioflavin T) were also used to contrast specific regions of the matrices (Bridier, Meylheuc, & Briandet, 2013; Hernández-Galán et al., 2017).

2.2.1.2 Microbial physiology

Several fluorophores have specific functions, providing information on the physiological state of the biofilm organisms, thereby the coupling of these fluorophores can provide a large panel of information on global lifestyle. Several fluorophore combinations can be used to discern living from dead bacteria (Tawakoli, Al-Ahmad, Hoth-Hannig, Hannig, & Hannig, 2013). For example, the use of the cell-permeant SYTO 9 which targets nucleic acids, marking the whole population in green, coupled with the cell impermeant propidium iodide that only marks the DNA of bacteria whose membrane is damaged, allows the spatial visualization and quantification of the dead microbial fraction (Dubois et al., 2019). Some non-fluorescent molecules can enter cells and be metabolized to release a fluorophore. Calcein-AM, cFDA or triembarine are used to visualize metabolically active bacteria by fluorescently reporting esterase activity *in situ* (Guéneau et al., 2021; Guilini et al., 2015). A bias of this labelling is the existence of strains able to expel these fluorophores by efflux pumps, especially within Gram-negative bacterial species (Reuter et al., 2020). Reactive nitrogen and oxygen intermediates involved in many metabolism pathways inside biofilms can also be quantified using fluorescent molecules (Barraud et al., 2006).

Studying the different expression profiles of several genes at the same time and at the single-cell level within a biofilm without the loss of structural information is a challenge. Using *P. aeruginosa* as a biofilm-forming bacterium model, Daniel Dar et al. recently developed the parallel sequential fluorescence *in situ* hybridization (par-seqFISH) technique for this purpose (Dar, Dar, Cai, & Newman, 2021).

Some general drawbacks of the use of chemical fluorophores within a biofilm are their non-specific reactions that can contrast untargeted biofilm compartments and possible diffusion-reaction limitations that can prevent their availability at the target sites (Flemming et al., 2016).

2.2.2 Genetically encoded fluorescent proteins

Genetically encoded reporters represent the second important family of microbial fluorescent markers. As for chemical reporters, they can be used for several types of analyses.

Soluble fluorescent proteins can be expressed under constitutive promoters for live geo-localization purposes (Bridier, Piard, Briandet, & Bouchez, 2020). They can also be expressed under the natural promoter of a specific gene of interest, which leads to fluorescence proportional to gene expression (transcriptional fusion) (Hautefort, Proença, & Hinton, 2003). DNA sequences can be engineered to fuse the fluorescent protein-coding sequence to a specific protein-coding sequence, which allows protein location analysis in the cell or in the environment (translational fusion) (Billaudeau, Yao, Cornilleau, Carballido-López, & Chastanet, 2019).

2.2.2.1 Fluorescent proteins

The Green Fluorescent Protein (GFP) has been, over the last decades, extensively used as a fluorescent marker in biological organisms. Originating from the medusa *Aequoria victoria,* this protein was purified in 1962 (Shimomura, Johnson, & Saiga, 1962). Since then, this protein has been much studied and the mechanism implicated in its fluorescence unravelled. The protein is composed of 11 beta-sheets enrolled in a cylinder structure that surrounds the fluorochrome, composed of three amino acids, Ser65-Tyr66-Gly67. This fluorochrome matures in three steps: cyclisation, dehydration and oxidation of these amino acids (Day & Davidson, 2009). This maturation is induced by a 488 nm wavelength and generates an emission of 509 nm wavelength, causing the green fluorescence of the protein. Through molecular engineering, this protein has been adapted in numerous clones, to enable emission in other wavelengths, covering a large part of the visible spectrum (Day & Davidson, 2009). The large list of fluorochromes available (GFP, YFP, CFP, etc.) allows *in vivo* multi staining and multispecies biofilm studies (Lee et al., 2014; Oliveira et al., 2015).

Another fluorescent protein is DsRed, originating from *Discosoma* corals, and has been one of the main precursors for Red Fluorescent Proteins (RFP). Several proteins derived from DsRed have been engineered and called mFruits (Shaner et al., 2004). These proteins emit in different wavelengths, between 550 and 650 nm, and are more efficient than the initial natural DsRed, in terms of photostability, maturation speed and brightness (Shaner et al., 2004). They also work in a similar manner to GFP, notably with the absolute need for oxygen to fluoresce. The best known of these proteins is mCherry, a protein emitting fluorescence at 610 nm. This efficient fluorescent protein has been used in many studies and notably

in several studies analysing multispecies biofilms, thanks to its different emission spectrum from GFP (Bridier et al., 2020; Lagendijk, Validov, Lamers, de Weert, & Bloemberg, 2010; Lee et al., 2014).

However, the main problem with these markers is the requirement of oxygen in the maturation steps of the fluorochromes. In fact, biofilms are 3-Dimensional structures wherein oxygen is consumed faster than it can diffuse, creating sharp gradients of oxygen that can be absent in the deepest layers where organisms can exhibit anaerobic metabolisms (de Beer, Stoodley, Roe, & Lewandowski, 1994; Karampatzakis et al., 2017). Fluorescence of these proteins can also be limited in mature biofilms by low microbial metabolism associated with low protein synthesis (Monmeyran et al., 2018). Another limitation is the energetic cost they burden the producing cells with by their large weight (27 kb for GFP and mCherry). This important size can also be disadvantageous in the observation of fusion proteins, increasing the risk of functional interference with the fused protein. Finally, their use is limited to pH above 5 which can be in specific conditions, an important limiting factor. Hence, the development of new fluorescent reporters, overcoming these constraints has been necessary as discussed in the next section.

2.2.2.2 FMN-binding proteins

FMN-binding proteins were developed to overcome the sensitivity of GFP and RFP to environmental conditions. This method relies on the Light Oxygen Voltage (LOV) domain present in the phototropin proteins found in certain bacteria and plants. This domain, under blue light excitation, binds the flavin mononucleotide protein (FMN) which induces a green fluorescence in the bacteria. In 2007, Drepper et al. engineered several of these proteins to enhance their fluorescence and created new fluorescent markers called BsFbFP, EcFbFP (derived from the YtvA protein in *B. subtilis*) and PpFbFP (derived from the SB2 protein in *P. putida*) (Drepper et al., 2007). Other markers including iLOV (Chapman et al., 2008) and creiLOV (Mukherjee et al., 2015) were developed later from other phototropins and consequently adapted to more photostable versions, such as phiLOV (Christie et al., 2012). The main advantage of these markers is that they do not require oxygen, making them a more efficient tool in biofilm studies. They are also smaller molecules than GFP and are not sensitive to pH (Christie et al., 2012). However, their use is limited by the very weak fluorescent signal they produce, thus often being difficult to differentiate from the fluorescent background. In addition, all these dyes emit fluorescence in the same wavelength range, limiting their use to one species studies or to the requirement of other markers.

2.2.3 Fluorogenic reporting systems

2.2.3.1 Self-labelling proteins

Fluorogenic systems consist of a non-fluorescent protein encoded in the genome that can bind various ligands, called fluorogens, which are able to fluoresce at different wavelengths. Several fluorogenic complexes were developed such as SNAP-Tag (Keppler et al., 2003) and HALO-Tag (Los et al., 2008). These new markers are

eliminating most of the disadvantages of the methods cited before. Indeed, they are not dependent on oxygen and have fluorescence levels comparable to the ones of GFP or mCherry. SNAP-Tag is relatively small (19 kDa) and HALO-Tag relatively fast to mature (15 min), enabling the choice to select the ideal method depending on the experiment. Nevertheless, most of the existing fluorogens are fluorescing even when not bound to the protein, requiring an additional washing step to eliminate free molecules. However, new fluorogens, notably for HALO-Tag, have been developed, in which fluorescence is only activated when bound to the protein (Streett, Charubin, & Papoutsakis, 2021). These fluorogenic systems have been used successfully in multispecies biofilms, such as for example SNAP-Tag, which was used in a dual-species biofilm model composed of *S. gordonii* and *Porphyromonas gingivalis* (Nicolle et al., 2010) and allowed an efficient differentiation thanks to the collection of fluorogens available. A possible limitation of these systems is that the diffusion of fluorogen molecules is not always efficient in the biofilm. Of note, the costs of these fluorogens can be an issue, particularly in flowcell systems.

2.2.3.2 FAST (fluorescence-activating and absorption-shifting-tag)

Recently, a new fluorogenic system, called "Fluorescence-Activating and absorption-Shifting-Tag" (FAST), has been developed by Plamont et al. (2016). Derived from the Blue-light receptor PYP of *Halorhodospira halophila*, this system works slightly differently from the previously described ones. First, the fluorogen only fluoresces when bound to the FAST protein tag, avoiding any extra washing step. Then, its fixation with its fluorogen is reversible, when other fluorogenic systems usually bind their ligands irreversibly. Its 14 kDa size makes it very useful in the construction of fusion proteins. Finally, a big advantage of FAST is its instantaneous maturation. Thus, its immediate fluorescence allows the study of transitory conditions while other fluorochromes can take a considerable amount of time to maturate and miss early transient phenomena. FAST available ligands are increasing quickly and are already covering a large part of the visible spectrum (Benaissa et al., 2021). FAST has already been tested in biofilm conditions and shown to be more efficient in displaying the biofilm growth than GFP or mCherry, whose signals quickly saturate (Monmeyran et al., 2018). FAST has also been used successfully with SNAP-Tag and HALO-Tag in multi-species cultures (Charubin, Streett, & Papoutsakis, 2020), without any cross-reactivity, demonstrating that it is an interesting complementary tool for multispecies biofilm studies.

2.2.4 Combining different families of fluorophores

To differentiate several species inside of a biofilm, a combination of chemical and genetic approaches can be done as described by the protocol proposed in Section 3. The association of a genetically labelled strain with other bacterial species marked with nonspecific chemicals was performed here using an *E. coli* GFP and *Bacillus* spp. In this case, the specific spatial organization of the pathogen inside the

community was studied. In our example, there is only one species background member. Therefore, the subtraction of the red signal from the green signal gives the localization of the *Bacillus*. The same approach can be used for environmental or defined mixed-species background communities.

2.3 Imaging biofilms

Imaging micro-organisms is a challenging field for optical microscopy systems, due to the small cell size but also due to delicate mounting strategies, such as for live cells, for instance. Between 10 and 100 µm into the biofilm, the analysis of biofilm spatial organization can be limited by its opacity and thickness that limits light penetration.

In this part, we compare different strategies of optical microscopy that can be applied to image biofilms or that need further development to be applied to biofilm imaging.

Individual bacterial cells range roughly from 0.5 µm large to a couple of microns long, so microscopes with good optical sectioning capabilities are needed to obtain information at single cell resolution. We refer here to Confocal Laser Scanning Microscopy (CLSM) systems, two or multi-photon confocal systems, light sheet microscopes, structured illumination (SIM), stimulated-emission-depletion (STED), super-resolution technologies that use Total Internal Reflection Fluorescence (TIRF) approaches, with respect to conventional wide field epi-fluorescence microscopy.

Since the invention of the confocal microscope by Marvin Minsky in the 1950s (Minsky, 1988) and the first commercial laser scanning confocal systems in the late 1980s, CLSM has become one of the most widely used optical sectioning approaches for fluorescence microscopy in biology during the last 20 years.

The CLSM uses a pinhole system, an opening of about 100 µm large in front of the light detectors, that eliminates out of focus emitted light, when a fluorescent sample undergoes laser excitation (Batt & Tortorello, 2014). The micrograph image is formed when the laser beam scans point by point the sample, and the photons are transformed into an electrical signal by a photomultiplier (PMT) detector or an avalanche photodiode, that is a more sensitive detector, such as the Hybrid system (HyD) from Leica Microsystems or the GaAsP produced by Zeiss. CLSM systems allow a good penetration of the light through the sample and a slightly increased lateral and mostly axial resolution, when the pinhole opening is not more than 1 AU (Airy Unit) (Batt & Tortorello, 2014). The micro-morphologies of microbe interaction within a porous material was achieved at a depth of around 50 µm without incising samples (Munir et al., 2021). Scanning the sample with the laser beam implies rather slow acquisition of large images (i.e. more than 512×512 pixels). To acquire images faster, the use of a resonant scanner coupled to the CLSM, that allows high frequency scanning is possible but the obtained images can be very noisy so less informative to answer biological questions. Another solution would be the spinning-disc confocal, that enables faster imaging as it uses a camera like widefield systems. The optical sectioning is generated when the emitted light is filtered through

a fast spinning Nipkow disc. A major drawback for this kind of confocal technology is the poor penetration depth of the light, but recent commercial systems have implemented different pinhole sizes to overcome this limitation.

Conventional commercial CLSM systems allow functional measures for live samples such as precise decaging or photoconversion of fluorophores to follow a subpopulation (Costache et al., 2017) or FRAP (fluorescence recovery after photobleaching) to measure a flux, drift or protein turn-over (Hauth, Chodorski, Wirsen, & Ulber, 2020; Schulmeister et al., 2008).

If phototoxicity to the cells, photobleaching of fluorophores or the penetration depth of the light becomes an issue when imaging a biofilm with a conventional CLSM, this may be overcome by using a two-photon (2P) or a multi-photon (MP) excitation laser (Olpe, Glatt, Laszlo, & Schellenberg, 1980; Tran et al., 2021). 2P microscopy uses femtosecond pulsed lasers. Compared to a conventional monophoton laser, 2P lasers deliver twice the wavelength of the desired excitation wavelength in a non-linear way. For instance, to excite a GFP at 488 nm, the 2P laser generates photons of 976 nm that travel at different speeds, so two photons of 976 nm meet exactly at the focal plane, where the excitation light will become 488 nm. The advantage of this technique is that longer wavelength photons, i.e., near infrared light, produce less photodamage, as they display lower energy than blue and UV photons. The penetration depth of 2P lasers is greater, for instance 143 µm for a Kombucha biofilm (Schulmeister et al., 2008). MP like 2P lasers induce the excitation wavelength at the focal plane. Two or more photons with long wavelengths are generated in a more stochastic manner, to restore the desired excitation light at the focal plane (Thomsen, Graf, Farewell, & Ericson, 2018). Thus, 2P and MP illumination induces an optical sectioning that is limited by the size of the point spread function (PSF) in z at the focal plane, even though most of the commercial microscopes couple the MP excitation laser to a CLSM system, to benefit also from the pinhole optical sectioning. Another advantage of MP lasers is that they can be used for precise laser ablation experiments while acquiring images on the microscope and this can be useful for functional imaging of live cells, for instance, to measure force generation at the cell wall or within the matrix of a biofilm.

When analysing many samples, high content screening modules (HCS) within CLSM systems allow 5D imaging (3D+multi-position+time-lapse) of multiple conditions for live biofilms that develop on 2D support, such as the coverslip glass bottom of a multi-well plate.

Studying biofilms that develop on a 3D support would enhance understanding of biofilm formation, dynamics and functioning mechanisms. To overcome this technical challenge, light sheet microscopy is a well adapted optical sectioning approach that illuminates only the focal plane using a second objective rather than the whole sample as in CLSM (Fig. 2). This approach has low phototoxicicity and is very fast, as the image is formed on one or two cameras, like for widefield conventional microscopes. The optical sectioning in common commercial light sheet solutions does not perform as well as CLSM and the detection objective needs greater working distance, but the illumination techniques allow very fast imaging of large samples

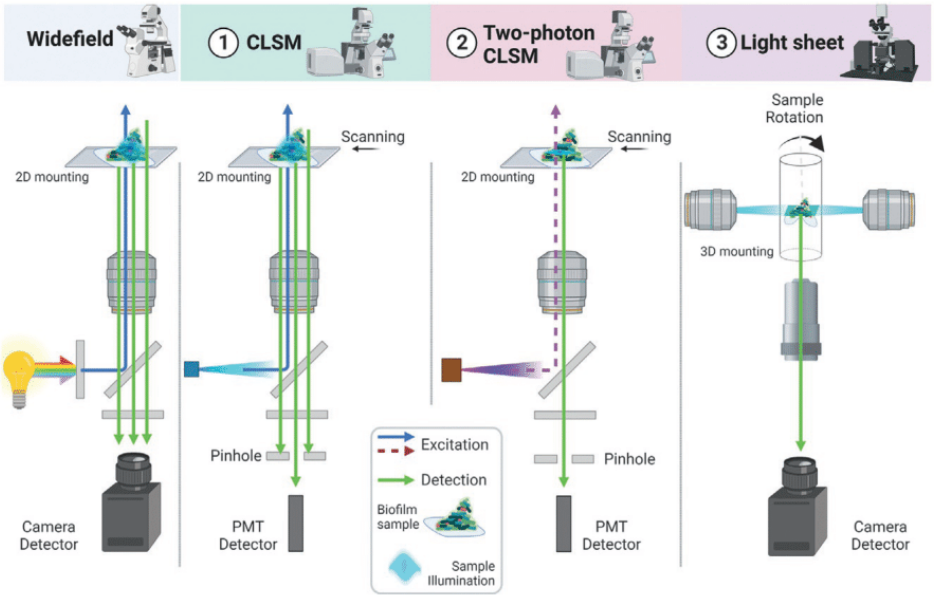

FIG. 2

Comparison of microscopy excitation strategies to detect fluorescence emission of a biofilm, using three optical sectioning approaches: Confocal Laser Scanning Microscopy (CLSM), Two-photon (2P) and Lightsheet (LS) microscopy, with respect to widefield epifluorescence (left). Here, the light from a multichromatic halogene lamp is filtered (grey rectangles), illuminates the whole sample and the signal is detected by a camera. The excitation optical trajectory is in blue and the emission signal in green. (1) CLSM often uses monochromatic laser excitation and the emission signal is filtered through a pinhole that eliminates out of focus blur. Thus, the PMT detects only signal coming from the focal plane. (2) 2P CLSM uses pulsed laser, often in the infrared domain. The excitation wavelength (twice lower) is reached only at the focal plane, which diminishes the photoxicity. See the sample illumination (at the desired excitation wavelength) that is less than in widefield and conventional CLSM. (3) LS microscope allows mounting on large 3D supports that can be rotated while imaging the sample. This is useful to overcome shaded areas comparing to conventional 2D mounting with a cover slip. Excitation light often comes from two objectifs, each one illuminating as a light sheet at the focal plane only. The excitation lightpath is orthogonal and fast camera detectors can be used, as for widefield microscopy. Figure created with https://biorender.com/.

and biofilms or cultures in 3D (Qin et al., 2020). This is mostly thanks to the alternative mounting strategies, i.e., within agarose cylinders or directly suspended in front of the objective with the possibility of rotating the sample for different view angles. Thus, the advantage of light sheet imaging is that the sample is more homogeneously illuminated as most commercial microscopes use two light sheets, on each side of the sample. This favours more precise volume reconstruction during 3D segmentation of the acquired images.

A milestone in optical imaging is the development of super resolution techniques bringing down lateral resolution to about 50 nm with respect to the light diffraction limited resolution that is about 200 nm. A major challenge for biofilm imaging is to better adapt super resolution techniques to help biofilm assessment at the nanoscale by using structured illumination (SIM), stimulated-emission-depletion (STED), and blinking strategies (PALM, STORM) (Berk et al., 2012; Billaudeau et al., 2017; Neu & Lawrence, 1999).

SIM uses several acquired images (3–7) on a camera through differently oriented grids that produce Moiré patterns enabling the enhancement of lateral resolution up to 150 nm, after image processing.

STED technology is coupled to CLSM and uses specific fluorescent dyes and a supplementary laser for emission-depletion as a donut shape during scanning to diminish the dimensions of each PSF to about 80 nm (xy). The laser power used is often too high for living cells, but there is no need for image processing to obtain the super-resolved image at the end of the acquisition.

The STORM/PALM strategies need the acquisition of many images, i.e., 2500–5000 frames, each one having only several fluorophores that emit, and that their precise localization allows to obtain a lateral resolution of the final image of about 10–30 nm (Altinoglu, Merrifield, & Yamaichi, 2019). These stochastic blinking methods are implemented in a TIRF microscope (Total Internal Reflection Fluorescence) that is one of the best optical sectioning strategies, illuminating only about 100 nm in thickness (z), but this illumination section has to be next to a coverslip. So, it is impossible to acquire images deeper than a couple of microns, even when near-TIRF or HILO (Highly Inclined Laminated Optics) are used.

Biofilm imaging would greatly benefit from super-resolved acquired images, but further development and adaptation of these technologies are needed to efficiently provide biological information, mostly for time-lapse of live biofilms.

2.4 Image analysis

Following acquisition, image analysis constitutes a crucial step enabling the extraction of meaningful qualitative and quantitative data from raw fluorescence microscopy image series. Recent advances in image analysis techniques open novel opportunities for spatial and temporal characterization of cells inside biofilms, and tremendous effort has been put into the development of powerful software tools for this purpose as recently reviewed (Jeckel & Drescher, 2021). Technically, several steps are required from pre-processing of raw images to spatial statistic extraction and object detection.

First, raw images from microscopic acquisition, which can be single 2D-images, 3D- or even 4D-image confocal series, should often be filtered to enable background noise reduction and enhance fluorescence signal contrast. Then, in the case of biofilms, 3D reconstructions, volumetric or isosurface projections or sections are mostly performed after filtering using dedicated commercial or freely available software

from confocal z-stack series to visualize 3D structure (Canette et al., 2019). In the example of Section 3, we used Imaris 9.31 (Bitplane).

Filtered images can also be quantified to extract numeric structural descriptors of biofilm and cell morphology that mostly require an upstream segmentation step. Segmentation is a critical step because it governs downstream analyses and greatly depends on image quality and resolution. The goal of segmentation is the partition of raw images into multiple regions to facilitate its quantitative analysis through the detection of objects (for instance, bacteria) and their separation from the background. Different methods of segmentation can be considered: semantic segmentation, instance segmentation or their combination (panoptic segmentation (Petrovai & Nedevschi, 2022). Semantic segmentation assigns a class label to each pixel, whereas instance segmentation detects and segments each object individually. With regards to biofilms, biovolume detection is an illustration of semantic segmentation as multiple objects identified as bacteria are treated as a single entity, and biofilm biomass can be quantified. Likewise, other global descriptors of biofilm architecture can be extracted as roughness, mean and maximum thickness, surface area, etc. Otherwise, instance segmentation treats multiple objects identified as bacteria as distinct individual instances. These features make instance segmentation a relevant approach for single-cell scale downstream analyses (Jeckel & Drescher, 2021). Recently, the concept of biofilm image cytometry was proposed in the BiofilmQ tool (Hartmann et al., 2021). BiofilmQ typically divides biofilm volume into cubes with user-defined size (which can correspond to the volume occupied by a single bacterium, i.e., *pseudo-cell* cubes), and fluorescence data and other cytometric properties in each cube are measured. This allows computing local spatio-temporal data in the biofilm as fluorescence intensity, the local density of cells, local porosity, local structure and texture, the spatial distribution of different markers, etc.

When using different fluorescent markers and reporters or working with differentially labelled bacterial strains, it is possible to analyse multi-channel fluorescent images to better decipher how the different fluorescent signals spatially interact. Focusing on multispecies bacterial biofilms is especially relevant for studying the nature of interactions in the 3D structure by analysing the spatial distribution patterns of bacterial species. Different methods can be applied to analyse colocalization from fluorescence images and can be divided into pixel-based methods and object-based methods (Lagache, Sauvonnet, Danglot, & Olivo-Marin, 2015). In pixel-based methods, individual pixels are analysed by the spectral information that they contain for the different channels and the overlap between fluorescence signals is measured. In object-based methods, the upstream segmentation of bacterial/cluster spots enables their representation as objects and the subsequent analysis of spatial distributions (Lagache et al., 2015).

The point-pattern analysis is classically used in spatial organization studies to extract quantitative spatial area-based or distance-based statistics (Lagache, Lang, Sauvonnet, & Olivo-Marin, 2013). Different coefficients such as Ripley's K function and derivative, pair-correlation or nearest neighbour functions for

instance constitute reference tools in this perspective (Lagache et al., 2015). Numerous studies have applied such analysis to bacterial communities to test if bacteria (points) are randomly distributed or colocalized, and therefore help to better understand interspecies microscale interactions (Esser, Leveau, Meyer, & Wiegand, 2015; Steinberg et al., 2021). The daime image analysis programme (Daims, Lücker, & Wagner, 2006) has been widely used for quantifying spatial arrangement patterns and relations between different species in FISH images using co-localization/co-aggregation and pair cross-correlation functions in mixed biofilms (Almstrand, Daims, Persson, Sörensson, & Hermansson, 2013; Ramírez-Puebla et al., 2022; Schillinger et al., 2012). These approaches enable a better understanding of the link between the spatial organization of strains and the biological activities of the community (Liu et al., 2016). The recent BiofilmQ tool also offers various parameters to quantify correlation and separation distances between species clusters in multispecies biofilm through comparisons of their respective biovolumes and other descriptors such as the Mander's or the Pearson's correlation coefficients (see examples in Section 3) (Hartmann et al., 2021). Complex bacterial 3D organization can thereby be quantitatively characterized including data on bacterial interactions based on spatial distribution. Both these coefficients have also been widely used to quantify probe co-localization in biological microscopy including to elucidate molecule functions in subcellular processes for instance (Dunn, Kamocka, & McDonald, 2011; Lagache et al., 2015).

The rise of artificial intelligence (AI) with machine and deep learning using convolutional neural networks (CNN) has provided an unprecedented opportunity to increase the flow and the power of image analysis. Therefore, the building and use of AI-driven automated workflows stand out as promising approaches for structural analysis of bacterial communities and complex biofilms from microscopy images (Ragi et al., 2021). Recently, a new deep-learning based 2D segmentation tool called Misic that is able to perform automatic semantic and instance segmentation of bacteria inside of bacterial communities images was proposed (Panigrahi et al., 2021). As a major advantage, this tool can be applied for the analysis of species interactions in 2D multispecies bacterial communities images using an interaction model, at a very high throughput independently from imaging modalities. Likewise, using an agent-based model combined with deep learning from both *in silico* and experimental microscopic data, a new network inference method was developed that allows prediction of interspecies interactions from self-organized spatiotemporal patterns (Lee et al., 2020). Toolboxes for studying 3D biofilms are also emerging as BCM3D or the already mentioned BiofilmQ (Hartmann et al., 2021; Zhang et al., 2020). These software tools enable automated morphometric cell classifications in multispecies biofilms and the deciphering of cell-to-cell interactions within the 3D structure.

Furthermore, the increase of computing power makes it possible to directly optimize images during acquisition through adaptive microscopy relying on feedback between acquisition, live AI-based image analysis, and microscope control (Jeckel & Drescher, 2021). All-in-one solutions are being proposed by microscope manufacturers in commercial systems (e.g. MICA from Leica) that will really extend our ability to explore biofilms at the single-cell scale and bacterial interactions within the 3D structure.

3 Experimental protocol

The objective of this experimental protocol is to study the spatial bacterial interactions within a mixed bi-species biofilm. The experimental protocol described here was used to generate the multispecies biofilm images presented Fig. 3 and the

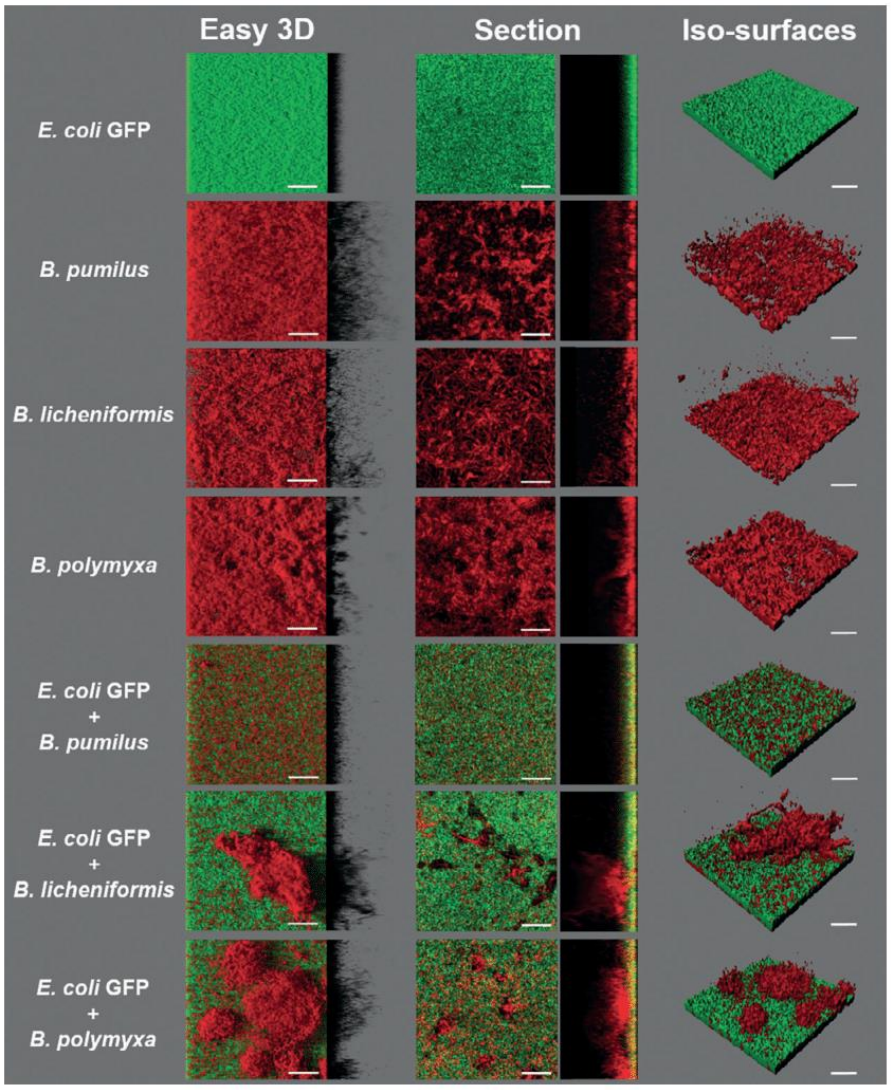

FIG. 3

Biofilm visualization using CLSM images with different modes of representation. *Bacillus* spp. strains were observed alone, or in a mixture with an *E. coli* strain that expresses GFP constitutively. SYTO 61 was used as a nonspecific marker to label in red all the cells. 3D projections of stacks using easy 3D mode are shown. The section mode allows the visualization of a fine (x,y) section of the base of the biofilm with a (z,y) section. 3D observation of isosurfaces of the mixed biofilm after binarization of both channels was made. All images were analysed using IMARIS software. The white scale bar represents 40 μm.

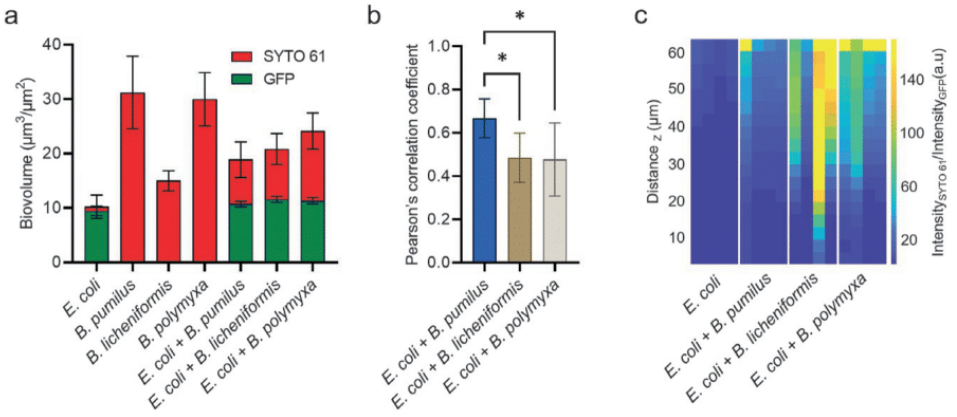

FIG. 4

Spatial analysis of mixed *E. coli* and *Bacillus* spp. biofilms. (A) Biovolume of each partner in mixed biofilms. The entire biofilm was labelled with SYTO 61 which targets nucleic acids and penetrates the cells allowing the labelling of the entire population (red). The monitoring of each partner is possible because *E. coli* expressed constitutively the GFP. The green bars in the graph correspond to the *E. coli* biovolume values in the total biofilm corresponding to the red bar values ($n=4$). (B) Pearson's correlation coefficient of mixed biofilms ($n=12$). (C) Kymographs of mixed biofilms fluorescence ratio intensity as a function of the distance to the substrate. A ratio value >1 means that there is more red intensity than green, so the higher the value, the more *Bacillus* spp. there are compared to *E. coli*. The yellow in the mixed biofilms of *E. coli* with *B. licheniformis* or *B. polymyxa* is consistent with the clusters of *Bacillus* spp. on the top of *E. coli* biofilm (Fig. 3). Each column corresponds to a replicate ($n=4$). The image stacks were taken with a CLSM. Error bars correspond to standard deviation and the asterisks correspond to $P< 0.05$. Statistical analysis were performed using two-way ANOVA and the uncorrected Fisher's least with PRISM software (GraphPad, San Diego, California, USA).

associated quantitative spatial analysis presented in Fig. 4. *E. coli* and *Bacillus* spp. biofilms were used as an example of multi-species biofilms to illustrate the experimental protocol.

3.1 Before you begin

Using fluorescent imaging to visualize spatial patterns of colonization in a multispecies biofilm is feasible only when it is possible to contrast both species with specific fluorophores. Having one partner expressing a fluorescent reporter (i.e. GFP) is enough as it can be combined with a second dye (i.e. nucleic acid probe SYTO 61) to label all the population in a second colour. The contrast between strains can be obtained with Gram staining, fluorescently labelled antibody or DNA probe (see Section 2.2).

All bacterial strains do not exhibit a similar adhesion rate on a specific surface. Hence to obtain a target initial ratio of adhering cells, it is necessary to calibrate the

relation between the number of planktonic cells added in the well and the number of adherent cells after incubation and rinsing.

In our example, we target a ratio of 0.50 ± 0.25 of each bacterial partner as estimated by quantifying the biovolume of adherent cells by CLSM using their respective fluorescent signatures (GFP or SYTO 61). If the value is not in the range, adjust the relative proportion of *Bacillus* spp. and *E. coli* to perform the adhesion phase. The protocol for this step is described below.

3.2 Materials

Equipment

- Laboratory incubator at 30 °C
- Polystyrene 96-well microtiter plate with a μclear® base (Greiner Bio-one, France)
- Leica SP8 AOBS inverted confocal laser scanning microscope (CLSM, LEICA Microsystems, Germany) equipped with a water immersion X63 objective (Numerical aperture = 1.2), a water pump, high-content screening module, two next-generation ultrasensitive detectors (HyD®)
- Leica Application Suite X (LAS X) software (LEICA Microsystems, Germany)
- IMARIS® 9.3.1 software (Bitplane, Zürich, Switzerland) with the batch option
- BiofilmQ software (Hartmann et al., 2021)

Chemicals and media

- SYTO 61 (Invitrogen, Carlsbad, CA, USA)
- Tryptic Soy Broth (TSB)
- TSB agar (1.5%) plate supplemented with ampicillin at 100 μg/mL (TSA Amp 100)

Strains

- A strain that constitutively expresses GFP. Here, we used *E. coli* CIRMBP 0248 isolated from a chick intestine that contains the pCM11 plasmid carrying the *gfp* expression system and *amp* gene encoding ampicillin (Amp) resistance for its selection (Malone et al., 2009).
- Non-labelled strains. Here, we used *B. pumilus* 1273, *B. licheniformis* 1218, and *B. polymyxa* 1167.

3.3 Methods

Growth of multi-species biofilms

1. From a −80 °C cryotube, plate the *E. coli* strain on a TSA Amp 100 Petri dish and incubate it for 24 h at 30 °C
2. Transfer a representative clone into a tube containing 5 mL of TSB without antibiotics. Scrape the surface of the −80 °C cryotubes containing the *Bacillus* spp. strains and inoculate tubes containing 5 mL of TSB. Incubate the cultures over night (~16 h) at 30 °C without agitation

3. Vortex the overnight cultures 3 s to homogenize the cell suspensions, and dilute at 1:100 in TSB for all the strains. For mixed biofilms, do the same but dilute in the same tube at 1:100 *E. coli* and one of the *Bacillus* spp. cultures

   Note: Read part "Quantification to make the ratio of the initial adhesion". If the ratio GFP/SYTO 61 is not between 0.25 and 0.75 with 1:100 dilution, adjust the proportion of *Bacillus* spp. in this step.
4. Adhesion phase: load 200 µL of the diluted solution in 2 different wells as technical replicates in polystyrene 96-well microtiter plates with a µclear® base. Incubate the plate for 90 min at 30 °C
5. Replace the medium in each well with 200 µL of fresh TSB. The plate is ready for labelling to verify initial adhesion. Once the ratio check has been performed, incubate the plate for 24 h at 30 °C for observation of the mixed biofilm.

Fluorescence labelling

1. Add SYTO 61 in 1 mL of TSB to obtain 15 µM final. Vortex the solution for 5 s
2. Load 50 µL of the SYTO 61 solution into each well
3. Protect from light and incubate for 10 min at room temperature. The plate is ready for image acquisition

Image acquisition

1. Turn on the confocal microscope with all the necessary components for its use (water pump, computer, microscope stand, controller, scan head, laser power and security)
2. Open LAS X software to set up the confocal microscope. Set the intensity of the 488 nm argon laser to 30% and switch on the HeNe 633 nm laser. Wait for 15 min to reach the power stability
3. Set one HyD detector photon collection between 500 and 550 nm to detect the fluorescence emitted by GFP. Use a second HyD detector to collect the fluorescence emitted by SYTO 61 between 650 and 750 nm. For both detectors, use the gain of 10%
4. Use the 63× water immersion lens. Turn on the water pump to get a drop of water on the lens. Remove air bubbles if needed. Carefully place the 96-well plate on the confocal platform and check the stability of the plate. Open shutter or brightfield and find the right well with the light intensity. Position the lens in the centre of the well
5. Set the image acquisition parameters. Set image definition at 512 × 512 pixels (pixel size = 360 nm). Choose a scan frequency value of 600 Hz for acquisition with the bidirectional scanning mode (image rate = 1.90/s). Use 1 as the pinhole value (value calculated with the Airy algorithm that optimizes the pinhole size for the acquisition parameters). Each image is taken by choosing a z-step of 1 µm for bacterial biofilms
6. Set the 488 nm laser intensity at 70% and the 633 nm at 40% with the acousto optical tunable filter (AOTF)
7. Raise the objective to find the base of the well
8. Create a new project for each well where the different stacks of images will be saved

9. Select the area to be imaged, in our case from the bottom of the well to the top of the biofilm and acquire the stack. In our example, two stacks of images per well were taken (4 zones per condition as there were two identical wells per plate)
10. Save image stacks in ".LIF" format

Image analysis

Visualization of the biofilms

(1) Open IMARIS and create a new "observed file" with the stacks in LIF format

(2) A background substraction with a threshold automatically calculated by the software is applied manually before each image stack observation

Notes: A batch can be created to do this step automatically if all images are in the same observed file.

(3) Open an image stack in the file to be analysed

(4) Select the easy 3D visualization with the blend mode, the section mode or 3D mode to visualize the mixed-species biofilm. The blend mode allows to obtain a reconstruction of the biofilm seen from above by the compilation of the stack images with a projection of the yz axis given by the shadow on the right of the image to obtain a representation of the relief. Thin sections of the biofilm along the xy, xz and yz axes are given by the section mode which allows a more precise visualization of the species between them. In the 3D mode, you have the possibility to binarize fluorescence signals of the two channels to perform isosurfaces. To do that, select the surface option and follow the steps indicated.

Notes: For all different representations, adjust the range of fluorescence of the two channels for optimized visualization.. For iso-surface, the binarization threshold can be adjusted manually.

(5) Take a snapshot to save the processed image projection

Quantification of the ratio of the initial adhesion

(1) Open BiofilmQ software and browse the LIF image stacks. In the folder where all the images are located, a new folder per project is created

(2) With BiofilmQ, open one newly created folder content and load the image stacks in the software

Notes: If there are a lot of images (i.e. confocal project), you have the possibility to make batches to analyse everything in the same way. To do this, create new files and copy the contents of each new folder into it. Set all desired parameters of "image preparation", "segmentation", "parameter calculation", "time-series analysis" and "data export" before going to "processe shortcuts" and select task that you want to batch. Click on "perform selected tasks on current experiment folder" to start the batch.

(3) Select channel 1 that corresponds to the GFP in the segmentation option. Set thresholding using OTSU class 2 with a sensitivity of 0.5. Segment image stacks using other default parameters of the segmentation option window. Check every image stack if the two segmentations correspond to the raw

image stack without background noise and over- or under-interpreting the size of the biofilm. Do the same with channel 2, which corresponds to SYTO 61

Notes: If the segmentation is not good, all the following steps must be restarted: adjust the segmentation sensitivity if needed.

(4) In parameter calculation, check the "global biofilm properties" option. Click on "Calculate object parameter" for both channels

(5) In data export, extract .csv files for both channels. One file is created per channel

(6) In every .csv file, extract the biovolume value. Calculate the GFP/SYTO 61 ratio with the control (*E. coli* alone). If the ratio is between 0.95 and 1.05, go to the next step. If not, check that the segmentations are correct with the segmentation preview option and adjust if necessary

(7) Calculate the GFP/SYTO 61 ratio with all images using the biovolume value of the csv files. The ratio must be between 0.25 and 0.75. If not, adjust the amount of *Bacillus* spp. in the 96-well plate and repeat all steps to be within the range.

Spatial analysis of the 24 h mix species biofilms

1. As in the above steps, images of 24 h mixed biofilms are loaded into BiofilmQ. The segmentation using thresholding OTSU class 2 with a sensitivity of 0.5 and a dissection method using cubes of 10 voxels side length (3.61 μm) is performed

   Notes: As above, a good segmentation is needed for the next steps. Adjust the sensitivity if needed.
2. In parameter calculation, check "Global biofilm properties", "Distance to surface", and "Fluorescence properties" withfor the last, "Mean intensity ratio per object channel 1 and channel 2" and the "Pearson coefficient calculation"
3. Export .csv files as previously described and extract values to graph biovolume and Pearson coefficient
4. Kymographs are made using the visualization window in BiofilmQ. One channel is loaded and in the Options window, choose "3D Heatmap/kymograph as calculated per title according method" as graph type. In the parameter choose "Frame" for X-axis, "Distance_From substrate" for Y_axis and "Intensity_Mean_Ch2_Ch1" for the colour code.

Arrange the range and Bins as needed to get the desired graph size (i.e. column size and sensitivity of the column split) and plot to obtain the Kymograph.

Summary of the analysis

The example analysis that was done to illustrate the experimental protocol has the objective to study the bacterial interaction inside a mixed bi-species biofilm. First, the structure of mono-specie biofilm was generated with IMARIS software and compared to mixed bi-species biofilm of *E. coli* GFP and the *Bacillus* spp. (Fig. 3). All mono-specie biofilm covered the surface, very densely for *E. coli* GFP. The *Bacillus* spp. strains formed 3D structured biofilms filamentous for *B. licheniformis* and clusters for *B. pumilus* and *B. polymyxa*.

Bi-species mixed biofilms showed different phenotypes in comparaison to mono-specie biofilms. Large clusters of *B. licheniformis* or *B. polymyxa* with a dense and flat biofilm of *E. coli* GFP around them are observed in mixed biofilm. These clusters seems to be on the biofilm of *E. coli* GFP.
To validate these observations, quantitative analysis were performed using BiofilmQ software with 4 images for each conditions (Fig. 4). The total biovolume of mono- and bi-species biofilms were calculated with the *E. coli* GFP and *Bacillus* spp. fractions (Fig. 4A). The biovolume of *E. coli* GFP was lower than the *Bacilus* spp. and *B. pumilus* and *B. polymyxa* had more biovolume in comparaison to *B. licheniformis*. The biovolume of *E. coli* GFP in bi-species biofilms were the same as the mono-specie biofilm of *E. coli* GFP unlike *Bacillus* spp. which decrease their biovolume in the presence of *E. coli* GFP. To quantify the organization of one partner in relation to the other within the mixed biofilm, the calculation of the Pearson's correlation coefficient was done (Fig. 4B). The value of *E. coli* GFP with *B. pumilus* was higher compared to the other two mixed biofilms, showing a more homogeneous organization of both partners in this case. To completment these analysis, a kymograph showing ratio of the $\text{intensity}_{\text{SYTO61}}/\text{Intensity}_{\text{GFP}}$ was performed to further investigate the stratification of bi-species biofilms (Fig. 4C). The results showed more SYTO61 intensity values on the top of the biofilm for *B. licheniformis* and *B. polymyxa* with *E. coli* GFP, corresponding to the clusters observed previously. All quantitative analyses confirmed the observations.

Acknowledgements

V.G. doctoral fellowship was funded by the "Association Nationale de la Recherche et de la Technologie" (contract 2020/0548) in the framework of a collaboration between INRAE and LALLEMAND SAS. R.C. was a recipient of an Anses-INRAE doctoral fellowship. This work was also supported by ANR JCJC BAoBAb (ANR-21-35CE-0001). Biofilm imaging was done at the INRAE MIMA2 imaging platform https://doi.org/10.15454/1.5572348210007727E12. Some figures were created with https://biorender.com/.

References

Almstrand, R., Daims, H., Persson, F., Sörensson, F., & Hermansson, M. (2013). New methods for analysis of spatial distribution and coaggregation of microbial populations in complex biofilms. *Applied and Environmental Microbiology*, *79*(19), 5978–5987. https://doi.org/10.1128/AEM.01727-13.

Altinoglu, I., Merrifield, C. J., & Yamaichi, Y. (2019). Single molecule super-resolution imaging of bacterial cell pole proteins with high-throughput quantitative analysis pipeline. *Scientific Reports*, *9*(1), 6680. https://doi.org/10.1038/s41598-019-43051-7.

Amieva, M., & Peek, R. M. (2016). Pathobiology of *Helicobacter pylori*-induced gastric cancer. *Gastroenterology*, *150*(1), 64–78. https://doi.org/10.1053/j.gastro.2015.09.004.

Arnaouteli, S., Bamford, N. C., Stanley-Wall, N. R., & Kovács, Á. T. (2021). *Bacillus subtilis* biofilm formation and social interactions. *Nature Reviews. Microbiology*, *19*(9), 600–614. https://doi.org/10.1038/s41579-021-00540-9.

Azeredo, J., Azevedo, N. F., Briandet, R., Cerca, N., Coenye, T., Costa, A. R., et al. (2017). Critical review on biofilm methods. *Critical Reviews in Microbiology*, *43*(3), 313–351. https://doi.org/10.1080/1040841X.2016.1208146.

Barnes, A. M. T., Dale, J. L., Chen, Y., Manias, D. A., Greenwood Quaintance, K. E., Karau, M. K., et al. (2017). *Enterococcus faecalis* readily colonizes the entire gastrointestinal tract and forms biofilms in a germ-free mouse model. *Virulence*, *8*(3), 282–296. https://doi.org/10.1080/21505594.2016.1208890.

Barraud, N., Hassett, D. J., Hwang, S.-H., Rice, S. A., Kjelleberg, S., & Webb, J. S. (2006). Involvement of nitric oxide in biofilm dispersal of *Pseudomonas aeruginosa*. *Journal of Bacteriology*, *188*(21), 7344–7353. https://doi.org/10.1128/JB.00779-06.

Bassères, E., Endres, B. T., Montes-Bravo, N., Pérez-Soto, N., Rashid, T., Lancaster, C., et al. (2021). Visualization of fidaxomicin association with the exosporium layer of *Clostridioides difficile* spores. *Anaerobe*, *69*, 102352. https://doi.org/10.1016/j.anaerobe.2021.102352.

Batt, C. A., & Tortorello, M. L. (Éds.). (2014). Encyclopedia of food microbiology (2nd ed.). AP, Academic Press/Elsevier.

Béchon, N., Mihajlovic, J., Lopes, A.-A., Vendrell-Fernández, S., Deschamps, J., Briandet, R., et al. (2022). *Bacteroides thetaiotaomicron* uses a widespread extracellular DNase to promote bile-dependent biofilm formation. *Proceedings of the National Academy of Sciences of the United States of America*, *119*(7), e2111228119. https://doi.org/10.1073/pnas.2111228119.

Benaissa, H., Ounoughi, K., Aujard, I., Fischer, E., Goïame, R., Nguyen, J., et al. (2021). Engineering of a fluorescent chemogenetic reporter with tunable color for advanced live-cell imaging. *Nature Communications*, *12*(1), 6989. https://doi.org/10.1038/s41467-021-27334-0.

Berk, V., Fong, J. C. N., Dempsey, G. T., Develioglu, O. N., Zhuang, X., Liphardt, J., et al. (2012). Molecular architecture and assembly principles of *Vibrio cholerae* biofilms. *Science (New York, N.Y.)*, *337*(6091), 236–239. https://doi.org/10.1126/science.1222981.

Billaudeau, C., Chastanet, A., Yao, Z., Cornilleau, C., Mirouze, N., Fromion, V., et al. (2017). Contrasting mechanisms of growth in two model rod-shaped bacteria. *Nature Communications*, *8*, 15370. https://doi.org/10.1038/ncomms15370.

Billaudeau, C., Yao, Z., Cornilleau, C., Carballido-López, R., & Chastanet, A. (2019). MreB forms subdiffraction nanofilaments during active growth in *Bacillus subtilis*. *MBio*, *10*(1). e01879-18 https://doi.org/10.1128/mBio.01879-18.

Blanchard, A. E., & Lu, T. (2015). Bacterial social interactions drive the emergence of differential spatial colony structures. *BMC Systems Biology*, *9*, 59. https://doi.org/10.1186/s12918-015-0188-5.

Bonicoli, F., Angelini, S., Riela, A., & Taiani, V. (1987). Anteposition of the tibial tuberosity in femoral-patellar arthrosis (4 to 7-year results). *La Chirurgia Degli Organi Di Movimento*, *72*(4), 327–332.

Bowler, P., Murphy, C., & Wolcott, R. (2020). Biofilm exacerbates antibiotic resistance: Is this a current oversight in antimicrobial stewardship? *Antimicrobial Resistance and Infection Control*, *9*(1), 162. https://doi.org/10.1186/s13756-020-00830-6.

Bridier, A., & Briandet, R. (2022). Microbial biofilms: Structural plasticity and emerging properties. *Microorganisms*, *10*(1), 138. https://doi.org/10.3390/microorganisms10010138.

Bridier, A., Briandet, R., Bouchez, T., & Jabot, F. (2014). A model-based approach to detect interspecific interactions during biofilm development. *Biofouling*, *30*(7), 761–771. https://doi.org/10.1080/08927014.2014.923409.

Bridier, A., Briandet, R., Thomas, V., & Dubois-Brissonnet, F. (2011). Resistance of bacterial biofilms to disinfectants: A review. *Biofouling*, *27*(9), 1017–1032. https://doi.org/10.1080/08927014.2011.626899.

Bridier, A., Dubois-Brissonnet, F., Boubetra, A., Thomas, V., & Briandet, R. (2010). The biofilm architecture of sixty opportunistic pathogens deciphered using a high throughput CLSM method. *Journal of Microbiological Methods*, *82*(1), 64–70. https://doi.org/10.1016/j.mimet.2010.04.006.

Bridier, A., Meylheuc, T., & Briandet, R. (2013). Realistic representation of *Bacillus subtilis* biofilms architecture using combined microscopy (CLSM, ESEM and FESEM). *Micron (Oxford, England: 1993)*, *48*, 65–69. https://doi.org/10.1016/j.micron.2013.02.013.

Bridier, A., Piard, J. C., Briandet, R., & Bouchez, T. (2020). Emergence of a synergistic diversity as a response to competition in *Pseudomonas putida* biofilms. *Microbial Ecology*, *80*(1), 47–59. https://doi.org/10.1007/s00248-019-01470-z.

Bridier, A., Piard, J.-C., Pandin, C., Labarthe, S., Dubois-Brissonnet, F., & Briandet, R. (2017). Spatial organization plasticity as an adaptive driver of surface microbial communities. *Frontiers in Microbiology*, *8*, 1364. https://doi.org/10.3389/fmicb.2017.01364.

Canette, A., Deschamps, J., & Briandet, R. (2019). High content screening confocal laser microscopy (HCS-CLM) to characterize biofilm 4D structural dynamic of foodborne pathogens. *Methods in Molecular Biology (Clifton, N.J.)*, *1918*, 171–182. https://doi.org/10.1007/978-1-4939-9000-9_14.

Chapman, S., Faulkner, C., Kaiserli, E., Garcia-Mata, C., Savenkov, E. I., Roberts, A. G., et al. (2008). The photoreversible fluorescent protein iLOV outperforms GFP as a reporter of plant virus infection. *Proceedings of the National Academy of Sciences of the United States of America*, *105*(50), 20038–20043. https://doi.org/10.1073/pnas.0807551105.

Charubin, K., Streett, H., & Papoutsakis, E. T. (2020). Development of strong anaerobic fluorescent reporters for *Clostridium acetobutylicum* and *Clostridium ljungdahlii* using HaloTag and SNAP-tag proteins. *Applied and Environmental Microbiology*, *86*(20), e01271-20. https://doi.org/10.1128/AEM.01271-20.

Chitlapilly Dass, S., Bosilevac, J. M., Weinroth, M., Elowsky, C. G., Zhou, Y., Anandappa, A., et al. (2020). Impact of mixed biofilm formation with environmental microorganisms on *E. coli* O157:H7 survival against sanitization. *NPJ Science of Food*, *4*, 16. https://doi.org/10.1038/s41538-020-00076-x.

Choong, F. X., Huzell, S., Rosenberg, M., Eckert, J. A., Nagaraj, M., Zhang, T., et al. (2021). A semi high-throughput method for real-time monitoring of curli producing Salmonella biofilms on air-solid interfaces. *Biofilms*, *3*, 100060. https://doi.org/10.1016/j.bioflm.2021.100060.

Christie, J. M., Hitomi, K., Arvai, A. S., Hartfield, K. A., Mettlen, M., Pratt, A. J., et al. (2012). Structural tuning of the fluorescent protein iLOV for improved photostability. *The Journal of Biological Chemistry*, *287*(26), 22295–22304. https://doi.org/10.1074/jbc.M111.318881.

Clevers, H. (2016). Modeling development and disease with organoids. *Cell*, *165*(7), 1586–1597. https://doi.org/10.1016/j.cell.2016.05.082.

Connell, J. L., Ritschdorff, E. T., Whiteley, M., & Shear, J. B. (2013). 3D printing of microscopic bacterial communities. *Proceedings of the National Academy of Sciences of the United States of America*, *110*(46), 18380–18385. https://doi.org/10.1073/pnas.1309729110.

Costache, V., Hebras, C., Pruliere, G., Besnardeau, L., Failla, M., Copley, R. R., et al. (2017). Kif2 localizes to a subdomain of cortical endoplasmic reticulum that drives asymmetric spindle position. *Nature Communications*, *8*(1), 917. https://doi.org/10.1038/s41467-017-01048-8.

Daims, H., Lücker, S., & Wagner, M. (2006). Daime, a novel image analysis program for microbial ecology and biofilm research. *Environmental Microbiology*, *8*(2), 200–213. https://doi.org/10.1111/j.1462-2920.2005.00880.x.

Dar, D., Dar, N., Cai, L., & Newman, D. K. (2021). Spatial transcriptomics of planktonic and sessile bacterial populations at single-cell resolution. *Science (New York, N.Y.)*, *373*(6556), eabi4882. https://doi.org/10.1126/science.abi4882.

Day, R. N., & Davidson, M. W. (2009). The fluorescent protein palette: Tools for cellular imaging. *Chemical Society Reviews*, *38*(10), 2887–2921. https://doi.org/10.1039/b901966a.

de Beer, D., Stoodley, P., Roe, F., & Lewandowski, Z. (1994). Effects of biofilm structures on oxygen distribution and mass transport. *Biotechnology and Bioengineering*, *43*(11), 1131–1138. https://doi.org/10.1002/bit.260431118.

Dekkers, J. F., Alieva, M., Wellens, L. M., Ariese, H. C. R., Jamieson, P. R., Vonk, A. M., et al. (2019). High-resolution 3D imaging of fixed and cleared organoids. *Nature Protocols*, *14*(6), 1756–1771. https://doi.org/10.1038/s41596-019-0160-8.

Deshmukh, R. A., Joshi, K., Bhand, S., & Roy, U. (2016). Recent developments in detection and enumeration of waterborne bacteria: A retrospective minireview. *MicrobiologyOpen*, *5*(6), 901–922. https://doi.org/10.1002/mbo3.383.

Díaz-Pascual, F., Lempp, M., Nosho, K., Jeckel, H., Jo, J. K., Neuhaus, K., et al. (2021). Spatial alanine metabolism determines local growth dynamics of *Escherichia coli* colonies. *eLife*, *10*, e70794. https://doi.org/10.7554/eLife.70794.

Doiron, K., Linossier, I., Fay, F., Yong, J., Abd Wahid, E., Hadjiev, D., et al. (2012). Dynamic approaches of mixed species biofilm formation using modern technologies. *Marine Environmental Research*, *78*, 40–47. https://doi.org/10.1016/j.marenvres.2012.04.001.

Douterelo, I., Jackson, M., Solomon, C., & Boxall, J. (2016). Microbial analysis of in situ biofilm formation in drinking water distribution systems: Implications for monitoring and control of drinking water quality. *Applied Microbiology and Biotechnology*, *100*(7), 3301–3311. https://doi.org/10.1007/s00253-015-7155-3.

Drepper, T., Eggert, T., Circolone, F., Heck, A., Krauss, U., Guterl, J.-K., et al. (2007). Reporter proteins for in vivo fluorescence without oxygen. *Nature Biotechnology*, *25*(4), 443–445. https://doi.org/10.1038/nbt1293.

Dubois, T., Tremblay, Y. D. N., Hamiot, A., Martin-Verstraete, I., Deschamps, J., Monot, M., et al. (2019). A microbiota-generated bile salt induces biofilm formation in Clostridium difficile. *NPJ Biofilms and Microbiomes*, *5*(1), 14. https://doi.org/10.1038/s41522-019-0087-4.

Dunn, K. W., Kamocka, M. M., & McDonald, J. H. (2011). A practical guide to evaluating colocalization in biological microscopy. *American Journal of Physiology. Cell Physiology*, *300*(4), C723–C742. https://doi.org/10.1152/ajpcell.00462.2010.

Elias, S., & Banin, E. (2012). Multi-species biofilms: Living with friendly neighbors. *FEMS Microbiology Reviews*, *36*(5), 990–1004. https://doi.org/10.1111/j.1574-6976.2012.00325.x.

Esser, D. S., Leveau, J. H. J., Meyer, K. M., & Wiegand, K. (2015). Spatial scales of interactions among bacteria and between bacteria and the leaf surface. *FEMS Microbiology Ecology*, *91*(3), fiu034. https://doi.org/10.1093/femsec/fiu034.

Fagerlund, A., Langsrud, S., & Møretrø, T. (2021). Microbial diversity and ecology of biofilms in food industry environments associated with *Listeria monocytogenes* persistence. *Current Opinion in Food Science*, *37*, 171–178. https://doi.org/10.1016/j.cofs.2020.10.015.

Farasin, J., Koechler, S., Varet, H., Deschamps, J., Dillies, M.-A., Proux, C., et al. (2017). Comparison of biofilm formation and motility processes in arsenic-resistant *Thiomonas* spp. strains revealed divergent response to arsenite. *Microbial Biotechnology*, *10*(4), 789–803. https://doi.org/10.1111/1751-7915.12556.

Flemming, H.-C., Neu, T. R., & Wingender, J. (Eds.). (2017). *The perfect slime: Microbial extracellular polymeric sibstances (EPS)*. IWA Publishing.

Flemming, H.-C., Wingender, J., Szewzyk, U., Steinberg, P., Rice, S. A., & Kjelleberg, S. (2016). Biofilms: An emergent form of bacterial life. *Nature Reviews. Microbiology*, *14*(9), 563–575. https://doi.org/10.1038/nrmicro.2016.94.

Frickmann, H., Zautner, A. E., Moter, A., Kikhney, J., Hagen, R. M., Stender, H., et al. (2017). Fluorescence in situ hybridization (FISH) in the microbiological diagnostic routine laboratory: A review. *Critical Reviews in Microbiology*, *43*(3), 263–293. https://doi.org/10.3109/1040841X.2016.1169990.

Giaouris, E., Heir, E., Desvaux, M., Hébraud, M., Møretrø, T., Langsrud, S., et al. (2015). Intra- and inter-species interactions within biofilms of important foodborne bacterial pathogens. *Frontiers in Microbiology*, *6*, 841. https://doi.org/10.3389/fmicb.2015.00841.

Grand, I., Bellon-Fontaine, M.-N., Herry, J.-M., Hilaire, D., Moriconi, F.-X., & Naïtali, M. (2011). Possible overestimation of surface disinfection efficiency by assessment methods based on liquid sampling procedures as demonstrated by in situ quantification of spore viability. *Applied and Environmental Microbiology*, *77*(17), 6208–6214. https://doi.org/10.1128/AEM.00649-11.

Guéneau, V., Rodiles, A., Piard, J.-C., Frayssinet, B., Castex, M., Plateau-Gonthier, J., et al. (2021). Capture and ex-situ analysis of environmental biofilms in livestock buildings. *Microorganisms*, *10*(1), 2. https://doi.org/10.3390/microorganisms10010002.

Guilbaud, M., Piveteau, P., Desvaux, M., Brisse, S., & Briandet, R. (2015). Exploring the diversity of *listeria monocytogenes* biofilm architecture by high-throughput confocal laser scanning microscopy and the predominance of the honeycomb-like morphotype. *Applied and Environmental Microbiology*, *81*(5), 1813–1819. https://doi.org/10.1128/AEM.03173-14.

Guilini, C., Baehr, C., Schaeffer, E., Gizzi, P., Rufi, F., Haiech, J., et al. (2015). New fluorescein precursors for live bacteria detection. *Analytical Chemistry*, *87*(17), 8858–8866. https://doi.org/10.1021/acs.analchem.5b02100.

Habimana, O., Guillier, L., Kulakauskas, S., & Briandet, R. (2011). Spatial competition with *Lactococcus lactis* in mixed-species continuous-flow biofilms inhibits *Listeria monocytogenes* growth. *Biofouling*, *27*(9), 1065–1072. https://doi.org/10.1080/08927014.2011.626124.

Hall, D. C., Palmer, P., Ji, H.-F., Ehrlich, G. D., & Król, J. E. (2021). Bacterial biofilm growth on 3D-printed materials. *Frontiers in Microbiology*, *12*, 646303. https://doi.org/10.3389/fmicb.2021.646303.

Han, X., Mslati, M. A., Davies, E., Chen, Y., Allaire, J. M., & Vallance, B. A. (2021). Creating a more perfect union: Modeling intestinal Bacteria-epithelial interactions using organoids. *Cellular and Molecular Gastroenterology and Hepatology*, *12*(2), 769–782. https://doi.org/10.1016/j.jcmgh.2021.04.010.

Hartmann, R., Jeckel, H., Jelli, E., Singh, P. K., Vaidya, S., Bayer, M., et al. (2021). Quantitative image analysis of microbial communities with BiofilmQ. *Nature Microbiology*, *6*(2), 151–156. https://doi.org/10.1038/s41564-020-00817-4.

Hautefort, I., Proença, M. J., & Hinton, J. C. D. (2003). Single-copy green fluorescent protein gene fusions allow accurate measurement of *Salmonella* gene expression in vitro and during infection of mammalian cells. *Applied and Environmental Microbiology*, *69*(12), 7480–7491. https://doi.org/10.1128/AEM.69.12.7480-7491.2003.

Hauth, J., Chodorski, J., Wirsen, A., & Ulber, R. (2020). Improved FRAP measurements on biofilms. *Biophysical Journal*, *118*(10), 2354–2365. https://doi.org/10.1016/j.bpj.2020.03.017.

Hernández-Galán, L., Cattenoz, T., Le Feunteun, S., Canette, A., Briandet, R., Le-Guin, S., et al. (2017). Effect of dairy matrices on the survival of *Streptococcus thermophilus*, *Brevibacterium aurantiacum* and *Hafnia alvei* during digestion. *Food Research International (Ottawa, Ont.)*, *100*(Pt 1), 477–488. https://doi.org/10.1016/j.foodres.2017.07.044.

Heumann, A., Assifaoui, A., Da Silva Barreira, D., Thomas, C., Briandet, R., Laurent, J., et al. (2020). Intestinal release of biofilm-like microcolonies encased in calcium-pectinate beads increases probiotic properties of *Lacticaseibacillus paracasei*. *NPJ Biofilms and Microbiomes*, *6*(1), 44. https://doi.org/10.1038/s41522-020-00159-3.

Høiby, N., Bjarnsholt, T., Givskov, M., Molin, S., & Ciofu, O. (2010). Antibiotic resistance of bacterial biofilms. *International Journal of Antimicrobial Agents*, *35*(4), 322–332. https://doi.org/10.1016/j.ijantimicag.2009.12.011.

Huang, Y., Xia, A., Yang, G., & Jin, F. (2018). Bioprinting living biofilms through optogenetic manipulation. *ACS Synthetic Biology*, *7*(5), 1195–1200. https://doi.org/10.1021/acssynbio.8b00003.

Jeckel, H., & Drescher, K. (2021). Advances and opportunities in image analysis of bacterial cells and communities. *FEMS Microbiology Reviews*, *45*(4), fuaa062. https://doi.org/10.1093/femsre/fuaa062.

Jo, J., Price-Whelan, A., & Dietrich, L. E. P. (2022). Gradients and consequences of heterogeneity in biofilms. *Nature Reviews. Microbiology*. https://doi.org/10.1038/s41579-022-00692-2.

Johnson, M. B., & Criss, A. K. (2013). Fluorescence microscopy methods for determining the viability of bacteria in association with mammalian cells. *Journal of Visualized Experiments: JoVE*, *79*. https://doi.org/10.3791/50729.

Karampatzakis, A., Sankaran, J., Kandaswamy, K., Rice, S. A., Cohen, Y., & Wohland, T. (2017). Measurement of oxygen concentrations in bacterial biofilms using transient state monitoring by single plane illumination microscopy. *Biomedical Physics & Engineering Express*, *3*(3), 035020. https://doi.org/10.1088/2057-1976/aa6db7.

Karygianni, L., Ren, Z., Koo, H., & Thurnheer, T. (2020). Biofilm Matrixome: Extracellular components in structured microbial communities. *Trends in Microbiology*, *28*(8), 668–681. https://doi.org/10.1016/j.tim.2020.03.016.

Keppler, A., Gendreizig, S., Gronemeyer, T., Pick, H., Vogel, H., & Johnsson, K. (2003). A general method for the covalent labeling of fusion proteins with small molecules in vivo. *Nature Biotechnology*, *21*(1), 86–89. https://doi.org/10.1038/nbt765.

Kim, D., Barraza, J. P., Arthur, R. A., Hara, A., Lewis, K., Liu, Y., et al. (2020). Spatial mapping of polymicrobial communities reveals a precise biogeography associated with human dental caries. *Proceedings of the National Academy of Sciences of the United States of America*, *117*(22), 12375–12386. https://doi.org/10.1073/pnas.1919099117.

Krishna Kumar, R., Meiller-Legrand, T. A., Alcinesio, A., Gonzalez, D., Mavridou, D. A. I., Meacock, O. J., et al. (2021). Droplet printing reveals the importance of micron-scale structure for bacterial ecology. *Nature Communications*, *12*(1), 857. https://doi.org/10.1038/s41467-021-20996-w.

Kristensen, M. F., Leonhardt, D., Neland, M. L. B., & Schlafer, S. (2020). A 3D printed microfluidic flow-cell for microscopy analysis of in situ-grown biofilms. *Journal of Microbiological Methods*, *171*, 105876. https://doi.org/10.1016/j.mimet.2020.105876.

Kühbacher, A., Cossart, P., & Pizarro-Cerdá, J. (2021). Internalization assays for *Listeria monocytogenes*. *Methods in Molecular Biology (Clifton, N.J.)*, *2220*, 189–200. https://doi.org/10.1007/978-1-0716-0982-8_15.

Lagache, T., Lang, G., Sauvonnet, N., & Olivo-Marin, J.-C. (2013). Analysis of the spatial organization of molecules with robust statistics. *PLoS One*, *8*(12), e80914. https://doi.org/10.1371/journal.pone.0080914.

Lagache, T., Sauvonnet, N., Danglot, L., & Olivo-Marin, J.-C. (2015). Statistical analysis of molecule colocalization in bioimaging. *Cytometry. Part A: The Journal of the International Society for Analytical Cytology*, *87*(6), 568–579. https://doi.org/10.1002/cyto.a.22629.

Lagendijk, E. L., Validov, S., Lamers, G. E. M., de Weert, S., & Bloemberg, G. V. (2010). Genetic tools for tagging Gram-negative bacteria with mCherry for visualization in vitro and in natural habitats, biofilm and pathogenicity studies. *FEMS Microbiology Letters*, *305*(1), 81–90. https://doi.org/10.1111/j.1574-6968.2010.01916.x.

Lee, K. W. K., Periasamy, S., Mukherjee, M., Xie, C., Kjelleberg, S., & Rice, S. A. (2014). Biofilm development and enhanced stress resistance of a model, mixed-species community biofilm. *The ISME Journal*, *8*(4), 894–907. https://doi.org/10.1038/ismej.2013.194.

Lee, J.-Y., Sadler, N. C., Egbert, R. G., Anderton, C. R., Hofmockel, K. S., Jansson, J. K., et al. (2020). Deep learning predicts microbial interactions from self-organized spatiotemporal patterns. *Computational and Structural Biotechnology Journal*, *18*, 1259–1269. https://doi.org/10.1016/j.csbj.2020.05.023.

Li, Q., Liu, L., Guo, A., Zhang, X., Liu, W., & Ruan, Y. (2021). Formation of multispecies biofilms and their resistance to disinfectants in food processing environments: A review. *Journal of Food Protection*, *84*(12), 2071–2083. https://doi.org/10.4315/JFP-21-071.

Liu, W., Røder, H. L., Madsen, J. S., Bjarnsholt, T., Sørensen, S. J., & Burmølle, M. (2016). Interspecific bacterial interactions are reflected in multispecies biofilm spatial organization. *Frontiers in Microbiology*, *7*, 1366. https://doi.org/10.3389/fmicb.2016.01366.

Los, G. V., Encell, L. P., McDougall, M. G., Hartzell, D. D., Karassina, N., Zimprich, C., et al. (2008). HaloTag: A novel protein labeling technology for cell imaging and protein analysis. *ACS Chemical Biology*, *3*(6), 373–382. https://doi.org/10.1021/cb800025k.

Lu, M., Wang, X., Sun, G., Qin, B., Xiao, J., Yan, S., et al. (2014). Fine structure of Tibetan kefir grains and their yeast distribution, diversity, and shift. *PLoS One*, *9*(6), e101387. https://doi.org/10.1371/journal.pone.0101387.

Malone, C. L., Boles, B. R., Lauderdale, K. J., Thoendel, M., Kavanaugh, J. S., & Horswill, A. R. (2009). Fluorescent reporters for Staphylococcus aureus. *Journal of Microbiological Methods*, *77*(3), 251–260. https://doi.org/10.1016/j.mimet.2009.02.011.

Mark Welch, J. L., Rossetti, B. J., Rieken, C. W., Dewhirst, F. E., & Borisy, G. G. (2016). Biogeography of a human oral microbiome at the micron scale. *Proceedings of the National Academy of Sciences of the United States of America*, *113*(6), E791–E800. https://doi.org/10.1073/pnas.1522149113.

Minsky, M. (1988). Memoir on inventing the confocal scanning microscope: Memoir on inventing the confocal scanning microscope. *Scanning*, *10*(4), 128–138. https://doi.org/10.1002/sca.4950100403.

Monmeyran, A., Thomen, P., Jonquière, H., Sureau, F., Li, C., Plamont, M.-A., et al. (2018). The inducible chemical-genetic fluorescent marker FAST outperforms classical fluorescent proteins in the quantitative reporting of bacterial biofilm dynamics. *Scientific Reports*, *8*(1), 10336. https://doi.org/10.1038/s41598-018-28643-z.

Mukherjee, A., Weyant, K. B., Agrawal, U., Walker, J., Cann, I. K. O., & Schroeder, C. M. (2015). Engineering and characterization of new LOV-based fluorescent proteins from *Chlamydomonas reinhardtii* and *Vaucheria frigida*. *ACS Synthetic Biology*, *4*(4), 371–377. https://doi.org/10.1021/sb500237x.

Munir, M. T., Maneewan, N., Pichon, J., Gharbia, M., Oumarou-Mahamane, I., Baude, J., et al. (2021). Confocal spectral microscopy, a non-destructive approach to follow contamination and biofilm formation of mCherry *Staphylococcus aureus* on solid surfaces. *Scientific Reports*, *11*(1), 15574. https://doi.org/10.1038/s41598-021-94939-2.

Neu, T. R., & Lawrence, J. R. (1999). Lectin-binding analysis in biofilm systems. *Methods in Enzymology*, *310*, 145–152. https://doi.org/10.1016/s0076-6879(99)10012-0.

Nicolle, O., Rouillon, A., Guyodo, H., Tamanai-Shacoori, Z., Chandad, F., Meuric, V., et al. (2010). Development of SNAP-tag-mediated live cell labeling as an alternative to GFP in *Porphyromonas gingivalis*. *FEMS Immunology and Medical Microbiology*, *59*(3), 357–363. https://doi.org/10.1111/j.1574-695X.2010.00681.x.

Ning, E., Turnbull, G., Clarke, J., Picard, F., Riches, P., Vendrell, M., et al. (2019). 3D bioprinting of mature bacterial biofilms for antimicrobial resistance drug testing. *Biofabrication*, *11*(4), 045018. https://doi.org/10.1088/1758-5090/ab37a0.

Noirot-Gros, M.-F., Shinde, S. V., Akins, C., Johnson, J. L., Zerbs, S., Wilton, R., et al. (2020). Functional imaging of microbial interactions with tree roots using a microfluidics setup. *Frontiers in Plant Science*, *11*, 408. https://doi.org/10.3389/fpls.2020.00408.

O'Donnell, A. G., Young, I. M., Rushton, S. P., Shirley, M. D., & Crawford, J. W. (2007). Visualization, modelling and prediction in soil microbiology. *Nature Reviews. Microbiology*, *5*(9), 689–699. https://doi.org/10.1038/nrmicro1714.

Oliveira, N. M., Oliveria, N. M., Martinez-Garcia, E., Xavier, J., Durham, W. M., Kolter, R., et al. (2015). Biofilm formation as a response to ecological competition. *PLoS Biology*, *13*(7), e1002191. https://doi.org/10.1371/journal.pbio.1002191.

Olpe, H. R., Glatt, A., Laszlo, J., & Schellenberg, A. (1980). Some electrophysiological and pharmacological properties of the cortical, noradrenergic projection of the locus coeruleus in the rat. *Brain Research*, *186*(1), 9–19. https://doi.org/10.1016/0006-8993(80)90251-6.

Pamp, S. J., Sternberg, C., & Tolker-Nielsen, T. (2009). Insight into the microbial multicellular lifestyle via flow-cell technology and confocal microscopy. *Cytometry. Part A: The Journal of the International Society for Analytical Cytology*, *75*(2), 90–103. https://doi.org/10.1002/cyto.a.20685.

Pandin, C., Darsonval, M., Mayeur, C., Le Coq, D., Aymerich, S., & Briandet, R. (2019). Biofilm formation and synthesis of antimicrobial compounds by the biocontrol agent *Bacillus velezensis* QST713 in an Agaricus bisporus compost micromodel. *Applied and Environmental Microbiology*, *85*(12). e00327-19 https://doi.org/10.1128/AEM.00327-19.

Panigrahi, S., Murat, D., Le Gall, A., Martineau, E., Goldlust, K., Fiche, J.-B., et al. (2021). Misic, a general deep learning-based method for the high-throughput cell segmentation of complex bacterial communities. *eLife*, *10*, e65151. https://doi.org/10.7554/eLife.65151.

Petrovai, A., & Nedevschi, S. (2022). Fast panoptic segmentation with soft attention Embeddings. *Sensors (Basel, Switzerland)*, *22*(3), 783. https://doi.org/10.3390/s22030783.

Plamont, M.-A., Billon-Denis, E., Maurin, S., Gauron, C., Pimenta, F. M., Specht, C. G., et al. (2016). Small fluorescence-activating and absorption-shifting tag for tunable protein imaging in vivo. *Proceedings of the National Academy of Sciences of the United States of America*, *113*(3), 497–502. https://doi.org/10.1073/pnas.1513094113.

Pouget, C., Dunyach-Remy, C., Pantel, A., Schuldiner, S., Sotto, A., & Lavigne, J.-P. (2021). New adapted in vitro technology to evaluate biofilm formation and antibiotic activity using live imaging under flow conditions. *Diagnostics (Basel, Switzerland)*, *11*(10), 1746. https://doi.org/10.3390/diagnostics11101746.

Qin, B., Fei, C., Bridges, A. A., Mashruwala, A. A., Stone, H. A., Wingreen, N. S., et al. (2020). Cell position fates and collective fountain flow in bacterial biofilms revealed by light-sheet microscopy. *Science (New York, N.Y.)*, *369*(6499), 71–77. https://doi.org/10.1126/science.abb8501.

Ragi, S., Rahman, M. H., Duckworth, J., Kalimuthu, J., Chundi, P., & Gadhamshetty, V. (2021). Artificial intelligence-driven image analysis of bacterial cells and biofilms. *IEEE/ACM Transactions on Computational Biology and Bioinformatics*. https://doi.org/10.1109/TCBB.2021.3138304.

Ramírez-Puebla, S. T., Weigel, B. L., Jack, L., Schlundt, C., Pfister, C. A., & Mark Welch, J. L. (2022). Spatial organization of the kelp microbiome at micron scales. *Microbiome*, *10*(1), 52. https://doi.org/10.1186/s40168-022-01235-w.

Reuter, A., Virolle, C., Goldlust, K., Berne-Dedieu, A., Nolivos, S., & Lesterlin, C. (2020). Direct visualisation of drug-efflux in live *Escherichia coli* cells. *FEMS Microbiology Reviews*, *44*(6), 782–792. https://doi.org/10.1093/femsre/fuaa031.

Romani, M., Carrion, C., Fernandez, F., Lebaron, P., & Lami, R. (2021). Methyl potassium Siliconate and siloxane inhibit the formation of multispecies biofilms on ceramic roof tiles: Efficiency and comparison of two common water repellents. *Microorganisms*, *9*(2), 394. https://doi.org/10.3390/microorganisms9020394.

Sadiq, F. A., Burmølle, M., Heyndrickx, M., Flint, S., Lu, W., Chen, W., et al. (2021). Community-wide changes reflecting bacterial interspecific interactions in multispecies biofilms. *Critical Reviews in Microbiology*, *47*(3), 338–358. https://doi.org/10.1080/1040841X.2021.1887079.

Saint Martin, C., Darsonval, M., Grégoire, M., Caccia, N., Midoux, L., Berland, S., et al. (2022). Spatial organisation of *Listeria monocytogenes* and *Escherichia coli O157:H7* cultivated in gel matrices. *Food Microbiology*, *103*, 103965. https://doi.org/10.1016/j.fm.2021.103965.

Sanchez-Vizuete, P., Dergham, Y., Bridier, A., Deschamps, J., Dervyn, E., Hamze, K., et al. (2022). The coordinated population redistribution between *Bacillus subtilis* submerged biofilm and liquid-air pellicle. *Biofilms*, *4*, 100065. https://doi.org/10.1016/j.bioflm.2021.100065.

Sanchez-Vizuete, P., Orgaz, B., Aymerich, S., Le Coq, D., & Briandet, R. (2015). Pathogens protection against the action of disinfectants in multispecies biofilms. *Frontiers in Microbiology*, *6*, 705. https://doi.org/10.3389/fmicb.2015.00705.

Schillinger, C., Petrich, A., Lux, R., Riep, B., Kikhney, J., Friedmann, A., et al. (2012). Co-localized or randomly distributed? Pair cross correlation of in vivo grown subgingival biofilm bacteria quantified by digital image analysis. *PLoS One*, *7*(5), e37583. https://doi.org/10.1371/journal.pone.0037583.

Schulmeister, S., Ruttorf, M., Thiem, S., Kentner, D., Lebiedz, D., & Sourjik, V. (2008). Protein exchange dynamics at chemoreceptor clusters in *Escherichia coli*. *Proceedings of the National Academy of Sciences of the United States of America*, *105*(17), 6403–6408. https://doi.org/10.1073/pnas.0710611105.

Shaner, N. C., Campbell, R. E., Steinbach, P. A., Giepmans, B. N. G., Palmer, A. E., & Tsien, R. Y. (2004). Improved monomeric red, orange and yellow fluorescent proteins derived from *Discosoma* sp. red fluorescent protein. *Nature Biotechnology*, *22*(12), 1567–1572. https://doi.org/10.1038/nbt1037.

Shank, E. A., Klepac-Ceraj, V., Collado-Torres, L., Powers, G. E., Losick, R., & Kolter, R. (2011). Interspecies interactions that result in *Bacillus subtilis* forming biofilms are mediated mainly by members of its own genus. *Proceedings of the National Academy of Sciences of the United States of America*, *108*(48), E1236–E1243. https://doi.org/10.1073/pnas.1103630108.

Shimomura, O., Johnson, F. H., & Saiga, Y. (1962). Extraction, purification and properties of aequorin, a bioluminescent protein from the luminous hydromedusan, *Aequorea*. *Journal of Cellular and Comparative Physiology*, *59*, 223–239. https://doi.org/10.1002/jcp.1030590302.

Silva, T. S. O., Freitas, A. R., Pinheiro, M. L. L., do Nascimento, C., Watanabe, E., & Albuquerque, R. F. (2018). Oral biofilm formation on different materials for dental implants. *Journal of Visualized Experiments: JoVE*, *136*. https://doi.org/10.3791/57756.

Steinberg, S., Grinberg, M., Beitelman, M., Peixoto, J., Orevi, T., & Kashtan, N. (2021). Two-way microscale interactions between immigrant bacteria and plant leaf microbiota as revealed by live imaging. *The ISME Journal*, *15*(2), 409–420. https://doi.org/10.1038/s41396-020-00767-z.

Streett, H., Charubin, K., & Papoutsakis, E. T. (2021). Anaerobic fluorescent reporters for cell identification, microbial cell biology and high-throughput screening of microbiota and genomic libraries. *Current Opinion in Biotechnology*, *71*, 151–163. https://doi.org/10.1016/j.copbio.2021.07.005.

Tawakoli, P. N., Al-Ahmad, A., Hoth-Hannig, W., Hannig, M., & Hannig, C. (2013). Comparison of different live/dead stainings for detection and quantification of adherent microorganisms in the initial oral biofilm. *Clinical Oral Investigations*, *17*(3), 841–850. https://doi.org/10.1007/s00784-012-0792-3.

Thomsen, H., Graf, F. E., Farewell, A., & Ericson, M. B. (2018). Exploring photoinactivation of microbial biofilms using laser scanning microscopy and confined 2-photon excitation. *Journal of Biophotonics*, *11*(10), e201800018. https://doi.org/10.1002/jbio.201800018.

Tolker-Nielsen, T., & Sternberg, C. (2011). Growing and analyzing biofilms in flow chambers. *Current Protocols in Microbiology*. *Chapter 1*, Unit 1B.2 https://doi.org/10.1002/9780471729259.mc01b02s21.

Tolker-Nielsen, T., & Sternberg, C. (2014). Methods for studying biofilm formation: Flow cells and confocal laser scanning microscopy. *Methods in Molecular Biology (Clifton, N.J.)*, *1149*, 615–629. https://doi.org/10.1007/978-1-4939-0473-0_47.

Tran, T., Grandvalet, C., Winckler, P., Verdier, F., Martin, A., Alexandre, H., et al. (2021). Shedding light on the formation and structure of Kombucha biofilm using two-photon fluorescence microscopy. *Frontiers in Microbiology*, *12*, 725379. https://doi.org/10.3389/fmicb.2021.725379.

van Tatenhove-Pel, R. J., Rijavec, T., Lapanje, A., van Swam, I., Zwering, E., Hernandez-Valdes, J. A., et al. (2021). Microbial competition reduces metabolic interaction distances to the low µm-range. *The ISME Journal*, *15*(3), 688–701. https://doi.org/10.1038/s41396-020-00806-9.

Wu, B. C., Haney, E. F., Akhoundsadegh, N., Pletzer, D., Trimble, M. J., Adriaans, A. E., et al. (2021). Human organoid biofilm model for assessing antibiofilm activity of novel agents. *NPJ Biofilms and Microbiomes*, *7*(1), 8. https://doi.org/10.1038/s41522-020-00182-4.

Xu, J.-G., Hu, H.-X., Han, B.-Z., & Chen, J.-Y. (2022). Interactions between *Salmonella enteritidis* and food processing facility isolate *Bacillus paramycoides* B5 in dual-species biofilms. *LWT*, *156*, 113053. https://doi.org/10.1016/j.lwt.2021.113053.

Yarwood, J. M., Bartels, D. J., Volper, E. M., & Greenberg, E. P. (2004). Quorum sensing in *Staphylococcus aureus* biofilms. *Journal of Bacteriology*, *186*(6), 1838–1850. https://doi.org/10.1128/JB.186.6.1838-1850.2004.

Yuan, L., de Haan, P., Peterson, B. W., de Jong, E. D., Verpoorte, E., van der Mei, H. C., et al. (2020). Visualization of bacterial colonization and cellular layers in a gut-on-a-chip system using optical coherence tomography. *Microscopy and Microanalysis: The Official Journal of Microscopy Society of America, Microbeam Analysis Society, Microscopical Society of Canada*, *26*(6), 1211–1219. https://doi.org/10.1017/S143192762002454X.

Zaborskytė, G., Wistrand-Yuen, E., Hjort, K., Andersson, D. I., & Sandegren, L. (2021). Modular 3D-printed peg biofilm device for flexible setup of surface-related biofilm studies. *Frontiers in Cellular and Infection Microbiology*, *11*, 802303. https://doi.org/10.3389/fcimb.2021.802303.

Zhang, M., Zhang, J., Wang, Y., Wang, J., Achimovich, A. M., Acton, S. T., et al. (2020). Non-invasive single-cell morphometry in living bacterial biofilms. *Nature Communications*, *11*(1), 6151. https://doi.org/10.1038/s41467-020-19866-8.

Zijnge, V., van Leeuwen, M. B. M., Degener, J. E., Abbas, F., Thurnheer, T., Gmür, R., et al. (2010). Oral biofilm architecture on natural teeth. *PLoS One*, *5*(2), e9321. https://doi.org/10.1371/journal.pone.0009321.

3 PRESENTATION DES RESULTATS

3.1 CHAPITRE 1 - CARACTERISATION DES COMMUNAUTES MICROBIENNES ASSOCIEES AUX SURFACES DE BATIMENTS D'ELEVAGE ET OBSERVATION DE LEURS MODULATIONS PAR L'APPLICATION D'UN BIOFILM POSITIF

3.1.1 Préambule

Le premier objectif de mon projet de recherche a été de développer une méthode de prélèvement des communautés microbiennes spatialement organisées sur les surfaces des bâtiments d'élevage. Cette approche, basée sur l'échantillonnage de coupons, a été associée à une analyse *ex-situ* en laboratoire. Dans ce chapitre, je présente dans un premier temps les résultats des études terrains qui ont permis de mettre au point cette méthode, la rendant standardisée et reproductible. Les techniques couramment utilisées, basées sur les écouvillonnages, boîtes de contact, chiffonnettes, ou éponges ne permettent pas le décrochement total des microorganismes associés et déstructurent les biofilms [37]. Or, cette formation du biofilm est une caractéristique importante car elle est intimement liée à la tolérance des microorganismes aux stress environnementaux et est impliquée dans les mécanismes d'interaction entre les différentes espèces de la communauté. L'utilisation de la MCBL, couplée à l'analyse d'image, a permis d'étudier la structuration en 3D des biofilms. Parallèlement, des dénombrements sur différents milieux sélectifs ont été effectués pour étudier le nombre de bactéries viables et cultivables présentes dans ces communautés. Enfin, une analyse de la diversité des espèces a été réalisée par séquençage à haut débit du gène de l'ARNr 16S.

L'approche d'étude des biofilms de surface a tout d'abord été testée dans un élevage de poulet expérimental de la société Lallemand. Cette étude a constitué un préalable à sa mise en œuvre au sein d'élevages commerciaux à plus grande échelle. La même stratégie de prélèvement et d'étude des biofilms a également été reproduite dans un élevage commercial porcin. Des coupons composés de

matériaux représentatifs de bâtiment d'élevage tels que le PVC, l'acier galvanisé ou inoxydable ont été placés sur les surfaces en contact avec les animaux avant leur arrivée dans le bâtiment. L'échantillonnage au fil du temps, suivi d'une analyse *ex-situ* au laboratoire, a permis d'étudier de manière globale les communautés attachées aux surfaces des coupons dans ces environnements. Suite aux résultats obtenus, nous avons décidé de nous focaliser pour la suite du projet sur l'élevage avicole comme système d'étude, moins contraignant que le système porcin. L'observation de l'expérimentation préliminaire en élevage de poulet de chair est décrite en **annexe**, tandis que l'étude en élevage porcin est détaillée dans l'**article 3**.

La méthodologie d'échantillonnage à l'aide des coupons a également permis l'isolement de souches environnementales. Par exemple, des souches sporulantes d'intérêt ont été isolées sur un milieu gélosé riche (TSA) à partir des biofilms sur les coupons puis cultivées en milieu liquide (TSB). La suspension résultante a été traitée à 80°C pendant 10 minutes pour sélectionner les spores. Après criblage de leurs propriétés bénéfiques en condition de biofilm, ces souches pourront être considérées comme des candidates pour une utilisation potentielle en biofilm positif dans un contexte similaire (ou identique) à celui de leur isolement. Certaines de ces souches ont été caractérisées comme formant spontanément de larges quantités de biofilms et leurs génomes ont été séquencés. Un exemple avec la souche *B. velezensis* P1, isolée d'un coupon prélevé dans un élevage porcin, est décrit dans l'**article 4**.

L'effet d'un produit commercial (Lalfilm Pro®, Lallemand SAS, France) sur la modulation de la composition du microbiote de surface d'un bâtiment d'élevage de poulets de chair, après le processus de nettoyage et de désinfection, et avant l'entrée des animaux dans le bâtiment, a été étudié. Le microbiote de surface de 4 bâtiments (2 traités et 2 témoins) a été suivi au cours du temps, en présence des animaux, par la méthode de prélèvement précédemment établie. Les résultats ont mis en évidence l'effet des biofilms positifs sur la modulation du microbiote de surface des bâtiments d'élevage. De plus, cette étude a permis de générer des connaissances sur la composition et la structure des communautés microbiennes

qui composent les microbiotes présents dans ces environnements jusqu'alors peu étudiés dans la littérature. Les résultats de cette étude sont décrits dans l'**article5**.

Les communautés de microorganismes qui composent les biofilms de surfaces au sein des élevages ne sont pas connues alors même qu'elles exercent un impact direct sur la santé des animaux. La pré-existence, après l'application d'un processus de nettoyage et de désinfection tels que décrit dans l'article 5 [38], de grandes quantités de spores sur la surface des coupons avant l'arrivée des animaux dans le bâtiment, a constitué une observation cruciale. En effet, environ 3 log d'Unités Formant Colonie par cm^2 (UFC/cm^2) de spores bactériennes ont été dénombrées dans les deux bâtiments n'ayant jamais reçu de solution de biofilm positif. Le séquençage à haut débit du gène de l'ARNr 16S suivi d'une analyse de la diversité basée sur les séquences obtenues a mis en évidence une abondance relative du genre *Bacillus* représentant jusqu'à 30 % de la population totale endémique dans ces bâtiments. Certaines souches formant des spores et ayant des phénotypes de biofilm remarquables ont été prélevées au cours du temps dans les bâtiments témoins et leurs génomes séquencés. Une étude des génomes et des phénotypes de biofilms a été réalisée dans le but de caractériser ces souches, afin d'identifier de possibles bactéries indésirables ou, au contraire, des souches potentiellement candidates pour une utilisation en biofilm positif dans ces mêmes environnements. Les résultats de cette étude sont décrits dans l'**article 6**, en préparation.

En conclusion de ce chapitre, une approche combinée a été employée pour la première fois avec succès afin d'acquérir des images microscopiques de la structure des communautés présentes sur les surfaces des bâtiments élevages, tout en permettant de suivre de manière fiable, précise et reproductible leur évolution en termes de nombre et de composition au fil du temps. De plus, certaines souches du genre *Bacillus,* autochtones des bâtiments d'élevage, ont été caractérisées en se basant sur leur génome et leur phénotype en biofilm, révélant ainsi leur potentiel dans le cadre d'utilisations industrielles.

3.1.2 Article 3 : Capture and *ex-situ* analysis of environmental biofilms in livestock buildings

Virgile Guéneau, Ana Rodiles, Jean-Christophe Piard, Bastien Frayssinet, Mathieu Castex, Romain Briandet.

Microorganisms, 2022, 10 (1), pp.2. 10.3390/microorganisms10010002.

microorganisms

MDPI

Article

Capture and Ex-Situ Analysis of Environmental Biofilms in Livestock Buildings

Virgile Guéneau [1,2], Ana Rodiles [2], Jean-Christophe Piard [1], Bastien Frayssinet [2], Mathieu Castex [2], Julia Plateau-Gonthier [2] and Romain Briandet [1,*]

[1] Micalis Institute, INRAE, AgroParisTech, Université Paris-Saclay, 78350 Jouy-en-Josas, France; virgile.gueneau@inrae.fr (V.G.); jean-christophe.piard@inrae.fr (J.-C.P.)
[2] Lallemand SAS, 31702 Blagnac, France; arodiles@lallemand.com (A.R.); bfrayssinet@lallemand.com (B.F.); mcastex@lallemand.com (M.C.); jplateau@lallemand.com (J.P.-G.)
* Correspondence: romain.briandet@inrae.fr

Abstract: Little information about biofilm microbial communities on the surface of livestock buildings is available yet. While these spatially organized communities proliferate in close contact with animals and can harbor undesirable microorganisms, no standardized methods have been described to sample them non-destructively. We propose a reproducible coupon-based capture method associated with a set of complementary ex-situ analysis tools to describe the major features of those communities. To demonstrate the biofilm dynamics in a pig farm building, we analyzed the coupons on polymeric and metallic materials, as representative of these environments, over 4 weeks. Confocal laser scanning microscopy (CLSM) revealed a rapid coverage of the coupons with a thick layer of biological material and the existence of dispersed clusters of active metabolic microorganisms. After detaching the cells from the coupons, counts to quantify the CFU/cm^2 were done with high reproducibility. High-throughput sequencing of the 16S rRNA V3-V4 region shows bacterial diversity profiles in accordance with reported bacteria diversity in pig intestinal ecosystems and reveals differences between materials. The coupon-based methodology allows us to deepen our knowledge on biofilm structure and composition on the surface of a pig farm and opens the door for application in different types of livestock buildings.

Keywords: biofilm; sampling; livestock building; surfaces; diversity

Citation: Guéneau, V.; Rodiles, A.; Piard, J.-C.; Frayssinet, B.; Castex, M.; Plateau-Gonthier, J.; Briandet, R. Capture and Ex-Situ Analysis of Environmental Biofilms in Livestock Buildings. *Microorganisms* **2022**, *10*, 2. https://doi.org/10.3390/microorganisms10010002

Academic Editor: Rajesh Kumar Sani

Received: 30 November 2021
Accepted: 19 December 2021
Published: 21 December 2021

1. Introduction

In intensive breeding farms, animals live in a confined environment directly on inorganic floors (slatted floors, cages, aviary) or organic litter (straw, sawdust). In these environments, animal density can be very high, and the running parameters of farms (animal nutrition, temperature, humidity, light) are modulated to obtain their maximal growth rate. Concrete, metals, and polymers composed the majority of housing equipment materials in direct contact with animals in the livestock buildings, such as water and feed distribution systems, fences, pens, cages, walls, or gratings [1]. To reduce organic matter and microbial development on these surfaces, cleaning and disinfection (C&D) procedures are performed between two batches of animals, as well as regular removal of manure during the batch. However, these procedures are far from eradicating sessile microflora that can harbor pathogenic subpopulations [2–4]. Indeed, it is estimated that between 40 and 80% of living microorganisms are associated with a surface in so-called biofilms, which are present in all biotopes on earth [5]. Biofilms are three-dimensional biological structures composed of microbial communities embedded in cohesive self-produced extracellular polymeric substances (EPS) [6]. EPS can drastically vary between biofilms but is generally composed of water and a complex mixture of polysaccharides, extracellular DNA (eDNA), proteins, and amyloid fibers. The presence of EPS, along with spatial organization and specific signaling systems, triggers a diversification of cell types and emerging community

functions, including a fantastic adaptation to environmental fluctuations and the action of antimicrobials, in comparison to their free planktonic homologs [7–12].

Because of spatial proximity and high cell density, biofilms are considered as hot spots for the spreading of antibiotic resistance genes and virulence factors by horizontal gene transfer [13–15].

Current knowledge about surface-associated microbial communities in livestock buildings is still very limited, while of prime importance to decipher microbial pathogens dynamics in these environments and their interactions with animals. These questions enter in the One Health context by pinpointing the flow of pathogens between the environment, animals, and humans. Furthermore, national and international regulations are evolving to limit the use of antimicrobials such as antibiotics (to prevent antibiotic resistance) and disinfectants (to prevent environmental pollution) [16]. The development of innovative and alternative strategies are hence explored and are needed to create scientific knowledge and methodologies to analyze complex multispecies biofilms on livestock building surfaces and their dynamics under perturbations [17,18].

In farms, most pathogenic microorganisms responsible for zoonosis can be associated and protected within environmental biofilms. Holobiont of animals is in constant interplay with the biofilms from the farm environment. These biofilms may constitute an environmental route for animal and human contamination [19]. Quantification of undesirable species such as bacterial pathogens is hence carried out in livestock buildings regularly to monitor its hygienic status and to comply with eventual national or international regulations. The sampling methodologies used are principally swabs, sponges, and contact plates with specific media [20,21]. Nowadays, there is no chemical or physical methodology able to extract all surface-associated communities from a surface to study it [22,23], and the extracted fraction may not be representative of the initial sessile community [24]. Another strong limitation of these sampling methods is the definitive loss of the biofilm spatial organization that is, as mentioned previously, a major factor of microbial persistence on surfaces.

Indeed, protocols with coupons, defined here as a small surface of a specific material where the biofilm can develop, have been designed and used to capture in-situ and non-invasively the microbial community of interest in other systems [25]. These types of sampling methods were in particular successively applied to describe biofilms in aquatic conditions (biocorrosion in the sea, drinking water distribution system, and wastewater treatment) [26–29]. Coupons have also been recently used to detect the pathogenic bacteria *Listeria monocytogenes* in the food processing industry [30]. The coupon-based method allows structural analysis of the microbial community using microscopy techniques that can be combined with microbial diversity and bacterial counts. Moreover, it has been shown that biofilms growing on coupons are representative of the surface of the surroundings and that this method is more robust than classical environmental swabbing with less variability in bacterial counting [31].

In this study, we implemented a coupon-based methodology to capture native biofilms on livestock building surfaces (here a pig farm) along with a set of ex-situ analyses to describe the structural dynamics of these communities over one month. CLSM analysis was put in use to decipher non-invasively the three-dimensional structure of the biofilm, with a special interest in contrasting metabolically active cells. Bacterial plate counting was performed on non-selective media to allow quantification of viable and cultivable species, while an analysis of the bacterial diversity was performed by high-throughput sequencing of the 16S rRNA V3-V4 regions.

2. Materials and Methods

2.1. Livestock Building, Coupons Disposition, and Sampling

The coupons were placed in a French commercial pig farm during the post-weaning stage of piglets over 31 days (Blan, France). The livestock building was a slatted floor pen system. The temperature was 27 °C at animals' entry with a decrease of 1 °C every week to reach 24 °C until the end of breeding. Representative coupons of livestock building

surface materials were composed of polyvinyl chloride (PVC) or galvanized steel (steel) with dimensions: 2.5 cm × 6 cm × 3 mm (Leroy-Merlin, Colomiers, France). Coupons were sterilized in an autoclave (HMC EUROPE, Tuslin, Germany) and dried in a dry oven (FD 115 model, Binder, Tuttlingen, Germany) for 15 min at 120 °C.

In this work, 60 coupons of each material were analyzed (120 coupons in total) side by side on pen dividers using double-sided tape under the water lines close to animals in five pens of 3.73 m per 2.5 m of 25 piglets each (Figure 1).

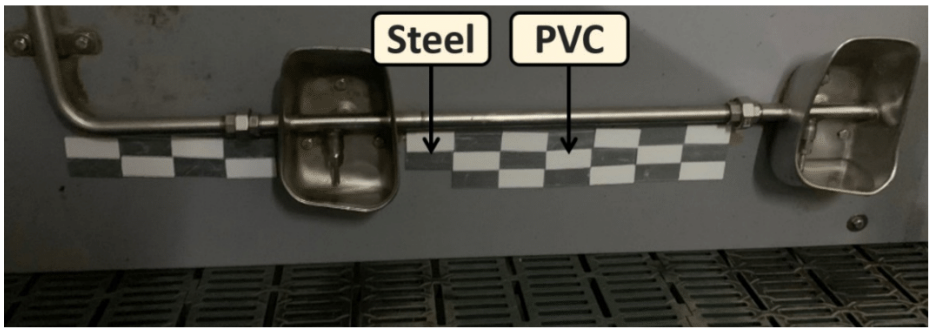

Figure 1. Arrangement of coupons on the wall. Steel and PVC coupons were placed on the walls under the water lines using double-sided tape in a staggered arrangement.

Per sampling day and in the same way for the 5 pens, 2 coupons of each material were extracted, one for microscopy study and the second one to perform the bacterial counts and DNA extraction for high-throughput sequencing analysis. The beginning of the experiment (day 0) corresponds to coupons implantation on pen dividers, after cleaning using the DECABAZ (HYDRACHIM, Étrelles, France) detergent and the VIROCID (CID lines, Ypres, Belgium) for the disinfection step, following manufacturer recommendations. A sampling of the coupons was made from the outside to the inside of the coupon line on days 2, 6, 7, 14, 21, and 31. The first sampling point on day 2 is just before the entry of animals. During sampling, coupons were aseptically removed with gloves from the pen dividers and placed in Petri dishes containing a sterile compress soaked in sterile water to avoid sample dehydration until analysis (<24 h after sampling).

2.2. Confocal Laser Scanning Microscopy

Biofilm structures on coupons were observed using a high-content screening confocal laser scanning microscope (LEICA, HCS-SP8, Wetzlar, Germany) at the INRAE MIMA2 microscopic platform (www6.jouy.inrae.fr/mima2_eng, accessed on 10 December 2021). Then, 50 µL of a 54 µM calcein acetoxymethyl (CAM), a metabolic fluorescent dye reporting esterase activity in green, was poured on the coupons and incubated in the dark for 30 min at 37 °C (Invitrogen, Carlsbad, CA, USA). The non-ionic molecules can enter passively into cells and be cleaved by intracellular esterase, releasing a fluorescent non-permeant ionic residue. Biofilms on the coupons were also counter labeled in red with 50 µL of a 3 µL/mL of SYTO 61 (Invitrogen, Carlsbad, CA, USA), a cell permanent red dye that labels nucleic acid.

A 600 Hz frequency was used to acquire images with the CLSM. SYTO 61 was excited with the HeNe laser at 633 nm, and the emitted fluorescence was collected with a hybrid detector in the range from 650 to 700 nm. CAM was excited with an argon laser set at 488 nm, and the emitted fluorescence was collected with a hybrid detector in the range from 500 to 550 nm. The surface topography was also captured using the reflection mode of the CLSM with the 488 nm laser line. A series of 512 × 512 pixels images was acquired using a 63× water lens (numerical aperture = 1.2) for the first samples (day 2) and a 40× air lens (numerical aperture = 0.8) for the other thick samples by taking one image per µm in

the *z*-axis to capture the full height of the biofilm. 2D projections and image analysis were performed using IMARIS 9.3.1 software (Bitplane, AG—Zurich, Switzerland).

Quantification of fluorescence signals was performed with the two labels to determine the evolution of each compartment (biovolume in $\mu m^3/\mu m^2$) over time for the two materials.

2.3. Enumeration of Bacteria Detached from Coupons

Coupons were placed in individual tubes containing 30 mL of a saline solution (NaCl 9 g/L) to cover halfway. With a sterile pipette tip, the biofilm was mechanically disrupted by successive round trips corresponding to 20 vertical and horizontal passages on the immersed side of the coupon, and then, the latter was turned over to do the same on the other side. Then, removing the coupon and suspending the bacteria by vortexing for 5 s the liquid, successive dilutions in saline solution were carried out in duplicate using 1mL of the resuspended biofilm solution. Counts into agar were made from 1 mL of the desired dilution. Trypticase soy broth with agar (TSA (*w/v*); 1% tryptone, 0.5% yeast extract, 0.5% NaCl, 1.5% agar; BioMérieux, Marcy-l'Étoile, France) was used as non-selective media under aerobic conditions for 24 h at 30 °C. To select the spores, 1mL of the biofilm solution was placed in a glass tube, in a water bath for 10 min at 80 °C, in duplicate for each coupon before enumeration by TSA. The Petri dishes in a CFU range between 30 and 300 were counted. The remaining 26 mL of the detached biofilm solution was centrifuged for 10 min at 6000× *g*, the supernatant was gently removed, and the pellets were placed at −20 °C to extract after the DNA.

2.4. High-Throughput Sequencing of the 16S rRNA and Diversity Analysis

2.4.1. DNA Extraction, PCR, and Sequencing

DNA from 60 bacterial pellets were extracted and purified using DNeasy PowerLyzer PowerSoil Kit manufacturer instructions (Qiagen, Hilden, Germany). PCR of V3–V4 regions of 16S rRNA marker genes was carried out on a thermocycler (Geneamp PCR system 9700, Applied Biosystems, USA) with universal primers F343 (5-CTTTCCCTACACGACGCTCTTCCGATCTTACGGRAGGCAGCAG-3) and R784 (5-GGAGTTCAGACGTGTGCTCTTCCGATCTTACCAGGGTATCTAATCCT-3) with an annealing temperature of 66 °C using Phusion High-Fidelity PCR kit (New England Biolabs, Ipswich, MA, USA) [32]. DNA was quantified on a NanoDrop Spectrophotometer ND-1000 (Thermo Fisher, Waltham, MA, USA). PCR products, including negative controls, were checked on 1% agarose gel electrophoresis to ensure PCR products. Illumina Miseq technology was used to sequence the amplicons (GeT-PlaGe INRAE platform, Toulouse, France).

2.4.2. Diversity Analysis Using Bioinformatics

Paired-end Fastq files were denoised with DADA2 [33] by default parameters, including consensus chimeras removal, as well removing primers and truncation by Demux with a final length of 411 ± 26 bp. Multiple alignment using fast Fourier transform (MAFFT) was used to perform de novo multiple sequence alignments [34], and mask as gap filtering Phylogeny was constructed with FastTree [35,36]. Data were rarefied to 10,120 sequences per sample; then low abundance amplicon sequence variants (ASVs) per pen were filtered out (<100 seqs in 2 samples, to improve accuracy on diversity estimates [37]). Rarefaction curves as observed AVSs and good coverage were studied to ensure a full sampling of the community was taken. Alpha diversity parameters (Shannon) and richness (Observed ASVs) were compared across materials per sampling point, as well as weighted UniFrac distances for Beta diversity. All bioinformatics results and graphs were obtained in QIIME2, using the Python-based microbiome data-science platform [38].

2.5. Statistical Analysis

Results are represented by the average and standard deviation (SD) or confidence interval (CI) of 5 coupons per day, and day was considered the experimental unit. Two-

way ANOVA using the uncorrected Fisher's least was used for the count and biovolume analysis with PRISM software (GraphPad, San Diego, California, USA). Taxonomy data were analyzed with Lefse [39] with default parameters, alpha diversity with Kruskal–Wallis, and beta diversity PERMANOVA in QIIME2 [38]. Data were considered significant when a p-value were smaller than 0.05.

3. Results

3.1. Coupons Are Colonized by a Densely Clustered Biofilm with Only a Minor Fraction of Cells Metabolically Active

Before being placed in the farm, coupons surface topography was analyzed with the reflection mode of a CLSM (Figure 2). The surface of steel was rougher than PVC with the presence of streaks and holes in abundance, while the PVC was very smooth. To estimate the hydrophilicity of the coupons, contact angles with water were measured [40]. The two side contact angles of 15 drops of 100 µL were measured with the image analysis software ImageJ (1.53 version). The water contact angles show that steel coupons (angle of 51.1° ± 7.4) were more hydrophilic ($p < 0.05$) than PVC coupons (angle of 84.8° ± 3.2).

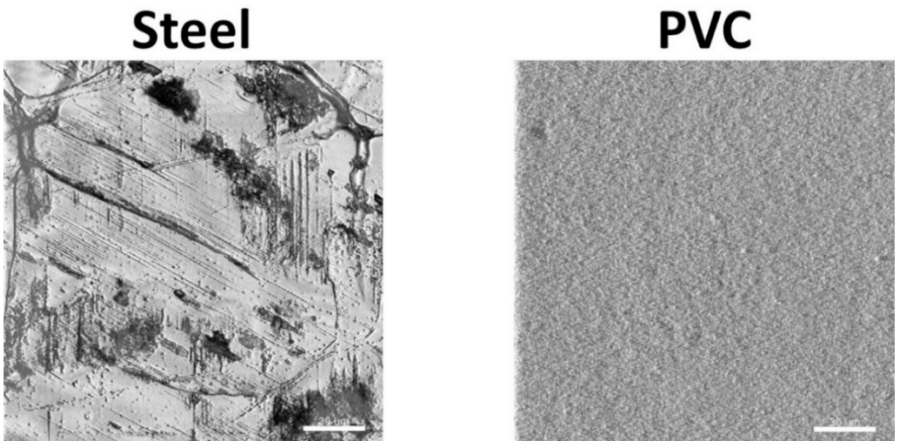

Figure 2. Characterization of the surface of coupons using confocal laser scanning microscopy. A detail of the surface topography of the steel and the PVC coupons by CLSM are shown (scale bar = 30 µm).

Coupons harvested in the building were labeled with SYTO 61 (red) to mark intra- and extracellular nucleic acids in the biofilms and CAM (green) to highlight metabolically active microorganisms inside the community (Figure 3a).

Images of the first sampling day after the cleaning and disinfection process and before the entry of animals in the farm (day 2) showed only a few sessile scattered microorganisms with the size around the micrometer compatible with bacteria. After animals entered, biovolumes in both channels sharply and significantly increased ($p < 0.05$) (Figure 3b). From sampling day 6 until the end of the experiment, material contrasted with SYTO 61 was covering all the coupons surfaces. An organization with clusters or compact structures with holes in both materials was visualized. The biovolume of SYTO 61-labeled material was significantly higher on steel than PVC from day 14, and a decrease of the signal was observed from day 7 in PVC ($p < 0.05$).

Green CAM-labeled clusters corresponding to metabolically active microorganisms were observed in all samples after animal entry. Biovolume of CAM was higher on steel in comparison to PVC on day 31 ($p < 0.05$), and a decrease of biovolume appeared for days 21 and 31 on PVC ($p < 0.05$) (Figure 3c).

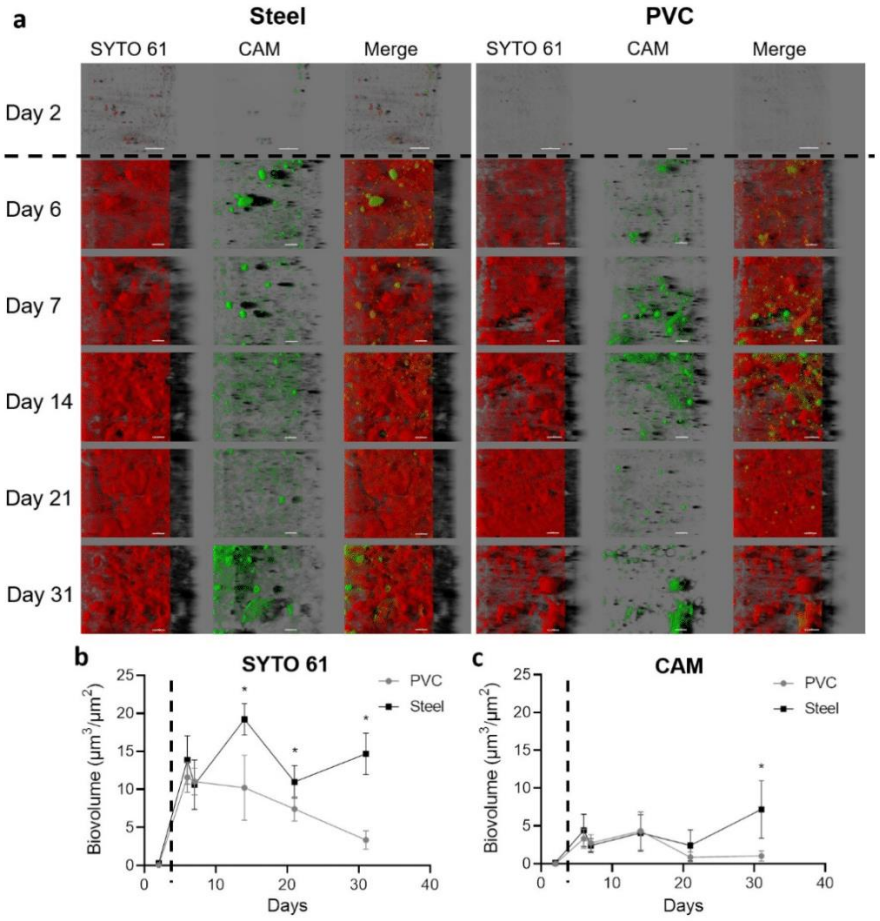

Figure 3. Confocal laser scanning microscopy visualization of biofilms settled on the steel and PVC coupons. Microorganisms and eDNA were labeled in red with SYTO61 and metabolically active cells in green with CAM. The easy 3D representative projections for each time point for steel and PVC coupons are shown (**a**). Day 2 corresponds to the first sampling, two days after the deposit of the coupons without animals in the farm; the scale bar represents 30 µm for day 2 and 40 µm for the other time points. The biovolume of SYTO 61 (**b**) and CAM (**c**) signals were extracted over time on PVC (grey lines) and steel (black lines). The dotted line indicates the animal's entry into the building. Results represent average ±CI 95% (* $p < 0.05$).

3.2. Enumeration of Aerobic Cultivable Bacteria from Coupons

Enumeration with TSA plates as a non-selective media to quantify total aerobic bacteria on coupons was performed. In addition, heat treatment of 10 min at 80 °C was carried out before TSA plating to select spores from the same samples (Figure 4).

Before the entry of animals and 2 days after coupon placement (day 2), 4 logs (CFU/cm^2) of total bacteria were enumerated in both materials. After animals entered, a significant increase of total aerobic cultivable bacteria was obtained on PVC in comparison to steel ($p < 0.05$) for all days, except at day 21. A stabilization of non-selective counting was obtained after animals entered with a value around 6 logs (CFU/cm^2) for PVC and 5 logs (CFU/cm^2) for steel. A peak was observed in both materials on day 21. With heat treatment, less than 1 log (CFU/cm^2) of spores were enumerated on both materials on the first sampling. Values increased on PVC and steel after day 2 to reach more than 2 logs (CFU/cm^2) of spores on day 21; no significant differences were observed on both materials for each time point. A higher number of total aerobic cultivable bacteria were counted

significantly on PVC compared to steel ($p < 0.05$), however, with a tendency to have fewer spores counted.

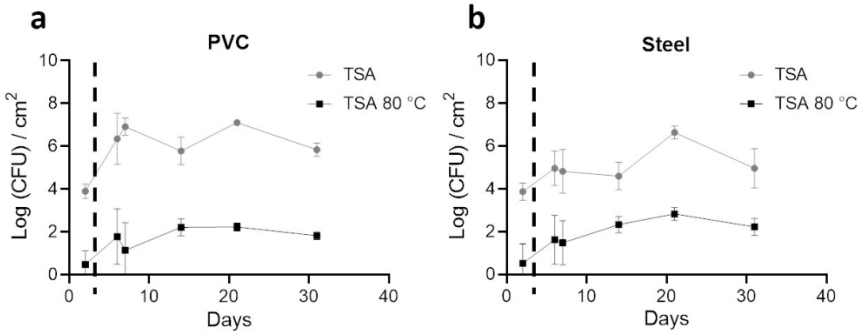

Figure 4. Enumeration profiles (Log CFU/cm^2) of the total aerobic bacteria (TSA) and spores (TSA, 80ºC, 10min) on steel and PVC coupons during the trial. Biofilms on coupons were removed mechanically by pipetting and by a round trip with saline solution. After successive dilutions, bacteria inside samples were enumerated on TSA (grey lines) and on TSA after a 10 min at 80 °C treatment to select spores (black lines). Results are average ±CI 95% of 2 enumeration profiles for PVC (**a**) and Steel (**b**) coupons. The dotted line indicates the animal's entry into the building.

3.3. 16S rRNA High-Throughput Sequencing Analysis to Decipher the Dynamic of Biofilm Bacterial Diversity

A total of 60 samples from PCR targeting the 16S rRNA coding gene were successfully sequenced. After error filtering, alignment, and chimera removal, 1,146,915 reads were generated, corresponding to 19,115 ± 6505 sequences per sample. Taxonomic analysis shows that *Firmicutes* phylum was the most represented in all samples, followed by *Proteobacteria*, *Actinobacteria*, and *Bacteroidetes*. *Lactobacillales*, *Clostridiales*, *Bacillales*, *Actinomycetales*, *Pseudomonadales*, *Bacteroidales*, and *Enterobacteriales* were the most dominant orders (Figure 5).

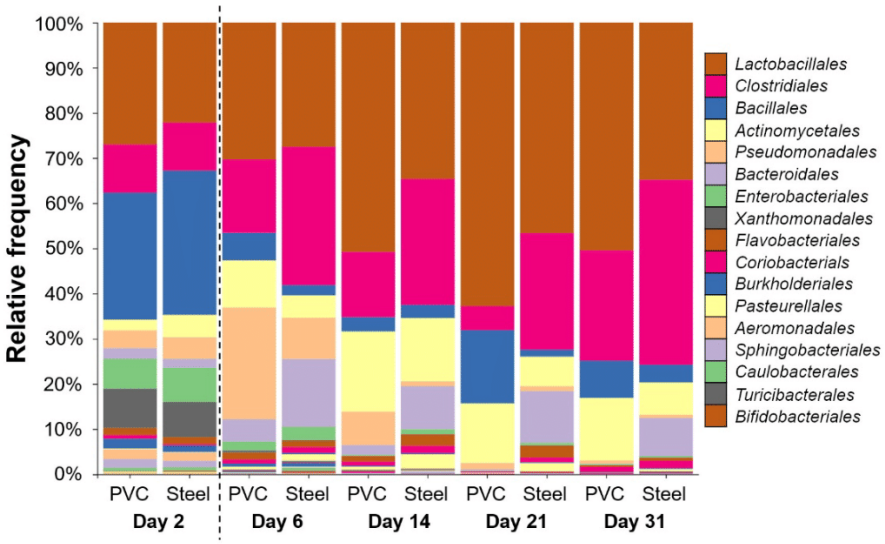

Figure 5. Taxonomic order profile of bacterial communities on the pig farm surface determined using PVC and steel coupons. Each color bar represents the relative frequency of one bacterial order inside the total bacterial community. For each day, PVC and steel taxonomic profiles are shown. The dotted line indicates the animal's entry into the building.

Lactobacillales was the most represented order in both materials when samples were compiled for days with significantly more relative frequency on PVC (40%) compared to steel (31%). The trends are reversed with *Clostridiales* that is the second most represented significantly on steel (25%) compared to PVC (14%) ($p < 0.05$). Other orders were also significantly different per material: *Bacillales*, *Actinomycetales*, and *Pseudomonadales* on PVC and *Bacteroidales*, *Rhodocyclales*, *Enterobacteriales*, *Coriobacteriales*, and *Flavobacteriales* on steel ($p < 0.05$). The trends stated above are true for each time point except for day 2 (Figure 4). On day 2, after C&D procedures and before the animals enter the building, taxonomic profiles are different, with the larger abundance corresponding to *Bacillales* order on both materials (28–32%). Just after animals enter at day 6, *Pseudomonadales* order proportion increases to reach 25% of relative frequency on the PVC in comparison to a less increase on the steel of 9%. *Bacteroidales* are more detectable on steel than PVC for every time point except for day 2, which is at the same level. The level of *Enterobacteriales* decreased from day 2 to the end of the experiment (Figure 5).

Shannon indexes were used to compare α-diversity between steel and PVC materials during the experiment (Figure 6). On day 2, before animal entry, the diversity was the same on both materials (6.3 and 6.2). The Shannon index on PVC decreased on day 6 until day 21, in comparison to a significantly higher and stable diversity level on steel for all the breeding duration. Except for the first sampling on day 2, a significantly lower level of diversity is observed on PVC compared to steel ($p < 0.05$), corresponding to a decrease of richness and evenness in the bacterial population. Similar results were found for observed ASVs from 285 at day 2 to a peak on day 6 with 341–431, reaching 170–290 ASVs at the end of the trial, for PVC and steel, respectively. Weighted UniFrac distances of beta diversity showed significant differences between the compositional 16S of both materials per day ($p < 0.05$).

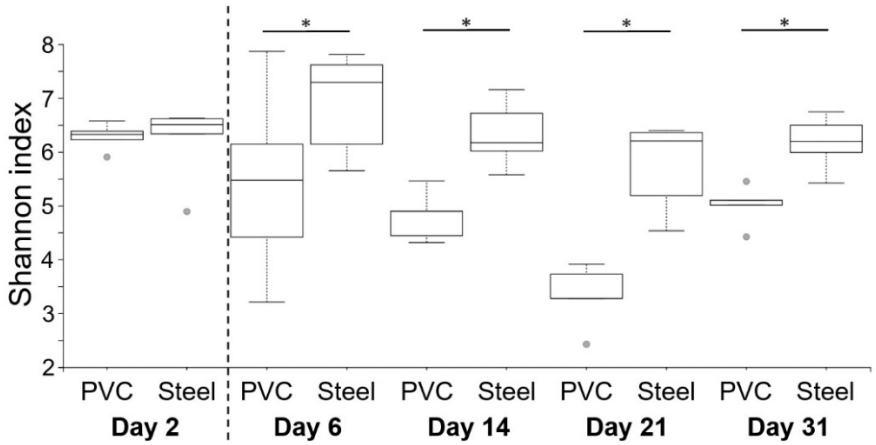

Figure 6. Comparison of α-diversity on PVC and steel coupons during the experiment. α-diversity was determined using the Shannon index value. The dotted line indicates the animal's entry into the building. Pairwise comparisons between materials per day are shown with an asterisk (* $p < 0.05$).

4. Discussion

Knowledge of the microbial communities living on surfaces of livestock buildings is still very limited in the literature. These communities, in close contact with animals, should be better characterized for their control. As mentioned previously, no standard or robust methodology is described to sample or analyze these spatially organized communities. Here, we propose a sampling and analyzing method of the biofilms by collecting them from coupons installed on site.

To apply and validate this methodology in the context of pig farms, coupons were placed after C&D protocol under the water lines, an area with frequent contact with animals. Coupons were sampled before animal entry that corresponds to 2 days of incubation (day 2),

and around 4 logs (CFU/cm^2) of bacteria were counted on TSA with both materials. After several days, the number of counts did not reach more than 7 logs (CFU/cm^2), showing low effectiveness of C&D protocol or rapid growth of bacteria after C&D. Analysis of coupons incubated throughout the breeding period exposed or not to a C&D process would allow answering this question.

The spatial organization of metabolically active bacteria inside the total biofilm was observed. By compiling the biovolume of both channels over time and by the ratio of CAM versus SYTO61, it was possible to estimate that for the two materials, around 30% of the biofilm was composed of metabolically active cells. The bacteria counted on TSA medium may be those detected by CAM without the viable but non-cultivable part. Metabolically active bacteria in the biofilm can have a commensal origin or can be those detected on surfaces before entry of animals which have developed, representing in our study around 4 logs (CFU/cm^2) for day 2, and which are by diversity analysis principally *Bacillales* and *Lactobacillales*. While CAM allowed the visualization of localized pockets of metabolically active cells, a limitation of such esterase activity markers is that some bacterial species can expulse the dye with efflux pumps, resulting in loss of intracellular fluorescence [41].

Here, coupons were contaminated with feces splashes from the arrival of the animals in the building (day 6). Fecal bacteria can hence be recruited in the preexisting biofilm and be integrated into the CFU counts. It has been shown that the bacterial quantity that lives in the gut achieves among the highest cell densities recorded for any ecosystem, with more than 10^{11} cells per gram of wet material in the colon [42]. The intestinal contents of pig harbor a fraction of strict microbial anaerobes that do not tolerate the presence of oxygen. Their release into open air can cause cell death and lysis and the release of eDNA [43]. In this study, the SYTO 61 can label live and dead microorganisms but also the abundant eDNA fraction in the matrix. Previous studies have shown that polysaccharides, proteins, and eDNA can play a role in the spatial structure of the biofilm [6,44]. The very compacted structure of biofilms may here be linked to the large amount of eDNA resulting from bacterial lysis.

A decrease in SYTO 61 signal on PVC is observed from day 6 to the end of the experiment. Biofilms on PVC could be less cohesive than on steel. The steel coupons showed high hydrophilic properties and harbored holes and cracks on their surface that could permit a better fixation of organic materials in comparison to PVC. The structure of the biofilm changed with a decrease of the biomass level during the experiment, but this was not correlated with a decrease in bacterial number. Biovolumes on steel were higher than on PVC, and this could also be explained by the properties of steel surface (hydrophobicity and rugosity). However, the number of bacteria counted on PVC was higher than on steel, which suggests that steel carries a greater matrix with fewer bacteria. Microscopic visualization of extracellular matrix compounds may be considered in future experiments. Alternative labeling methods can be used in future experiments to distinguish other components of the biofilm, such as fluorescent lectins that bind specifically to exopolysaccharides, thioflavin T for amyloid fiber labeling, or fluorescence in situ hybridization (FISH) technique by detecting specific species having access to their spatial organization [45,46].

The bacterial diversity was studied by 16S high-throughput sequencing analysis. Overall, in the absence of additional biological replicates, the insights brought by 16S sequencing were limited to the description of the microbial community. The results showed more richness and evenness in steel than PVC, and this was in line with the taxonomy results, with the presence of a large proportion of bacteria on coupons, such as *Lactobacillales*, *Clostridiales*, *Bacillales*, *Actinomycetales*, *Pseudomonadales*, *Bacteroidales*, and *Enterobacteriales*, already found in other pig studies [47–49]. A bias in this community profiling arises from the high quantities of bacterial eDNA from feces on the surface that can be sequenced in addition to the living bacteria that multiply in such biofilms. DNA of bacteria that can grow on the surface was amplified, but because of the eDNA release, dead bacteria are also detected with this approach. V3–V4 regions of the gene encoding the 16S RNA were chosen for DNA amplification to discriminate better the species as bringing higher

variability of the amplified sequences, in comparison to other regions like V4–V5 region, which can show as well the presence of archaea [50]. Internal transcribed spacer (ITS) regions from fungi that code for ribosomal RNA can also be used to study this diversity of surface communities [51]. A probable correlation exists between the composition of the animal microbiota and the microbial communities identified on the coupons. For future experiments, animal microbiota has to be sampled, analyzed, and compared to the biofilms.

This method has been validated in a pig farming context, allowing a better understanding of the dynamics of microbial communities over time in this production system. In the future, we could envision that a farmer could use this coupon method without the intervention of specialized technician and send them to the laboratory with a dedicated procedure for monitoring the building surface microbiological profile. Interesting trends such as the effect of the material stand out significantly and should be extended by other complementary studies in other farms to standardize the results. The method also makes it possible to isolate strains of interest from these surfaces. New high-throughput culturomic techniques compatible with our sampling methodology allow us to isolate and cultivate viable bacteria inside the community and could help to avoid the bias surface contamination by dead bacteria from feces that are detected by DNA sequencing [52–54]. In perspective, a study where coupons are placed at different heights to also study the formation of biofilm on these surfaces without splashes of feces could be considered. Other coupons composed of representative materials of the livestock building as concrete or stainless steel could also be analyzed.

Antimicrobial tolerance and resistance of such compact 3D communities will be also interesting to investigate. These microbial communities are also frequently exposed to antibiotic residues and can become reservoirs of antibiotic resistance genes.

5. Conclusions

A method to non-invasively capture biofilms of the surface of livestock buildings and their ex-situ analysis was developed in this work to be implemented and validated in a building of a pig farm. Bacterial density, diversity, and the three-dimensional structure of the surface biofilms were analyzed, thus increasing our knowledge of these microbial communities, poorly documented until now. In perspective, these results could contribute to better understanding the contamination risks of animals by pathogens present on the contact surfaces and directly associated with biofilms. In the future, this approach could be used to study surface biofilms in a variety of agricultural environments, including other types of livestock buildings.

Author Contributions: Conceptualization, V.G., J.-C.P., B.F., M.C., J.P.-G. and R.B.; methodology, V.G., J.-C.P., B.F., M.C., J.P.-G. and R.B.; validation, J.-C.P., M.C., J.P.-G. and R.B.; formal analysis, V.G. and A.R.; investigation, V.G., J.P.-G. and R.B.; resources, M.C. and R.B.; data curation, V.G.; writing—original draft preparation, V.G.; writing—review and editing, A.R., M.C., J.P.-G. and R.B.; supervision, J.-C.P., M.C., J.P.-G. and R.B.; project administration, M.C. and R.B.; funding acquisition, M.C. and R.B. All authors have read and agreed to the published version of the manuscript.

Funding: This research was funded by INRAE, LALLEMAND SAS and "Association Nationale de la Recherche et de la Technologie" (contract 2020/0548).

Institutional Review Board Statement: Not applicable.

Conflicts of Interest: The authors declare no conflict of interest.

References

1. Godyń, D.; Nowicki, J.; Herbut, P. Effects of environmental enrichment on pig welfare—A review. *Animals* **2019**, *9*, 383. [CrossRef]
2. Luyckx, K.Y.; Van Weyenberg, S.; Dewulf, J.; Herman, L.; Zoons, J.; Vervaet, E.; Heyndrickx, M.; De Reu, K. On-farm comparisons of different cleaning protocols in broiler houses. *Poult. Sci.* **2015**, *94*, 1986–1993. [CrossRef]
3. Mannion, C.; Leonard, F.C.; Lynch, P.B.; Egan, J. Efficacy of cleaning and disinfection on pig farms in Ireland. *Vet. Rec.* **2007**, *161*, 371–375. [CrossRef]

4. Misra, S.; van Middelaar, C.E.; Jordan, K.; Upton, J.; Quinn, A.J.; de Boer, I.J.M.; O'Driscoll, K. Effect of different cleaning procedures on water use and bacterial levels in weaner pig pens. *PLoS ONE* **2020**, *15*, e0242495. [CrossRef] [PubMed]
5. Flemming, H.-C.; Wuertz, S. Bacteria and archaea on earth and their abundance in biofilms. *Nat. Rev. Microbiol.* **2019**, *17*, 247–260. [CrossRef] [PubMed]
6. Flemming, H.-C. The Perfect Slime. *Colloids Surf. B Biointerface* **2011**, *86*, 251–259. [CrossRef] [PubMed]
7. Flemming, H.-C.; Wingender, J.; Szewzyk, U.; Steinberg, P.; Rice, S.A.; Kjelleberg, S. Biofilms: An emergent form of bacterial life. *Nat. Rev. Microbiol.* **2016**, *14*, 563–575. [CrossRef] [PubMed]
8. Bridier, A.; Piard, J.-C.; Pandin, C.; Labarthe, S.; Dubois-Brissonnet, F.; Briandet, R. Spatial organization plasticity as an adaptive driver of surface microbial communities. *Front. Microbiol.* **2017**, *8*, 1364. [CrossRef] [PubMed]
9. Bridier, A.; Briandet, R.; Thomas, V.; Dubois-Brissonnet, F. Resistance of bacterial biofilms to disinfectants: A review. *Biofouling* **2011**, *27*, 1017–1032. [CrossRef] [PubMed]
10. Chamignon, C.; Guéneau, V.; Medina, S.; Deschamps, J.; Gil-Izquierdo, A.; Briandet, R.; Mousset, P.-Y.; Langella, P.; Lafay, S.; Bermúdez-Humarán, L.G. Evaluation of the probiotic properties and the capacity to form biofilms of various lactobacillus strains. *Microorganisms* **2020**, *8*, 1053. [CrossRef]
11. Høiby, N.; Bjarnsholt, T.; Givskov, M.; Molin, S.; Ciofu, O. Antibiotic resistance of bacterial biofilms. *Int. J. Antimicrob. Agents* **2010**, *35*, 322–332. [CrossRef] [PubMed]
12. Coenye, T. Response of sessile cells to stress: From changes in gene expression to phenotypic adaptation. *FEMS Immunol. Med. Microbiol.* **2010**, *59*, 239–252. [CrossRef] [PubMed]
13. Lerminiaux, N.A.; Cameron, A.D.S. Horizontal transfer of antibiotic resistance genes in clinical environments. *Can. J. Microbiol.* **2019**, *65*, 34–44. [CrossRef] [PubMed]
14. Soucy, S.M.; Huang, J.; Gogarten, J.P. Horizontal gene transfer: Building the web of life. *Nat. Rev. Genet.* **2015**, *16*, 472–482. [CrossRef]
15. Madsen, J.S.; Burmølle, M.; Hansen, L.H.; Sørensen, S.J. The interconnection between biofilm formation and horizontal gene transfer. *FEMS Immunol. Med. Microbiol.* **2012**, *65*, 183–195. [CrossRef] [PubMed]
16. Taylor, K. Ten years of REACH—An animal protection perspective. *Altern. Lab. Anim.* **2018**, *46*, 347–373. [CrossRef]
17. McEwen, S.A.; Collignon, P.J. Antimicrobial resistance: A one health perspective. *Microbiol. Spectr.* **2018**, *6*, ARBA-0009-2017. [CrossRef]
18. Cross, A.R.; Baldwin, V.M.; Roy, S.; Essex-Lopresti, A.E.; Prior, J.L.; Harmer, N.J. Zoonoses under our noses. *Microbes Infect.* **2019**, *21*, 10–19. [CrossRef]
19. Chlebicz, A.; Śliżewska, K. Campylobacteriosis, salmonellosis, yersiniosis, and listeriosis as zoonotic foodborne diseases: A review. *Int. J. Environ. Res. Public Health* **2018**, *15*, 863. [CrossRef]
20. Valentine, N.B.; Butcher, M.G.; Su, Y.-F.; Jarman, K.H.; Matzke, M.; Webb-Robertson, B.-J.; Panisko, E.A.; Seiders, B.A.B.; Wahl, K.L. Evaluation of sampling tools for environmental sampling of bacterial endospores from porous and nonporous surfaces. *J. Appl. Microbiol.* **2008**, *105*, 1107–1113. [CrossRef]
21. Ismaïl, R.; Aviat, F.; Michel, V.; Le Bayon, I.; Gay-Perret, P.; Kutnik, M.; Fédérighi, M. Methods for recovering microorganisms from solid surfaces used in the food industry: A review of the literature. *Int. J. Environ. Res. Public Health* **2013**, *10*, 6169–6183. [CrossRef] [PubMed]
22. Gomes, I.B.; Lemos, M.; Mathieu, L.; Simões, M.; Simões, L.C. The action of chemical and mechanical stresses on single and dual species biofilm removal of drinking water bacteria. *Sci. Total Environ.* **2018**, *631–632*, 987–993. [CrossRef] [PubMed]
23. Stiefel, P.; Mauerhofer, S.; Schneider, J.; Maniura-Weber, K.; Rosenberg, U.; Ren, Q. Enzymes enhance biofilm removal efficiency of cleaners. *Antimicrob. Agents Chemother.* **2016**, *60*, 3647–3652. [CrossRef] [PubMed]
24. Grand, I.; Bellon-Fontaine, M.-N.; Herry, J.-M.; Hilaire, D.; Moriconi, F.-X.; Naïtali, M. Possible Overestimation of Surface Disinfection Efficiency by Assessment Methods Based on Liquid Sampling Procedures as Demonstrated by in Situ Quantification of Spore Viability. *Appl. Environ. Microbiol.* **2011**, *77*, 6208–6214. [CrossRef] [PubMed]
25. Goeres, D.M.; Loetterle, L.R.; Hamilton, M.A.; Murga, R.; Kirby, D.W.; Donlan, R.M. Statistical assessment of a laboratory method for growing biofilms. *Microbiology* **2005**, *151*, 757–762. [CrossRef] [PubMed]
26. Douterelo, I.; Boxall, J.B.; Deines, P.; Sekar, R.; Fish, K.E.; Biggs, C.A. Methodological approaches for studying the microbial ecology of drinking water distribution systems. *Water Res.* **2014**, *65*, 134–156. [CrossRef]
27. Deines, P.; Sekar, R.; Husband, P.S.; Boxall, J.B.; Osborn, A.M.; Biggs, C.A. A new coupon design for simultaneous analysis of in situ microbial biofilm formation and community structure in drinking water distribution systems. *Appl. Microbiol. Biotechnol.* **2010**, *87*, 749–756. [CrossRef]
28. Douterelo, I.; Jackson, M.; Solomon, C.; Boxall, J. Microbial analysis of in situ biofilm formation in drinking water distribution systems: Implications for monitoring and control of drinking water quality. *Appl. Microbiol. Biotechnol.* **2016**, *100*, 3301–3311. [CrossRef]
29. Krishnan, M.; Dahms, H.-U.; Seeni, P.; Gopalan, S.; Sivanandham, V.; Jin-Hyoung, K.; James, R.A. Multi metal assessment on biofilm formation in offshore environment. *Mater. Sci. Eng. C Mater. Biol. Appl.* **2017**, *73*, 743–755. [CrossRef]
30. Rodríguez-López, P.; Rodríguez-Herrera, J.J.; Cabo, M.L. Tracking bacteriome variation over time in listeria monocytogenes-positive foci in food industry. *Int. J. Food Microbiol.* **2020**, *315*, 108439. [CrossRef]

31. Moen, B.; Røssvoll, E.; Måge, I.; Møretrø, T.; Langsrud, S. Microbiota formed on attached stainless steel coupons correlates with the natural biofilm of the sink surface in domestic kitchens. *Can. J. Microbiol.* **2016**, *62*, 148–160. [CrossRef]
32. Verschuren, L.M.G.; Calus, M.P.L.; Jansman, A.J.M.; Bergsma, R.; Knol, E.F.; Gilbert, H.; Zemb, O. Fecal microbial composition associated with variation in feed efficiency in pigs depends on diet and sex. *J. Anim. Sci.* **2018**, *96*, 1405–1418. [CrossRef]
33. Callahan, B.J.; McMurdie, P.J.; Rosen, M.J.; Han, A.W.; Johnson, A.J.A.; Holmes, S.P. DADA2: High-resolution sample inference from illumina amplicon data. *Nat. Methods* **2016**, *13*, 581–583. [CrossRef] [PubMed]
34. Katoh, K.; Standley, D.M. MAFFT multiple sequence alignment software version 7: Improvements in performance and usability. *Mol. Biol. Evol.* **2013**, *30*, 772–780. [CrossRef] [PubMed]
35. Price, M.N.; Dehal, P.S.; Arkin, A.P. FastTree 2—Approximately maximum-likelihood trees for large alignments. *PLoS ONE* **2010**, *5*, e9490. [CrossRef]
36. Lane, D.J. 16s/23s RRNA sequencing. In *Nucleic Acid Techniques in Bacterial Systematics*; John Wiley and Sons: New York, NY, USA, 1991; pp. 115–175.
37. Bokulich, N.A.; Subramanian, S.; Faith, J.J.; Gevers, D.; Gordon, J.I.; Knight, R.; Mills, D.A.; Caporaso, J.G. Quality-filtering vastly improves diversity estimates from illumina amplicon sequencing. *Nat. Methods* **2013**, *10*, 57–59. [CrossRef]
38. Bolyen, E.; Rideout, J.R.; Dillon, M.R.; Bokulich, N.A.; Abnet, C.C.; Al-Ghalith, G.A.; Alexander, H.; Alm, E.J.; Arumugam, M.; Asnicar, F.; et al. Reproducible, Interactive, scalable and extensible microbiome data science using QIIME 2. *Nat. Biotechnol.* **2019**, *37*, 852–857. [CrossRef] [PubMed]
39. Segata, N.; Izard, J.; Waldron, L.; Gevers, D.; Miropolsky, L.; Garrett, W.S.; Huttenhower, C. Metagenomic biomarker discovery and explanation. *Genome Biol.* **2011**, *12*, R60. [CrossRef] [PubMed]
40. Menees, T.S.; Radhakrishnan, R.; Ramp, L.C.; Burgess, J.O.; Lawson, N.C. Contact angle of unset elastomeric impression materials. *J. Prosthet. Dent.* **2015**, *114*, 536–542. [CrossRef] [PubMed]
41. Joux, F.; Lebaron, P. Use of fluorescent probes to assess physiological functions of bacteria at single-cell level. *Microbes Infect.* **2000**, *2*, 1523–1535. [CrossRef]
42. Sender, R.; Fuchs, S.; Milo, R. Revised estimates for the number of human and bacteria cells in the body. *PLoS Biol.* **2016**, *14*, e1002533. [CrossRef] [PubMed]
43. Albenberg, L.; Esipova, T.V.; Judge, C.P.; Bittinger, K.; Chen, J.; Laughlin, A.; Grunberg, S.; Baldassano, R.N.; Lewis, J.D.; Li, H.; et al. Correlation between intraluminal oxygen gradient and radial partitioning of intestinal microbiota. *Gastroenterology* **2014**, *147*, 1055–1063.e8. [CrossRef]
44. Das, T.; Sehar, S.; Manefield, M. The roles of extracellular DNA in the structural integrity of extracellular polymeric substance and bacterial biofilm development. *Environ. Microbiol. Rep.* **2013**, *5*, 778–786. [CrossRef] [PubMed]
45. Golub, S.R.; Overton, T.W. Pellicle formation by escherichia coli K-12: Role of adhesins and motility. *J. Biosci. Bioeng.* **2021**, *131*, 381–389. [CrossRef] [PubMed]
46. Flemming, H.-C.; Wingender, J. The biofilm matrix. *Nat. Rev. Microbiol.* **2010**, *8*, 623–633. [CrossRef]
47. Wang, X.; Tsai, T.; Deng, F.; Wei, X.; Chai, J.; Knapp, J.; Apple, J.; Maxwell, C.V.; Lee, J.A.; Li, Y.; et al. Longitudinal investigation of the swine gut microbiome from birth to market reveals stage and growth performance associated bacteria. *Microbiome* **2019**, *7*, 109. [CrossRef]
48. Shin, D.; Chang, S.Y.; Bogere, P.; Won, K.; Choi, J.-Y.; Choi, Y.-J.; Lee, H.K.; Hur, J.; Park, B.-Y.; Kim, Y.; et al. Beneficial roles of probiotics on the modulation of gut microbiota and immune response in pigs. *PLoS ONE* **2019**, *14*, e0220843. [CrossRef] [PubMed]
49. Pollock, J.; Glendinning, L.; Smith, L.A.; Mohsin, H.; Gally, D.L.; Hutchings, M.R.; Houdijk, J.G.M. Temporal and nutritional effects on the weaner pig ileal microbiota. *Anim. Microbiome* **2021**, *3*, 58. [CrossRef]
50. Fadeev, E.; Cardozo-Mino, M.G.; Rapp, J.Z.; Bienhold, C.; Salter, I.; Salman-Carvalho, V.; Molari, M.; Tegetmeyer, H.E.; Buttigieg, P.L.; Boetius, A. Comparison of two 16S RRNA primers (V3-V4 and V4-V5) for studies of arctic microbial communities. *Front. Microbiol.* **2021**, *12*, 637526. [CrossRef]
51. Iwen, P.C.; Hinrichs, S.H.; Rupp, M.E. Utilization of the internal transcribed spacer regions as molecular targets to detect and identify human fungal pathogens. *Med. Mycol.* **2002**, *40*, 87–109. [CrossRef] [PubMed]
52. Lagier, J.-C.; Million, M.; Hugon, P.; Armougom, F.; Raoult, D. Human gut microbiota: Repertoire and variations. *Front. Cell. Infect. Microbiol.* **2012**, *2*, 136. [CrossRef] [PubMed]
53. Vartoukian, S.R.; Palmer, R.M.; Wade, W.G. Strategies for culture of "unculturable" bacteria. *FEMS Microbiol. Lett.* **2010**, *309*, 1–7. [CrossRef] [PubMed]
54. Lagier, J.-C.; Dubourg, G.; Million, M.; Cadoret, F.; Bilen, M.; Fenollar, F.; Levasseur, A.; Rolain, J.-M.; Fournier, P.-E.; Raoult, D. Culturing the human microbiota and culturomics. *Nat. Rev. Microbiol.* **2018**, *16*, 540–550. [CrossRef] [PubMed]

3.1.3 Article 4 : Genome sequence of *Bacillus velezensis* P1, a strain isolated from a biofilm captured on a pig farm building

Virgile Guéneau, Jean-Christophe Piard, Bastien Frayssinet, Valentin Loux, Hélène Chiapello, Romain Briandet.

Microbiology Resource Announcements, 2022, 10.1128/mra.01219-21.

AMERICAN SOCIETY FOR MICROBIOLOGY | Microbiology Resource Announcements

GENOME SEQUENCES

Genome Sequence of *Bacillus velezensis* P1, a Strain Isolated from a Biofilm Captured on a Pig Farm Building

Virgile Guéneau,[a,b] **Jean-Christophe Piard,**[a] **Bastien Frayssinet,**[b] **Valentin Loux,**[c,d] **Hélène Chiapello,**[c] **Julia Plateau-Gonthier,**[b] **Mathieu Castex,**[b] **Romain Briandet**[a]

[a]Université Paris-Saclay, INRAE, AgroParisTech, Micalis Institute, Jouy-en-Josas, France
[b]Lallemand SAS, Blagnac, France
[c]Université Paris-Saclay, INRAE, MaIAGE, Jouy-en-Josas, France
[d]Université Paris-Saclay, INRAE, BioinfOmics, MIGALE Bioinformatics Facility, Jouy-en-Josas, France

ABSTRACT The genome of the *Bacillus velezensis* P1 strain isolated from a biofilm on the wall of a pig farm was sequenced. The strain harbors many surface colonization genes involved in surfactant, matrix, and antibacterial synthesis.

Surface communities on the wall inside a pig farm building were sampled by using coupons installed on the surface for 31 days. Biofilms were recovered by scratching using a pipette cone and 30 mL of saline solution, and the bacterial suspension was treated for 10 min at 80°C to select heat-resistant spores. Plating the treated suspension on Trypticase soy (TS) agar at 30°C for 24 h allowed isolation of the P1 strain forming highly structured colonies on agar.

From a −80°C glycerol stock, the P1 strain was cultured in TS under agitation at 37°C overnight (~16 h). Genomic DNA was extracted and purified using the Monarch genomic DNA purification kit (New England Biolabs, Ipswich, MA, USA). DNA sequencing (DNA-seq) was performed at the GeT-PlaGe core facility (INRAE, Toulouse, France; www.genotoul.fr/en/). DNA-seq libraries were prepared according to Illumina's protocols using the TruSeq Nano DNA high-throughout (HT) library kit (Illumina, San Diego, CA, USA). Briefly, DNA was fragmented by sonication, size selection was performed using sample purification beads (SPBs) (kit beads), and adaptors were ligated to be sequenced. Library quality was assessed using the Agilent DNF-474 high-sensitivity (HS) next-generation sequencing (NGS) fragment kit (Agilent Technologies, Santa Clara, CA, USA), and libraries were quantified by quantitative PCR (qPCR) using the Kapa library quantification kit (Roche, Basel, Switzerland). DNA-seq experiments were performed on an Illumina NovaSeq 6000 system, using a paired-end read length of 2 × 150 bp with the Illumina NovaSeq 6000 reagent kits (Illumina). Verification of the libraries was done using NanoDrop quantification (NanoDrop 8000; Thermo Scientific, Waltham, MA, USA). The reads (5,299,802 sequences, sequence length of 150 bp) were analyzed using tools available in Galaxy with default parameters (https://galaxy.migale.inrae.fr/) (1). *De novo* assembly was performed using Unicycler (Galaxy version 0.4.8.0) with quality control done with Quast (Galaxy version 5.0.2 + Galaxy 3) (2, 3), and genome annotation was performed using the Prokaryotic Genome Annotation Pipeline (PGAP, annotation software revision 5.2) (4). The percent genome coverage is 201, and the size of the assembly is 3,901,648 bp, made of 26 contigs with a GC content of 47% and an N_{50} value of 564,796 nucleotides. A total of 3,766 predicted protein-coding genes were detected with 78 tRNAs, 3 rRNAs, and 5 noncoding RNAs (ncRNAs). The bacterial species identified with more than 99.9% identity is *Bacillus velezensis* as determined by a BLAST search of the genome of 100 kb, using the nucleotide database collection of *Bacillus* (taxid: 1386) optimized for highly similar sequences. The Staramr tool (Galaxy version 0.7.2 + Galaxy 0) revealed that *B. velezensis* P1 does not harbor antibiotic resistance genes (https://github.com/phac-nml/staramr) and that no plasmids were predicted.

Editor Steven R. Gill, University of Rochester School of Medicine and Dentistry

Address correspondence to Romain Briandet, romain.briandet@inrae.fr.

The authors declare no conflict of interest.

Received 21 December 2021
Accepted 9 January 2022
Published 27 January 2022

Different genes involved in biofilm formation were detected in the genome (i.e., *eps*, *sps*, *cap*, *tapA→tasA*, *bslA*) (5–7). Using the antiSMASH genome analysis tool, 5 antibacterial genes were detected, encoding with a coverage of more than 98% bacillibactin, macrolactin, bacillaene, difficidin, and bacilysin (8, 9).

The biofilm formation and antimicrobial secretion properties of *B. velezensis* P1 are assumed to confer significant fitness to live and persist in the livestock building surface biotope.

Data availability. This whole-genome shotgun project has been deposited at DDBJ/ENA/GenBank under the accession number JAHLGR000000000 and in the NCBI Sequence Read Archive (SRA) under BioProject accession number PRJNA736682. The draft genome assembly and annotation can be found under BioProject number PRJNA736682 and BioSample number SAMN19656044, respectively.

ACKNOWLEDGMENTS

This study was funded by Lallemand Animal Nutrition, INRAE, and the Association Nationale de la Recherche et de la Technologie (ANRT) as part of Virgile Guéneau's Ph.D.

We are grateful to the INRAE MIGALE bioinformatics facility (https://migale.inrae.fr/) for providing technical support.

REFERENCES

1. Afgan E, Baker D, Batut B, van den Beek M, Bouvier D, Cech M, Chilton J, Clements D, Coraor N, Grüning BA, Guerler A, Hillman-Jackson J, Hiltemann S, Jalili V, Rasche H, Soranzo N, Goecks J, Taylor J, Nekrutenko A, Blankenberg D. 2018. The Galaxy platform for accessible, reproducible and collaborative biomedical analyses: 2018 update. Nucleic Acids Res 46:W537–W544. https://doi.org/10.1093/nar/gky379.
2. Wick RR, Judd LM, Gorrie CL, Holt KE. 2017. Unicycler: resolving bacterial genome assemblies from short and long sequencing reads. PLoS Comput Biol 13:e1005595. https://doi.org/10.1371/journal.pcbi.1005595.
3. Mikheenko A, Prjibelski A, Saveliev V, Antipov D, Gurevich A. 2018. Versatile genome assembly evaluation with QUAST-LG. Bioinformatics 34:i142–i150. https://doi.org/10.1093/bioinformatics/bty266.
4. Li W, O'Neill KR, Haft DH, DiCuccio M, Chetvernin V, Badretdin A, Coulouris G, Chitsaz F, Derbyshire MK, Durkin AS, Gonzales NR, Gwadz M, Lanczycki CJ, Song JS, Thanki N, Wang J, Yamashita RA, Yang M, Zheng C, Marchler-Bauer A, Thibaud-Nissen F. 2021. RefSeq: expanding the Prokaryotic Genome Annotation Pipeline reach with protein family model curation. Nucleic Acids Res 49:D1020–D1028. https://doi.org/10.1093/nar/gkaa1105.
5. Diehl A, Roske Y, Ball L, Chowdhury A, Hiller M, Molière N, Kramer R, Stöppler D, Worth CL, Schlegel B, Leidert M, Cremer N, Erdmann N, Lopez D, Stephanowitz H, Krause E, van Rossum B-J, Schmieder P, Heinemann U, Turgay K, Akbey Ü, Oschkinat H. 2018. Structural changes of TasA in biofilm formation of Bacillus subtilis. Proc Natl Acad Sci U S A 115:3237–3242. https://doi.org/10.1073/pnas.1718102115.
6. Eichenberger P, Fujita M, Jensen ST, Conlon EM, Rudner DZ, Wang ST, Ferguson C, Haga K, Sato T, Liu JS, Losick R. 2004. The program of gene transcription for a single differentiating cell type during sporulation in Bacillus subtilis. PLoS Biol 2:e328. https://doi.org/10.1371/journal.pbio.0020328.
7. Earl C, Arnaouteli S, Bamford NC, Porter M, Sukhodub T, MacPhee CE, Stanley-Wall NR. 2020. The majority of the matrix protein TapA is dispensable for Bacillus subtilis colony biofilm architecture. Mol Microbiol 114:920–933. https://doi.org/10.1111/mmi.14559.
8. Blin K, Shaw S, Steinke K, Villebro R, Ziemert N, Lee SY, Medema MH, Weber T. 2019. antiSMASH 5.0: updates to the secondary metabolite genome mining pipeline. Nucleic Acids Res 47:W81–W87. https://doi.org/10.1093/nar/gkz310.
9. Chen XH, Koumoutsi A, Scholz R, Eisenreich A, Schneider K, Heinemeyer I, Morgenstern B, Voss B, Hess WR, Reva O, Junge H, Voigt B, Jungblut PR, Vater J, Süssmuth R, Liesegang H, Strittmatter A, Gottschalk G, Borriss R. 2007. Comparative analysis of the complete genome sequence of the plant growth-promoting bacterium Bacillus amyloliquefaciens FZB42. Nat Biotechnol 25:1007–1014. https://doi.org/10.1038/nbt1325.

3.1.4 Article 5 : Positive biofilms to control surface-associated microbial communities in a broiler chicken production system - a field study

Virgile Guéneau, Ana Rodiles, Bastien Frayssinet, Jean-Christophe Piard, Mathieu Castex, Romain Briandet.

Frontiers in Microbiology, 2022, 13, pp.981747. 10.3389/fmicb.2022.981747.

frontiers | Frontiers in Microbiology

TYPE Original Research
PUBLISHED 15 August 2022
DOI 10.3389/fmicb.2022.981747

OPEN ACCESS

EDITED BY
Nikos Chorianopoulos,
Hellenic Agricultural
Organization, Greece

REVIEWED BY
Efstathios D. Giaouris,
University of the Aegean, Greece
Essam S. Soliman,
Suez Canal University, Egypt

*CORRESPONDENCE
Romain Briandet
romain.briandet@inrae.fr

SPECIALTY SECTION
This article was submitted to
Food Microbiology,
a section of the journal
Frontiers in Microbiology

RECEIVED 29 June 2022
ACCEPTED 21 July 2022
PUBLISHED 15 August 2022

CITATION
Guéneau V, Rodiles A, Frayssinet B,
Piard J-C, Castex M,
Plateau-Gonthier J and Briandet R
(2022) Positive biofilms to control
surface-associated microbial
communities in a broiler chicken
production system - a field study.
Front. Microbiol. 13:981747.
doi: 10.3389/fmicb.2022.981747

Positive biofilms to control surface-associated microbial communities in a broiler chicken production system - a field study

Virgile Guéneau[1,2], Ana Rodiles[2], Bastien Frayssinet[2], Jean-Christophe Piard[1], Mathieu Castex[2], Julia Plateau-Gonthier[2] and Romain Briandet[1]*

[1]Université Paris-Saclay, INRAE, AgroParisTech, Micalis Institute, Jouy-en-Josas, France, [2]Lallemand SAS, Blagnac, France

In the One Health concept, the use of beneficial bacteria to form positive biofilms that prevent the settlement of undesirable bacteria is a promising solution to limit the use of antimicrobials on farms. However, there is a lack of field studies reporting the onset of these beneficial bacteria after application and the effects on autochthonous surface microbiota. In the study reported here, the inner surfaces of commercial broiler chicken houses were treated or not with a bacterial consortium composed of *Bacillus* spp. and *Pediococcus* spp. strains, able to form covering biofilms in different laboratory models. Preinstalled coupons were sampled over time to capture microbial biofilm dynamics on-farm surfaces. The results showed that the bacterial consortium can establish on the farm surfaces, modulate microbial communities, and limit the implantation of Enterobacteriaceae and Enterococcaceae, two families containing potential pathogens.

KEYWORDS

positive biofilms, biosecurity, livestock building surfaces, microbial community structure, bacterial pathogens

Introduction

In standard intensive broiler farms, chickens live all their life on the same floor mainly covered by straw litter, wood shavings, or sawdust. Animal density is high (up to 21 birds/m²), and physicochemical conditions (illumination, temperature, and humidity) are optimized to favor animal growth. These conditions obviously trigger the development of microorganisms on the farm surfaces among which potential undesirable microorganisms (Guéneau et al., 2022b). Cleaning and disinfection (C&D) procedures are applied between each production batch in order to eliminate potential pathogens and avoid cross-contamination through a reduction of the microbial load of livestock building surfaces. These procedures are typically composed of wet cleaning

with detergent, disinfection, rinsing, and vacancy period steps before new animals enter (Luyckx et al., 2015a). The disinfectants typically used are quaternary ammonium compounds, aldehydes, and alcohols applied on surfaces by spraying or fogging (Luyckx et al., 2015b). It has been shown that these procedures are not totally effective in eradicating surface-associated communities (Luyckx et al., 2015a). The presence of microbial communities spatially organized on surfaces has been invoked to explain the incomplete action of C&D procedures (Flemming and Wuertz, 2019). Those surface-associated communities often named biofilms are three-dimensional microbial structures adhering to the surface and enclosed in self-produced extracellular polymeric substances (EPSs; Flemming, 2011). The EPS composition can vary between biofilms but is typically composed of a complex mixture of water and biopolymers including polysaccharides, eDNA, proteins, and amyloid fibers. Thanks to their spatial structure, the protective effect of the EPS matrix, and cellular phenotypic heterogeneity, biofilms can adapt exceptionally to environmental fluctuation and are often strongly tolerant to the action of antimicrobials (Bridier et al., 2011; Flemming et al., 2016). In their biofilm form, pathogens such as *Campylobacter jejuni*, *Enterococcus* spp., *Escherichia coli*, or *Salmonella* spp. have been shown to survive C&D procedure, leading to cross-contaminations between batches of animals (Peyrat et al., 2008; Marin et al., 2009, 2011). As an example, the contamination of chickens with the main zoonotic bacterial pathogen *Campylobacter* spp. in Europe can be explained by its ability to form biofilms on surfaces (Trachoo et al., 2002; Newell and Fearnley, 2003; EFSA and ECDC, 2021). Similarly, the major pathogens responsible for zoonosis in Europe have been described as biofilm formers in livestock building (Guéneau et al., 2022b). These observations support the need to study deeper biofilms in animal production systems for their control.

The poultry sector is one of the fastest growing and most flexible livestock sectors representing half of the additional meat expected to be produced within the next 10 years (OECDE and FAO, 2021). The current societal context leads producers to increase the sustainability and the biosecurity of their farms while reducing the use of antimicrobials such as antibiotics and surface disinfectants. In addition to polluting the environment, nonspecific and abusive use of these antimicrobials triggers the emergence of resistance that can be carried by pathogenic agents (McEwen and Collignon, 2018). Thereby, the World Health Organization defines antimicrobial resistance as a world public health threat that has to be managed urgently. In order to prevent zoonoses and increase food safety, innovative biosecurity tools are implemented. Biosecurity procedures are a set of measures designed to protect against the entry and spread of pathogens. The use of bacteria able to form positive biofilms and guide the microbial ecology of surfaces after C&D procedures is a new and promising biosafety tool. The concept is based on the rapid onset of beneficial bacteria that will occupy ecological niches on surfaces. These beneficial bacteria are being selected for their biofilm-forming abilities and other features linked to spatial and nutritional competition (Alvarez-Ordóñez et al., 2019; Guéneau et al., 2022b). Surface bioprotection is already used by breeders, and some products composed of cocktails of beneficial bacteria are already on the market. However, to our knowledge, no scientific study reports their stepwise implantation on livestock surfaces and their effects on the autochthonous microbiota.

In this study, the modulation of surface-associated microbial communities by the addition of a product composed of a consortium of selected bacteria was studied. First, biofilm phenotypes of the strains that composed the product were studied in different laboratory models. Then, using a field methodology previously described based on preinstalled coupons, surface microbiota was captured over time in treated and untreated buildings (Guéneau et al., 2022c). An integrated global analysis was used to analyze (i) the *in-situ* spatial organization of the surface-attached communities by confocal laser scanning microscopy (CLSM), (ii) bacteria counting in specific agar media, and (iii) the microbial diversity by high-throughput sequencing of the 16S rRNA gene. The exclusion effect of the product on Enterobacteriaceae and Enterococcaceae was studied using relative abundance ratio (Morton et al., 2019). Indeed, these two families contain chicken pathogens of interest such as *Salmonella* spp., *Escherichia coli*, *Enterococcus faecalis*, and *Enterococcus cecorum* (Foley et al., 2013; Manges, 2016; Souillard et al., 2022).

Methods

Macro-colonies, pellicles, and swarming phenotypes

All axenic experiments began with 5 ml of trypticase soy broth (TSB; Biomerieux, France) at 30°C overnight cultures without agitation made from an −80°C glycerol stock. The bacterial consortium LALFILM PRO® (Lallemand SAS, Blagnac, France) was diluted in TSB at 0.4 g/30 ml and was used after agitating for 2 h at 180 rpm at 37°C.

For macro-colonies phenotypes, six-well plates were used with 4 ml of TSA 1.5% agar supplemented with Congo red 40 μg/ml (Sigma-Aldrich, France) to observe amyloid fiber production and 20 μg/ml Coomassie Brilliant Blue to contrast protein production (Sigma-Aldrich, France; Neumann et al., 1994; Jones and Wozniak, 2017). Around 3 μl of culture was deposited in the center of each well, left to dry for 10 min, and then incubated at 30°C for 6 days. For pellicle formation, 4 ml of TSB was inoculated in the same conditions and incubated for 2 days at 30°C.

To perform the swarming experiments, TSB plates supplemented with agar to obtain 0.8% final were prepared (TSB Agar, Biomerieux, France) and allowed to dry in a hood for half an hour. Around 10 µl of culture was deposited in the center of the plate and left to dry for 10 min before 1 day of incubation at 30°C. For each model, a representative picture from three biological replicates was selected.

Field experiments in livestock buildings

Two independent experiments were conducted in France (batch 1 and batch 2), each with a building treated with a positive biofilm and an untreated control building. Each commercial broiler chicken house building was 800 m^2 (one control building and one treated per batch). The buildings had identical and unconnected artificial cross-ventilation systems and contained ~18,000 chickens each. Batch 1 was the experiment performed in summer 2020, and batch 2 was the one performed in winter 2020. Buildings of the two batches have never been treated with positive bacteria before.

Similar C&D procedures were performed in the buildings before experiments. They consist of cleaning the building with water the day after the animals left and applying the HD4N detergent (Anti-Germ Deutschland GmbH, Memmingen, Germany) at 1 ml/L, followed by rinsing with water under pressure. Calcium oxide was then applied the next day at 500 g/m^2 followed by treatment with VIROCID disinfectant (CID lines, Ypres, Belgium) at 1 ml/L. Around 4 kg/m^2 of chopped straw was set up without new addition during the batch, and then a fumigation protocol with FUMAGRI OPP (LCB Food Safety, Boz, France) was done.

A recently developed protocol was used to study farm surface-associated microbiota (Guéneau et al., 2022c). Briefly, polyvinyl chloride (PVC) coupons were cut from a flat bar (LEROY MERLIN, France) to obtain dimensions of 2.5 cm × 6 cm × 3 mm. Coupons were sterilized in an autoclave (HMC EUROPE, Germany), and dried in a dry oven (FD 115 model, Binder, Germany) for 15 min at 120°C. Then, they were deposited after the C&D procedure 4 days before animal entry below the central water lines of the buildings. The 1st day of the experiments corresponded to the day when coupons were deposited. LALFILM PRO® (Lallemand SAS, France) (total count minimum is 2^{10} CFU/g) was resuspended in tap water and applied following the commercial instructions at a rate of 0.2 g/m^2. The application was performed with a low pressure (<4 bars) atomizer on all farm internal surfaces including litter, walls, ceiling, drinkers, and feeders without chickens inside the building. The same procedure was applied only with tap water in the control building. The coupons were collected over time, this is five coupons per condition and per sampling day with sterile gloves and analyzed.

Confocal laser scanning microscopy

Biofilm structures on coupons were observed using a Leica HCS-SP8 CLSM at the INRAE MIMA2 microscopic platform (https://doi.org/10.15454/1.5572348210007727E12).

Environmental biofilms from coupons were labeled with 50 µl of a 54 µM calcein acetoxymethyl (CAM) solution (metabolic fluorescent dye reporting esterase activity). The dye was poured on the coupons and incubated in dark for 30 min at 37°C (Invitrogen, Carlsbad, CA, USA). The non-ionic molecules can enter passively into cells and be cleaved by intracellular esterase releasing a fluorescent non-permeant ionic residue. Biofilms on the coupons were counter-labeled in red with 50 µl of a 3 µl/ml of SYTO 61 (Invitrogen, Carlsbad, CA, USA), a cell-permeant red dye that labels nucleic acid.

For submerged *in vitro* biofilms, $1/100^e$ dilution in TSB was performed from the overnight cultures of strains alone or a suspension of the product concentration in TSB of 0.4 g/30 ml placed in a 50-ml Falcon after agitating for 2 h at 37°C. In total, 200 µl of the solutions were poured into the wells of polystyrene 96-well microtiter plates with a µclear® base (Greiner Bio-one, France) for 1.5 h at 30°C for an adhesion step. Supernatants were removed, 200 µl of fresh media were added, and the plate was put at 30°C for 2 or 24 h. A solution of 3 µl/ml of SYTO 9, a cell-permeant green dye that labels nucleic acid (Invitrogen, Carlsbad, CA, USA) was prepared, and 50 µl of this solution was added to each well.

A 600-Hz frequency was used to acquire images with the CLSM. SYTO 61 was excited with the HeNe laser at 633 nm, and the emitted fluorescence was collected with a hybrid detector in the range of 650–700 nm. SYTO 9 and CAM were excited with an argon laser set at 488 nm, and the emitted fluorescence was collected with a hybrid detector in the range of 500–550 nm. For all acquisitions from this work, a series of four images for each coupon of 512 × 512 pixels was acquired using a 63x water objective lens (numerical aperture = 1.2) by taking one image per µm in Z to capture the full height of the biofilm.

The 2D projections of biofilms and the extracted biofilm biovolume ($\mu m^3/\mu m^2$) were obtained using IMARIS 9.3.1 software (Bitplane, AG - Zurich, Switzerland).

Enumeration of culturable microorganisms from coupons

Coupons were placed in individual tubes containing 30 ml of a saline solution (NaCl 9 g/L). With a pipette cone, the biofilm was mechanically disrupted by successive round trips. Twenty passages vertically and horizontally were made on both sides of the coupon. After homogenization by vortexing 5 s and pipetting, successive dilutions in saline solution were carried out in duplicate using 1 ml of the resuspended biofilm

solution. Counts into agar were made from 1 ml of the desired dilution. TSA (Biomerieux, France) was used as nonselective media under aerobic conditions for 24 h at 30°C. In order to estimate bacilli spores in environmental biofilms, 1 ml of detached biofilm suspension was placed in a glass tube that was immersed in a water bath for 10 min at 80°C, in duplicate for each coupon, before enumeration on TSA ("TSA 80°C" condition). PSA+A medium (MRS, supplemented with cysteine hydrochloride 0.05% (wt/vol) + 100 μg/L novobiocin + 10 mg/L vancomycin + 50,000 U/L nystatin + 1 mg/L ampicillin) was used to enumerate *Pediococcus* spp. (Simpson et al., 2006). The remaining 26 ml of the detached biofilm suspension was centrifuged for 10 min at 6,000 × *g*, the supernatant was gently removed, and the pellets were placed at −20°C for DNA extraction.

High-throughput sequencing of the 16S rRNA gene and diversity analysis

DNA extraction, PCR, and sequencing

DNA from 80 bacterial pellets was extracted using DNeasy PowerLyzer PowerSoil Kit following the manufacturer's instructions (Qiagen, Germany). For PCR strategy, the same methodology was used as reported in Guéneau et al. (2022c). In short, this is PCR of V3-V4 regions of 16S rRNA marker genes using Phusion High-Fidelity PCR Kit (New England Biolabs, UK) amplified with universal primers F343 (5-CTT TCCCTACACGACGCTCTTCCGATCTTACGGRAGGCAGC AG-3) and R784 (5-GGAGTTCAGACGTGTGCTCTTCCG ATCTTACCAGGGTATCTAATCCT-3) at 66°C of annealing temperature on a thermocycler (GeneAmp PCR System 9700, Applied Biosystems, USA; Verschuren et al., 2018). Around 1% of agarose gel electrophoresis was used to ensure the expected size of the amplicons in PCR products, including negative controls. The NanoDrop Spectrophotometer ND-1000 (Thermo Fisher, Waltham, MA, USA) was used to quantify the DNA. DNA amplicons were sequenced using Illumina MiSeq technology in the GeT-PlaGe INRAE platform (Toulouse, France).

Diversity and taxonomical analysis using bioinformatics

Paired-end fastq files were truncated and denoized with DADA2 (Callahan et al., 2016) under default parameters excluding primers length. *De novo* multiple sequence alignment was performed by fast Fourier transform (MAFFT; Katoh and Standley, 2013), and FastTree was used to construct the phylogeny (Price et al., 2010). Rarefaction curves as goods coverage and observed AVSs were studied to ensure a full sampling of the community was taken. Data were rarefied at sequence depth higher than 10,000 sequences per sample to study diversity. Alpha-diversity was studied with the Shannon index and beta-diversity using weighted UniFrac distances. Relative abundance and natural log ratios were used to analyze relevant taxonomical changes (Morton et al., 2019). QIIME2 (v2020.2) was used to obtain all bioinformatics results (Bolyen et al., 2019).

Statistical analysis

Results are represented by the average and standard deviation (SD) or confidence interval (CI) of five coupons per Day. "Coupon" was considered the experimental unit and treatment the fixed factor. A two-way ANOVA using the uncorrected Fisher's least was used for the count and biovolume analysis using PRISM software (GraphPad, USA, California) with treatment and time as fixed factors. Linear discriminant analysis (LDA) effect size (LEfSe; Segata et al., 2011) was used to identify significant differences in taxonomical relative abundances. Diversity profiles were analyzed with the Kruskal–Wallis, Spearman's correlation, and ANOSIM in QIIME2, and log ratios with the Mann–Whitney *U*-test with seaborn (v0.5.0) in Python (v3.7.6). Data were considered significant when a *p*-value was smaller than 0.05.

Results

Beneficial bacteria biofilm phenotypes

The positive biofilm applied to building surfaces was composed of six strains of *Bacillus* spp. and two strains of *Pediococcus* spp. Four laboratory biofilm models were used to study the phenotypes of the strains composing the positive biofilm bacterial consortium (Figure 1). In the macro-colony model, which is an agar–air interface biofilm model, *Bacillus* 3 was able to form a structured colony with wrinkles, whereas the other *Bacillus* spp. have a flat structure covering most of the Petri dish. The bacterial consortium forms wrinkles and a beginning of spread is observed on the agar plate. In contrast to *Pediococcus* spp., *Bacillus* spp. strains and the bacterial consortium were able to form pellicles at the liquid–air interface.

In a swarming model on semisolid-air, *Bacillus* 2 was able to colonize the totality of the Petri dish after 24 h. *Bacillus* 4 and *Pediococcus* spp. were not able to swarm.

A submerged biofilm model was studied using CLSM. At 2 h, all strains started to cover the surface. The bacterial consortium showed a diversity of cell morphologies with cocci and bacilli. At 24 h, *Bacillus* 6 formed a spectacular thick biofilm as visualized by the virtual lateral shadow projection. The other strains covered the majority of the surface of wells with a thin layer of bacteria. The LALFILM PRO® showed a structured and dense biofilm structure.

10.3389/fmicb.2022.981747

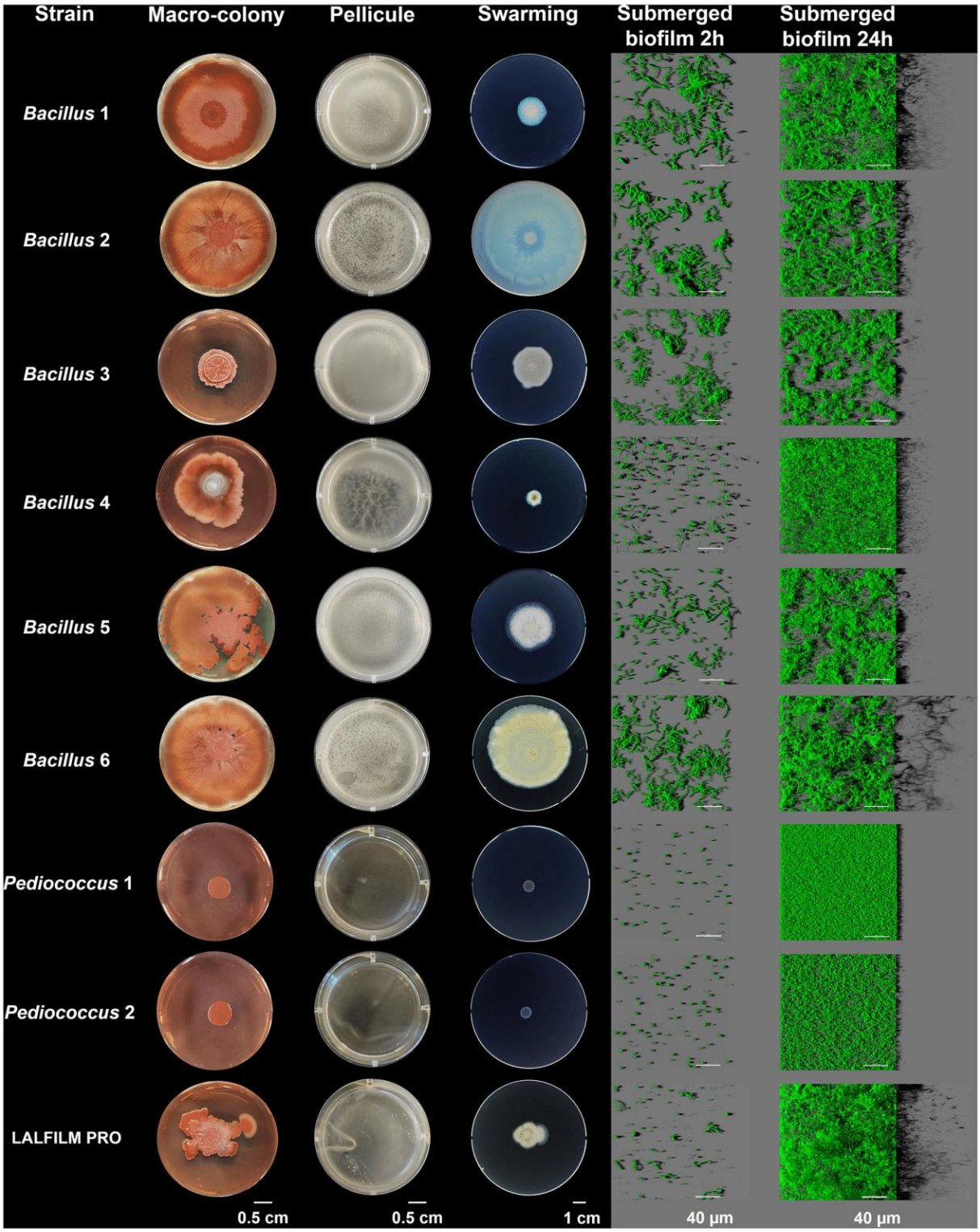

FIGURE 1
Biofilm phenotypes of the strains composing the bacterial consortium. Macro-colonies were used as a biofilm model at the solid–air interface and pellicles for the liquid–air interface. The swarming model allowed us to identify whether bacteria can colonize semisolid surfaces. Biofilm development of the submerged biofilm at 2 and 24 h using SYTO 9 to label the bacterial cells was observed using CLSM.

A stepwise installation of biofilms on farm surfaces

Microscopic quantification of the biofilm formation on coupons

Visualization of biofilms that developed on the surface of coupons was performed using CLSM. In batch 1, the day before the entrance of animals, a few microorganisms were detected, but the images show structured biofilms from day 10 with green clusters corresponding to metabolically active bacteria (CAM), especially in the treated condition (Figure 2A). Biovolume showed significantly more SYTO 61 signals corresponding to the entire microbial population on day 10 in the treated condition (Figure 2B). CAM biovolume signals showed no significant differences between the control and the treated condition (Figure 2C).

The surfaces of the second batch were less colonized by biofilms compared to the first batch, and no structured biofilm was observed for all time points (Figure 2D). On day 18, a higher SYTO 61 biovolume was detected in the treated condition ($p < 0.05$; Figure 2E).

As in batch 1, no significant differences with CAM biovolume were observed between the control and the treated conditions (Figure 2F). The range of biovolume values for SYTO 61 and CAM was 10 times smaller in batch 2 compared to batch 1.

Enumeration of cultivable bacteria

In the first batch, TSA counts of the control and the treated condition did not differ significantly across the experimental period (Figure 3A). An increase in TSA counts was measured after the entry of the animals and subsequently stabilize on day 10, reaching more than 6 logs (CFU)/cm^2. Initial values on TSA differed between conditions in batch 2 with significantly higher counts in the treated condition ($p < 0.05$; Figure 3B). A linear increase of CFU was observed in the treated condition, and a decrease appears between days 10 and 18 compared to the control ($p < 0.05$).

No significant differences between the two conditions of batch 1 were determined for TSA 80°C counts (Figure 3C). No increase in spore counts was observed after animal entry. In batch 2, more spores than the control were counted in the treated condition ($p < 0.05$; Figure 3D). A significantly lower number of spores was determined in the control of batch 1 compared to the control of batch 2 ($p < 0.05$). Interestingly for the two batches and in both conditions, the spore count values were very stable over time.

PSM + A counts were significantly higher in treated conditions for all samples except for day 18 in batch 1 (Figure 3E). For batch 2, the counts increased progressively in both conditions, whereas a decrease was observed on day 18 in the control condition (Figure 3F). With PSM + A medium, nothing was counted at the initial time point for the control condition of the two batches, whereas around 2 logs were observed in the treated conditions ($p < 0.05$; Figures 3E,F).

Modulation of livestock biofilm communities composition by the addition of beneficial bacteria

In total, 80 samples were successfully sequenced producing a total of 4,067,961 sequences of 411 ± 26 bp. After denoizing, a total of 1,997,152 corresponding to 2,187 ASVs were kept. Rarefaction curves showed a *plateau* and goods coverage close to 1 from about 5,000 sequences (Supplementary Figure 1). Two samples were discarded for the diversity analysis as <10,000 reads were recovered (3,760 and 5,316 sequences). Mitochondria and chloroplast were also removed (8 ASVs in total corresponding to 1,201 sequences) before the downstream taxonomical analysis.

Weighted UniFrac distances were studied by using ANOSIM (Table 1). For batch 1, distances between treatments were significantly different on days 4, 10, and 18 ($p < 0.05$). For batch 2, distances between treatments were significantly different on days 3, 10, and 18 ($p < 0.05$), with a trend for day 6 ($p = 0.068$).

The Shannon index was used to compare alpha-diversity between conditions (Figure 4). In general, the Shannon index was stable over time, specifically in batch 1 (Figure 4A). Lower values than control were observed in the treated condition for days 4, 5, and 10 in batch 1, and on days 3 and 18 in batch 2 ($p < 0.05$; Figure 4B). However, an increased Shannon diversity was noticed in treated vs. control on day 6 of batch 2 ($p < 0.05$; Figure 4B).

At phyla level 4, phylum described coupons composition as: Firmicutes (57.6%), Proteobacteria (38.6%), Actinobacteria (3.1%), and Bacteroidetes (0.6%; Supplementary Figure 2). The evolution of the phyla over time showed a predominance of Firmicutes (66.2%) over Proteobacteria (31.1%) and Actinobacteria (2.7%) before entry of the animals (day 3 or 4), then similar proportions of Firmicutes (51.7%) over Proteobacteria (47.4%) from day 5/6 to day 10, and finally a predominance of Firmicutes (64.5%) over Proteobacteria (25.7%), Actinobacteria (7.8%), and Bacteroidetes (2.1%) at day 18. When comparing conditions per batch, significant differences were found mainly in batch 2 on day 3 with a higher abundance of Firmicutes in the treated group and a higher relative abundance of Proteobacteria and Actinobacteria in the control ($p < 0.05$).

Individual sample profile at the family level reveals a relatively small variability across all five coupons per day and condition (Supplementary Figure 3). The entry of

10.3389/fmicb.2022.981747

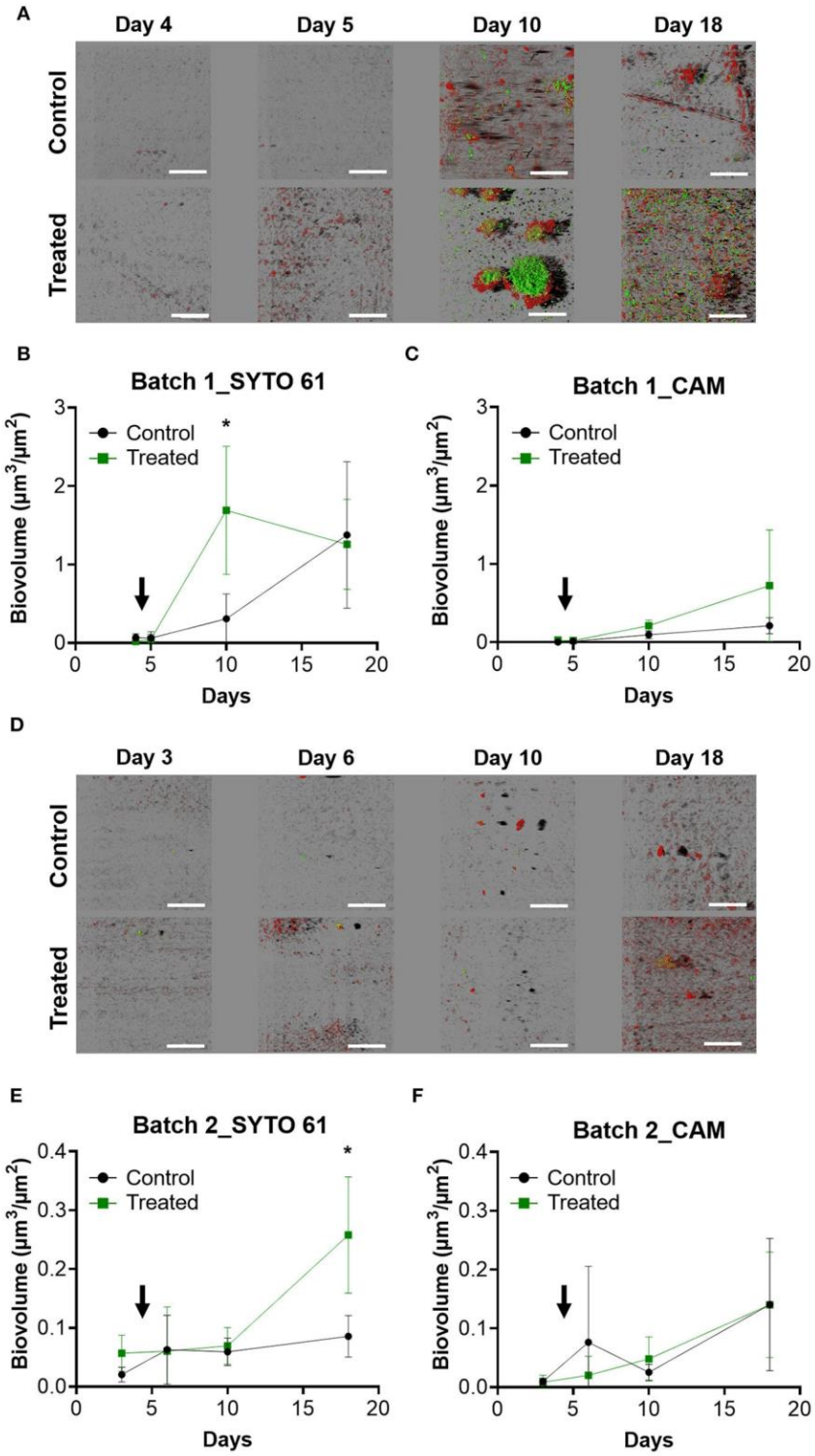

FIGURE 2
Visualization and quantification of surface-attached microbial communities of farms depending on the treatment and during the time. After sampling, coupons were labeled with SYTO 61 to detect the entire population in red and with CAM to contrast metabolically active populations and then observed with CLSM. IMARIS software was used to visualize images in blend mode **(A,D)** and to quantify SYTO 61 biovolume for batch 1 **(B)** and batch 2 **(E)**. Similarly, quantification of CAM was performed for batch 1 **(C)** and batch 2 **(F)**. The black arrow indicates the day when the animals enter the farm. Error bar shows standard deviation and asterisks represent significant differences between conditions on the same day ($p < 0.05$).

10.3389/fmicb.2022.981747

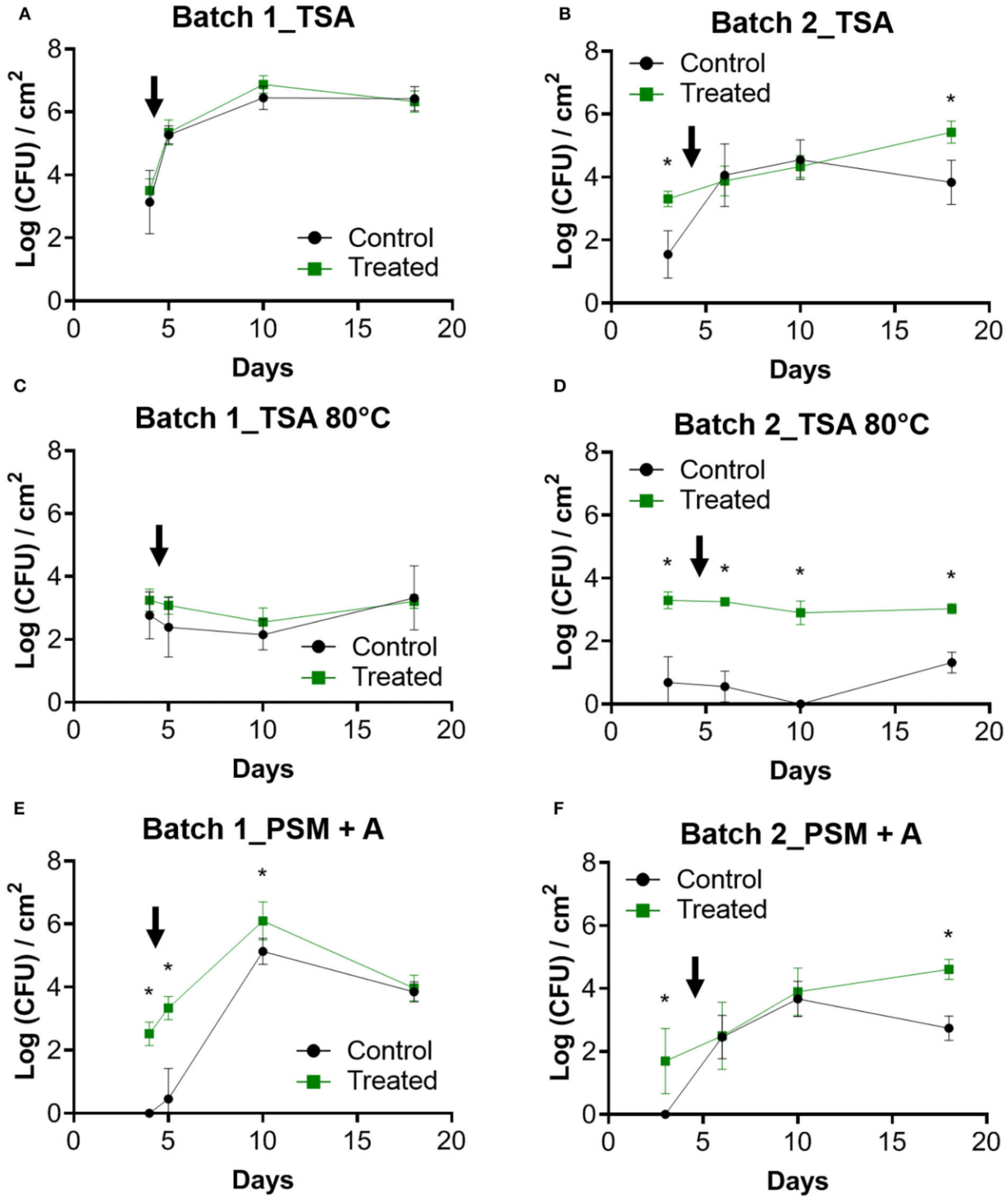

FIGURE 3
Enumeration of bacteria from coupons. Counts over time were performed on the biofilms previously removed from the coupons for batch 1 **(A,C,E)** and batch 2 **(B,D,F)**. TSA was used as a nonselective medium. Enumerations of these samples on TSA after treating them for 10 min at 80°C were performed to select spores forming bacteria. PSM + A medium was used to count *Pediococcus* genus. The black arrow indicates the day when the animals enter the farm. Error bar shows standard deviation and asterisks represent significant differences between conditions on the same day ($p < 0.05$).

10.3389/fmicb.2022.981747

the animals led to increases in the relative abundance of Enterobacteriaceae and Enterococcaceae families and decreases in Lactobacillaceae and Bacillaceae families. The relative abundance of *Bacillus* spp. and *Pediococcus* spp. and relevant ratios were analyzed. For both genera, abundance profiles across the experimental period differed between batches and treatments (Figure 5A). *Pediococcus* spp. relative abundance was significantly higher in the treated group for all days ($p < 0.05$), except on day 10 of batch 1, whereas *Bacillus* spp. relative abundance in the treated condition was higher compared to the control on days 4 and 5 for batch 1 and days 3, 6, and 10 for batch 2 ($p < 0.05$; Figure 5B). In the same way, the Enterobacteriaceae family was reduced on day 10 for batch 1 and on day 18 for batch 2 in the treated condition compared to the control ($p < 0.05$); Enterococcaceae family was also reduced on days 3, 6, and 18 for batch 2 in treated condition compared to control ($p < 0.05$; Supplementary Figure 4).

TABLE 1 ANOSIM of batch 1 and batch 2 per sampling day.

		Batch 1		Batch 2	
		R statistic	*p*-value	*R* statistic	*p*-value
Global	0.603	0.001*	0.700	0.001*	
Pairwise (control vs. treated)	Day 3			0.969	0.011*
	Day 4	0.506	0.025*		
	Day 5	0.08	0.207		
	Day 6			0.280	0.068
	Day 10	0.404	0.019*	0.564	0.007*
	Day 18	0.212	0.032*	0.644	0.008*

*Significant differences between control and treated groups ($p < 0.05$).

Enterobacteriaceae and Enterococcaceae families were compared against *Pediococcus* spp. and *Bacillus* spp. using natural log ratio (Figure 6). There was no Enterococcaceae detected on day 3 in the treated group of batch 2 at the earliest time point, making the ratio infinite on that day (not shown in plots; Figure 6A). Natural log ratio (*Bacillus*/Enterobacteriaceae) was enhanced by the treated condition, which was globally significant for batch 2 (Supplementary Figure 4) and specifically significant on days 18 and 6, respectively, for batches 1 and 2 ($p < 0.05$; Figure 6B). Similarly, treated conditions showed increases in natural log ratio (*Pediococcus*/Enterobacteriaceae) for all days with statistical significance for the first days (3–6 days) for both batches. At later time points, the same effect was significantly detected on days 10 and 18 of batch 2 (Figure 6C). Natural log ratio (*Pediococcus*/Enterococcaceae) in treated conditions was always higher vs. control, but significantly higher from day 3/4 to day 10 in batch 1 and until day 18 in batch 2 ($p < 0.05$; Figure 6C).

Discussion

The objective of this work was to analyze the modulating effect of a mixture of *Bacillus* spp. and *Pediococcus* spp. strains on the natural surface-attached microbial communities associated with poultry houses. Before testing in field conditions, several biofilm models were used in the laboratory to characterize the traits of the bacteria that have been applied on the farm. All the strains were able to form biofilms, and the combination of all of them constitutes the LALFILM PRO® product, which can form covering and structured biofilm *in vitro*. The set of complementary techniques used to analyze livestock building surfaces demonstrated that the mixture of beneficial bacteria can also be established on farm surfaces. It also revealed contrasted situations and heterogeneities between farm buildings (batches).

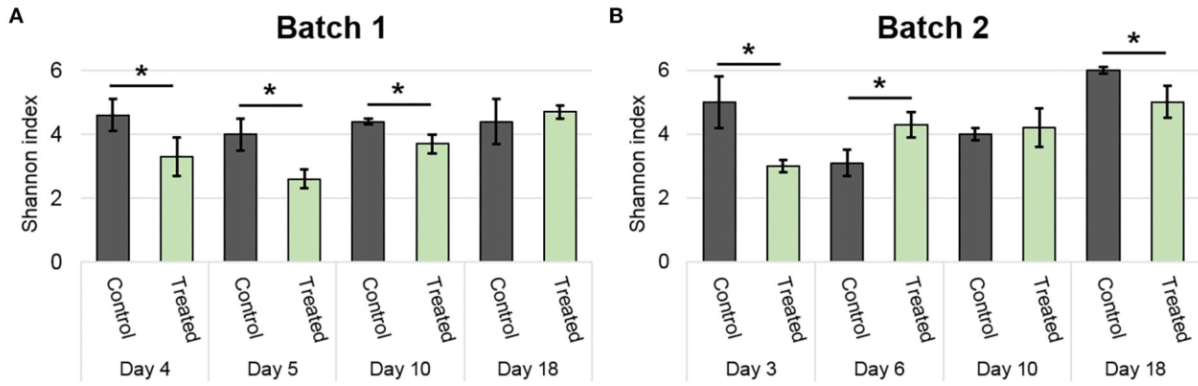

FIGURE 4
Modulation of bacterial community diversity by the addition of positive bacteria. The Shannon index of batch 1 **(A)** and batch 2 **(B)** during the experimental period. Error bar shows standard deviation and asterisks represent significant differences between conditions on the same day ($p < 0.05$).

10.3389/fmicb.2022.981747

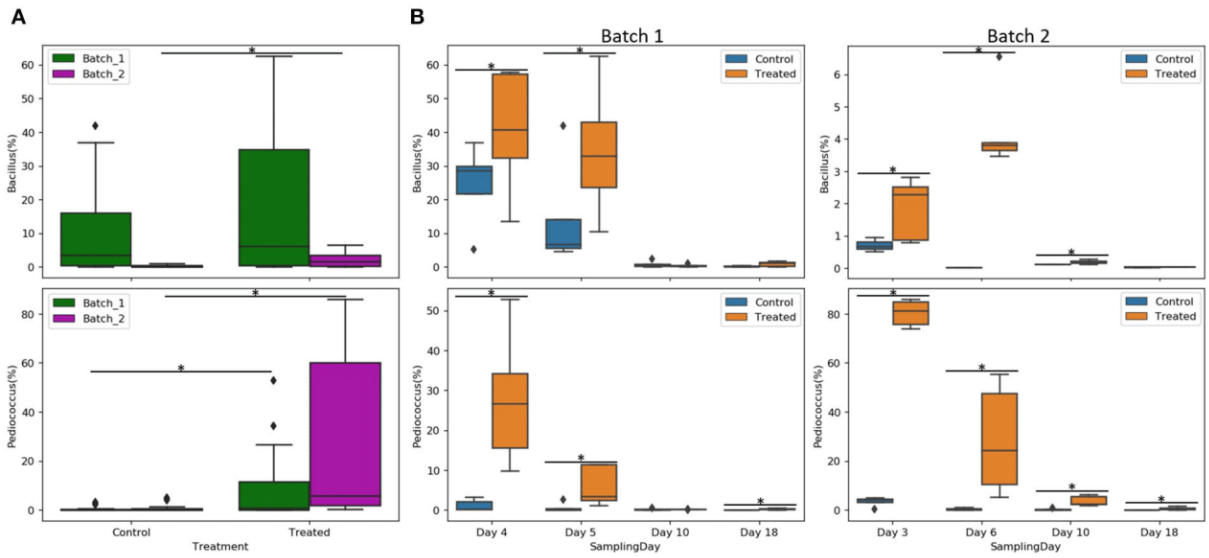

FIGURE 5
Relative abundance of *Bacillus* and *Pediococcus* per batch **(A)** and per sampling day **(B)** of different conditions (control or treated). Asterisks represent significant differences between conditions ($p < 0.05$).

Indeed, even if the observed environmental biofilms of the farm were sparse, quantification of the SYTO 61 biovolume allowed to show that more biomass was detected in the treated condition in both batches. Specific counts showed more *Pediococcus* spp. in the treated conditions, especially the first few days of sampling before the animals entered, with no *Pediococcus* spp. detected in the controls. Relative abundances of *Pediococcus* spp. were significantly higher in the treated condition for both batches. The large amount of *Bacillus* spp. detected in batch 1 control makes it difficult to differentiate the beneficial bacilli from the mixture that was applied in the treated building. In batch 2, significantly more total aerobic bacteria were counted in the treated condition, and *Bacillus* spp. relative abundance correlated with the spore counts on TSA 80°C for all time points, except for day 18.

In addition to being implanted on surfaces, the product can modulate the alpha diversity of the surface communities. In batch 1, a decrease of the Shannon index is observed for the treated group on days 4, 5, and 10 before returning to the same value as the control. Since the Shannon index is calculated based on species richness and evenness, adding a large number of bacteria of identical species lowers the value. These values are in line with the establishment of the products on the surfaces at least for the 1st days. The same observations were made for batch 2 on days 3 and 18, but a lower Shannon index value is calculated in the control on day 6, which could be explained by a higher relative proportion of Enterobacteriaceae (43%) and Enterococcaceae families (43%; e.g., *E. casseliflavus* and *E. cecorum*) due to animal entrance. As revealed by the weighted UniFrac distances of beta diversity, the distribution or composition of species was also modulated by the treatment in both batches and at all sampling points except the next days of animal entry (days 5–6) where a similar composition was found between coupon treatments.

The increase of *Bacillus* spp. and *Pediococcus* spp. abundance was correlated with a decrease in the Shannon diversity. The treatment increases *Bacillus* spp. and *Pediococcus* spp. quantities (i.e., abundance and counts) and the relevant ratios, probing a concomitant decrease of Enterobacteriaceae and Enterococcaceae families. Despite these promising results, further analysis would be required for a better resolution. Other techniques, such as qPCR, will be used in the future to track targeted pathogenic strains (Postollec et al., 2011).

The different approaches showed colonization of the applied consortium, but it is unclear whether the product is able to grow and be metabolically active on the surfaces and not just persistent "without growth" acting, hence more like a physical barrier as the main mode of action. No significant differences were observed with the quantification of CAM biovolume for both conditions and in both batches. More *Pediococcus* spp. were enumerated during the earlier days in the batches in the treated condition, but the increase in values that follow may be due to the detection of environmental *Pediococcus* spp. detected also in the controls. Moreover, the values of spores count were very stable during the experiment even in the control, which makes it impossible to conclude whether the *Bacillus* spp. of

10.3389/fmicb.2022.981747

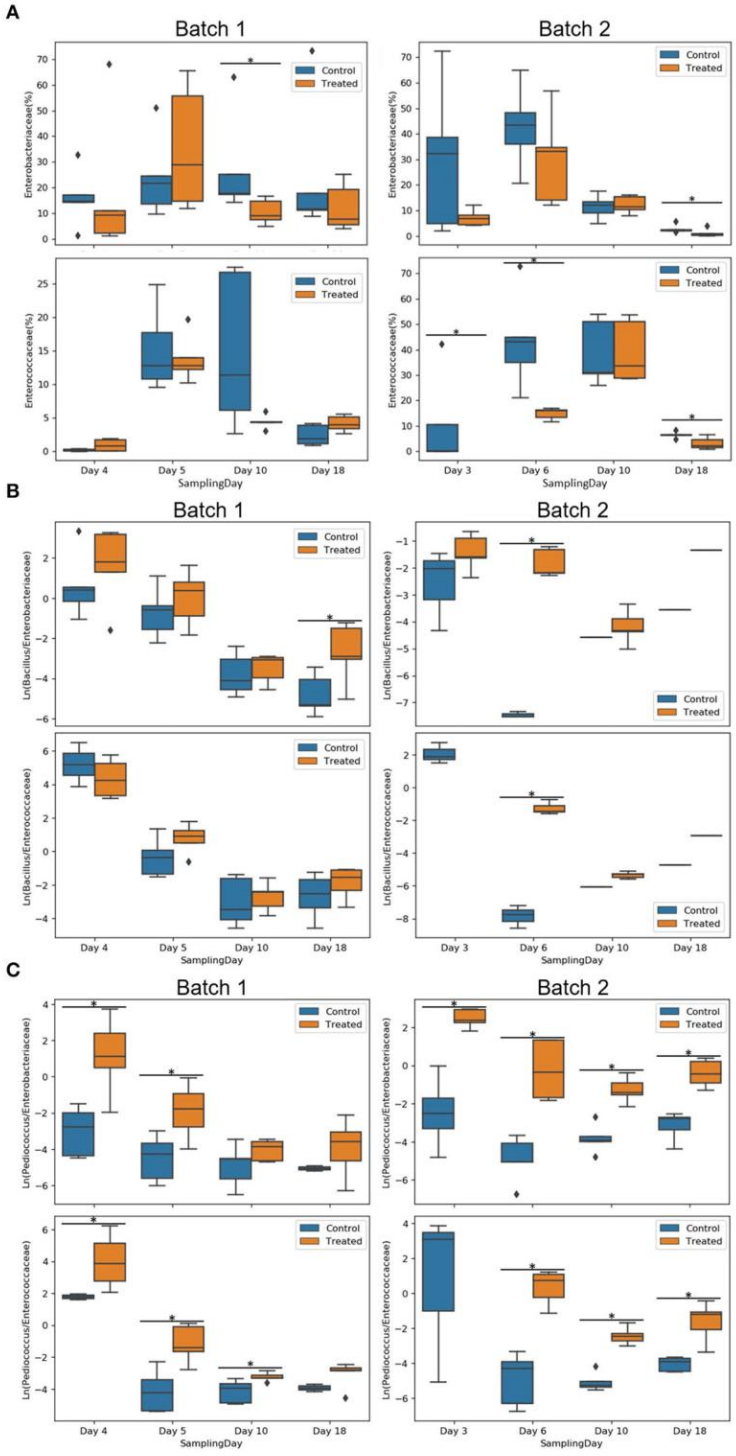

FIGURE 6
Comparison of Enterobacteriaceae and Enterococcaceae families against *Pediococcus* spp. and *Bacillus* spp. using natural log ratio. Relative abundance of Enterobacteriaceae and Enterococcaceae of batches 1 and 2 per condition (control and treated) and sampling day **(A)**. Natural log ratios of *Bacillus* **(B)** or *Pediococcus* **(C)** vs. Enterobacteriaceae or Enterococcaceae on the coupon biofilms of batch 1 and batch 2 per condition (control or treated) and sampling day. Sample representation per ratio was 76 biofilm coupons for *Pediococcus*/Enterobacteriaceae, 64 for *Bacillus*/Enterobacteriaceae, 66 for *Pediococcus*/Enterococcaceae, and 55 for *Bacillus*/Enterococcaceae coupons. Note that no Enterococcaceae was present in the treated condition on day 3 (infinite ratio), and other samples contained zeros on one side of their log ratio. Asterisks represent significant differences between conditions ($p < 0.05$).

the product, initially used in the form of spores, were able to grow. The relative abundance of the *Bacillus* spp. that decreases and the stable value of spores over time are consistent with the idea that the quantity of *Bacillus* spp. is stable during the time on the farm after the C&D protocols. The litter used in batch 1 was left outside for a longer period, which may have resulted in *Bacillus* spp. colonization. This could explain the higher number of spores detected in the batch 1 control compared to batch 2. Another hypothesis is that the C&D process before batch 1 was less efficient because the counts on TSA were also higher in the control building of batch 1 compared to batch 2.

Our results indicate that the initial situation between the two batches was different in terms of community profiles, microbial density, and spatial organization of the communities. Initial counts before animal entry were not identical across batches for control. The bacterial count and biovolume of the batch 1 control were higher than those of the batch 2 control. The CLSM images showed that at the beginning of the rearing cycle, biofilms were poorly developed and did not completely cover the surfaces of the coupons, especially for batch 2. Ten times less biovolume on batch 2 was quantified compared to batch 1. More total bacteria and spores were counted in batch 1 for all the experiments, with a very stable value of spores during the time for the two batches. The number of spores in the control of batch 1 was correlated with the relative abundance of *Bacillus* spp. These results show the importance of biological replicates for this type of field study. The biofilms of the product did not cover the entire surface of the coupons in this farm setting, although it was the case *in vitro*, in the laboratory. It can be interesting to develop a field model in the lab to study biofilm formation in conditions closer to those encountered on farms (temperature, humidity, poor nutritive medium, and materials). Modeling the interactions and testing the ecological theories within these positive bacterial consortia in simplified communities appear to be a promising step to improve the product composition (De Roy et al., 2014). In addition, the study of bacteria naturally present in farms would allow new selection criteria of strains (phenotypes and genomes), already identified as capable of living in these environments (Guéneau et al., 2022a).

A previous study compared the use of beneficial bacteria guiding surface microbial ecology with conventional C&D protocols in livestock buildings (Luyckx et al., 2016). In our study, the application of positive biofilm is a complement to the C&D protocol and not a simple substitution. Indeed, a surface with a reduced load of microorganisms obtained by C&D will be more favorable to the settlement of a positive biofilm. The observation of a decrease in the abundance of *Bacillus* spp. and *Pediococcus* spp. over time suggests that the product will be particularly effective at the beginning of the breeding process, when the microbial load is low, thus limiting the implantation and early development of harmful microorganisms. Other studies showed that natural positive resident microbiota of smear cheese wooden shelves had an effect on the exclusion of pathogens on surfaces by nutritional competition when the natural microbiota is already established or develops faster than the pathogen (Guillier et al., 2008). In addition, studies on *Agaricus bisporus* biocontrol have shown that the addition of positive biofilm-forming bacteria in compost with a low initial microorganism load was able to limit the early establishment of the main green mold mushroom pathogens (Pandin et al., 2019).

Conclusion

This field study demonstrated that the positive biofilm-forming bacteria used can establish on livestock building surfaces and to modulate the biofilm community structure and diversity, with special reference to the reduction of the ratio involving Enterobacteriaceae and Enterococcaceae families. Large-scale field experiments will be required to get significant statistics on the effect of positive biofilm on the prevalence of specific targeted pathogens. This study also highlights microbial variability between production batches of the same farm within the same building. These promising results encourage the innovative use of positive biofilms to guide these ecological systems.

Data availability statement

The datasets presented in this study can be found in online repositories. The names of the repository/repositories and accession number(s) can be found at: https://www.ncbi.nlm.nih.gov, PRJNA855604.

Author contributions

VG, J-CP, BF, MC, JP-G, and RB: conceptualization and methodology. J-CP, MC, JP-G, and RB: validation and supervision. VG and AR: formal analysis and data curation. VG, JP-G, and RB: investigation. MC and RB: resources, project administration, and funding acquisition. VG: writing the original draft preparation. AR, MC, JP-G, and RB: writing, reviewing, and editing. All authors have read and agreed to the published version of the manuscript.

Funding

This research was funded by INRAE, Lallemand SAS, and Association Nationale

de la Recherche et de la Technologie (contract 2020/0548).

Conflict of interest

Authors VG, AR, BF, MC, and JP-G were employed by Lallemand SAS marketing the product LALFILM PRO® used as a positive biofilm in this study.

The remaining authors declare that the research was conducted in the absence of any commercial or financial relationships that could be construed as a potential conflict of interest.

Publisher's note

Supplementary material

The Supplementary Material for this article can be found online at: https://www.frontiersin.org/articles/10.3389/fmicb.2022.981747/full#supplementary-material

References

Alvarez-Ordóñez, A., Coughlan, L. M., Briandet, R., and Cotter, P. D. (2019). Biofilms in food processing environments: challenges and opportunities. *Annu. Rev. Food Sci. Technol.* 10, 173–195. doi: 10.1146/annurev-food-032818-121805

Bolyen, E., Rideout, J. R., Dillon, M. R., Bokulich, N. A., Abnet, C. C., Al-Ghalith, G. A., et al. (2019). Reproducible, interactive, scalable and extensible microbiome data science using QIIME 2. *Nat. Biotechnol.* 37, 852–857. doi: 10.1038/s41587-019-0209-9

Bridier, A., Briandet, R., Thomas, V., and Dubois-Brissonnet, F. (2011). Resistance of bacterial biofilms to disinfectants: a review. *Biofouling* 27, 1017–1032. doi: 10.1080/08927014.2011.626899

Callahan, B. J., McMurdie, P. J., Rosen, M. J., Han, A. W., Johnson, A. J. A., and Holmes, S. P. (2016). DADA2: high-resolution sample inference from Illumina amplicon data. *Nat. Methods* 13, 581–583. doi: 10.1038/nmeth.3869

De Roy, K., Marzorati, M., Van den Abbeele, P., Van de Wiele, T., and Boon, N. (2014). Synthetic microbial ecosystems: an exciting tool to understand and apply microbial communities. *Environ. Microbiol.* 16, 1472–1481. doi: 10.1111/1462-2920.12343

EFSA and ECDC (2021). The European union one health 2019 zoonoses report. *EFSA J.* 19, e06406. doi: 10.2903/j.efsa.2021.6406

Flemming, H.-C. (2011). The perfect slime. *Colloids Surf. B Biointerfaces* 86, 251–259. doi: 10.1016/j.colsurfb.2011.04.025

Flemming, H.-C., Wingender, J., Szewzyk, U., Steinberg, P., Rice, S. A., and Kjelleberg, S. (2016). Biofilms: an emergent form of bacterial life. *Nat. Rev. Microbiol.* 14, 563–575. doi: 10.1038/nrmicro.2016.94

Flemming, H.-C., and Wuertz, S. (2019). Bacteria and archaea on Earth and their abundance in biofilms. *Nat. Rev. Microbiol.* 17, 247–260. doi: 10.1038/s41579-019-0158-9

Foley, S. L., Johnson, T. J., Ricke, S. C., Nayak, R., and Danzeisen, J. (2013). *Salmonella* pathogenicity and host adaptation in chicken-associated serovars. *Microbiol. Mol. Biol. Rev.* 77, 582–607. doi: 10.1128/MMBR.00015-13

Guéneau, V., Piard, J.-C., Frayssinet, B., Loux, V., Chiapello, H., Plateau-Gonthier, J., et al. (2022a). Genome sequence of *Bacillus velezensis* P1, a strain isolated from a biofilm captured on a pig farm building. *Microbiol. Resour. Announc.* 11, e0121921. doi: 10.1128/MRA.01219-21

Guéneau, V., Plateau-Gonthier, J., Arnaud, L., Piard, J.-C., Castex, M., and Briandet, R. (2022b). Positive biofilms to guide surface microbial ecology in livestock buildings. *Biofilm* 4, 100075. doi: 10.1016/j.bioflm.2022.100075

Guéneau, V., Rodiles, A., Piard, J.-C., Frayssinet, B., Castex, M., Plateau-Gonthier, J., et al. (2022c). Capture and *ex-situ* analysis of environmental biofilms in livestock buildings. *Microorganisms* 10, 2. doi: 10.3390/microorganisms10010002

Guillier, L., Stahl, V., Hezard, B., Notz, E., and Briandet, R. (2008). Modelling the competitive growth between *Listeria monocytogenes* and biofilm microflora of smear cheese wooden shelves. *Int. J. Food Microbiol.* 128, 51–57. doi: 10.1016/j.ijfoodmicro.2008.06.028

Jones, C. J., and Wozniak, D. J. (2017). Congo red stain identifies matrix overproduction and is an indirect measurement for c-di-GMP in many species of bacteria. *Methods Mol. Biol.* 1657, 147–156. doi: 10.1007/978-1-4939-7240-1_12

Katoh, K., and Standley, D. M. (2013). MAFFT multiple sequence alignment software version 7: improvements in performance and usability. *Mol. Biol. Evol.* 30, 772–780. doi: 10.1093/molbev/mst010

Luyckx, K., Dewulf, J., Van Weyenberg, S., Herman, L., Zoons, J., Vervaet, E., et al. (2015a). Comparison of sampling procedures and microbiological and non-microbiological parameters to evaluate cleaning and disinfection in broiler houses. *Poult. Sci.* 94, 740–749. doi: 10.3382/ps/pev019

Luyckx, K., Millet, S., Van Weyenberg, S., Herman, L., Heyndrickx, M., Dewulf, J., et al. (2016). Comparison of competitive exclusion with classical cleaning and disinfection on bacterial load in pig nursery units. *BMC Vet. Res.* 12, 189. doi: 10.1186/s12917-016-0810-9

Luyckx, K. Y., Van Weyenberg, S., Dewulf, J., Herman, L., Zoons, J., Vervaet, E., et al. (2015b). On-farm comparisons of different cleaning protocols in broiler houses. *Poult. Sci.* 94, 1986–1993. doi: 10.3382/ps/pev143

Manges, A. R. (2016). *Escherichia coli* and urinary tract infections: the role of poultry-meat. *Clin. Microbiol. Infect.* 22, 122–129. doi: 10.1016/j.cmi.2015.11.010

Marin, C., Balasch, S., Vega, S., and Lainez, M. (2011). Sources of *Salmonella* contamination during broiler production in Eastern Spain. *Prev. Vet. Med.* 98, 39–45. doi: 10.1016/j.prevetmed.2010.09.006

Marin, C., Hernandiz, A., and Lainez, M. (2009). Biofilm development capacity of *Salmonella* strains isolated in poultry risk factors and their resistance against disinfectants. *Poult. Sci.* 88, 424–431. doi: 10.3382/ps.2008-00241

McEwen, S. A., and Collignon, P. J. (2018). Antimicrobial resistance: a one health perspective. *Microbiol. Spectr.* 6, 2–6. doi: 10.1128/microbiolspec.ARBA-0009-2017

Morton, J. T., Marotz, C., Washburne, A., Silverman, J., Zaramela, L. S., Edlund, A., et al. (2019). Establishing microbial composition measurement standards with reference frames. *Nat. Commun.* 10, 2719. doi: 10.1038/s41467-019-10656-5

Neumann, U., Khalaf, H., and Rimpler, M. (1994). Quantitation of electrophoretically separated proteins in the submicrogram range by dye elution. *Electrophoresis* 15, 916–921. doi: 10.1002/elps.11501501132

Newell, D. G., and Fearnley, C. (2003). Sources of *Campylobacter* colonization in broiler chickens. *Appl. Environ. Microbiol.* 69, 4343–4351. doi: 10.1128/AEM.69.8.4343-4351.2003

OECDE and FAO (2021). *OECD-FAO Agricultural Outlook 2021-2030*. Paris: FAO

Pandin, C., Darsonval, M., Mayeur, C., Le Coq, D., Aymerich, S., and Briandet, R. (2019). Biofilm formation and synthesis of antimicrobial compounds by the biocontrol agent *Bacillus velezensis* QST713 in an agaricus bisporus compost micromodel. *Appl. Environ. Microbiol.* 85, e00327–e00319. doi: 10.1128/AEM.00327-19

Peyrat, M. B., Soumet, C., Maris, P., and Sanders, P. (2008). Recovery of *Campylobacter jejuni* from surfaces of poultry slaughterhouses after cleaning and disinfection procedures: analysis of a potential source of carcass contamination. *Int. J. Food Microbiol.* 124, 188–194. doi: 10.1016/j.ijfoodmicro.2008.03.030

Postollec, F., Falentin, H., Pavan, S., Combrisson, J., and Sohier, D. (2011). Recent advances in quantitative PCR (qPCR) applications in food microbiology. *Food Microbiol.* 28, 848–861. doi: 10.1016/j.fm.2011.02.008

Price, M. N., Dehal, P. S., and Arkin, A. P. (2010). FastTree 2–approximately maximum-likelihood trees for large alignments. *PLoS ONE* 5, e9490. doi: 10.1371/journal.pone.0009490

Segata, N., Izard, J., Waldron, L., Gevers, D., Miropolsky, L., Garrett, W. S., et al. (2011). Metagenomic biomarker discovery and explanation. *Genome Biol.* 12, R60. doi: 10.1186/gb-2011-12-6-r60

Simpson, P. J., Fitzgerald, G. F., Stanton, C., and Ross, R. P. (2006). Enumeration and identification of pediococci in powder-based products using selective media and rapid PFGE. *J. Microbiol. Methods* 64, 120–125. doi: 10.1016/j.mimet.2005.04.019

Souillard, R., Laurentie, J., Kempf, I., Le Caër, V., Le Bouquin, S., Serror, P., et al. (2022). Increasing incidence of *Enterococcus*-associated diseases in poultry in France over the past 15 years. *Vet. Microbiol.* 269, 109426. doi: 10.1016/j.vetmic.2022.109426

Trachoo, N., Frank, J. F., and Stern, N. J. (2002). Survival of *Campylobacter jejuni* in biofilms isolated from chicken houses. *J. Food Prot.* 65, 1110–1116. doi: 10.4315/0362-028X-65.7.1110

Verschuren, L. M. G., Calus, M. P. L., Jansman, A. J. M., Bergsma, R., Knol, E. F., Gilbert, H., et al. (2018). Fecal microbial composition associated with variation in feed efficiency in pigs depends on diet and sex. *J. Anim. Sci.* 96, 1405–1418. doi: 10.1093/jas/sky060

3.1.5 Article 6 : Insights into the genomic and phenotypic characteristics of *Bacillus* spp. strains isolated from biofilms in broiler farms

Virgile Guéneau, Guillermo Jiménez, Mathieu Castex, Romain Briandet.

En préparation.

Insights into the genomic and phenotypic characteristics of *Bacillus* spp. strains isolated from biofilms in broiler farms

Virgile Guéneau[a,b], Guillermo Jiménez[b], Mathieu Castex[b], Romain Briandet[a,*]

[a] Université Paris-Saclay, INRAE, AgroParisTech, Micalis Institute,78350 Jouy-en-Josas, France

[b] Lallemand SAS, 31702, Blagnac, France

* Address correspondence to Romain Briandet, romain.briandet@inrae.fr

Keywords: Biofilm, *Bacillus* spp., eDNA, antibiotics resistance genes, antimicrobials secretion, broiler farms, microbial ecology

Abstract

The characterization of surface microbiota living in biofilms within livestock buildings has been relatively unexplored, despite its potential impact on animal health. To enhance our understanding of these microbial communities, we characterized eleven spore-forming strains isolated from two commercial broiler chicken farms. Sequencing of the strains revealed them to belong to three species *Bacillus velezensis*, *Bacillus subtilis*, and *Bacillus licheniformis*. Genomic analysis revealed of the presence of antimicrobial resistance genes (ARG) and genes associated with antimicrobial secretion specific to each species. We conducted a comprehensive characterization of the biofilm formed by these strains under various conditions and we revealed significant structural heterogeneity across the different strains. A macro-colony interaction model was employed to assess the compatibility of these strains to coexist in mixed biofilms. We identified highly competitive *B. velezensis* trains, which cannot coexist with other *Bacillus* spp. Using confocal laser scanning microscopy along with a specific dye for extracellular DNA (eDNA), we uncovered the importance of extracellular DNA for the formation of *B. licheniformis* biofilms. All together, the results highlight the heterogeneity in both genome and biofilm structure among *Bacillus* spp. isolated from biofilms present within livestock buildings.

Introduction

Livestock building surfaces are reservoirs of potential undesirable microorganisms and so, considered a vector for disease transmission in animals [1]. Yet, scientific studies investigating the microbial composition, diversity and the structure of biofilms associated to animal production systems remain scarce. To minimize the presence of undesirable microorganisms on the surfaces of livestock buildings between successive batches of animals, cleaning and disinfection procedures using biocides are implemented. However, the efficacy of these procedures can be reduced by the formation of biofilm structures formed by the microbial community, which can adhere to surfaces [2].

The majority of microorganisms on Earth live in a biofilm lifestyle [3]. Biofilms are spatially organized microbial communities embedded in a self-produced extracellular matrix [4]. The extracellular matrix of biofilms consists mainly of water, exopolysaccharides, proteins, and extracellular DNA (eDNA) [5]. Due to the matrix and resulting gradients, these communities possess emergent properties compared to the planktonic form, such as greater tolerance to environmental fluctuations like the application of biocides or antibiotics [6,7].

Antibiotics are sometimes used on a massive scale in animal production systems as curative or preventive measures to control pathogens as well as growth promoter for animals on livestock farms, depending on the regulations in force to control their use. The use of antibiotics inevitably leads to the emergence of resistances. Antimicrobial Resistance Genes (ARGs) can be carried by pathogens or by other members of the microbial community, including the ones attached to surfaces [8,9]. Strains carrying mobilizable ARGs of clinical relevance are then considered undesirable because they can confer resistance to microbial pathogens and pose safety concerns for animals, humans, and the environment.

We recently described that *Bacillus* spp. can be very abundant on commercial poultry farm surfaces, even after cleaning and disinfection procedures and this even prior to the entrance of animals [10]. The *Bacillus* genus is ubiquitous in the environment and known for its ability to form biofilms [11,12]. Some *Bacillus* spp. may be undesirable and carry mobile ARGs, or be pathogenic such as *B. cereus* or *B. anthracis*. Characterization of *Bacillus* spp. strains encountered on farms can therefore be important to i) identify strains potentially posing safety concerns and find ways to limit their establishment on farm surfaces, and ii) select for safe

strains with high biofilm forming capacity which could be used as competitive exclusion agents. Indeed, the biotechnological potential of beneficial strains of *Bacillus* spp. have already largely investigated and in various industrial applications and products have been developed, such as probiotics [13,14], biocontrol agents [15] or positive biofilms [1].

The presented study aimed at characterising 11 spore-forming strains isolated from poultry farms surfaces [10] using genomic analysis and biofilm characterization using different laboratory models. In order to increase our knowledge of the microbial ecology of these biotopes, we studied the compatibility links between these strains with a macro-colony biofilm model used to observe the potential of biofilms to merge and cover the surface [16]. Confocal laser scanning microscopy (CLSM) coupled with image analysis was used to visualize and quantify submerged biofilm formation with a focus on eDNA quantification and its involvement in the formation of biofilms.

Methods

Isolation of strains from farm surface biofilms

Strains were isolated from the surfaces of 2 commercial poultry farms (i.e. building 1 and 2) [10] using a coupon sampling method [17]. After sampling, the polyvinyl chloride (PVC) coupons (2.5 cm × 6 cm × 3 mm) were placed in individual tubes containing 30 mL of a saline solution (NaCl 9 g/L). The microbiota attached to the surface was mechanically detached using a pipette cone in successive round trips. In order to count spores in the environmental biofilms, 1 ml of detached biofilm suspension was placed in a glass tube that was immersed in a water bath for 10 min at 80°C, before enumeration on TSA (TSB Agar, Biomérieux, France). Representative colonies were picked and grown overnight (~16 h) in TSB (TSB; Biomérieux, France) before being stored in glycerol tubes at -80°C.

DNA extraction and sequencing

The same protocol as described by Guéneau et al. [18] was used to extract and sequence the genomes. Concisely, from a -80°C glycerol stock, the strains were cultured in TSB under agitation at 37°C overnight. Genomic DNA was extracted and purified using the Monarch genomic DNA purification kit (New England Biolabs, Ipswich, MA, USA). DNA sequencing

(DNA-seq) was performed at the GeT-PlaGe core facility (INRAE, Toulouse, France; www.genotoul.fr/en/). DNA-seq libraries were prepared according to Illumina's protocols using the TruSeq Nano DNA high-throughout (HT) library kit (Illumina, San Diego, CA, USA). DNA-seq experiments were performed on an Illumina NovaSeq 6000 system, using a paired-end read length of 2 × 150 bp with the Illumina NovaSeq 6000 reagent kits (Illumina).

Phylogenetic analysis of *Bacillus* spp. and species assignments

De novo assembly was performed using Unicycler (Galaxy version 0.4.8.0) [19] and genome annotation was performed using the PROKA (Rapid prokaryotic genome annotation)(Galaxy version 1.14.6) [20]. The phylogenetic tree analysis of the 18 Bacillus spp. strains was performed using the bacterial Phylogenetic Tree Service of BV-BRC [21]. The whole genome sequence FASTA file of each of the 18 *Bacillus* spp. strains were uploaded to BV-BRC, set to the "contigs" object type. The phylogenetic tree was then built with the default Codon Tree method. For species assignments, the genome sequences were compared to the genomes sequences of the closest species within *Bacillus* spp. genus in the BV-BRC database, with the requested use of 1,000 genes (up from the default 100), with 5 allowed deletions.

Identification of ARGs

ARGs were searched in genomes using three different tools. The first tool is ARG-ANNOT (Antibiotic Resistance Gene-ANNOTation) [22] that was used with the default threshold percentages for identity and minimum sequence length. A blast of the WGS of each *Bacillus* spp. strains in FASTA format was applied against the latest database ARG-ANNOT-NT-V6-July2019.

CARD (Comprehensive Antibiotic Resistance Database) [23] analysis was performed with the same genomes. For this, each genome sequence was screened with CARD's Resistance Gene Identifier (RGI) version 5.2.0 and CARD database version 3.1.4. "Perfect", "Strict", and "Loose" hits were evaluated for the provided genome sequence, and for complete and partial gene predictions with the default filter parameters.

ResFinder [24] was used to screen for ARGsin each of the *Bacillus* spp. genome sequences. The genome sequence in FASTA format was analysed online at https://cge.cbs.dtu.dk/services/ResFinder/ in ResFinder 4.1 software version and database

version 2021-09-23. The analysis was run against all available antibiotics with the following settings: 80 % threshold for ID and 60 % for minimum sequence length (coverage). The results presented are a compilation of the hits found by the three tools.

The intrinsic or acquired nature of the ARGs found in each of the *Bacillus* spp. was evaluated by checking the presence of such genes in strains of the same species (e.g. blasting each ARGs against the NCBI genomes database of the same species), and the search of any genetic mobile element (MGE) associated to such ARGs to evaluate their non-transferability (e.g. using the online tool MobileElementFinder available at https://cge.cbs.dtu.dk/services/MobileElementFinder).

Identification of biosynthetic gene clusters related with antimicrobial

The whole genome sequence FASTA file of each of the 18 *Bacillus* spp. strains were uploaded to antiSMASH 5.0 tool (https://antismash.secondarymetabolites.org/#!/start) [25]. The detection strictness > 90 % was chosen to detect well-defined clusters containing all required parts.

Biofilm experiments

Macro-colony

All experiments began with 5 ml cultures in trypticase soy broth (TSB; Biomérieux, France) were made from glycerol stock at -80°C and placed at 30°C overnight without shaking. After 5 seconds of rapid vortexing to homogenise the cultures, 3 µL of two cultures were collected and deposited in one well of 6 wells plate containing 4 ml of TSA 1.5% agar supplemented with Congo red 40 µg/ml (Sigma-Aldrich, France) to observe amyloid fiber production and 20 µg/ml Coomassie Brilliant Blue to contrast protein production [26,27]. For kin discrimination drops were deposited on a well containing TSA 1.5% agar so that their edges were about 2 mm distance from each other. Samples were dried for 10 min under a hood in case of agar plates, and then incubated 6 days at 30°C.

Swarming

In swarming experiments, 20 mL of TSB supplemented with agar to obtain 0.8% final (TSB Agar, Biomerieux, France) was prepared in a Petri dish and dried in a hood for half an hour. 10 µL of culture was deposited in the center of the plate and left to dry for 10 min before 1 day of incubation at 30°C. For each model, a representative picture from three biological replicates was selected.

Pellicule

Experiments began with 5 ml cultures in trypticase soy broth (TSB; Biomérieux, France) made from glycerol stock at -80°C and placed at 30°C overnight without shaking. After 5 seconds of rapid vortexing to homogenise the cultures, 3 µL of two cultures were collected and deposited in one well of 6 wells plate containing 4 ml of TS. Samples were incubated at 30°C for 2 days.

Submerged biofilm

1/100e dilution in TSB was performed from the overnight cultures of strains. 200 µl of the solutions were poured into the wells of polystyrene 96-well microtiter plates with a µclear® base (Greiner Bio-one, France) compatible with microscopy for 1.5 h at 30°C for an adhesion step. Supernatants were removed, 200 µl of fresh media were added with or without DNAse I (Thermo Scientific, VF304452) at 98 U/mL [28], and the plate was put at 30°C 24 h. A solution of 3 µl/ml of SYTO 9, a cell-permeant green dye that labels nucleic acid (Invitrogen, Carlsbad, CA, USA) mixed with 3 µl of TOTO3 a red dye that labels extracellular nucleic acid (Invitrogen, Carlsbad, CA, USA), was prepared, and 50 µl of this solution was added to each well before CLSM acquisitions.

Confocal laser scanning microscopy

Acquisitions were performed using a Leica SP8 AOBS inverted high content screening confocal laser scanning microscope (HCS-CLSM, LEICA Microsystems, Germany). Image acquisitions were performed on the MIMA2 platform (https://www6.jouy.inra.fr/mima2_eng/). Images every µm to capture the full height of the biofilm of 512 × 512 pixels (147.62 × 147.62 µm, pixel size 0.361 µm) were taken at 600 Hz frequency using the 63x water objective lens (numerical aperture = 1.2). The SYTO9 was excited with an argon laser set at 488 nm, and the emitted fluorescence was collected with a hybrid detector (HyD LEICA Microsystems, Germany) in the

range of 500-550 nm. The TOTO3 was excited with the helium-neon laser at 633 nm, and the emitted fluorescence was collected with a hybrid detector in the range of 650-800 nm. For each experiment, 3 biological replicates were carried out, representing at least 12 technical values per condition.

CLSM Image analysis

2D projections of biofilms and movies were obtained using IMARIS 9.3.1 software (Bitplane, Zurich, Switzerland). BiofilmQ software was used to extract quantitative values from image stacks [29]. Channels were analysed separately using the OTSU thresholding method and "global biofilm properties" were selected to extract the biovolume of the binarized images.

Statistical analysis

Two-way ANOVA using the uncorrected Fisher's least was used using PRISM software (GraphPad, USA, California). Data were considered significant when a p-value was smaller than 0.05.

Results

Genomic analysis of *Bacillus* spp.

Genomes characteristics

Genome analysis was carried out after the sequencing of the eleven strains (**Table 1**). The assignment of species through genome analysis was conducted, and the strains were sorted according to their phylogenetic distance. Three strains were identified as *B. velezensis*, two as *B. subtilis,* and six as *B. licheniformis*.

Table 1: Genomic characterization of the strains used in this study. All strains were isolated from two separate broiler buildings [10].

Name	Completeness	Genome size (bases)	N50	Genome size (bp)	%GC	CDS	rRNA	rRNA	tmRNA	Building number	BioSample accession
Bacillus velezensis B18	99.5	3915595	315607	3915595	46	3771	3	82	1	1	SAMN30015524
Bacillus velezensis B8	99.67	3938456	390404	3938456	46	3738	3	79	1	1	SAMN30015523
Bacillus velezensis B1	99.67	4158515	381251	4158515	46	4143	4	84	1	1	SAMN30015521
Bacillus subtilis C15	99.62	4047208	1049618	4047208	44	4032	3	73	1	2	SAMN30015532
Bacillus subtilis B2	99.6	4188957	654724	4188957	44	4241	3	77	1	1	SAMN30015522
Bacillus licheniformis C3	99.57	4167229	349485	4167229	46	4247	3	79	1	2	SAMN30015528
Bacillus licheniformis C2	99.46	4309318	313710	4309318	44	4445	3	80	1	2	SAMN30015527
Bacillus licheniformis C1	98.5	4204947	44804	4204947	45	4306	4	52	1	2	SAMN30015526
Bacillus licheniformis C10	99.45	4319637	347658	4319637	46	4486	4	80	1	2	SAMN30015530
Bacillus licheniformis C11	99.17	4176285	1084421	4176285	46	4234	5	79	1	2	SAMN30015531
Bacillus licheniformis C5	99.17	4256195	399216	4256195	45	4349	4	79	1	2	SAMN30015529

ARG

The genome-based identification of ARG reveals patterns linked to the species and are represented in a presence/absence heat map (**Fig. 1**). The detailed analysis is shown in **Sup. 1**.

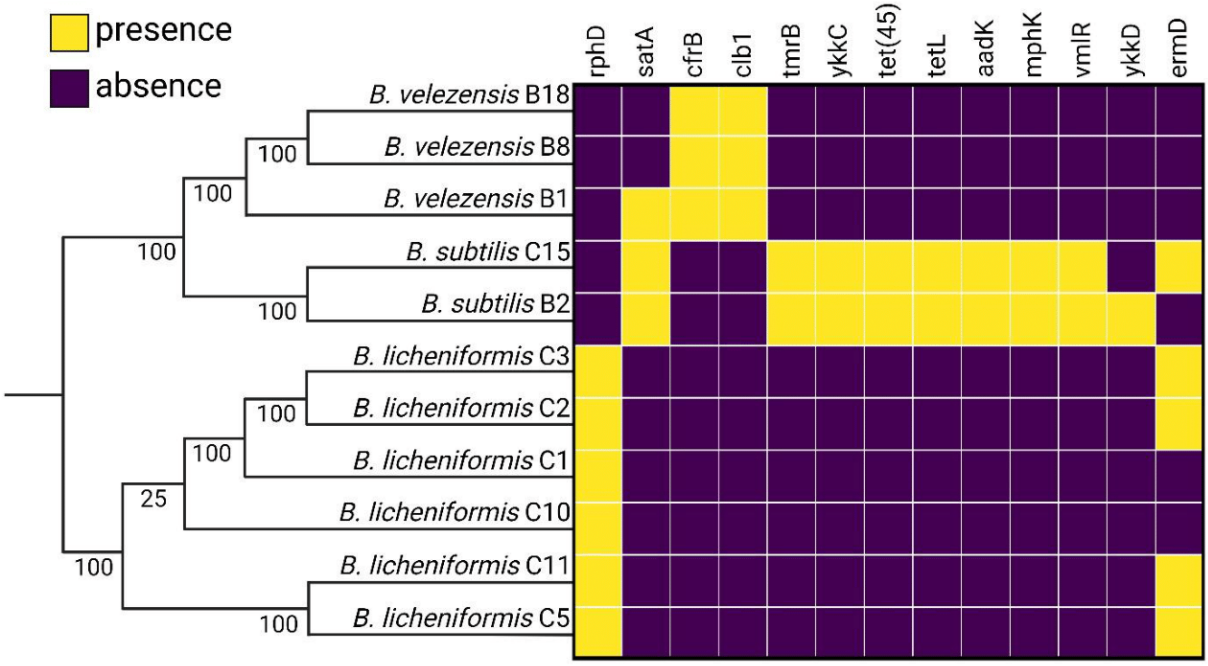

Figure 1: Identification of *Bacillus* spp. species classified according to phylogenetic distance and identification of ARG in genomes. The Bootstrap value is shown in the tree. The presence or absence of ARG in the genome identified by the tree tools ARG-ANNOT, CARD and ResFinder are represented in the heat map.

A relationship between the presence of ARGs and the species was observed. The three *B. velezensis* has 2 hits (*cfrB*, *clbA*) and in addition *satA* for the strain B1 and *tetL* and *tet45* for the strain B8. The two *B. subtilis* strains each have 10 hits, with *rphD* only found in C15. *B. licheniformis* strains all showed hits against *rphD*, and *ermD* for strains C3, C2, C5 and C11. When blasting the ARGs in the NCBI, the coverage and identity of these putative ARGs matches with typical genes commonly encountered into the genomes of the respective species and characterised as chromosomally located intrinsic resistance genes. For *B. velezensis* these include genes encoding a streptothricin N-acetyltransferase related to streptothricin resistance, a Methyltransferases resulting in resistance via methylation of the 50S ribosomal complex and genes related to tetracycline as well as a gene conferring broader resistance to to lincosamides, streptogramin, oxazolidinones, phenicols and pleuromutilins. These resistance genes are common in *B. velezensis*, *B. amyloliquefaciens* and others *Bacillus* spp. and are reported to be located on the chromosome with no indication of mobile elements. For *B. subtilis* these include

notably genes encoding resistance to lincosamycin (LmrB), streptomycin (aadK/aadE), tetracycline (tet(45)/tetL), macrolide antibiotics (mph(K)) and a broad specificity multidrug (ykkC/ykkD) resistance genes. These resistance genes are common in *B. subtilis* and are found located on the chromosome with no indication of mobile elements. Finally for *B. licheniformis* these includes *rphD* encoding resistance to rifamycin and *ermD* encoding broad spectrum resistance to macrolides (e.g. erythromycin), streptogramin b (e.g. virginiamycin s, quinupristin, pristinamycin ia) and lincosamides (e.g. clindamycin, lincomycin). These resistance genes are common in *B. licheniformis* and *B. paralicheniformis* and are also reported to be located on the chromosome with no indication of mobile elements.

No Mobile Genetic Elements associated with antibiotic resistance genes were found in the genomes of any of the 11 isolated *Bacillus* strains analysed using the online tool CGE-MobileElementFinder (**see results in Sup. 2 and 3**).

Biosynthetic gene clusters related with antimicrobials

Antimicrobial secretion genes were searched in the genomes and species patterns were revealed (**Fig. 2**). The detailed analysis is shown in **Sup. 4**.

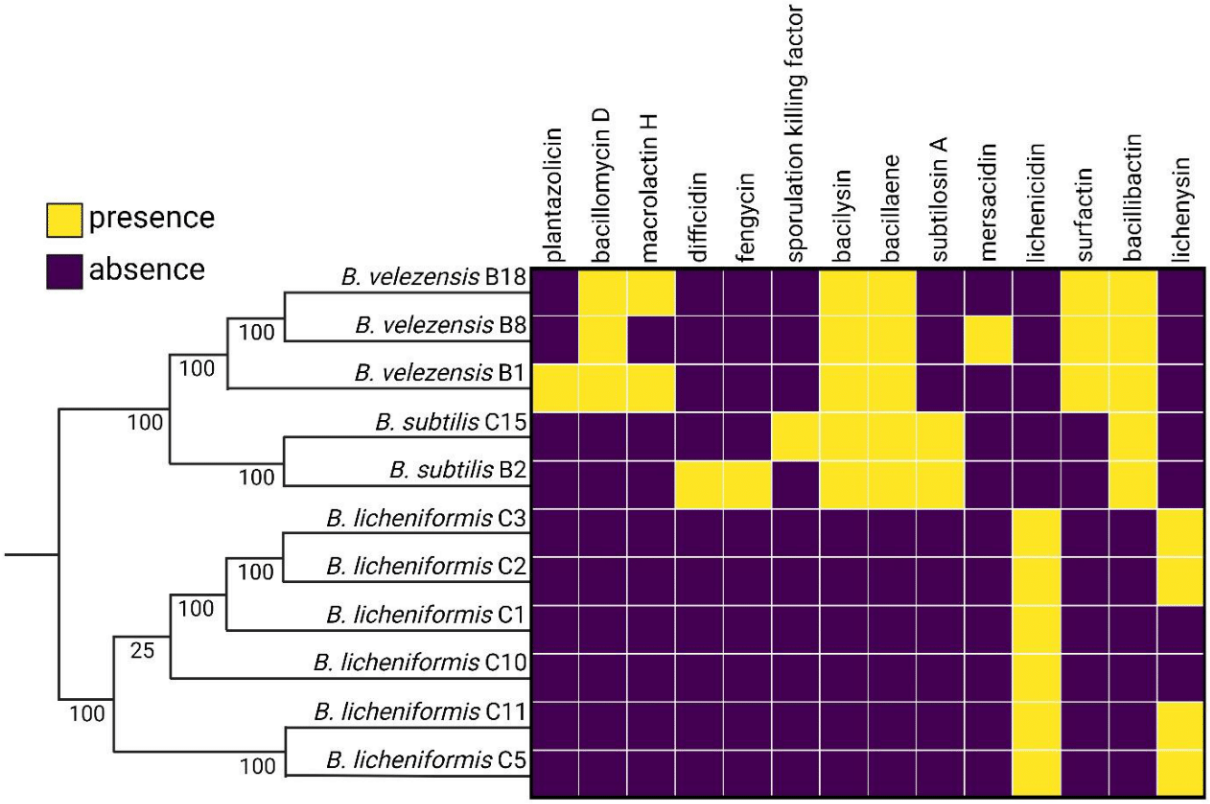

Figure 2: Identification of genes involved in antimicrobial secretion in *Bacillus* spp. genomes. Highly conserved hits (> 90 %) of antimicrobial secreted molecules were identified through genome analysis using the antiSMASH tool and represented by a yellow box in the heat map. Bootstrap values are represented on the tree.

Bacilysin, bacillaene and bacillibactin were found in *B. subtilis* and *B. velezensis* while lichenicidin and lichenysin were detected in *B. licheniformis*. Subtilosin A was identified only for *B. subtilis*, bacillomycin D, and surfactin were specific to *B. velezensis*. However, some strain-specific hits were also identified. Mersacidin for *B. velezensis* B8, plantazolicin for *B. velezensis* B1, the sporulation killing factor for *B. subtilis* C15 and difficidin and fengycin for *B. subtilis B2*.

Description of *Bacillus* spp. biofilms isolated from livestock building surfaces

Biofilm formation capability

All the *Bacillus* spp. isolates were able to form structured biofilms in the different laboratory models used. Macro-structures are described in **figure 3**.

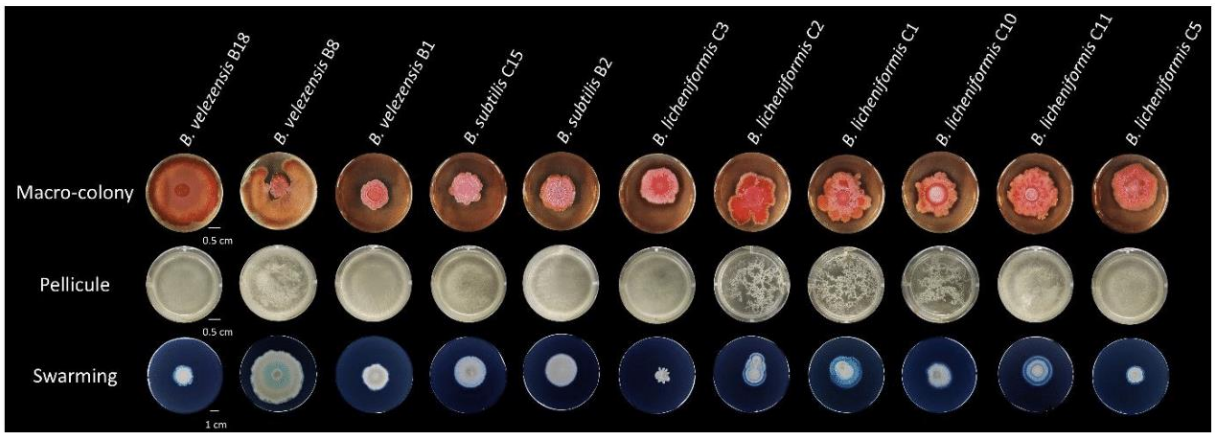

Figure 3: Representative images of the 11 *Bacillus* spp. grown on macrocolony, pellicle and swarming biofilm models. Macro-colony and swarm biofilm models enable bacterial growth at the agar-air interface. Pellicles form at the interface between liquid and air. Representative images of the three biological replicates performed are shown.

Structural heterogeneity was observed among the different isolates and within the same species. Macro-colony staining differed between strains, demonstrating the diversity of extracellular matrix composition. The red colony contains amyloid fibers because of the staining with Congo red. A lighter coloration, such as the one observed at the center of *B. licheniformis* C11 colony was associated with concentrated protein because of Coomassie

Brilliant Blue labelling. Some colonies, such as the ones from *B. subtilis* strains and *B. velezensis* B1, formed tall, wrinkled structures, while others, such as *B. velezensis* B18, were flat but showed ability to colonize the entire surface of the well. Likewise, remarkable phenotypes were observed with the pellicle model. *B. licheniformis* strains C1, C2 and C10 formed a fine, highly structured pellicle, while all other strains showed flat pellicle. *B. velezensis* B8 was the strongest colonizer in the swarming model. Phenotypes differed between strains, with the remarkable presence of pronounced halo-like growth for *B. licheniformis* strains C1, C2 and C11. As shown in other biofilm models, a significant degree of heterogeneity in 3D structures was likewise observed in submerged biofilms. SYTO9 staining visualized the entire population, while TOTO3 only enabled detection of eDNA or bacteria with damaged cell walls (**Fig. 5A**). The biofilms of *B. velezensis* and *B. subtilis* strains were homogeneous, whereas *B. licheniformis* formed biofilms with a large number of dense structures, making them highly heterogeneous. Certain structures exhibited a notable abundance of eDNA. The amount of eDNA was higher in *B. licheniformis* biofilms than in other *Bacillus* spp. except for *B. velezensis* B8.

Evaluation of strain interactions using a macro-colony model

An interaction experiment was performed (**Fig. 4**).

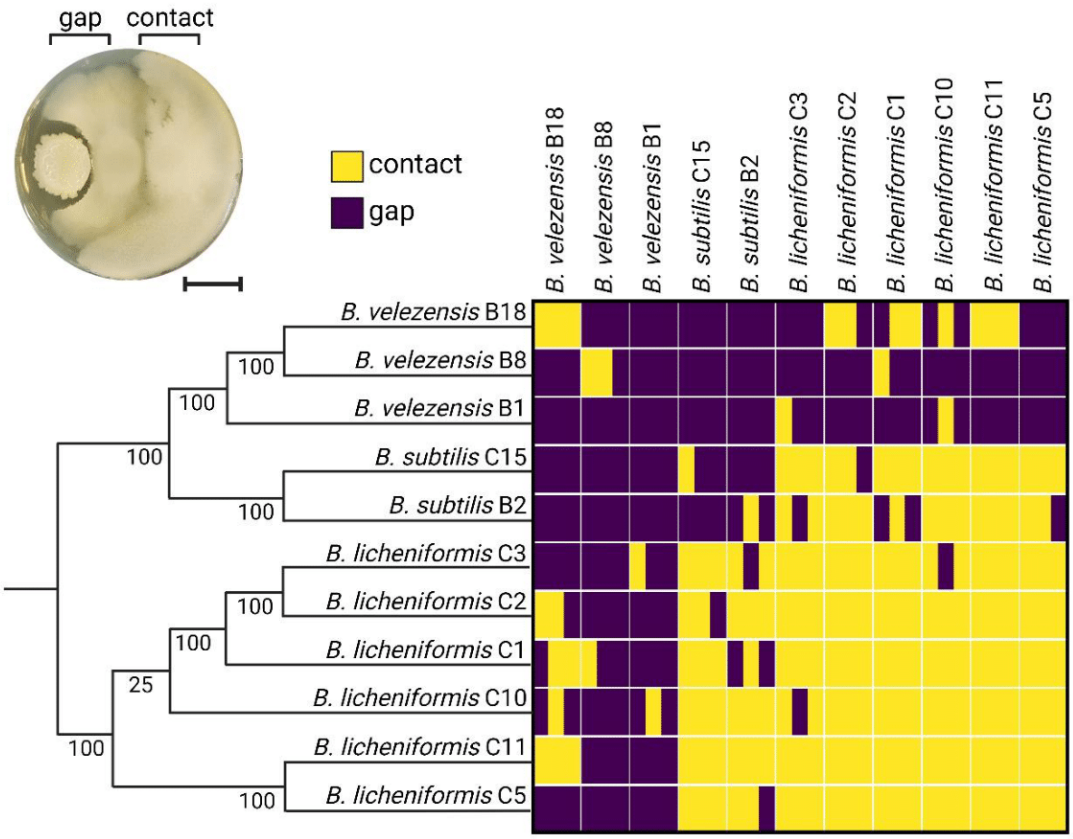

Figure 4: Compatibility assessment of *Bacillus* spp. according to the phylogenetic distance of strains in a macro-colonie biofilm model. A representative image of the contact and gap phenotypes is shown as an example. Scale bar = 1 cm. One square represents three biological replicates, each showing an interaction.

A relationship between the phylogenetic distance of the strains and their ability to form mixed biofilms was observed. *B. velezensis* B8, B18, and B1 primarily demonstrate a tendency towards negative recognition, as evidenced by the spatial separation between their colonies and other neighboring colonies. This suggests that these strains likely secrete a diffusible molecule into the agar medium. The colonies of all the other strains were able to form contacts with each other, except for certain replicates and for strains *B. velezensis* B2 and *B. subtilis* C15 for which did not form a contact. Interestingly, some interactions between the same strain from different cultures showed some sort of antagonism with a distance between the two colonies. This was the case for *B. velezensis* B1, B2 or *B. subtilis* C15.

eDNA differentially influences bacilli biofilms organization

DNAse I had an effect on the structure of all *B. licheniformis* strains and *B. subtilis* C15 (**Fig. 5A, B**). The enzyme treatment reduced significantly ($p < 0.01$) biofilm formation for all strains of *B. licheniformis* save strain C11 (**Fig. 5C**) and this was associated with a significant reduction of eDNA (**Fig. 5D**).

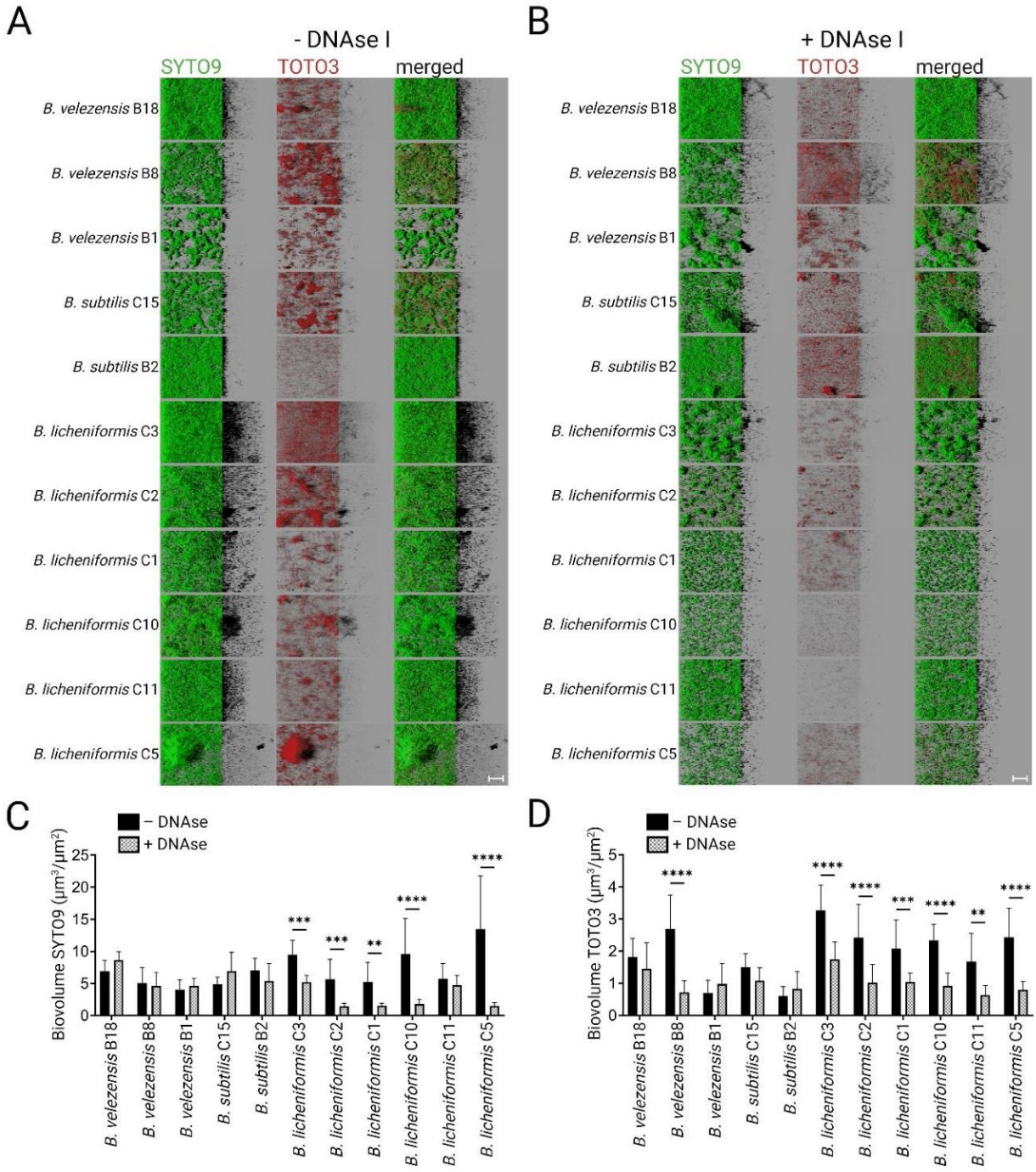

Figure 5: Effect of DNAse I on the formation of *Bacillus* spp. biofilms isolated from the surface of poultry farm buildings. (A) Representative images captured using CLSM of 24h *Bacillus* spp. biofilms within the culture medium following adhesion. Chemical labeling using SYTO9 to highlight the entire population, and TOTO3 to mark the DNA were used. (B) Same experiment with DNAse I incorporated in the medium after the adhesion step. Scale bar = 40 µm. (C) Quantification of the biovolume of the SYTO9 signal. (D) Quantification of the biovolume of the TOTO3 signal. Error bars correspond to standard deviation.

Discussion

Eleven sporulated strains were isolated from two poultry farms and we investigated some of their genomic and biofilm forming features. All the strains were able to form biofilms in different laboratory models with a high diversity of morphology between strains. However, it is crucial to note that a more extensive strain collection would be necessary to draw general conclusions at the species level, particularly for *B. subtilis* and *B. velezensis*.

A detailed *in silico* analysis was conducted to identify putative ARG genes in the genomes of the *Bacillus* strains. Based on the results it can be concluded that the hits identified relate to genes inherent and intrinsic to the respective *Bacillus* species of the 11 *Bacillus* strains studied. Indeed these genes were all found to be located in chromosomic regions and detected in published genomes of strains from the same bacterial species including the respective type strains. Besides the absence of any mobile genetic element associated with these genes in the genomes of the 11 strains further supports that these genes are unlikely to pose a safety concern. Phenotypic testing for resistance towards clinically relevant antibiotics would however be required to complete the safety assessment of these strains in term of ARG.

Each strain showed different biofilm characteristics. Submerged biofilms were subjected to more comprehensive characterization. CLSM enables quantification of structural parameters, such as biovolume, which describe the morphology of biofilms. There seems to be no link between the presence of eDNA and the biovolume reduction. It is plausible that eDNA may influence the early stages of biofilm formation, possibly preventing strains from aggregating during the initial phases. This could hinder the establishment of cell-to-cell density dependent communication systems such as Quorum Sensing (QS) [32]. It would therefore be relevant to carry out the same experiments using kinetics (HCS-CLSM) to decipher the growth dynamics of biofilms with or without DNAse [33]. Considering DNase treatment for surface decontamination, its potential to remove clusters prompts the idea of conducting such treatments before animal introduction or during the application of positive biofilms. This might mitigate the initial stages of biofilm development.

We highlight a correlation association between the ability of the strains to merge their macro-colonies and the presence of genes related to antimicrobial secretion. For instance, *B. subtilis* B2 and C15 exhibit a compatibility between each other and the *B. licheniformis*. Despite this,

they secrete antimicrobials that are distinct from those of *B. velezensis*, which are mostly unable to mix. Essential compounds like bacillomycin D, bacilysin, bacillaene, surfactin, and bacillibactin are consistent across all three *B. velezensis* strains. Moreover, strain B18 displays more kin-positive traits when compared to B1 and B8. The specificity of B1 lies in its production of plantazolicin, while B8 synthesises mersacidin. In contrast, all *B. licheniformis* strains are compatible among themselves and predominantly secrete lichenicidin, with the additional presence of lichenysin in strains C3, C2, C11, and C5. It would be interesting to investigate further the ability of strains to form mixed biofilms in the same colony. Indeed, based on kin discrimination, it has been shown that colonies able to merge can form stable mixed biofilms and colonise environments such as plant roots [34].

The selection of competitive strains with *Bacillus* spp. potentially tolerant to C&D procedure due to their biofilm from the breeding process, therefore possessing strong competitive potential and resistance to DNase, is being considered for incorporation into a novel product formulation. This product aims to combine strains that form positive biofilms with DNase enzymatic treatment to help positive biofilm establish itself by destroying the community already in place.

Conclusion

In conclusion, this research has illuminated various aspects of bacterial strains isolated from the broiler breeding environment, revealing their genetic diversity and biofilm structures. *B. velezensis* appears to be highly competitive in these environments compared to other *Bacillus* species. Characterization of submerged biofilms has uncovered the role of eDNA in *Bacillus* species biofilm structures. In particular, we have demonstrated that DNAse treatment prevents *B. licheniformis* biofilms formation, but not those of *B. velezensis*. Finally, the lack of mobilizable antibiotic resistance genes (ARGs) enables the consideration of some of these strains for biotechnological applications.

Data availability

The original contributions presented in the study are included in the article. Further inquiries can be directed to the corresponding author. The whole-genome shotgun project has been deposited in the NCBI Sequence Read Archive (SRA) under BioProject accession number PRJNA863099.

Author Contributions

VG, MC and RB: conceptualization and methodology. MC and RB: validation and supervision. VG, GJ: formal analysis and data curation. VG, GJ, MC, and RB: investigation. MC and RB: resources, project administration, and funding acquisition. VG, GJ, MC: writing the original draft preparation. MC and RB: reviewing, and editing. All authors have read and agreed to the published version of the manuscript.

Funding

This research was funded by INRAE, LALLEMAND SAS and “Association Nationale de la Recherche et de la Technologie” (contract 2020/0548).

Conflict of interest

The authors declare that the research was conducted in the absence of any commercial or financial relationships that could be construed as a potential conflict of interest.

Acknowledgments

We thank the MIMA2 platform (Microscopie et Imagerie des Microorganismes, Animaux et Aliments, https://doi.org/10.15454/1.5572348210007727E12) for the Leica SP8-HCS microscopy observations.

References

[1] Guéneau V, Plateau-Gonthier J, Arnaud L, Piard J-C, Castex M, Briandet R. Positive biofilms to guide surface microbial ecology in livestock buildings. Biofilm 2022;4:100075. https://doi.org/10.1016/j.bioflm.2022.100075.

[2] Luyckx K, Millet S, Van Weyenberg S, Herman L, Heyndrickx M, Dewulf J, et al. A 10-day vacancy period after cleaning and disinfection has no effect on the bacterial load in pig nursery units. BMC Vet Res 2016;12:236. https://doi.org/10.1186/s12917-016-0850-1.

[3] Flemming H-C, Wuertz S. Bacteria and archaea on Earth and their abundance in biofilms. Nat Rev Microbiol 2019;17:247–60. https://doi.org/10.1038/s41579-019-0158-9.

[4] Sauer K, Stoodley P, Goeres DM, Hall-Stoodley L, Burmølle M, Stewart PS, et al. The biofilm life cycle: expanding the conceptual model of biofilm formation. Nat Rev Microbiol 2022;20:608–20. https://doi.org/10.1038/s41579-022-00767-0.

[5] Flemming H-C, van Hullebusch ED, Neu TR, Nielsen PH, Seviour T, Stoodley P, et al. The biofilm matrix: multitasking in a shared space. Nat Rev Microbiol 2023;21:70–86. https://doi.org/10.1038/s41579-022-00791-0.

[6] Flemming H-C, Wingender J, Szewzyk U, Steinberg P, Rice SA, Kjelleberg S. Biofilms: an emergent form of bacterial life. Nat Rev Microbiol 2016;14:563–75. https://doi.org/10.1038/nrmicro.2016.94.

[7] Bridier A, Briandet R, Thomas V, Dubois-Brissonnet F. Resistance of bacterial biofilms to disinfectants: a review. Biofouling 2011;27:1017–32. https://doi.org/10.1080/08927014.2011.626899.

[8] Munita JM, Arias CA. Mechanisms of Antibiotic Resistance. Microbiol Spectr 2016;4. https://doi.org/10.1128/microbiolspec.VMBF-0016-2015.

[9] Larsson DGJ, Flach C-F. Antibiotic resistance in the environment. Nat Rev Microbiol 2022;20:257–69. https://doi.org/10.1038/s41579-021-00649-x.

[10] Guéneau V, Rodiles A, Frayssinet B, Piard J-C, Castex M, Plateau-Gonthier J, et al. Positive biofilms to control surface-associated microbial communities in a broiler chicken production system - a field study. Front Microbiol 2022;13:981747. https://doi.org/10.3389/fmicb.2022.981747.

[11] Arnaouteli S, Bamford NC, Stanley-Wall NR, Kovács ÁT. Bacillus subtilis biofilm formation and social interactions. Nat Rev Microbiol 2021;19:600–14. https://doi.org/10.1038/s41579-021-00540-9.
[12] Majed R, Faille C, Kallassy M, Gohar M. Bacillus cereus Biofilms-Same, Only Different. Front Microbiol 2016;7:1054. https://doi.org/10.3389/fmicb.2016.01054.
[13] Mingmongkolchai S, Panbangred W. Bacillus probiotics: an alternative to antibiotics for livestock production. J Appl Microbiol 2018;124:1334–46. https://doi.org/10.1111/jam.13690.
[14] Muras A, Romero M, Mayer C, Otero A. Biotechnological applications of Bacillus licheniformis. Crit Rev Biotechnol 2021;41:609–27. https://doi.org/10.1080/07388551.2021.1873239.
[15] Pandin C, Le Coq D, Deschamps J, Védie R, Rousseau T, Aymerich S, et al. Complete genome sequence of Bacillus velezensis QST713: A biocontrol agent that protects Agaricus bisporus crops against the green mould disease. J Biotechnol 2018;278:10–9. https://doi.org/10.1016/j.jbiotec.2018.04.014.
[16] Rendueles O, Zee PC, Dinkelacker I, Amherd M, Wielgoss S, Velicer GJ. Rapid and widespread de novo evolution of kin discrimination. Proc Natl Acad Sci U S A 2015;112:9076–81. https://doi.org/10.1073/pnas.1502251112.
[17] Guéneau V, Rodiles A, Piard J-C, Frayssinet B, Castex M, Plateau-Gonthier J, et al. Capture and Ex-Situ Analysis of Environmental Biofilms in Livestock Buildings. Microorganisms 2021;10:2. https://doi.org/10.3390/microorganisms10010002.
[18] Guéneau V, Piard J-C, Frayssinet B, Loux V, Chiapello H, Plateau-Gonthier J, et al. Genome Sequence of Bacillus velezensis P1, a Strain Isolated from a Biofilm Captured on a Pig Farm Building. Microbiol Resour Announc 2022;11:e0121921. https://doi.org/10.1128/mra.01219-21.
[19] Wick RR, Judd LM, Gorrie CL, Holt KE. Unicycler: Resolving bacterial genome assemblies from short and long sequencing reads. PLoS Comput Biol 2017;13:e1005595. https://doi.org/10.1371/journal.pcbi.1005595.
[20] Seemann T. Prokka: rapid prokaryotic genome annotation. Bioinformatics 2014;30:2068–9. https://doi.org/10.1093/bioinformatics/btu153.
[21] Olson RD, Assaf R, Brettin T, Conrad N, Cucinell C, Davis JJ, et al. Introducing the Bacterial and Viral Bioinformatics Resource Center (BV-BRC): a resource combining PATRIC, IRD and ViPR. Nucleic Acids Res 2023;51:D678–89. https://doi.org/10.1093/nar/gkac1003.
[22] Gupta SK, Padmanabhan BR, Diene SM, Lopez-Rojas R, Kempf M, Landraud L, et al. ARG-ANNOT, a new bioinformatic tool to discover antibiotic resistance genes in bacterial genomes. Antimicrob Agents Chemother 2014;58:212–20. https://doi.org/10.1128/AAC.01310-13.
[23] Alcock BP, Raphenya AR, Lau TTY, Tsang KK, Bouchard M, Edalatmand A, et al. CARD 2020: antibiotic resistome surveillance with the comprehensive antibiotic resistance database. Nucleic Acids Res 2020;48:D517–25. https://doi.org/10.1093/nar/gkz935.
[24] Zankari E, Hasman H, Cosentino S, Vestergaard M, Rasmussen S, Lund O, et al. Identification of acquired antimicrobial resistance genes. J Antimicrob Chemother 2012;67:2640–4. https://doi.org/10.1093/jac/dks261.
[25] Blin K, Shaw S, Steinke K, Villebro R, Ziemert N, Lee SY, et al. antiSMASH 5.0: updates to the secondary metabolite genome mining pipeline. Nucleic Acids Res 2019;47:W81–7. https://doi.org/10.1093/nar/gkz310.

[26] Jones CJ, Wozniak DJ. Congo Red Stain Identifies Matrix Overproduction and Is an Indirect Measurement for c-di-GMP in Many Species of Bacteria. Methods Mol Biol 2017;1657:147–56. https://doi.org/10.1007/978-1-4939-7240-1_12.
[27] Kiersztyn B, Siuda W, Chróst R. Coomassie Blue G250 for Visualization of Active Bacteria from Lake Environment and Culture. Pol J Microbiol 2017;66:365–73. https://doi.org/10.5604/01.3001.0010.4867.
[28] Béchon N, Mihajlovic J, Lopes A-A, Vendrell-Fernández S, Deschamps J, Briandet R, et al. Bacteroides thetaiotaomicron uses a widespread extracellular DNase to promote bile-dependent biofilm formation. Proc Natl Acad Sci U S A 2022;119:e2111228119. https://doi.org/10.1073/pnas.2111228119.
[29] Hartmann R, Jeckel H, Jelli E, Singh PK, Vaidya S, Bayer M, et al. Quantitative image analysis of microbial communities with BiofilmQ. Nat Microbiol 2021;6:151–6. https://doi.org/10.1038/s41564-020-00817-4.
[30] EFSA Panel on Additives and Products or Substances used in Animal Feed (FEEDAP), Bampidis V, Azimonti G, Bastos M de L, Christensen H, Dusemund B, et al. Safety and efficacy of the feed additive consisting of Bacillus licheniformis DSM 28710 (B-Act®) for laying hens, minor poultry species for laying, poultry species for breeding purposes and ornamental birds (HuvePharma N.V.). EFSA J 2021;19:e06449. https://doi.org/10.2903/j.efsa.2021.6449.
[31] Agersø Y, Bjerre K, Brockmann E, Johansen E, Nielsen B, Siezen R, et al. Putative antibiotic resistance genes present in extant Bacillus licheniformis and Bacillus paralicheniformis strains are probably intrinsic and part of the ancient resistome. PLoS One 2019;14:e0210363. https://doi.org/10.1371/journal.pone.0210363.
[32] Mukherjee S, Bassler BL. Bacterial quorum sensing in complex and dynamically changing environments. Nat Rev Microbiol 2019;17:371–82. https://doi.org/10.1038/s41579-019-0186-5.
[33] Canette A, Deschamps J, Briandet R. High Content Screening Confocal Laser Microscopy (HCS-CLM) to Characterize Biofilm 4D Structural Dynamic of Foodborne Pathogens. Methods Mol Biol 2019;1918:171–82. https://doi.org/10.1007/978-1-4939-9000-9_14.
[34] Stefanic P, Kraigher B, Lyons NA, Kolter R, Mandic-Mulec I. Kin discrimination between sympatric Bacillus subtilis isolates. Proc Natl Acad Sci U S A 2015;112:14042–7. https://doi.org/10.1073/pnas.1512671112.
[35] Fan B, Blom J, Klenk H-P, Borriss R. Bacillus amyloliquefaciens, Bacillus velezensis, and Bacillus siamensis Form an "Operational Group B. amyloliquefaciens" within the B. subtilis Species Complex. Front Microbiol 2017;8:22. https://doi.org/10.3389/fmicb.2017.00022.
[36] Dunlap CA, Kwon S-W, Rooney AP, Kim S-J. Bacillus paralicheniformis sp. nov., isolated from fermented soybean paste. Int J Syst Evol Microbiol 2015;65:3487–92. https://doi.org/10.1099/ijsem.0.000441.

Supplementary

	Anti-Microbial Resistance								
	ARG-ANNOT			CARD-RGI (strict and perfect hits)			CGE-RESFINDER		
Strains	AMR gene	Identity (%)	Coverage (%)	AMR gene	Identity (%)	Coverage (%)	AMR gene	Identity (%)	Coverage (%)
Bacillus licheniformis C1	(Rif)rphD	80	100	**NO STRICT OR PERFECT HITS**			**NO AMR GENES DETECTED**		
Bacillus licheniformis C2	(MLS)erm (D) (Rif)rphD	97 80	100 100	ErmD (strict)	97	100	erm(D)	100	100
Bacillus licheniformis C3	(Rif)rphD (MLS)erm (D)	80 97	100 100	ErmD (strict)	97	100	erm(D)	100	100
Bacillus licheniformis C5	(Rif)rphD (MLS)erm (D)	80 95	100 99	ErmD (strict)	97	100	erm(D)	96	99
Bacillus licheniformis C10	(Rif)rphD	80	100	**NO STRICT OR PERFECT HITS**			**NO AMR GENES DETECTED**		
Bacillus licheniformis C11	(Rif)rphD (MLS)erm (D)	80 95	100 99	ErmD (strict)	94	100	erm(D)	96	99
Bacillus subtilis C15	(Rif)rphD (Tet)tetL (AGly)sat A (MLS)Lmr B	79 80 94 99	100 99 100 100	ykkD (strict) vmlR (strict) mphK (strict) aadK (strict) tet(45) (strict) ykkC (perfect) tmrB (perfect)	99 98 98 98 75 100 100	100 100 100 100 100 100 100	aadK tet(L) mph(K)	99 99 98	100 100 100
Bacillus subtlis B2	(AGLY)sat A (MLS)Lmr B	94 98	100 100	ykkD (strict) vmlR (strict) aadK (strict) mphK (strict) tet(45) (strict) ykkC (perfect) tmrB (perfect)	99 99 98 98 76 100 100	100 100 100 100 100 100 100	mph(K) tet(L) aadK	98 99 99	100 100 100
Bacillus velezensis B1	(AGLY)sat A (MLS)cfrB	84 89	98 99	clbA (strict)	100	100	cfr(B)	89	99
Bacillus velezensis B8	Tet(tetL) (MLS)cfrB	79 89	100 99	clbA (strict) tet(45) (strict)	100 76	100 71	cfr(B) tet(L)	89 87	99 100
Bacillus velezenis B18	(MLS)cfrB	89	99	clbA (strict)	100	100	cfr(B)	89	99

Supplementary data 1: Details of ARG gene analysis using ARG-ANNOT, CARD-RGI and CGE-RESFINDER tools.

Strains	AMR genes found in genomes (80% identity & 70% coverage)	Mobile Genetic Elements (MGEs) associated to AMR genes
Bacillus velezensis B1	satA	0
	cfrB	0
	cblA	0
Bacillus subtilis B2	satA	0
	LmrB	0
	ykkD	0
	vmlR	0
	aadK	0
	mphK	0
	tet(45)	0
	tet(L)	0
	ykkC	0
	tmrB	0
Bacillus velezensis B8	tet(tetL)	0
	tet(45)	0
	cfrB	0
	clbA	0
Bacillus velezensis B18	cfrB	0
	clbA	0
Bacillus licheniformis C1	rphD	0
Bacillus licheniformis C2	erm(D)	0
	rphD	0
Bacillus licheniformis C3	erm(D)	0
	rphD	0
Bacillus licheniformis C5	erm(D)	0
	rphD	0
Bacillus licheniformis C10	rphD	0
Bacillus licheniformis C11	erm(D)	0
	rphD	0
Bacillus subtilis C15	rphD	0
	tetL	0
	tet(45)	0
	satA	0
	LmrB	0
	ykkD	0
	vmlR	0
	mphK	0
	aadK	0
	ykkC	0
	tmrB	0

Supplementary data 2: Results of the Mobile Genetic Elements (MGEs) associated with ARG genes analysis using the CGE-MobileElementFinder tool.

The five ARG genes found in three *Bacillus velezensis* strains were blasted against the genomes NCBI database showing the following results:

- *satA* gene resulted in 59 top hits belonging to *Bacillus amyloliquefaciens*, among them the type strain *Bacillus amyloliquefaciens* DSM 7 = ATTCC 23350, with a 73% coverage and a 85.71% identity.
- *cfrB* gene resulted in 71 top hits belonging to *Bacillus amyloliquefaciens*, among them the type strain *Bacillus amyloliquefaciens* DSM 7 = ATTCC 23350, with a 99% coverage and a 88.80% identity.
- *cblA* gene resulted in 71 top hits belonging to *Bacillus amyloliquefaciens*, among them the type strain *Bacillus amyloliquefaciens* DSM 7 = ATTCC 23350, with a 100% coverage and a 93.05% identity.
- *tetL* gene resulted in 72 top hits belonging to *Bacillus amyloliquefaciens*, among them the type strain *Bacillus amyloliquefaciens* DSM 7 = ATTCC 23350, with a 99% coverage and a 78.83% identity.
- *tet45* gene resulted in 77 top hits belonging to *Bacillus amyloliquefaciens*, among them the type strain *Bacillus amyloliquefaciens* DSM 7 = ATTCC 23350, with a 99% coverage and a 75.73% identity.

(In 2017, Fen et al. proposed that the close relatedness of *Bacillus amyloliquefaciens, Bacillus velezensis* and *Bacillus siamensis* is well reflected by the novel taxonomic unit named "Operational group *B.amyloliquefaciens*", [35])

The ten ARG genes found in two *Bacillus subtilis* strains were blasted against the genomes NCBI database showing the following results:

- *satA* gene resulted in 100 top hits belonging to *Bacillus subtilis*, among them the type strain *Bacillus subtilis subsp. subtilis str. 168*, with a 100% coverage and a 100% identity.
- *lmrB* gene resulted in 100 top hits belonging to *Bacillus subtilis*, among them the type strain *Bacillus subtilis subsp. subtilis str. 168*, with a 100% coverage and a 100% identity.
- *ykkD* gene resulted in 100 top hits belonging to *Bacillus subtilis*, among them the type strain *Bacillus subtilis subsp. subtilis str. 168*, with a 100% coverage and a 100% identity.

- *ykkC* gene resulted in 100 top hits belonging to *Bacillus subtilis*, among them the type strain *Bacillus subtilis subsp. subtilis str. 168*, with a 100% coverage and a 100% identity.
- *vmlR* gene resulted in 100 top hits belonging to *Bacillus subtilis*, among them the type strain *Bacillus subtilis subsp. subtilis str. 168*, with a 100% coverage and a 100% identity.
- *aadK* gene resulted in 100 top hits belonging to *Bacillus subtilis*, among them the type strain *Bacillus subtilis subsp. subtilis str. 168*, with a 100% coverage and a 100% identity.
- *mphK* gene resulted in 100 top hits belonging to *Bacillus subtilis*, among them the type strain *Bacillus subtilis subsp. subtilis str. 168*, with a 100% coverage and a 100% identity.
- *tet45* gene resulted in 17 top hits belonging to *Bacillus subtilis*, among them the type strain *Bacillus subtilis subsp. subtilis str. 168*, with a 97% coverage and a 80.65% identity.
- *tetL* gene resulted in 34 top hits belonging to *Bacillus subtilis*, among them the type strain *Bacillus subtilis subsp. subtilis str. 168*, with a 100% coverage and a 100% identity.
- *tmrB* gene resulted in 34 top hits belonging to *Bacillus subtilis*, among them the type strain *Bacillus subtilis subsp. subtilis str. 168*, with a 100% coverage and a 100% identity.
- *rphD* gene resulted in 101 top hits belonging to *Bacillus subtilis*, among them the type strain *Bacillus subtilis subsp. subtilis str. 168*, with a 100% coverage and a 79.0% identity.

The ARG gene found in the six *Bacillus licheniformis* strains was blasted against the genomes NCBI database showing the following results:

- *rphD* gene resulted in 47 top hits belonging to *Bacillus licheniformis*, among them the type strain *B. licheniformis* DSM 13 = ATTCC 14580, with a 100% coverage and a 79.68% identity.

The ARG gene found in four out of six *Bacillus licheniformis* strains was blasted against the genomes NCBI database showing the following results:

- *ermD* gene resulted in 100 top hits belonging to *Bacillus paralicheniformis*, among them the type strain *B. paralicheniformis* strain KJ-16, with a 100% coverage and a 99.53% identity.

(In 2015, Dunlop et al. described *B. paralicheniformis* as a new species [36], since that date, many *B. licheniformis* strains were taxonomically moved to *B. paralicheniformis* in the NCBI databases).

Supplementary data 3: Detailed results of AGR research in other representatives of the species studied (i.e. *B. velezensis*, *B. subtilis*, *B. licheniformis*).

	Anti-microbial secretion		
	AntiSMASH (detection strictness > 90 %)		
Strains	Type	Most similar know cluster	Similarity (%)
Bacillus licheniformis C1	lanthipeptide-class-II	lichenicidin VK21 A1 / lichenicidine VK21 A2	100
Bacillus licheniformis C2	NRPS lanthipeptide-class-II	lichenysin lichenicidin VK21 A1 / lichenicidine VK21 A2	100 100
Bacillus licheniformis C3	NRPS lanthipeptide-class-II	lichenysin lichenicidin VK21 A1 / lichenicidine VK21 A2	100 100
Bacillus licheniformis C5	NRPS lanthipeptide-class-II	lichenysin lichenicidin VK21 A1 / lichenicidine VK21 A2	100 100
Bacillus licheniformis C10	lanthipeptide-class-II	lichenicidin VK21 A1 / lichenicidine VK21 A2	100
Bacillus licheniformis C11	NRPS lanthipeptide-class-II	lichenysin lichenicidin VK21 A1 / lichenicidine VK21 A2	100 100
Bacillus subtilis C15	transAT-PKS, PKS-like, T3PKS, NRPS NRPS sactipeptide other sactipeptide, ranthipeptide	bacillaene bacillibactine subtilosin A bacilysin sporulation killing factor	100 100 100 100 100
Bacillus subtlis B2	other sactipeptide NRPS NRPS, transAT-PKS, T3PKS, PKS-like NRPS, batalactone lanthipeptide-classe-I	bacilysin subtilosin A bacillibactin bacillaene fengycin subtilomycin	100 100 100 100 100 100
Bacillus velezensis B1	other RiPP-like,NRPS transAT-PKS transAT-PKS transAT-PKS, T3PKS, NRPS betalactone, transAT-PKS, NRPS NRPS	bacilysin bacillibactin difficidin macrolactin H bacillaene bacillomycin D surfactin	100 100 100 100 100 100 91
Bacillus velezensis B8	other RiPP-like, NRPS transAT-PKS transAT-PKS, T3PKS, NRPS lanthipeptide-class-II NRPS LAP, PRE-containing	bacilysin bacillibactin macrolactin H bacillane mersacidin surfactin plantazolicin	100 100 100 100 100 91 91
Bacillus velezenis B18	transAT-PKS transAT-PKS, NRPS, T3PKS NRPS other NRPS, RiPP-like RRE-containing, LAP transAT-PKS	difficidin bacillaene surfactin bacilysin bacillibactin plantazolicin macrolactin H	100 100 91 100 100 91 100

Supplementary data 4: Details of antimicrobial secretion detected in genomes using antiSMASH tool.

3.2 CHAPITRE 2 - ÉLABORATION D'UNE STRATEGIE INNOVANTE PERMETTANT LA SELECTION ET L'ASSOCIATION DE SOUCHES BENEFIQUES FORMANT DES BIOFILMS CAPABLES DE LIMITER L'IMPLANTATION ET LA CROISSANCE DES AGENTS PATHOGENES

3.2.1 Préambule

Bien que des produits commerciaux à base de consortiums de souches formant des biofilms positifs soient disponibles sur le marché depuis quelques années, il est essentiel de mener des recherches approfondies pour mieux comprendre le devenir des souches individuelles du consortium au cours du temps et les mécanismes sous-jacents à leurs propriétés compétitrices vis-à-vis de bactéries indésirables. Ces produits sont principalement constitués d'assemblages de souches d'espèces du genre *Bacillus* spp. et de bactéries lactiques. Les souches sont sélectionnées pour leur compétitivité élevée, souvent évaluée en condition de vie planctonique. Toutefois, étant donné la prédominance du mode de vie en biofilm sur les surfaces des bâtiments d'élevage, il était impératif de vérifier leur compétitivité au sein de ces structures microbiennes.

Ce chapitre présente une stratégie innovante visant à la sélection et à l'association raisonnée de souches en vue du développement et de la formulation de produits commerciaux de nouvelle génération (**Figure 3**).

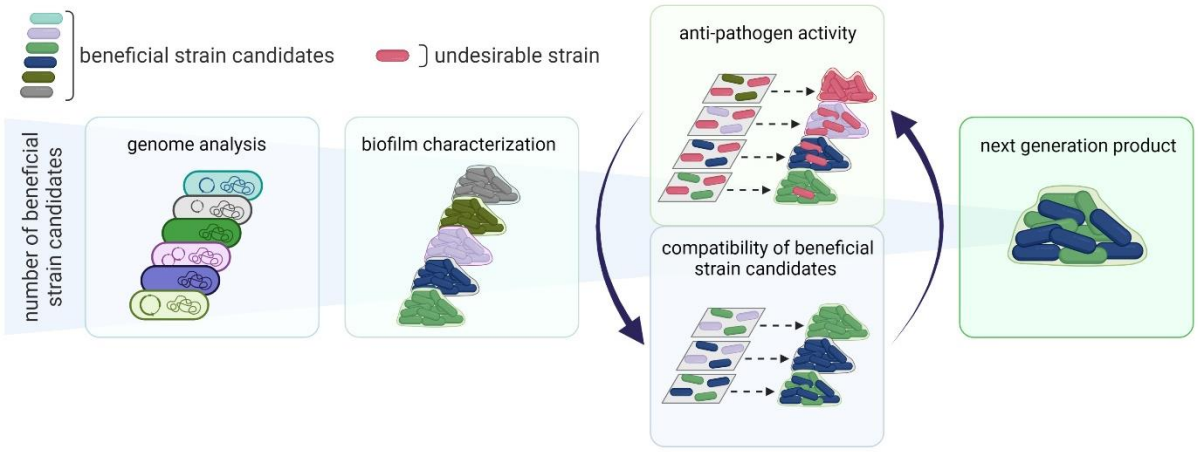

Figure 3: Schématisation de la méthodologie employée pour sélectionner et assembler des souches candidates mobilisant des propriétés d'intérêt pour une application en biofilm positif, avec comme perspective le développement de produits de nouvelle génération.

Dans un premier temps, nous avons sélectionné 230 souches candidates du genre *Bacillus* et *Paenibacillus*, provenant à la fois de la collection Delaporte (équipe B3D), de la collection Aquapharm (Lallemand) et isolées à partir d'un élevage dans le cadre des études présentées dans le chapitre précédent. L'analyse des génomes de ces souches a permis de sélectionner des espèces présentes sur la liste de QPS de l'EFSA (*B. velezensis, B. subtilis, B. licheniformis*), ainsi que 2 souches de *Paenibacillus* spp. formant des biofilms très structurés en macro-colonies. La capacité de ces souches à former des biofilms immergés a été visualisée par MCBL. Une sélection de 18 souches présentant des morphologies remarquables (hauteur, rugosité, volume, macro-structures), a été effectuée tout en conservant une diversité d'espèces.

Les méthodes utilisées par la suite reposent sur une analyse phénotypique combinant l'utilisation de la MCBL avec des souches génétiquement modifiées pour exprimer des protéines fluorescentes, ainsi qu'une analyse d'images à haut débit. Les souches candidates ont été mises en compétition avec 4 bactéries pathogènes problématiques des élevages avicoles (*Staphylococcus aureus*, *Enterococcus cecorum*, *Escherichia coli* et *Salmonella enterica*). Nous avons introduit dans ces souches pathogènes un plasmide exprimant constitutivement le gène codant pour la GFP (green fluorescent protein), afin de suivre leur croissance

au sein de biofilm mixes. L'impact de la présence des souches bénéfiques candidates sur la croissance des souches pathogènes a été quantifié en se basant sur le volume des biofilms formés par les souches fluorescentes pathogènes après 24h d'incubations dans différentes conditions, dans deux modèles de biofilms mixtes immergés décrits dans l'**article 7**.

Cette quantification, après 24h heures d'incubation, a permis de sélectionner des souches de *Bacillus* spp. à fort potentiel antagoniste. Toutefois, les mécanismes impliqués restaient à élucider. En effet, plusieurs processus écologiques de compétition peuvent s'établir entre deux espèces bactériennes, conduisant à la dominance de l'une et à l'exclusion de l'autre. *Bacillus* spp., par exemple, peut exclure le pathogène par une croissance plus rapide, en exploitant plus efficacement une ressource nutritive ou en bloquant l'accès de l'autre espèce à la ressource. Ces stratégies sont désignées sous le terme de **compétition nutritionnelle**. La production abondante par les *Bacillus* spp de matrice d'exopolysaccharides peut également contribuer à limiter l'implantation d'un organisme exogène dans le biofilm (**compétition spatiale**). Enfin, les bactéries sont capables de secréter un arsenal de molécules pouvant inhiber la croissance ou tuer une autre espèce, telles que des toxines et des antimicrobiens [39]. On parle alors de **compétition d'interférence**, phénomène qui intègre également la sécrétion de molécules comme les sidérophores impliquées dans l'acquisition du fer dans l'environnement [40]. Dans ce cas, il s'agit d'une **compétition nutritionnelle par interférence**. Chacun de ces mécanismes d'exclusion peut être représenté au moyen d'outils mathématiques de modélisation dédiés reposant sur des analyses temporelles. C'est par exemple le cas du modèle proie-prédateur de Lotka-Volterra qui incrimine la sécrétion de molécules interférentes [41] ou le modèle de Jameson pour une compétition spatial et nutritionnelle [42,43]. Ces modèles permettent d'obtenir des paramètres quantitatifs décrivant l'évolution des partenaires et leur influence mutuelle. Cela ouvre la voie à une interprétation biologique des mécanismes sous-jacents. Par cette approche, nous avons étudié les grandes familles de mécanismes impliqués dans l'exclusion d'*E. cecorum* et de *S. enterica* par 3 souches de *B. velezensis*, seules ou en consortiums 2 et 3 souches,

à travers les cinétiques de formation de biofilms mixtes au cours du temps. Expérimentalement, une étude spatio-temporelle du devenir de la bactérie pathogène marquée par la GFP en présence de différentes souches de *B. velenzensis* (x,y,z,t) couplée à l'analyse des images, a été réalisée. Les trois souches de *B. velezensis* présentent des paramètres de croissance (tels que le temps de génération et le volume maximal atteint) similaires, mais distincts de ceux des deux pathogènes. Le modèle de Jameson décrit de manière exhaustive les interactions compétitives, sur le plan nutritionnel et spatial. Une souche ayant un temps de génération plus court se développera plus rapidement, excluant ainsi son partenaire concurrent. Dans le scénario où *E. cecorum* est majoritaire au début de l'interaction, un modèle proie-prédateur de type Lotka-Volterra décrit cette dynamique. En effet, *E. cecorum* se développe simultanément avec *B. velezensis*, mais à partir d'une certaine concentration des deux partenaires, *B. velezensis* exclut *E. cecorum* en produisant certainement des composés bactéricides pour le pathogène. Cela indique que *B. velezensis* détecte la présence d'*E. cecorum* et adapte son métabolisme pour éviter son exclusion. De plus, cette étude souligne aussi l'importance du mode de vie en biofilm de *B. velezensis* dans l'exclusion de *S. enterica*. En effet, avec une concentration initiale identique de *B. velezensis* et de *S. enterica*, le pathogène est exclu lorsque *B. velezensis* se trouve sous forme de biofilm, et pas dans un état planctonique, dès le début de l'expérience.

Tout comme les propriétés de colonisation des surfaces, le potentiel compétitif des souches de *Bacillus* spp. envers des bactéries pathogènes ou indésirables est en général évalué pour des souches individuelles, mais pas en combinaison. Étant donné la forte activité compétitrice, il est crucial de s'assurer au préalable de l'absence de compétition interne au sein du consortium bénéfique. La compatibilité de chacune des 3 souches de *B. velezensis* avec les 18 souches précédemment étudiées a été testée au sein de biofilms mixtes. A cette fin, les 3 souches de *B. velezensis* d'intérêt ont été génétiquement étiquetées en introduisant un plasmide exprimant constitutivement le gène codant une protéine fluorescente (GFP ou mCherry) afin d'étudier leur spatialisation et de les quantifier dans des biofilms mixtes. Les résultats ont montré que ces 3 souches de

B. velezensis, phylogénétiquement très proches, étaient compatibles entre elles et sont capables de coexister dans les biofilms. En revanche, les combinaisons binaires entre ces souches de *B. velezensis* et les autres souches de *Bacillus* ont toutes montré l'exclusion d'une souche par une autre, ce qui est en accord avec la théorie de la discrimination de parenté *kin* [44]. Ce phénomène est observé chez *Bacillus subtilis* où les cellules sont en mesure de différencier les individus apparentés (phylogénétiquement liés) des individus non apparentés (phylogénétiquement non liés) [45]. En effet, la reconnaissance des membres de leur propre communauté est importante chez les microbes, car elle est à l'origine du développement de comportement de mutualisation et d'entraide favorisant les voisins (kin) de la même espèce [44]. Les microorganismes démontrent une coopération multiple pour s'alimenter, se déplacer, développer leur virulence, acquérir du fer, se défendre, détecter le quorum, et engendrer des biofilms multicellulaires ou des organes de fructification. L'entraide trouve sa justification dans l'évolution lorsqu'elle profite aux individus partageant les mêmes gènes. Cependant, la véritable distinction peut s'effectuer dans le cas des systèmes poison-antidote, tels que les bactériocines, où les cellules favorisent leur propre espèce en empoisonnant les autres, ou dans les systèmes d'adhésion, où les cellules de la même espèce se lient entre elles. Ces comportements peuvent contribuer à renforcer les liens de parenté en général, facilitant ainsi l'évolution et la préservation de la coopération. Une fois les associations stables identifiées, des expériences similaires d'interaction entre des bactéries pathogènes et les 3 souches de *B. velezensis*, seules ou en consortium 2 et 3 souches, ont été entreprises dans le but de comparer les effets des mélanges de souches aux souches individuelles. Ainsi, les consortiums compatibles ne possèdent pas plus d'effet d'exclusion des pathogènes par rapport aux souches seules les composants. Les résultats de cette série d'expériences sont exposés dans l'**article 7**, en cours de finalisation.

L'influence des bactéries lactiques sur la croissance des bactéries pathogènes a également été investiguée en utilisant la même stratégie que précédemment décrite. Les souches de bactéries lactiques étudiées sont les deux souches de

Pediococcus spp. présentes dans le produit commercial Lalfilm Pro. Dans le but d'améliorer le potentiel d'un produit de nouvelle génération, nous avons évalué la capacité de ces souches de bactéries lactiques à coexister au sein d'un biofilm mixte avec les trois souches de *B. velezensis* préalablement sélectionnées. Les *Pediococcus* spp. et les trois souches de *B. velezensis*, dans ce cas éloignées phylogénétiquement, ont démontré leur aptitude à former des biofilms stables à deux espèces. Pour la première fois, un effet antagoniste accru des associations entre *Pediococcus* spp. et *B. velezensis* sur les bactéries pathogènes a été démontré. Les résultats sont décrits dans l'**article 8**, en préparation.

En parallèle des études réalisées au MCBL, des expériences d'interaction au sein de macro-colonies ont été réalisées. La formation d'une macro-colonie structurée de cellules et d'une matrice extracellulaire est un modèle de biofilm qui se développe à l'interface entre un milieu gélosé et l'air. La capacité des différentes souches candidates (*Bacillus* spp. ; *Paenibacillus* spp. ; *Pediococcus* spp.) à former des co-macro-colonies, en combinaison ou associées à des souches pathogènes, a été étudiée. L'objectif de ces expériences était d'analyser les antagonismes dans un modèle de biofilm distinct de celui précédemment décrit en biofilm immergé. Des comparaisons entre ces deux modèles de biofilm ont été effectuées. Le modèle de biofilm en macro-colonie présente l'avantage d'une mise en place plus simple que le modèle en biofilm immergé, même si la quantification et l'identification des mécanismes d'interactions reste spécifique à chacun des modèles. Les résultats de cette partie sont décrits dans la section "**Exploration des biofilms en macro-colonies : étude des interactions pour une sélection de souches à fort potentiel anti-pathogène**".

En conclusion, une méthode novatrice basée sur l'imagerie en temps réel et l'analyse des biofilms mixes par MCBL a été élaborée pour la sélection de souches et de consortiums, présentant des propriétés d'intérêt en tant que biofilms positifs dans les élevages. Au cours de cette étude, nous avons corrélé les mécanismes responsables de l'antagonisme envers les agents pathogènes avec différents modes de compétition, tels que la compétition spatiale/nutritionnelle et l'interférence. De plus, des souches individuelles prometteuses ont été identifiées,

de même que des consortiums démontrant un effet significativement renforcé par rapport aux souches individuelles qui les composent. Enfin, notre contribution se manifeste par un complément du processus de sélection des souches, en introduisant l'utilisation d'un modèle basé sur les macro-colonies.

3.2.2 Article 7 : Guided assembly of positive biofilms targeting pathogenic bacteria using live-cell imaging

Virgile Guéneau, Laurent Guillier, Guillermo Jiménez, Julia Plateau-Gonthier, Marie-Françoise Noirot-Gros, Pascale Serror, Mathieu Castex, Romain Briandet.

En préparation.

Guided assembly of positive biofilms targeting pathogenic bacteria using live-cell imaging

Virgile Guéneau[a,b], Laurent Guillier[c], Guillermo Jiménez[b], Julia Plateau-Gonthier[b], Marie-Françoise Noirot-Gros[a], Pascale Serror[a], Mathieu Castex[b], Romain Briandet[a*]

[a] Université Paris-Saclay, INRAE, AgroParisTech, Micalis Institute, 78350, Jouy-en-Josas, France

[b] Lallemand SAS, 31702, Blagnac, France

[c] French Agency for Food, Environmental and Occupational Health & Safety (ANSES), Laboratory for Food Safety, Salmonella and Listeria Unit, Paris-Est University, 14 rue Pierre et Marie Curie, 94701, Maisons-Alfort, France.

* Address correspondence to Romain Briandet, romain.briandet@inrae.fr

Keywords: biofilms, microbial pathogens, *Bacillus* species, kin discrimination, microbial growth modeling, live-cell imaging

Abstract

The use of chemical antimicrobials to control undesirable microbial agents contributes to the rise of antimicrobial resistance (AMR) and environmental pollution. In alignment with the One Health paradigm, there is a growing emphasis on developing innovative alternatives, such as harnessing beneficial microorganisms with strong competitive traits. This approach aims to sculpt the microbial ecology of surfaces, ultimately restraining the proliferation of undesirable microorganisms. In this contribution, we introduce a novel methodology that enables a rational and systematic selection and combination of strains for such applications. Our approach leverages live-cell fluorescent imaging through High Content Screening Confocal Laser Scanning Microscopy (HCS-CLSM). This method was used to assess a collection of *Bacillus* species strains in diverse multi-species biofilm scenarios, aiming to understand their impact on the growth of different bacterial pathogens and unravel the nature of the mechanisms underlying their exclusion. Our study results reveal the exceptional antagonistic influence of three *Bacillus velezensis* strains against pathogens. Moreover, these strains demonstrated the ability to form a stable *kin*-compatible consortium, resulting in enhanced surface colonisation of the biofilm compared to individual strains. By leveraging live-cell imaging kinetics and modelling, we were able to demonstrate Jameson nutritional competition in most explored scenarios. Additionally, regarding antagonist interactions between *B. velezensis* against *Enterococcus cecorum*, our modelling revealed a Lotka-Volterra prey-predator dynamic, indicating an active interference mechanism. Furthermore, we observed a notable increase in the inhibition of *Salmonella enterica* serovar Enteritidis when *B. velezensis* was pre-established on the surface, suggesting a disctinct biofilm-associated exclusion effect. This methodology establishes an innovative approach for constructing robust positive biofilms with potent effects against pathogens.

Introduction

Microorganisms mainly live in the form of biofilms, capable of colonising diverses biotopes on Earth [1]. Biofilms are complex communities of spatially organised microorganisms embedded in a self-produced matrix growing at interfaces, and interacting with each other and with their environment [2]. This spatial arrangement and cellular diversity within microbial communities result in unique biofilm properties compared to planktonic lifestyles [3–6]. Consequently, microorganisms living in biofilms exhibit greater tolerance to environmental fluctuations, such as exposure to disinfectants [7], antibiotics [8] or passage through the digestive tract [9]. These communities often consist of multiple species engaged in various interactions, including resource competition, cooperation for mutual benefit, or even the inhibition of other species [10,11]. Understanding these interactions to predict overall biofilm behaviour and function is a critical challenge in microbial ecology.

As an application of the One Health concept, biotechnology is developing solutions that employ guided microbial ecology principles to regulate interactions within complex biofilm communities. Specific strains or consortia of beneficial strains with antagonistic activity against undesirable microorganisms, like pathogens, can be intentionally introduced to surfaces [12], foods [13] or directly to hosts [14]. This approach recognizes microbial communities as complex systems, where manipulating a few key components can significantly impact the entire system [15]. This approach modifies the microbial composition to promote a targeted ecosystem [16]. Beneficial strains are selected for their antagonistic effect against undesirable microorganisms, which may involve nutritional and spatial competition [17] or the secretion of active molecules [18]. The quantification of antagonism is typically assessed in planktonic form of interacting species, which inadequately reflects real-world conditions where microbial communities reside in biofilms. Additionally, commercial products frequently contain multiple strains, with no clear justification for their inclusion and no assurance of their compatibility.

Here, we present a pipeline for the rational selection and combination of strains to create positive biofilms on livestock building surfaces, an approach already employed in the field. This method relies on phenotype analysis using High Content Screening-Confocal Laser Scanning Microscopy (HCS-CLSM) combined with genetically engineered fluorescent strains and dedicated image analysis [19]. For this study, we meticulously analysed more than 23220 image

z-stacks to extract quantitative data on the effectiveness of positive biofilm. Using this pipeline, we screened a collection of *Bacillus* species for their impact on the growth and establishment of several bacterial pathogens including *Staphylococcus aureus*, *Enterococcus cecorum*, *Escherishia coli* and *Salmonella enterica* serovar Enteritidis (*S. enterica*) in two submerged mixed species biofilm models. *Bacillus* species are part of the natural microbiota of biofilm in livestock buildings and renowned for their versatile applications in biotechnology, making them attractive candidates for exploring their biocontrol potential. By modelling live-cell CLSM imaging of interspecies interactions, we elucidate the underlying family of mechanisms involved in antagonistic interactions, encompassing spatial and nutritional competition [17,20], as well as Lotka-Volterra prey-predator interference [21].

To further comprehend and optimise the use of bacterial cocktails in biotechnological applications, we leveraged the concept of kin discrimination to prevent interference between beneficial organisms and combine only compatible beneficial strains. Kin discrimination is observed when organisms can distinguish between genetically related (kin) and genetically unrelated (non-kin) individuals [22]. This concept is based on the detection of small signalling molecules, or specific flagellin motifs in *B. velezensis* [23]. Kin discrimination is crucial for the evolution of cooperative behaviours, allowing genetically related individuals to cooperate and enhance their overall fitness. Our study demonstrated that phylogenetically related *Bacillus* species strains could coexist, whereas more distant strains exhibited mutual exclusivity in a submerged mixed biofilm model. We selected strains capable of forming stable three-strains kin biofilms, and demonstrated enhanced surface colonisation with antagonistic activity against pathogens.

Methods

Bacterial strains and genetic constructions

The WT bacterial strains and genetic constructions used in the study are described in **Table 1**. The experiments were conducted using Tryptic Soy Broth (TSB) medium (Biomérieux, France) at a temperature of 30°C. To initiate each experiment, a 5 mL overnight culture was prepared from a glycerol stock at -80°C. If the strain carried a plasmid with a gene encoding for fluorescent proteins, the culture was supplemented with the selection antibiotics (5 µg/mL erythromycin for Gram-positive species or 100 µg/mL ampicillin for Gram-negative species). The overnight cultures were then centrifuged at 5000 g for 5 minutes, and the supernatant was replaced with fresh TSB before beginning the experiments.

Table 1: Bacterial strains used in the study.

Name	Origine and genotype	Reference
Bacillus velezensis 11285	Marine	Lallemand AQP
Bacillus velezensis 12048	Marine	Lallemand AQP
Bacillus velezensis B8	Surfaces of commercial broiler chicken houses	[12]
Bacillus velezensis 12701	Marine	Lallemand AQP
Bacillus velezensis 11457	Marine	Lallemand AQP
Bacillus velezensis B18	Surfaces of commercial broiler chicken houses	[12]
Bacillus velezensis B1	Surfaces of commercial broiler chicken houses	[12]
Bacillus velezensis 12832	Marine	Lallemand AQP
Bacillus velezensis 1273	Very wet soil of a snow combe, 2400m altitude	Delaporte collection
Bacillus velezensis 12001	Plant	Lallemand AQP
Bacillus subtilis 1202	Water from a river	Delaporte collection
Bacillus licheniformis 1234	Small greenish pebbles	Delaporte collection
Bacillus licheniformis C5	Surfaces of commercial broiler chicken houses	[12]
Bacillus licheniformis 1218	Sea urchin intestine in sea water	Delaporte collection
Bacillus licheniformis 1298	Pinkish grey gravel	Delaporte collection
Bacillus licheniformis 1219	Greyish sandy soil	Delaporte collection
Paenibacillus sp. 1167	Black soil	Delaporte collection
Peanibacillus sp. 1399	Dark brown soil	Delaporte collection
Bacillus velezensis 11285 mCherry	*Bacillus velezensis* 11285 with pCM11-*mcherry* (ery)	This study
Bacillus velezensis 12048 GFP	*Bacillus velezensis* 12048 with pCM11-*gfp* (ery)	This study
Bacillus velezensis B8 GFP	*Bacillus velezensis* B8 with pCM11-*gfp* (ery)	This study
Bacillus velezensis B8 mCherry	*Bacillus velezensis* B8 with pCM11-*mcherry* (ery)	This study
Staphylococcus aureus RN4220	Laboratory strain with pALC2084-*gfp* (ery)	[24]
Enterococcus cecorum DSM20682	Strain from DSM collection, isolated from chicken caecum with pCM11-*gfp* (ery)	This study
Salmonella enterica serovar Enteritidis NCTC6676	Strain from NCTC collection, isolated from a dead cow with pCM11-*gfp* (amp)	This study
Escherichia coli CIRMBP0248	Strain from CIRMBP collection, isolated from chicken intestine with pCM11-*gfp* (amp)	This study

The phylogenetic tree analysis of the 18 *Bacillus* strains was performed using the bacterial Phylogenetic Tree Service of BV-BRC [25]. The whole genome sequence FASTA file of each of the 18 *Bacillus* strains were uploaded to BV-BRC, set to the "contigs" object type. The

phylogenetic tree was then built with the default Codon Tree method. For species assignments, the genome sequences were compared to the genomes sequences of the closest species within *Bacillus* genus in the BV-BRC database, with the requested use of 1,000 genes (up from the default 100), with 5 allowed deletions.

Transformation protocol using PCM11 plasmid to enable expression of GFP or mCherry to visualise CLSM strains [26] was adapted for each strain, described in detail in the supplementary material (**Fig. S1)**. Briefly, wild type *E. coli* and *S. enterica* were transformed using a standard heat shock protocol. The protocols used to prepare the electrocompetent cells and to transform *E. cecorum* were inspired by Dunny *et al.* [27]. For *B. velezensis*, the transformation protocol presented takes advantage of the ability of some species to be naturally competent [28] and was inspired by Dergham *et al.* [29].

Submerged biofilm models

All biofilm structures were performed in 96-well plates µclear® base (Greiner Bio-one, France) compatible with high resolution fluorescence microscopy. Images were acquired automatically using the HCS mode of the confocal for kinetic experiments.

Co-inoculation biofilm model to study interaction after adhesion stage

Multi-species biofilms were established using genetically labelled strains (GFP-labelled pathogen, GFP-labelled *B. velezensis*, mCherry-labelled *B. velezensis*) alongside non-genetically labelled *Bacillus* species strains (one, two, or three strains), beginning with an equivalent initial adhesion biovolume of 0.50 +/- 0.25 between the fluorescent strain and the non-genetically labelled strains. Adhesion ratios were determined following the protocol outlined by Guéneau *et al.* [19] employing a GFP/SYTO61 (Invitrogen, Carlsbad, CA, USA; a bright cell-permeant red dye that labels nucleic acid) dual labelling. In this system, cells labelled only in red correspond to the non-genetically labelled strains, and cells labelled both in red and green correspond to the genetically tagged ones. GFP strains with SYTO61 were used to study biofilms at a given time point. For kinetics measurements, SYTO61 was replaced by the vital dye FM4-64 (Invitrogen, Carlsbad, CA, USA; a lipophilic dye that labels cell membranes in red) at a vital concentration of 1 µg/mL [30].

Concisely, the overnight cultures of the GFP-labelled pathogen and *Bacillus* strains were diluted in TSB at 1/100e, except for the poorly adhesive strains *B. licheniformis* 1298, *Paenibacillus* sp. 1399, and *Paenibacillus* sp. 1167, which were diluted at 5/100e. The same volume previously determined for *Bacillus* strains was used for monospecific biofilm growth. We added 200 µL of the bacterial solution to 96-well plates and performed an adhesion step of 1h30 at 30°C. Then, the supernatant was replaced with fresh TSB and incubated for 24 h at 30°C.

In the case of kinetics in the co-inoculation model, three initial ratios of the two partners were employed to investigate the formation of multi-species biofilm. The experiment was based on planktonic culture volumes to achieve previously validated 1:1 adhesion ratio values. These three ratios correspond to 10 times more volume of GFP pathogens for one volume of *B. velezensis*, the same volumes as those determined for the 1:1 ratio, and one volume of GFP pathogens for 10 volumes of *B. velezensis*.

The same protocol was used to study the interaction of unlabelled *Bacillus* species with GFP-labelled *B. velezenesis*. Adhesion ratios were determined with *B. velezensis* 12048 GFP and applied in the same way with *B. velezensis* 11285 GFP and *B. velezensis* B8 GFP. For two-strains *Bacillus* strains biofilms, the labelled strains and a *Bacillus* strains were diluted at 1/200e each after centrifugation in the same way as described above , except for the strains *B. licheniformis* 1298, *Paenibacillus* sp. 1399 and *Paenibacillus* sp. 1167, which were diluted at 5/100e. For three-strain *B. velezensis* biofilms, the three strains were diluted at 1/333e in TSB before performing an adhesion phase and incubated for 24 h at 30°C.

After incubation, 50 µL of SYTO9 (Invitrogen, Carlsbad, CA, USA; a cell-permeant green dye that labels nucleic acid) for monospecific *Bacillus* strains or SYTO61 for two-strain biofilms with a GFP-labelled strain were added, diluted in TSB at 2 µg/mL. Images were captured using CLSM. In the case of *B. velezensis* WT grown with GFP and mCherry labelled *B. velezensis* strains, 50 µL of 4′-6-diamino-2′phenylindole (DAPI) at 2 µg/mL was added to visualise the entire biofilm.

Recruitment biofilm model to study pathogen adhesion and growth on established *Bacillus* spp. biofilm

This experiment investigated pathogen recruitment and growth on mature *Bacillus* biofilms. *Bacillus* biofilms were developed using the same protocol as previously described with an adhesion phase followed by 24 h growth at 30°C without agitation. Overnight pathogen

cultures were centrifuged at 5000 g for 10 min and the supernatants were replaced with fresh TSB (supplemented with FM4-64 at 1 µg/mL for the kinetics experiment) to remove the antibiotics. 50 µL of a GFP pathogen solution was added to wells containing *Bacillus* biofilms for an adhesion step of 1h30 at 30°C. Supernatants were carefully replaced with 200 µL of fresh TSB and CLSM acquisitions were performed directly (recruitment t=0h) or after 24h growth at 30°C (recruitment t=24h). Prior CLSM acquisition, 50 µL of a TSB solution containing SYTO61 at 2 µg/mL or FM4-64 at 1 µg/mL for kinetics until the end of the experiment was added to the wells.

Live-cell fluorescent imaging

Live-cell fluorescent imaging was conducted using a Leica SP8 AOBS inverted high-content screening confocal laser scanning microscope (HCS-CLSM, LEICA Microsystems, Germany) at the MIMA2 platform (https://doi.org/10.15454/1.5572348210007727E12). Biofilm images were captured using a 63x water objective with a numerical aperture of 1.2. Imaging was performed at a frequency of 600 Hz, with each image taken every micrometre to ensure full height coverage of the biofilm. The acquired images had a resolution of 512 × 512 pixels, corresponding to a physical area of 184.52 µm x 184.52 µm and a pixel size of 0.361 µm. The SYTO9 and the GFP were excited with an argon laser set at 488 nm, and the emitted fluorescence was collected with a hybrid detector (HyD LEICA Microsystems, Germany) in the range 500-550 nm. FM4-64 was excited with a helium-neon laser at 561 nm, and the emitted fluorescence was collected with a hybrid detector in the range of 600-750 nm. SYTO 61 was excited with a helium-neon laser at 633 nm and the emitted fluorescence was collected with a hybrid detector in the range of 650-750 nm.

For 4D (xyzt) acquisitions, the temperature was maintained at 30°C and 150 µm stacks of images were acquired every hour. For each experiment, between 3 and 6 biological replicates were carried out with 4 technical replicates, representing at least 12 technical values per condition.

A specific experiment to observe biofilms with the three compatible *B. velezensis* strains was performed using a Zeiss LSM 700 inverted CLSM (Carl Zeiss, Germany) equipped with a 405 nm laser that allows excitation of the blue nucleic acid dye DAPI. A Plan-Apochromat 63x oil immersion objective with a numerical aperture of 1.4 was used to capture images at every

micrometre. The images had a resolution of 1024 × 1024 pixels, covering an area of 203.2 × 203.2 µm. The pixel size of each image was 0.20 µm. Biofilms visualisation of the 3 *B. velezensis* growing in the same sample was performed using 3 different fluorescent molecules. DAPI was excited with a diode laser at 405 nm to label the entire population. The emitted fluorescence of DAPI was collected with a photomultiplier detector (PMT) in the range of 410-550 nm. mCherry protein was excited with a diode laser at 555 nm and the emitted fluorescence was collected with a PMT detector in the range of 560-700 nm. GFP was excited with an argon laser set at 488 nm and the emitted fluorescence was collected with a PMT detector in the range of 490-550 nm. Acquisitions were performed sequentially, starting with the DAPI channel and then the mCherry and GFP channels together.

CLSM image analysis

2D projections of biofilms and movies were obtained using IMARIS 9.3.1 software (Bitplane, Zurich, Switzerland). BiofilmQ software was used to extract quantitative values from image stacks [31]. Channels were analyzed separately using the OTSU thresholding method and "global biofilm properties" were selected to extract the biovolume of the binarized images.

To assess the anti-pathogenic activity of *Bacillus* species strains against pathogens, the biovolume ($\mu m^3/\mu m^2$) of the GFP channel of submerged mixed biofilms was measured and normalised to the biovolume of monospecific GFP pathogen biofilms. To standardise a score reporting biofilm anti-pathogenic activity, values were centre-reduced to fall between 0 (indicating the lowest activity) and 1 (representing the highest activity). This approach allowed for the use of a simple score ranging from 0 to 1 to compare the anti-pathogenic activity of different *Bacillus* strains and identify the most promising potential.

Modeling microbial growth and competition

GFP-measured biovolumes served as model inputs for both pathogens. For *Bacillus* in monoculture, biovolumes corresponding to the FM4-464 marker were used. In co-culture, *Bacillus* biovolumes were determined by subtracting the GFP-biovolume of the co-inoculated pathogen, from the total biovolume.

For monoculture experiments, biovolume increase was described using a generic primary growth model [32]:

$$\frac{1}{N(t)}\frac{dN(t)}{dt} = \mu_{max} \cdot \alpha(t) \cdot f(t)$$

Where μ_{max} is the exponential growth rate, α(t) is the adjustment function and f(t) is the inhibition function.

The nlsMicrobio package was used to fit Baranyi & Roberts primary growth model to estimate μ_{max}, lag (derived from α(t)), Nmax (derived from f(t)), and N_0 .

Two types of model were fitted to the competition data between pathogens and bioprotective flora.

The first type of model is the Jameson-type model [33]. The Jameson effect can be described as competition between species to use environmental resources in order to maximise their growth and population. When the common resource(s) are exhausted, the competition is over and the growth of each species in the population stops.

The growth stops simultaneously by both populations. Both competitors share the inhibition function (f(t)) of the exponential growth.

$$\frac{1}{N_A(t)}\frac{dN_A(t)}{dt} = \mu_{\max A} \cdot f_A(t)$$

$$\frac{1}{N_B(t)}\frac{dN_B(t)}{dt} = \mu_{\max B} \cdot f_B(t)$$

The inhibition function being

$$f_A(t) = f_B(t) = \begin{cases} 1 \; if \; t < t_{max} \\ 0 \; if \; t \geq t_{max} \end{cases}$$

where t_{max} is the time at which the stationary phase begins for populations A and B.

The second type of model is the Lotka-Volterra model. In this model, the inhibition functions can be described as follow:

$$\begin{cases} f_A(t) = \left(1 - \dfrac{N_A(t) + \alpha_{AB} N_B(t)}{N_{\max A}}\right) \\ f_B(t) = \left(1 - \dfrac{N_B(t) + \alpha_{BA} N_A(t)}{N_{\max B}}\right) \end{cases}$$

where the parameters α_{AB} and α_{BA} are the coefficients of interaction measuring the effects of one species on the other.

It makes no specific assumptions about the mechanisms underlying species interactions, they can be parameterized in ways that approximate any combination of underlying mechanisms. For example, in a system with two species, if both α_{AB} and α_{BA} are less than zero, species suppress each other's growth, indicating competition.

μ_{max} estimates were expressed in generation time (*GT*)

$$GT = \frac{ln(2)}{\mu_{max}}$$

The nlsMicrobio [34] and gauseR [35] packages were respectively used to fit the Jameson-type and Lotka-Volterra models.

Statistical analysis

Results were presented as mean and standard deviation (SD). Two-way ANOVA with uncorrected Fisher's least was used with PRISM software (GraphPad, USA, California). Statistical significance was determined when the *p*-value associated with the Fisher test was less than 0.05.

Results

Selection of *Bacillus* strains capable of limiting bacterial pathogens colonisation in different biofilm models

A collection of 18 *Bacillus* strains from different isolation origins was characterised in three biofilm models revealing a wide range of phenotypic diversity (**Fig. S2**). Utilising two co-incubation biofilm models, we conducted a screening process to identify *Bacillus* strains with the capacity to restrict the growth and establishment of pathogens (**Fig. 1**).

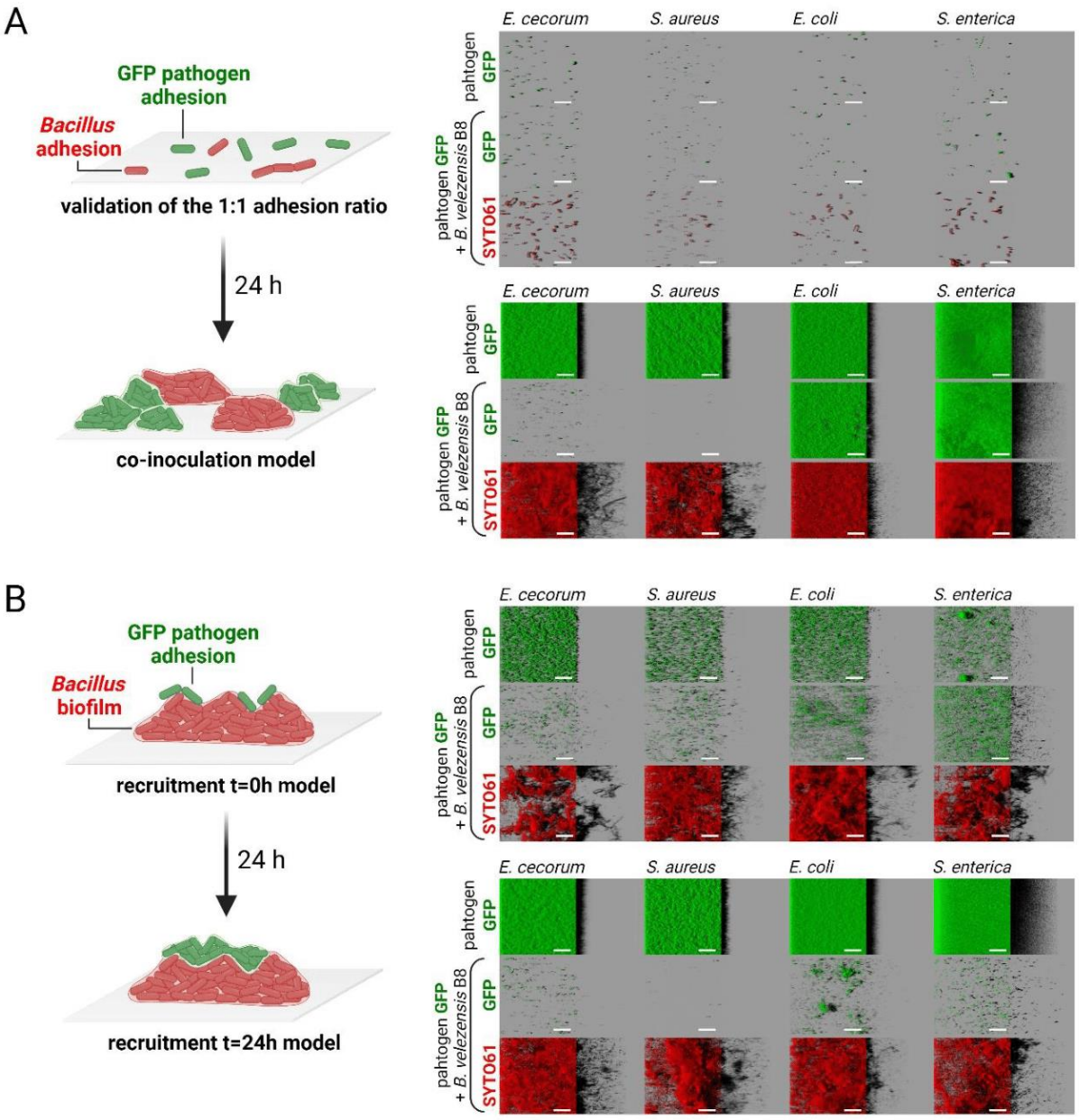

Figure 1: Co-incubation models between the 18 *Bacillus* strains and the 4 pathogens GFP used in the study. (A) To implement the co-inoculation model, the equal adhesion ratio of both pathogen and a *Bacillus* strain is first verified to ensure that both adhere to the surface in the same biovolume. Then, a 24-hour incubation is carried out and the quantification of the pathogen GFP is performed. (B) A planktonic culture of pathogens is introduced for an adhesion step on an installed *Bacillus* biofilm. This is followed by the quantification of the pathogen GFP biovolume, which is used to study the impact of the *Bacillus* biofilm on the pathogen's adhesion. The same steps as previously described

are repeated before a 24-hour incubation to examine the pathogen's development on a *Bacillus* biofilm, followed by the quantification of the pathogen GFP. In both models, SYTO61 is used to visualise the whole population in red, i.e., the pathogen and the *Bacillus*. The quantification of the pathogen GFP biovolumes is done to identify *Bacillus* that reduce pathogen growth compared to pathogens growing without *Bacillus* under the same conditions. Representative images were shown using *B. velezensis* B8. Scale bar = 40 µm.

In these models, pathogens carrying a GFP marker on a stable plasmid throughout the experiment were employed (**Fig. S3**). To ensure an equitable starting point for the co-inoculation interaction model in terms of *Bacillus* and pathogen quantities, we conducted adhesion ratio experiments and validated them across all 18 *Bacillus* strains with respect to the four pathogens (**Fig. S4**). Subsequently, we extracted raw biovolumes of GFP-expressing pathogens from image z-stacks captured during co-inoculation (**Fig. S5**), recruitment t=0 h (**Fig. S6**) and recruitment t=24 h (**Fig. S7**) models. This data was used to calculate antagonistic scores for each of the *Bacillus* strains (**Fig. 2**).

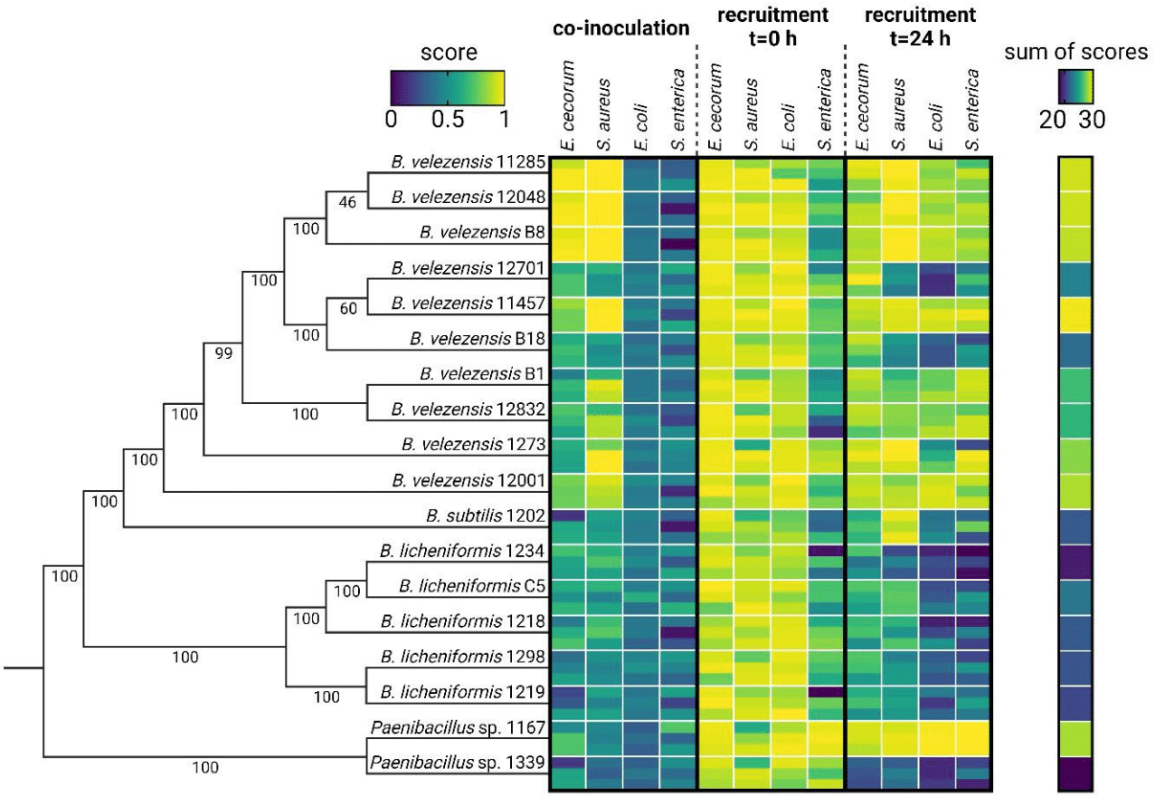

Figure 2: Antagonism score of the *Bacillus* strains against pathogens in the 2 co-incubation models. Pathogens are grouped by models and the 18 *Bacillus* strains are ordered according to the phylogenetic tree reflecting their relatedness. The Bootstrap values are placed before each node. In this heat map, 1 represents the highest antagonist score and 0 the lowest, calculated based on pathogen GFP biovolume in presence of one *Bacillus* strain normalised by the value of the pathogen GFP growing alone. Every square represents one interaction and displays the means

of three biological replicates, which in turn are calculated using four technical replicates. The sum of *Bacillus* scores against each pathogen in all models was calculated to total the antagonistic power of each strain. 2736 stacks of images were analysed to produce this heat map.

The results showed that the *B. velezensis* species display a notably superior overall antagonistic activity compared to other represented species. In particular, *Paenibacillus* sp. 1167 exhibited strong antagonist activity against all pathogens in the recruitment model, whereas it demonstrated relatively limited inhibitory effect on pathogens in the co-inoculation model. Among the *B. licheniformis* strains, pathogen adhesion was reduced in most cases, except for *S. enterica*. However, the t=24 h recruitment analysis revealed that pathogens were able to grow on the biofilm. Remarkably, *B. velezensis* 11285, *B. velezensis* 12048 and *B. velezensis* B8 consistently achieved the highest score sums and display superior performance against *E. cecorum* and *S. aureus*. To confirm that the reduction in GFP signal resulted from a decrease in the number of cells rather than issues related to GFP fluorescence, cell counts were conducted at the conclusion of the experiment using *B. velezensis* B8, a strain that showed a high antagonistic score (**Fig. S8**).

Establishing a *kin*-compatible *B. velezensis* synthetic consortium

Adhesion ratios between *B. velezensis* 12048 GFP and the 18 *Bacillus* strains were determined and applied to *B. velezensis* 11285 GFP and *B. velezensis* B8 GFP (**Fig. S9**). The co-inoculation model was used to simultaneously quantify the biovolume of GFP and SYTO61 channels (**Fig. S10**). The results show that none of the combinations exhibited a total biovolume (SYTO61) significantly different from that of either strain when grown individually. In instances of associations, the GFP to SYTO61 biovolume ratio was determined after a 24 h incubation period (**Fig. 3A**). Notably, two-strain biofilm formation was consistently observed only between the three GFP-tagged strains and their non-tagged counterparts, resulting in homogeneous biofilm mixtures (**Fig. 3B**). No other strain associations allowed for homogeneous mixed biofilm formation.

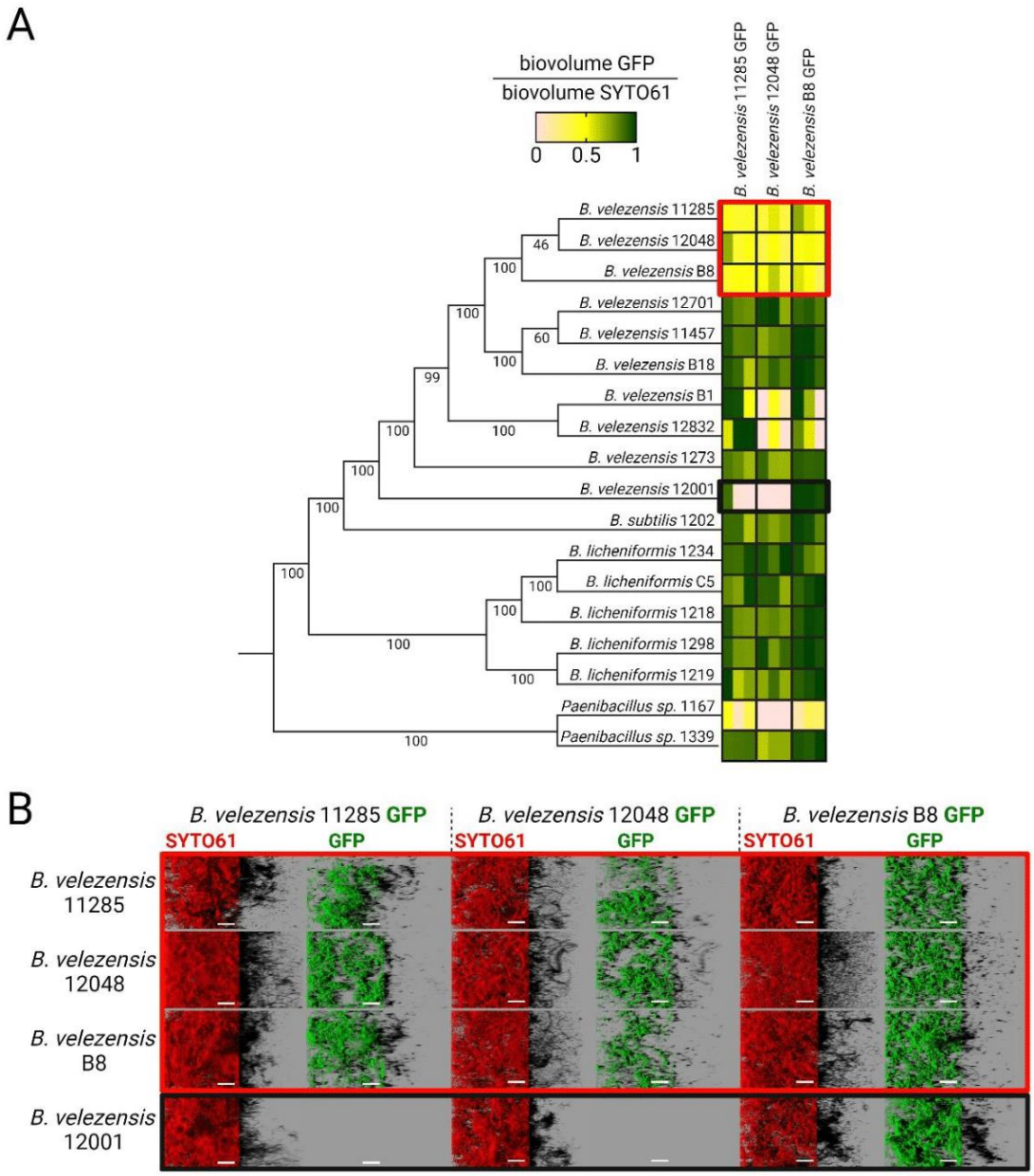

Figure 3 : Kin discrimination in a submerged biofilm model of 18 *Bacillus* strains against 3 *B. velezensis* GFP possessing a high antagonistic effect against pathogens. (A) The ability of three *B. velezensis* strains expressing GFP and exhibiting potent antagonistic activity against pathogens to form a mixed submerged biofilm with other *Bacillus* strains ordered by phylogenetic distance was evaluated using the co-inoculation model. The SYTO61 and GFP signals were quantified to perform the ratio biovolume GFP / biovolume SYTO61. A ratio of 0.5 means that there is the same biovolume of the *B. velezensis* GFP as non-genetically labelled *Bacillus* strain (labelled chemically using SYTO61). The red rectangles represent the examples illustrated below. Every square represents one interaction and displays the means of three biological replicates, which in turn are calculated using four technical replicates. 684 stacks of images were analysed to produce this heat map. (B) Examples are shown to illustrate the interactions between the 3 *B. velezensis* GFP strains capable of forming mixed bi-strain biofilms. The case of exclusion is demonstrated by *B. velezensis* 12001, which excludes *B. velezensis* 11285 and *B. velezensis* 12048 and is excluded by *B. velezensis* B8. Scale bar = 40 µm.

Further investigations were carried out to evaluate the capacity of the three selected *B. velezensis* strains to form a three-strains biofilm. To this end, a co-incubation experiment was performed, incorporating two genetically tagged *B. velezensis* strains with GFP and mCherry, along with a wild-type strain. The cell-permeant nucleic acid dye DAPI was also added before observations to visualise the entire population in blue. The population solely displaying blue fluorescence corresponds to the wild strain. An experiment was conducted using the *B. velezensis* B8 strain as an exemplar, involving the wild-type strain as well as strains genetically tagged with GFP or mCherry (**Fig. 4A**). Observations and quantification showed that the three strains were able to mix homogeneously in the same biofilm (**Fig. 4B**). The combination of strains did not show any differences in biovolume (**Fig. 4C**). However, the biofilm formed by the three strains covered significantly more surface area than the one and two strains combinations (**Fig. 4D**).

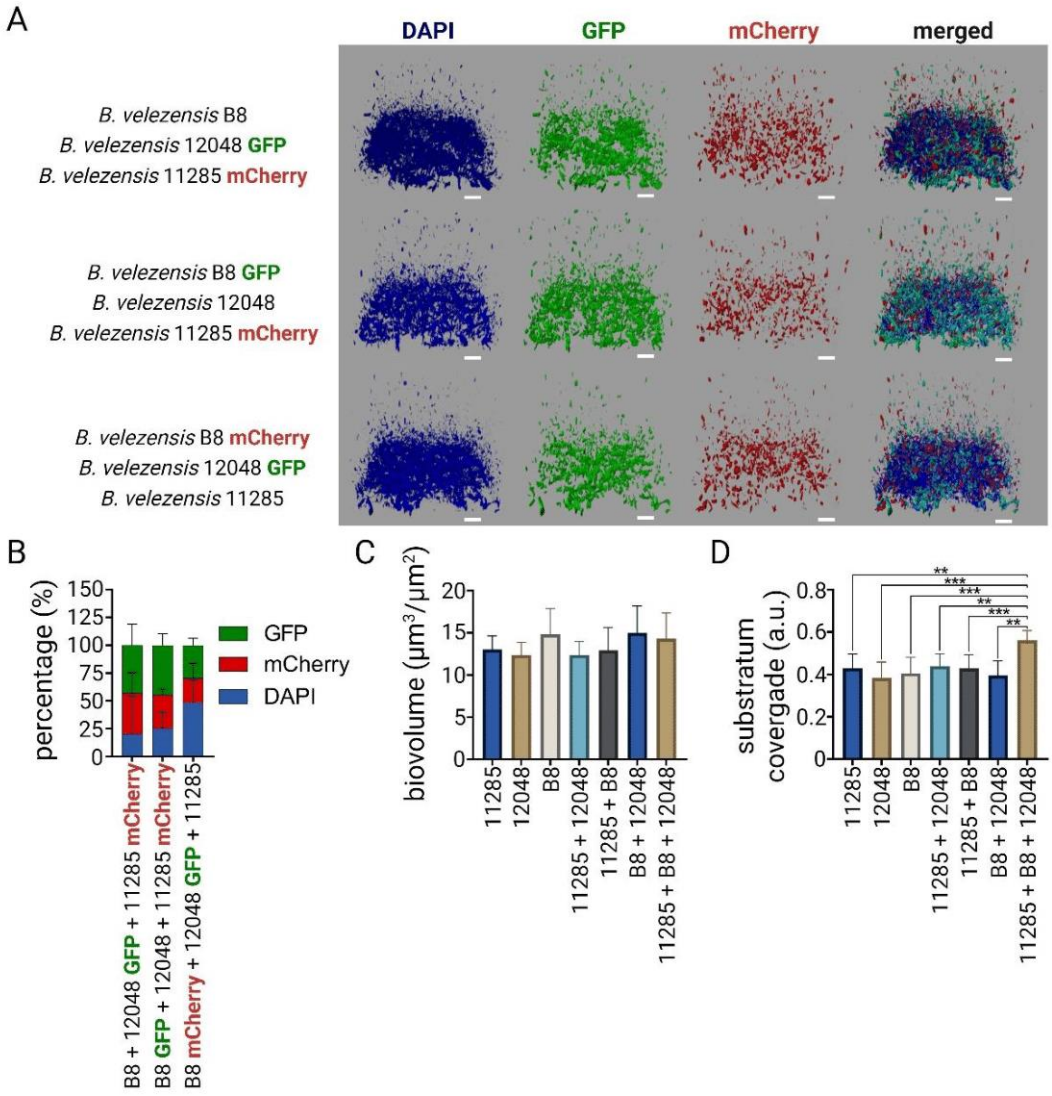

Figure 4: Mixed biofilm composed of 3 strains of *B. velezensis*. (A) Observation was performed using *B. velezensis* B8 strains wild type, or genetically labelled with GFP or mCherry, along with the addition of DAPI in the biofilm to visualise the entire population in blue. Combinations with other partners, including wild type, GFP or mCherry, were conducted to differentiate between each of the partners. Scale bar = 30 µm. (B) Percentage of signal from GFP, mCherry and DAPI-labelled cells only relative to total biovolume of DAPI in biofilms of the 3 strains (C) The co-inoculation model was employed using each wild type strains, whether combined or not, and the biofilms were labelled with SYTO9 to investigate their overall structure. The biovolume was extracted and shown on the graph. (D) Substratum coverage quantification of wild type strains alone or in consortia. 168 image stacks were analysed for quantification, corresponding to 6 biological replicates, each with 4 technological replicates per condition. Error bars correspond to standard deviation.

Antagonism within the mixtures was investigated and compared to that of individual strains, revealing no discernible distinctions (**Fig. S11**). Subsequently, interaction kinetics were employed to explore temporal dynamics, aiming to highlight potential significant differences and effectively distinguish among various families of antagonistic mechanisms.

Identification of mechanism families describing *B. velezensis* antagonism to pathogens

The addition of FM4-64 to visualise biofilm had no effect on pathogen growth kinetics (**Fig. S12**). Over 18720 image stacks were analysed to study interaction mechanisms.

B. velezensis and E. cecorum interactions

Monoculture experiments (**Fig. 5**) showed that *E. cecorum* exhibits significantly faster generation times (42 minutes) compared to the three *B. velezensis* strains (mean generation times ranging from to 62 to 74 minutes). Furthermore, the maximum biovolumes achieved by *E. cecorum* after the exponential growth phase are also greater than those of the three *B. velezensis* strains (8.9 $\mu m^3/\mu m^2$ compared to the mean of 4.8 $\mu m^3/\mu m^2$).

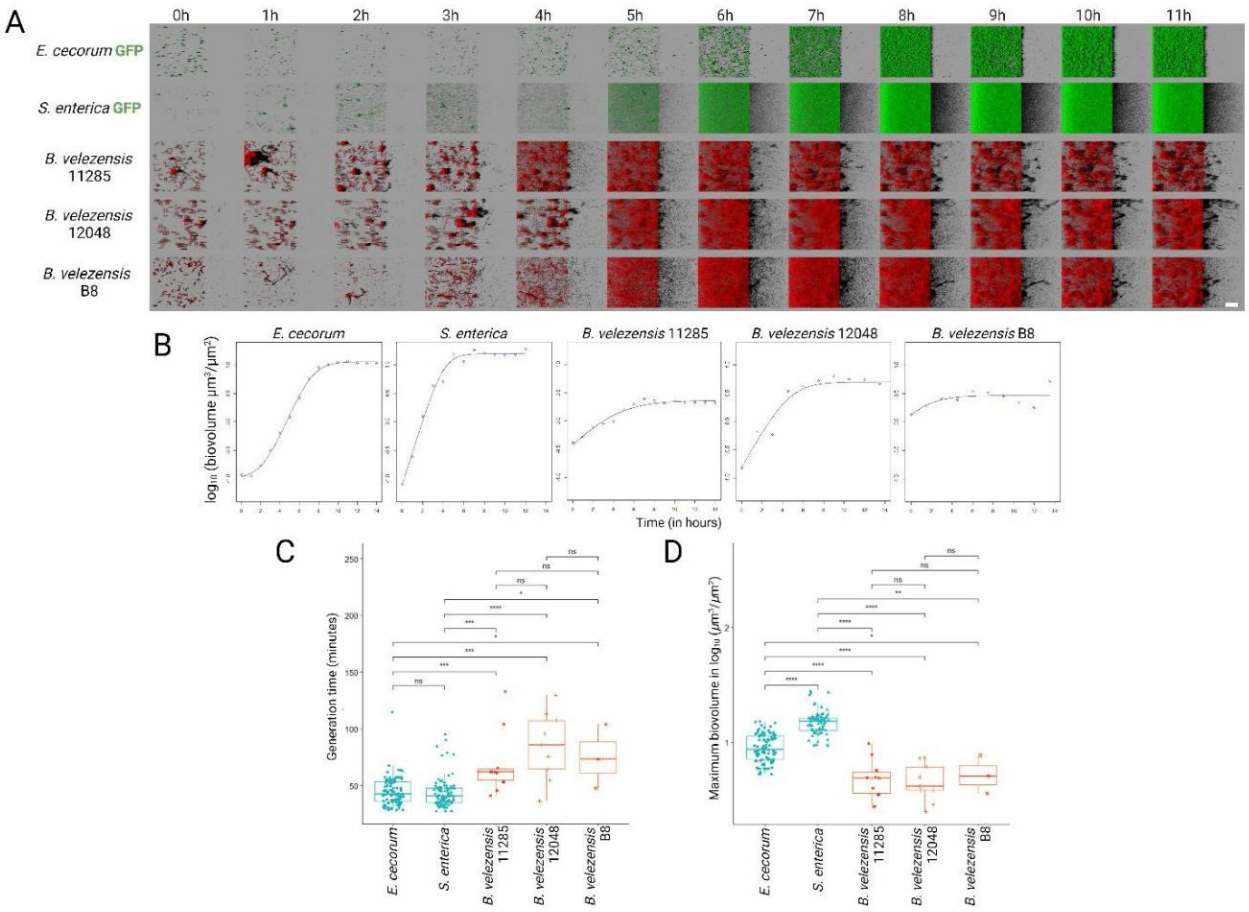

Figure 5: Monoculture biofilms growth. (A) CLSM visualisation of biofilm growth over time with a representative example per condition. The green colour corresponds to GFP labelling, while the red colour represents FM4-64. Scale bar = 40 µm. (B) Illustration (1 of the replicate) of the growth in monoculture. The dots correspond to measured biovolumes, the line to the primary growth model fitted to observations. (C) Comparaison of the generation times (D) and maximum biovolumes reached during monoculture experiments.

To explore the competition between *B. velezensis* and *E. cecorum,* three initial conditions were tested (**Fig. 6A,B**).

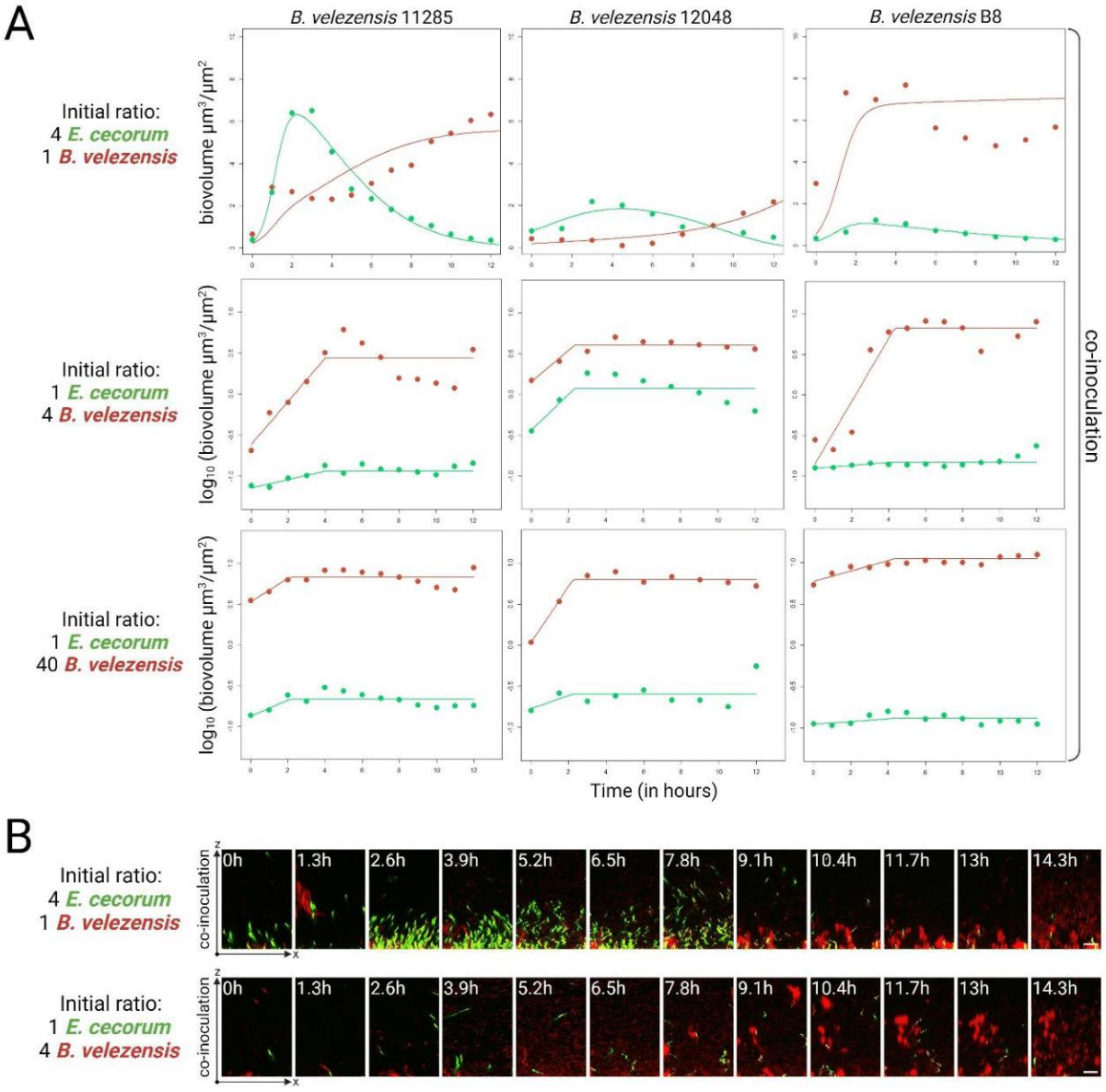

Figure 6: Interaction between *B. velezensis* and *E. cecorum*. (A) Illustration (one of the replicate) of the competition between *E. cecorum* and the three *B. velezensis* in the co-inoculation model. The dots correspond to measured biovolumes, the line to the primary growth models fitted to observations. (B) CLSM visualisation of 2 species biofilm growth over time with a representative example describing the Lotka-Volterra and Jameson models. The green colour corresponds to GFP labelling, while the red colour represents FM4-64. Scale bar = 50 µm.

In co-inoculation experiments with more *B. velezensis* inoculated (either 1 biovolume of *E. cecorum* vs 4 of *B. velezensis* or versus 40 of *B. velezensis*), regardless of the co-inoculated *B. velezensis* strains used, the generation time of *E. cecorum* is substantially extended (increasing from 42 minutes to 129 minutes). The exponential growth of *E. cecorum* ceases simultaneously with that of the co-inoculated *B. velezensis,* following the Jameson inhibition model.

In co-inoculation experiments with more *E. cecorum* initial biovolume compared to *B. velezensis* (4/1 ratio), regardless of the *B. velezensis* species, the behaviour of *E. cecorum* was different. Initially, exponential growth is observed with a generation time similar to that observed in monoculture, followed by a decline in population. The Lotka-Volterra model described this behaviour. The final levels of *E. cecorum* reached at the end of the experiments were lower than the initial biovolume (**fig. S13**).

While the competition patterns against *E. cecorum* are similar for the three *B. velezensis* strains, the final level reached at the end of the co-inoculation showed that *B. velezensis* B8 presents higher inhibition ability compared to the two other *B. velezensis* strains in experiments with 4/1 ratio and 1/4 ratios (Supplementary material 13).

All possible associations of the three *B. velezensis* were tested as well in co-inoculation experiments. However, compared to what is observed for simple competition (i.e. one *B. velezensis* vs *E. cecorum*), none of the association improved nor limited the competition against *E. cecorum* (**fig. S14**).

B. velezensis and S. enterica interactions

Monoculture experiments showed that *S. enterica* exhibits shorter generation times (41 minutes) compared to the three *B. velezensis* strains (Figure 5B). The maximum biovolumes reached by *S. enterica* in the stationary phase (N_{max}) are the highest among all studied microorganisms with a mean biovolume of 14.8 $\mu m^3/\mu m^2$ (Figure 5C).

In co-inoculation experiments, *B. velezensis* strains were consistently outperformed by *S. enterica*, even when the initial biovolumes of *S. enterica* were 40 times lower than those of *B. velezensis* (**Fig. 7**).

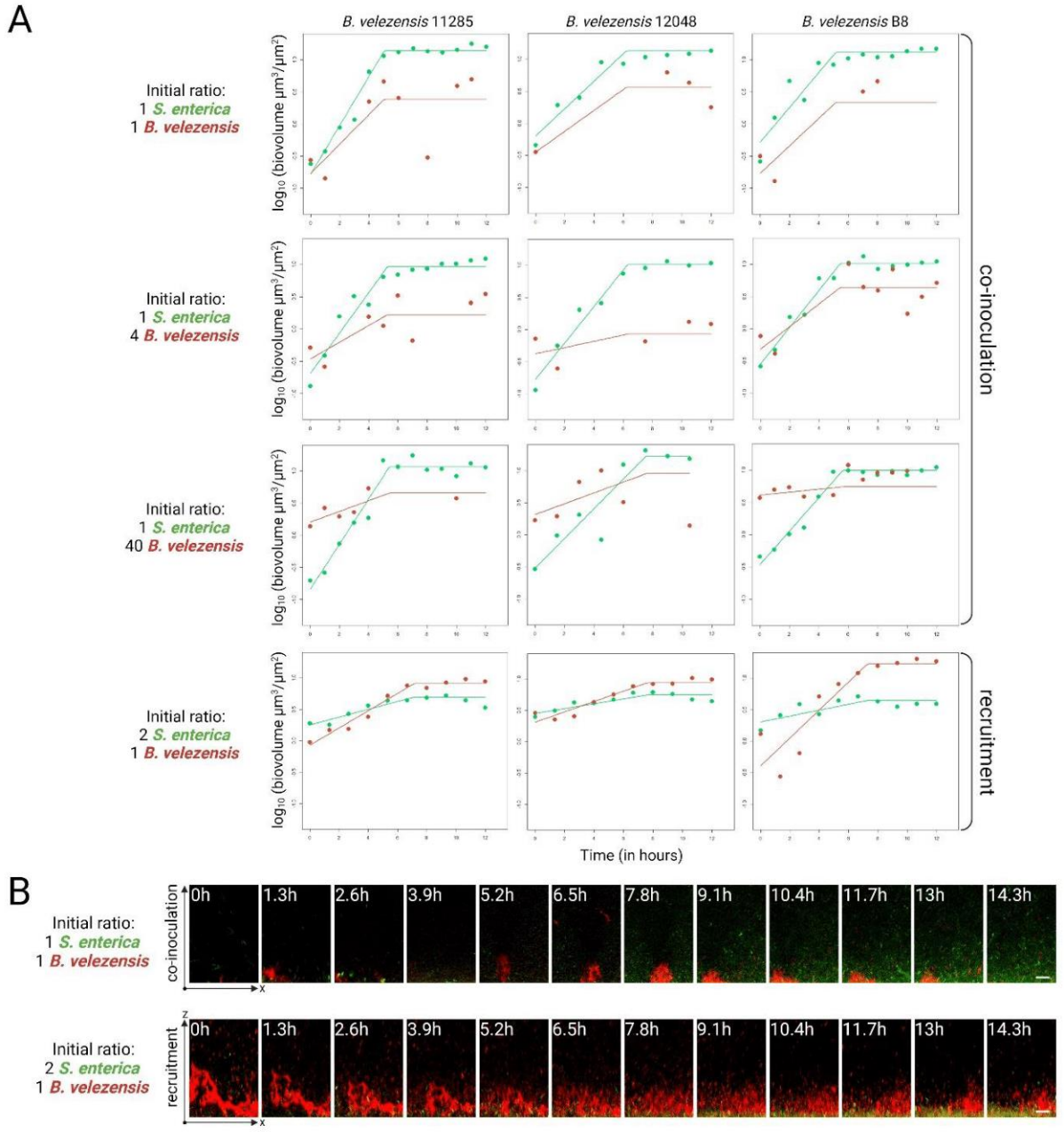

Figure 7: Interaction between *B. velezensis* and *S. enterica*. (A) Illustration (one of the replicate) of the competition between *S. enterica* and the three *B. velezensis* in co-inoculation and recruitment models. The dots correspond to measured biovolumes, the line to the primary growth models fitted to observations. (B) CLSM visualisation of 2 species biofilm growth over time with a representative example describing the Lotka-Volterra and Jameson models. The green colour corresponds to GFP labelling, while the red colour represents FM4-64. Scale bar = 50 µm.

Co-inoculations had a relatively minor effect on *S. enterica*'s growth parameters. Generation times were slightly longer compared to monoculture experiments, with mean generation times increasing from 41 minutes to 53 minutes. The maximum biovolumes reached in the stationary phase were also slightly reduced. The generation times of *B. velezensis* are doubled compared

to those observed in monoculture experiments (**fig. S14**), and their growth stops simultaneously with that of *S. enterica*, following the Jameson-type competition model.

Associations of *B. velezensis* (combination of two or three species) were not found to inhibit the growth of *S. enterica* either. The co-inoculated pathogen outperformed mixed populations of *B. velezensis* in the same manner as competition with singles species.

competition favoured the three *B. velezensis* strains when *S. enterica* competes with cells that have already established a biofilm (**Fig. 7**). The generation time for *S. enterica* increased considerably from 40 minutes to more than 300 minutes. The cessation of *S. enterica* growth at the same time as that of *B. velezensis* indicated a Jameson-type competition.

Discussion

Positive biofilms are employed on the surfaces of livestock buildings to restrict the colonisation of undesirable bacteria, consequently reducing the risk of disease and the need for chemical inputs in animal treatment [16]. The presented study enabled a rational selection and combination of strains forming positive biofilms with a robust antagonistic activity against pathogen growth. To accomplish this, a systematic in-vitro cell-imaging pipeline based on two biofilm models was used to investigate interactions within controlled microbial communities. The results presented are the outcome of a high-throughput analysis of over 23220 image z-stacks, predominantly utilising two colour channels (around 3 millions images in total per channel), which has made it possible to decipher the main families of mechanisms involved in pathogen antagonism.

In existing literature, studies on microbial interactions often start with a calibration of partners using optical density (OD) or counting in solid medium of planktonic cultures [18,36,37] and not on the quantification of the volume at the bottom of the well before the start of the experiment [38]. However, these methods fail to account for differences in adhesion rate or the propency of bacilli cells to aggregate and form filamentous structures [2,4]. To mitigate this bias, the models used were systematically initiated with a biovolume-based calibration process after the adhesion period, ensuring precise initial quantification over the quantities of both partners adhering to the substrate.

Concerning *S. enterica*, the results of the co-inoculation model with the three selected *B. velezensis* strains showed varying kinetics, with subsequent inhibition observed. In experiments conducted at the final time-point, stacks were manually captured based on the height of the biofilms, as opposed to kinetics where image capture were standardised across all samples. Since *B. velezensis* biofilms were thicker than those of *S. enterica*, a larger quantity of planktonic cells was quantified, thereby overestimating the pathogen signal compared to the control. Kinetics experiments were, therefore, more representative of reality.

Numerous commercial products in the market consist of strain assemblies which individually exhibit optimal performance in a specific identified property for various applications such as probiotics [39], biocontrol agents in plants [40], or food preservation [41]. In the case of positive biofilms, the consortia of strains used are selected primarily for their strong antagonistic activity against pathogen growth when used individually and then mixed during formulation. Consequently, the long-term behaviour of multi-strain biofilms, as well as the description of the effects of these mixtures compared to individual strains in terms of surface colonisation properties or antagonism against pathogens and the bacteria within the mixture itself, is not typically observed.

The compatibility of the *Bacillus* strains was studied in biofilms of two strains to ensure that one strain did not exclude the other. As the candidate strains were selected for their strong competitiveness against many pathogens, it is likely that the mechanisms involved also affect other *Bacillus* strains. In this study, we genetically engineered three wild-type *B. velezensis* strains that are highly antagonist to pathogens to fluoresce, an essential step for CLSM interaction studies. Competition between these three phylogenetically related *B. velezensis* GFP against other candidates has shown that only these strains together are capable of forming a stable, reproducible mixed biofilm. This is consistent with kin-compatibility theory [22,42] but a larger number of interactions with more *Bacillus* strains would be required to establish correlations between phylogenetic distance and interaction phenotype. Such experiments would demand genetically engineered wild-type strains expressing GFP, which may be difficult to obtain. Our approach, for the first time, allows for a rational selection of consortiums of strains forming positive biofilms. We demonstrate that mixtures of strains, including up to 3 *B. velezensis*, form homogeneous mixed biofilms but do not exhibit increased antagonistic activity compared to the individual strains comprising the consortium.

In most situations of our experiments, the Jameson model provides a suitable modelling framework for describing competitions. It highlights that growth ceases when one of the species has consumed an essential resource. In the case of biofilms, this essential resource is likely the available volume. The study of these two pathogens reveals other distinct competition mechanisms. For *S. enterica*, in co-inoculation experiments, regardless of the initial "power balance" with *B. velezensis*, the pathogen outpaces the growth of *B. velezensis*. These growth parameters of *S. enterica* are minimally affected by the presence of *B. velezensis*. The slight increase in *S. enterica*'s generation time during co-inoculation can be attributed to the limitation of available space caused by *B. velezensis*. The competition is completely reversed if *S. enterica* encounters an established *B. velezensis* biofilm. The significant increase in *S. enterica*'s generation time in the presence of these established biofilms indicates the presence of interferent molecules. Therefore, the outcome of the competition between *B. velezensis and S. enterica* depends more on the physiological state of the competitors within biofilms than on their initial numbers at the beginning of the competition. Moreover, certain *B. velezensis* strains have an effect only on recruitment at t= 0h, but this is not maintained at t= 24h, suggesting limited interaction with the matrix or pathogen mortality during the adhesion stage due to the presence of interfering molecules in the supernatant.

Regarding *E. cecorum*, when it is in the minority at the initial time point, its generation time is significantly prolonged in the case of co-inoculation with *B. velezensis*. This substantial slowdown can be explained by the presence of an inhibitory compound associated with the presence of *B. velezensis*. Our results are in agreement with those obtained in the study conducted by Medina Fernández et al. [43], who demonstrated the antagonistic activity of *Bacillus* supernatants on different *E. cecorum* isolates. A Jameson-type competition also occurs, with the pathogen ceasing its growth when *B. velezensis* reaches its stationary phase. The situation observed when *E. cecorum* is more abundant than *B. velezensis* is unique. *E. cecorum* initiates exponential growth, and after a few hours, inactivation of the pathogen is observed. This suggests a different mechanism of inhibition for competition ratios initially unfavorable to the pathogen (no inactivation is observed in these cases, only a slowing/cessation of growth). The parameter values of the Lotka-Volterra model indicate that competition is established between the pathogen and *B. velezensis* in the early hours. *B. velezensis*'s impact on *E. cecorum* is greater than that of *E. cecorum* on *B. velezensis*. This competition may be the trigger for a

reaction in *B. velezensis* that does not occur when *E. cecorum* is present at low levels. The similar behaviour of *E. cecorum* competing with established *B. velezensis* indicates that the outcome of the competition is a question of the relative number of competitors rather than their initial physiological state. The study and modelling of kinetics are essential tools for understanding these competitions. The simple characterization of Nfinal - N0 would not have allowed us to elucidate these competition mechanisms.

B. velezensis is well known to secrete broad-spectrum interfering molecules that impede microbial growth [44,45], and which may be previously produced by the *B. velezensis* biofilm prior to the introduction of the pathogen onto the sample. The production of specific interfering molecules by *B. velezensis* remains to be identified and characterised through biochemical analysis of the compounds using methods such as mass spectrometry or nuclear magnetic resonance [46].

Our experiments did not reveal greater antagonism against the tested pathogens in the different *B. velezensis* consortia compared to a single strain. However, it is important to emphasise that activity is not reduced when a consortium is used. Higher surface colonisation was observed with the three-strain *B. velezensis* consortium compared to single-strain and two-strain biofilms.

To generalise the antagonistic effects of *B. velezensis* strains to other pathogen species, further experiments with different isolates are needed. The chosen strains of *B. velezensis* exhibit comparable sets of antagonistic activities against pathogens and share a close phylogenetic relationship, likely indicating the presence of redundant molecular mechanisms.

All experiments were conducted in controlled laboratory conditions, which are conducive to setup, control, and high throughput. However, it is essential to study interactions under field conditions, as biofilm growth, structure, and interactions are influenced by the physicochemical conditions of the environment and the autochthonous microbiota [47,48].

The prospects of this work involve the incorporation of artificial intelligence (AI). Indeed, these tools initially allow for improved image segmentation and error reduction [49], which is particularly common when segmenting images from kinetics where fluorescence intensity varies over time. In addition, AI could be used to predict the antagonism of beneficial strains using their genomes and biofilm morphology descriptors [50], saving considerable time and

improving the selection of beneficial candidate strains. This research was carried out in the context of positive biofilms in livestock building environments. It is conceivable to extend the pipeline used to other farming systems, such as aquaculture or other application domains as biocontrol, bioremediation or probiotics.

Data availability

The original contributions presented in the study are included in the article. Further inquiries can be directed to the corresponding author.

Funding

This research was funded by INRAE, LALLEMAND SAS and "Association Nationale de la Recherche et de la Technologie" (contract 2020/0548).

Ethics declarations

The authors declare that the research was conducted in the absence of any commercial or financial relationships that could be construed as a potential conflict of interest.

Acknowledgments

This study was funded by INRAE and Lallemand SAS. We thank the MIMA2 platform (Microscopie et Imagerie des Microorganismes, Animaux et Aliments, https://doi.org/10.15454/1.5572348210007727E12) for microscopic observations. Thanks to Julien Deschamps for the Leica SP8-HCS training, Pierre Adenot for the Zeiss LSM 700 observations, Martine Letheule and Christine Longin for TEM observations. Thanks to Harold Guéneau for the Python programming that enabled us to sort the data generated by BiofilmQ. Some figures were created with BioRender (https://www.biorender.com/).

Contributions

VG, LG, MC and RB: conceptualization and methodology. MC and RB: validation and supervision. VG, LG and GJ formal analysis and data curation. VG, JP-G, MC, and RB: investigation. PS et M-FN-G contribute to develop the transformation protocol of the strains.

MC and RB: resources, project administration, and funding acquisition. VG, LG: writing the original draft preparation. MC and RB: reviewing, and editing. All authors have read and agreed to the published version of the manuscript.

References

[1] Flemming H-C, Wuertz S. Bacteria and archaea on Earth and their abundance in biofilms. Nat Rev Microbiol 2019;17:247–60. https://doi.org/10.1038/s41579-019-0158-9.

[2] Sauer K, Stoodley P, Goeres DM, Hall-Stoodley L, Burmølle M, Stewart PS, et al. The biofilm life cycle: expanding the conceptual model of biofilm formation. Nat Rev Microbiol 2022;20:608–20. https://doi.org/10.1038/s41579-022-00767-0.

[3] Flemming H-C, Wingender J, Szewzyk U, Steinberg P, Rice SA, Kjelleberg S. Biofilms: an emergent form of bacterial life. Nat Rev Microbiol 2016;14:563–75. https://doi.org/10.1038/nrmicro.2016.94.

[4] Arnaouteli S, Bamford NC, Stanley-Wall NR, Kovács ÁT. Bacillus subtilis biofilm formation and social interactions. Nat Rev Microbiol 2021;19:600–14. https://doi.org/10.1038/s41579-021-00540-9.

[5] Flemming H-C, van Hullebusch ED, Neu TR, Nielsen PH, Seviour T, Stoodley P, et al. The biofilm matrix: multitasking in a shared space. Nat Rev Microbiol 2023;21:70–86. https://doi.org/10.1038/s41579-022-00791-0.

[6] Dergham Y, Coq DL, Nicolas P, Deschamps J, Huillet E, Sanchez-Vizuete P, et al. Multi-scale transcriptome unveils spatial organisation and temporal dynamics of Bacillus subtilis biofilms 2023:2023.01.06.522868. https://doi.org/10.1101/2023.01.06.522868.

[7] Bridier A, Briandet R, Thomas V, Dubois-Brissonnet F. Resistance of bacterial biofilms to disinfectants: a review. Biofouling 2011;27:1017–32. https://doi.org/10.1080/08927014.2011.626899.

[8] Ciofu O, Moser C, Jensen PØ, Høiby N. Tolerance and resistance of microbial biofilms. Nat Rev Microbiol 2022;20:621–35. https://doi.org/10.1038/s41579-022-00682-4.

[9] Heumann A, Assifaoui A, Da Silva Barreira D, Thomas C, Briandet R, Laurent J, et al. Intestinal release of biofilm-like microcolonies encased in calcium-pectinate beads increases probiotic properties of Lacticaseibacillus paracasei. NPJ Biofilms Microbiomes 2020;6:44. https://doi.org/10.1038/s41522-020-00159-3.

[10] Ghoul M, Mitri S. The Ecology and Evolution of Microbial Competition. Trends Microbiol 2016;24:833–45. https://doi.org/10.1016/j.tim.2016.06.011.

[11] Palmer JD, Foster KR. Bacterial species rarely work together. Science 2022;376:581–2. https://doi.org/10.1126/science.abn5093.

[12] Guéneau V, Rodiles A, Frayssinet B, Piard J-C, Castex M, Plateau-Gonthier J, et al. Positive biofilms to control surface-associated microbial communities in a broiler chicken production system - a field study. Front Microbiol 2022;13:981747. https://doi.org/10.3389/fmicb.2022.981747.

[13] Borges F, Briandet R, Callon C, Champomier-Vergès M-C, Christieans S, Chuzeville S, et al. Contribution of omics to biopreservation: Toward food microbiome engineering. Front Microbiol 2022;13:951182. https://doi.org/10.3389/fmicb.2022.951182.

[14] Woo SL, Pepe O. Microbial Consortia: Promising Probiotics as Plant Biostimulants for Sustainable Agriculture. Front Plant Sci 2018;9:1801. https://doi.org/10.3389/fpls.2018.01801.
[15] Xu Z, Sun X, Xie J, Zheng D, Xia R, Wang W, et al. Keystone species determine the productivity of synthetic microbial biofilm communities 2023. https://doi.org/10.21203/rs.3.rs-2527818/v1.
[16] Guéneau V, Plateau-Gonthier J, Arnaud L, Piard J-C, Castex M, Briandet R. Positive biofilms to guide surface microbial ecology in livestock buildings. Biofilm 2022;4:100075. https://doi.org/10.1016/j.bioflm.2022.100075.
[17] Guillier L, Stahl V, Hezard B, Notz E, Briandet R. Modelling the competitive growth between Listeria monocytogenes and biofilm microflora of smear cheese wooden shelves. Int J Food Microbiol 2008;128:51–7. https://doi.org/10.1016/j.ijfoodmicro.2008.06.028.
[18] Podnar E, Erega A, Danevčič T, Kovačec E, Lories B, Steenackers H, et al. Nutrient Availability and Biofilm Polysaccharide Shape the Bacillaene-Dependent Antagonism of Bacillus subtilis against Salmonella Typhimurium. Microbiol Spectr 2022;10:e0183622. https://doi.org/10.1128/spectrum.01836-22.
[19] Guéneau V, Charron R, Costache V, Bridier A, Briandet R. Chapter 9 - Spatial analysis of multispecies bacterial biofilms. In: Gurtler V, Patrauchan M, editors. Methods in Microbiology, vol. 53, Academic Press; 2023, p. 275–307. https://doi.org/10.1016/bs.mim.2023.03.002.
[20] Habimana O, Guillier L, Kulakauskas S, Briandet R. Spatial competition with Lactococcus lactis in mixed-species continuous-flow biofilms inhibits Listeria monocytogenes growth. Biofouling 2011;27:1065–72. https://doi.org/10.1080/08927014.2011.626124.
[21] Dedrick S, Warrier V, Lemon KP, Momeni B. When does a Lotka-Volterra model represent microbial interactions? Insights from in vitro nasal bacterial communities. mSystems 2023;8:e0075722. https://doi.org/10.1128/msystems.00757-22.
[22] Stefanic P, Kraigher B, Lyons NA, Kolter R, Mandic-Mulec I. Kin discrimination between sympatric Bacillus subtilis isolates. Proc Natl Acad Sci U S A 2015;112:14042–7. https://doi.org/10.1073/pnas.1512671112.
[23] Liu Y, Huang R, Chen Y, Miao Y, Štefanič P, Mandic-Mulec I, et al. Involvement of Flagellin in Kin Recognition between Bacillus velezensis Strains. mSystems 2022;7:e0077822. https://doi.org/10.1128/msystems.00778-22.
[24] Malone CL, Boles BR, Lauderdale KJ, Thoendel M, Kavanaugh JS, Horswill AR. Fluorescent reporters for Staphylococcus aureus. J Microbiol Methods 2009;77:251–60. https://doi.org/10.1016/j.mimet.2009.02.011.
[25] Olson RD, Assaf R, Brettin T, Conrad N, Cucinell C, Davis JJ, et al. Introducing the Bacterial and Viral Bioinformatics Resource Center (BV-BRC): a resource combining PATRIC, IRD and ViPR. Nucleic Acids Res 2023;51:D678–89. https://doi.org/10.1093/nar/gkac1003.
[26] Lauderdale KJ, Malone CL, Boles BR, Morcuende J, Horswill AR. Biofilm dispersal of community-associated methicillin-resistant Staphylococcus aureus on orthopedic implant material. J Orthop Res 2010;28:55–61. https://doi.org/10.1002/jor.20943.
[27] Dunny GM, Lee LN, LeBlanc DJ. Improved electroporation and cloning vector system for gram-positive bacteria. Appl Environ Microbiol 1991;57:1194–201. https://doi.org/10.1128/aem.57.4.1194-1201.1991.
[28] Serrano E, Carrasco B, Gilmore JL, Takeyasu K, Alonso JC. RecA Regulation by RecU and DprA During Bacillus subtilis Natural Plasmid Transformation. Front Microbiol 2018;9:1514. https://doi.org/10.3389/fmicb.2018.01514.

[29] Dergham Y, Sanchez-Vizuete P, Le Coq D, Deschamps J, Bridier A, Hamze K, et al. Comparison of the Genetic Features Involved in Bacillus subtilis Biofilm Formation Using Multi-Culturing Approaches. Microorganisms 2021;9. https://doi.org/10.3390/microorganisms9030633.
[30] Pogliano J, Osborne N, Sharp MD, Abanes-De Mello A, Perez A, Sun YL, et al. A vital stain for studying membrane dynamics in bacteria: a novel mechanism controlling septation during Bacillus subtilis sporulation. Mol Microbiol 1999;31:1149–59. https://doi.org/10.1046/j.1365-2958.1999.01255.x.
[31] Hartmann R, Jeckel H, Jelli E, Singh PK, Vaidya S, Bayer M, et al. Quantitative image analysis of microbial communities with BiofilmQ. Nat Microbiol 2021;6:151–6. https://doi.org/10.1038/s41564-020-00817-4.
[32] Cornu M, Billoir E, Bergis H, Beaufort A, Zuliani V. Modeling microbial competition in food: Application to the behavior of Listeria monocytogenes and lactic acid flora in pork meat products. Food Microbiology 2011;28:639–47. https://doi.org/10.1016/j.fm.2010.08.007.
[33] Ross T, Dalgaard P, Tienungoon S. Predictive modelling of the growth and survival of Listeria in fishery products. International Journal of Food Microbiology 2000;62:231–45. https://doi.org/10.1016/S0168-1605(00)00340-8.
[34] Possas A, Valero A, Pérez-Rodríguez F. New software solutions for microbiological food safety assessment and management. Current Opinion in Food Science 2022;44:100814. https://doi.org/10.1016/j.cofs.2022.100814.
[35] Mühlbauer LK, Schulze M, Harpole WS, Clark AT. gauseR: Simple methods for fitting Lotka-Volterra models describing Gause's "Struggle for Existence." Ecology and Evolution 2020;10:13275–83. https://doi.org/10.1002/ece3.6926.
[36] Henriksen NNSE, Hansen MF, Kiesewalter HT, Russel J, Nesme J, Foster KR, et al. Biofilm cultivation facilitates coexistence and adaptive evolution in an industrial bacterial community. NPJ Biofilms Microbiomes 2022;8:59. https://doi.org/10.1038/s41522-022-00323-x.
[37] Bolješić M, Kraigher B, Dogsa I, Jerič Kokelj B, Mandic-Mulec I. Kin Discrimination Modifies Strain Distribution, Spatial Segregation, and Incorporation of Extracellular Matrix Polysaccharide Mutants of Bacillus subtilis Strains into Mixed Floating Biofilms. Appl Environ Microbiol 2022;88:e0087122. https://doi.org/10.1128/aem.00871-22.
[38] Tai J-SB, Mukherjee S, Nero T, Olson R, Tithof J, Nadell CD, et al. Social evolution of shared biofilm matrix components. Proc Natl Acad Sci U S A 2022;119:e2123469119. https://doi.org/10.1073/pnas.2123469119.
[39] Cheng Y, Chen Y, Li X, Yang W, Wen C, Kang Y, et al. Effects of synbiotic supplementation on growth performance, carcass characteristics, meat quality and muscular antioxidant capacity and mineral contents in broilers. J Sci Food Agric 2017;97:3699–705. https://doi.org/10.1002/jsfa.8230.
[40] Wong CKF, Saidi NB, Vadamalai G, Teh CY, Zulperi D. Effect of bioformulations on the biocontrol efficacy, microbial viability and storage stability of a consortium of biocontrol agents against Fusarium wilt of banana. J Appl Microbiol 2019;127:544–55. https://doi.org/10.1111/jam.14310.
[41] González-González F, Delgado S, Ruiz L, Margolles A, Ruas-Madiedo P. Functional bacterial cultures for dairy applications: Towards improving safety, quality, nutritional and health benefit aspects. J Appl Microbiol 2022;133:212–29. https://doi.org/10.1111/jam.15510.

[42] Kraigher B, Butolen M, Stefanic P, Mandic Mulec I. Kin discrimination drives territorial exclusion during Bacillus subtilis swarming and restrains exploitation of surfactin. ISME J 2022;16:833–41. https://doi.org/10.1038/s41396-021-01124-4.
[43] Medina Fernández S, Cretenet M, Bernardeau M. In vitro inhibition of avian pathogenic Enterococcus cecorum isolates by probiotic Bacillus strains. Poult Sci 2019;98:2338–46. https://doi.org/10.3382/ps/pey593.
[44] Byun H, Brockett MR, Pu Q, Hrycko AJ, Beld J, Zhu J. An Intestinal Bacillus velezensis Isolate Displays Broad-Spectrum Antibacterial Activity and Prevents Infection of Both Gram-Positive and Gram-Negative Pathogens In Vivo. J Bacteriol 2023;205:e0013323. https://doi.org/10.1128/jb.00133-23.
[45] Wilson J, Cui J, Nakao T, Kwok H, Zhang Y, Kayrouz CM, et al. Discovery of Antimicrobial Phosphonopeptide Natural Products from Bacillus velezensis by Genome Mining. Appl Environ Microbiol 2023;89:e0033823. https://doi.org/10.1128/aem.00338-23.
[46] Mielko KA, Jabłoński SJ, Milczewska J, Sands D, Łukaszewicz M, Młynarz P. Metabolomic studies of Pseudomonas aeruginosa. World J Microbiol Biotechnol 2019;35:178. https://doi.org/10.1007/s11274-019-2739-1.
[47] Ly S, Bajoul Kakahi F, Mith H, Phat C, Fifani B, Kenne T, et al. Engineering Synthetic Microbial Communities through a Selective Biofilm Cultivation Device for the Production of Fermented Beverages. Microorganisms 2019;7:206. https://doi.org/10.3390/microorganisms7070206.
[48] Sengupta D, Datta S, Biswas D. Towards a better production of bacterial exopolysaccharides by controlling genetic as well as physico-chemical parameters. Appl Microbiol Biotechnol 2018;102:1587–98. https://doi.org/10.1007/s00253-018-8745-7.
[49] Jelli E, Ohmura T, Netter N, Abt M, Jiménez-Siebert E, Neuhaus K, et al. Single-cell segmentation in bacterial biofilms with an optimized deep learning method enables tracking of cell lineages and measurements of growth rates. Mol Microbiol 2023;119:659–76. https://doi.org/10.1111/mmi.15064.
[50] Guo T, Li X. Machine learning for predicting phenotype from genotype and environment. Curr Opin Biotechnol 2023;79:102853. https://doi.org/10.1016/j.copbio.2022.102853.

Supplementary

E. coli and *S. enterica*:

Briefly, competent cells were prepared by adding 1 ml of overnight culture of the wild type strain in 80 ml of LB (Difco™) and placed at 37°C until reaching OD600=0.3-0.4. The culture was placed on ice for 15 min, split in two 50 mL tubes and then centrifuged at 6000 g, 10 min. The supernatants were removed and the pellets were homogenised in 30 mL of 0.1 M CaCl2. The cultures were incubated 30 min at 30 °C before centrifugation at 6000 g, 10 min. Supernatants were removed and the pellets were suspended in 3 mL of 0.1M Cacl2 at 15 % glycerol. 50 µL tubes are prepared and stored at -80°C.

For transformation, a tube of competent cells was put on ice to defrost gently. 1 µg of pCM11 plasmid was incorporated in the tube, placed on ice for 15 min. The tube was incubated at 42 °C for 90 s before being put on ice for a few seconds. 250 µL of SOC medium was incorporated, the tube was put 1h at 37 °C with agitation. The culture was plate on LB supplemented with ampicillin at 100 µg/mL and incubated 1 day at 37 °C. The clones that have grown and thus integrated the plasmid were stored.

E. cecorum:

To obtain electrocompetent cells, SGM17 medium (37,25 g M17 Broth from Difco™; 5 g/L glucose; 0.16 M saccharose; 2 % glycine) was inoculated 1:100 (v;v) with an overnight culture of wild type *E. cecorum* and placed at 37°C until to reach a OD600=0.5. The bacteria were put on ice for 10 min. All the following steps were performed on ice. Bacteria were centrifuged at 3800 g, 10 min, 4°C. The supernatant was removed and the pellet was suspended in the same volume carefully with a Sac-Gly solution at 4°C (saccharose 0.5 M, glycerol 10%, pH 7,0). This washing step was performed 5 times by dividing each time per 2 the volume of Sac-Gly to suspend the pellet. A final wash is performed with a pellet resuspended in Sac-Gly with 1/150e of the initial culture volume. Aliquots of 40 µL were prepared, frozen in liquid nitrogen and stored at -80°C.

40 µL of competent cells were defrosted on ice and 1 µg of pCM11 plasmid was added. The whole was placed in an electroporation cuvette and the electric pulse was applied (25 µF, 200 Ohms, 2.4 kV). Immediately, 1 mL of SGM17 supplemented with 0.5 M MgCl2 and 10 mM CaCl2

before the tube was put on ice for 5 min. The cuvette is placed at 30°C without agitation for 3h. The culture was plate on M17 supplemented with 0.5 g/L of glucose and erythromycin at 1 µg/mL and incubated 2 days at 30 °C. The clones that have grown and thus integrated the plasmid were stored.

B. velezensis:

Before starting, 5 µg of plasmid pCM11 was digested at a single site with the ECORI restriction enzyme (NEB), then the enzyme was inactivated. A ligation protocol using the Quick ligation kit (NEB) was performed with the 5 µg of plasmid to obtain concatemers of the plasmid. From a TSA plate, one colony was taken and put in 1 mL MC medium (20 g/L glucose; 10 g/L potassium glutamate; 1 M pH7 potassium phosphate buffer; 0.1 M sodium trisodium citrate; 10 g/L ferric ammonium citrate; 5 % casein hydrolysate; 1% tryptophan; 1M MgSO4; completed with H2O). The culture was incubated 4 h at 37°C, 180 rpm. 500 µL was collected and added into a new tube containing the 5 µg of pCM11 concatemers. The two tubes were incubated 1h30 at 37°C, 180 rpm. 200 µL of each culture was plated on TSA supplemented with erythromycin 0.5 µg/mL and lincomycin 25 µg/mL. The plates were put at 30°C for 2 days. The clones that have grown and thus integrated the plasmid were stored.

Supplementary data 1: Transformation protocols to obtain fluorescent strains.

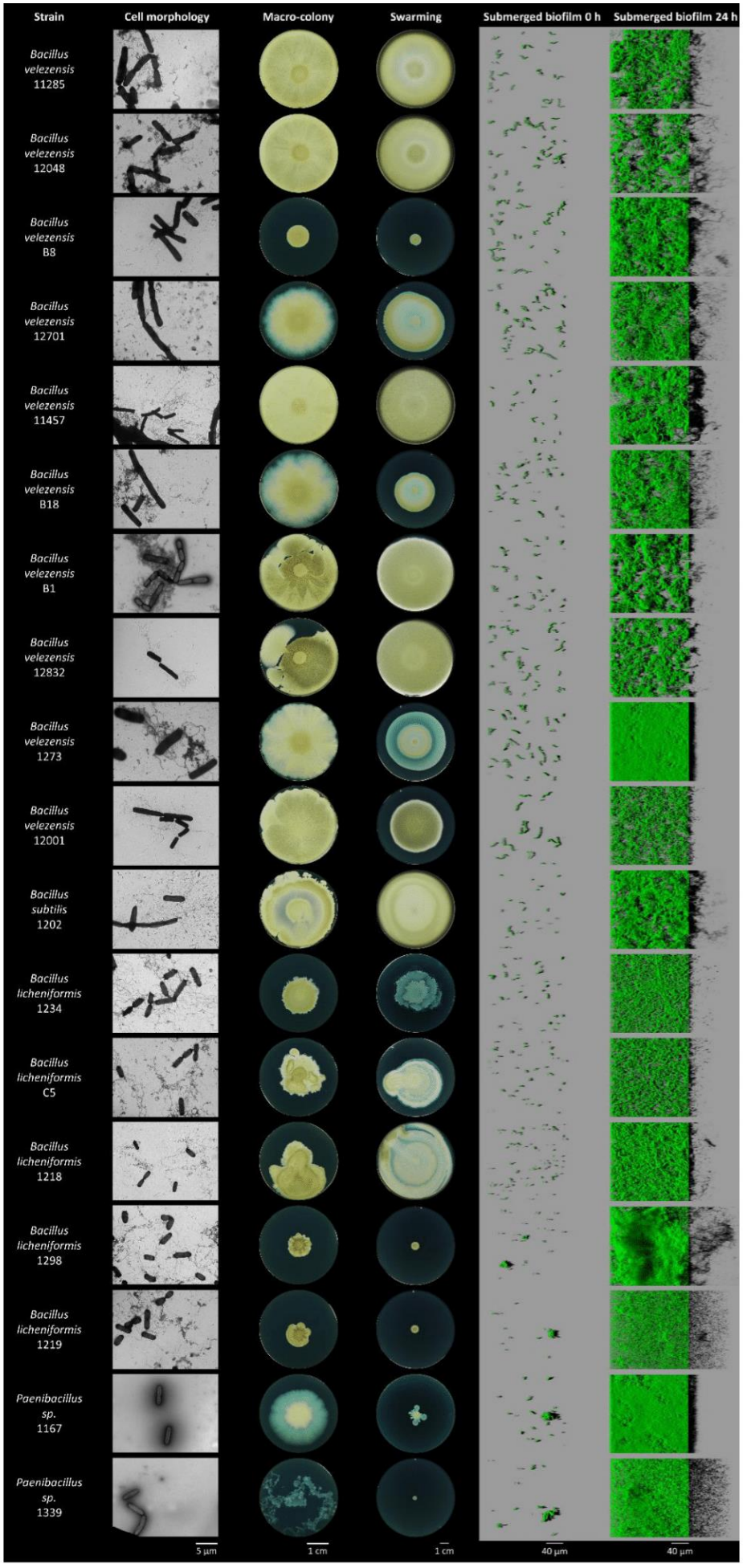
Strain
Cell morphology
Macro-colony
Swarming
Submerged biofilm 0 h
Submerged biofilm 24 h
Bacillus velezensis 11285
Bacillus velezensis 12048
Bacillus velezensis B8
Bacillus velezensis 12701
Bacillus velezensis 11457
Bacillus velezensis B18
Bacillus velezensis B1
Bacillus velezensis 12832
Bacillus velezensis 1273
Bacillus velezensis 12001
Bacillus subtilis 1202
Bacillus licheniformis 1234
Bacillus licheniformis C5
Bacillus licheniformis 1218
Bacillus licheniformis 1298
Bacillus licheniformis 1219
Paenibacillus sp. 1167
Paenibacillus sp. 1339
5 µm
1 cm
1 cm
40 µm
40 µm

Supplementary data 2: Phenotypic characterisation of the *Bacillus* strains.

To initiate the macro-colony model experiments, 5 ml cultures were prepared in trypticase soy broth (TSB; Biomérieux, France) from glycerol stock stored at -80°C. The cultures were left at 30°C overnight without any agitation. After homogenising the cultures by rapid vortexing for 5 seconds, 3 µL of culture were collected and deposited in one well of a six-well plate containing 4 ml of TSA 1.5% agar. The samples were then dried under a hood for 10 minutes and incubated at 30°C for 4 days. The swarming experiment followed a similar protocol, with 20 mL of TSA 0.7% agar being used in a Petri dish and incubated for one night at 30°C. For transmission electron microscopy (TEM), 1 ml of overnight culture of *Bacillus* strains was collected and centrifuged at 1000 g for 10 minutes. The supernatant was then changed with 500 µL of salt water (9g/L NaCl), and the culture was placed onto 200-mesh copper grids and counterstained with lead citrate. The grids were examined using a Hitachi HT7700 electron microscope (Hitachi, Japan) operated at 80 kV (Elexience, France). Images were acquired with a charge-coupled device camera (Advanced Microscopy Techniques Corp., Japan). Mono-species submerged biofilms were observed using the CLSM. To initiate the experiment, the overnight cultures were diluted at 1/100e in TSB. Next, 200 µL of this diluted solution was added to each well of a 96-well plate and allowed to adhere for 1 hour and 30 minutes. After the adhesion phase, the supernatant was carefully removed and replaced with fresh TSB. The plates were then incubated for 24 h at 30°C without agitation, and 432 stacks of images were observed. Representative images are shown.

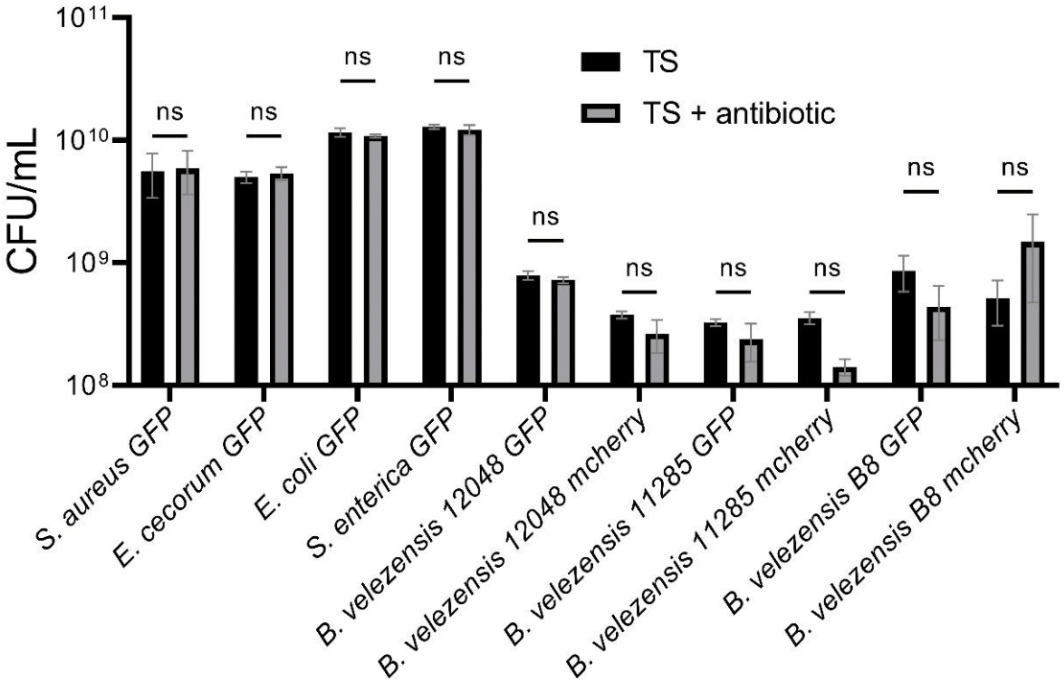

Supplementary data 3: Stability of the plasmid in biofilm experiments.

Biofilms grew without antibiotics for 24 h from overnight cultures of bacteria grown with antibiotics. Biofilms were detached and homogenised to verify plasmid stability by enumeration on TSA or TSA + antibiotics (ery 5 µg/mL for *S. aureus* and *E. cecorum* and amp 100 µg/mL for *E. coli* and *S. enterica*). 3 biological replicates were performed. Error bars correspond to standard deviation.

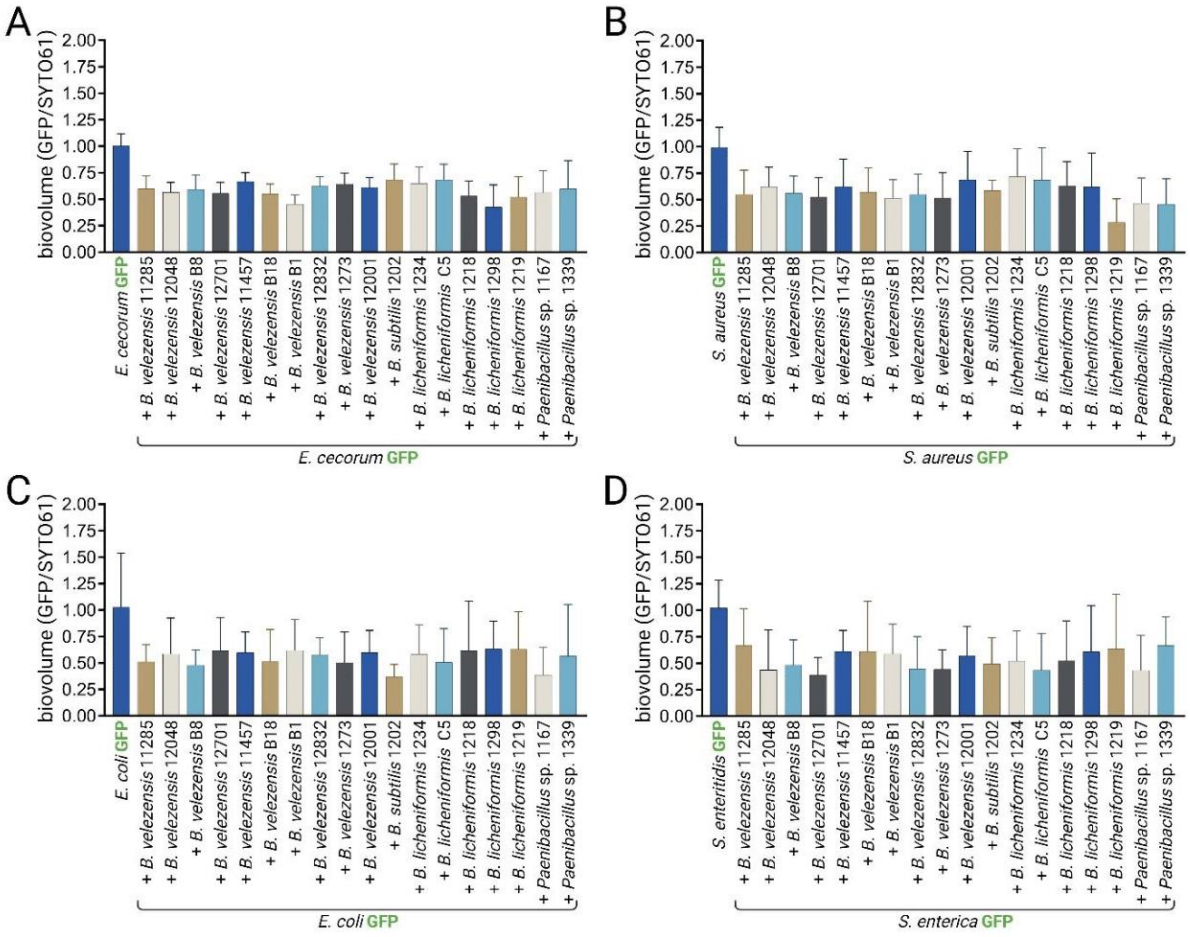

Supplementary data 4: Adhesion ratio of *Bacillus* strains and pathogens in the co-inoculation growth model.

Volumes of non-labeled *Bacillus* strains overnight cultures were calibrated to achieve the same biovolume of pathogens and *Bacillus* strains adhered to the bottom of the wells. To accomplish this, the pathogen was genetically marked with GFP, and the entire population was chemically labelled with SYTO61 after 1 h 30 min of adhesion. The GFP biovolume to SYTO61 biovolume ratio of 0.5 indicates an equal quantity of pathogens and *Bacillus* strai. The results are shown for (A) GFP-labelled *E. cecorum*, (B) GFP-labelled *S. aureus*, (C) GFP-labelled *E. coli*, and (D) GFP-labelled *S. enterica*. 912 stacks of images were performed with 3 biological replicates. Error bars correspond to standard deviation.

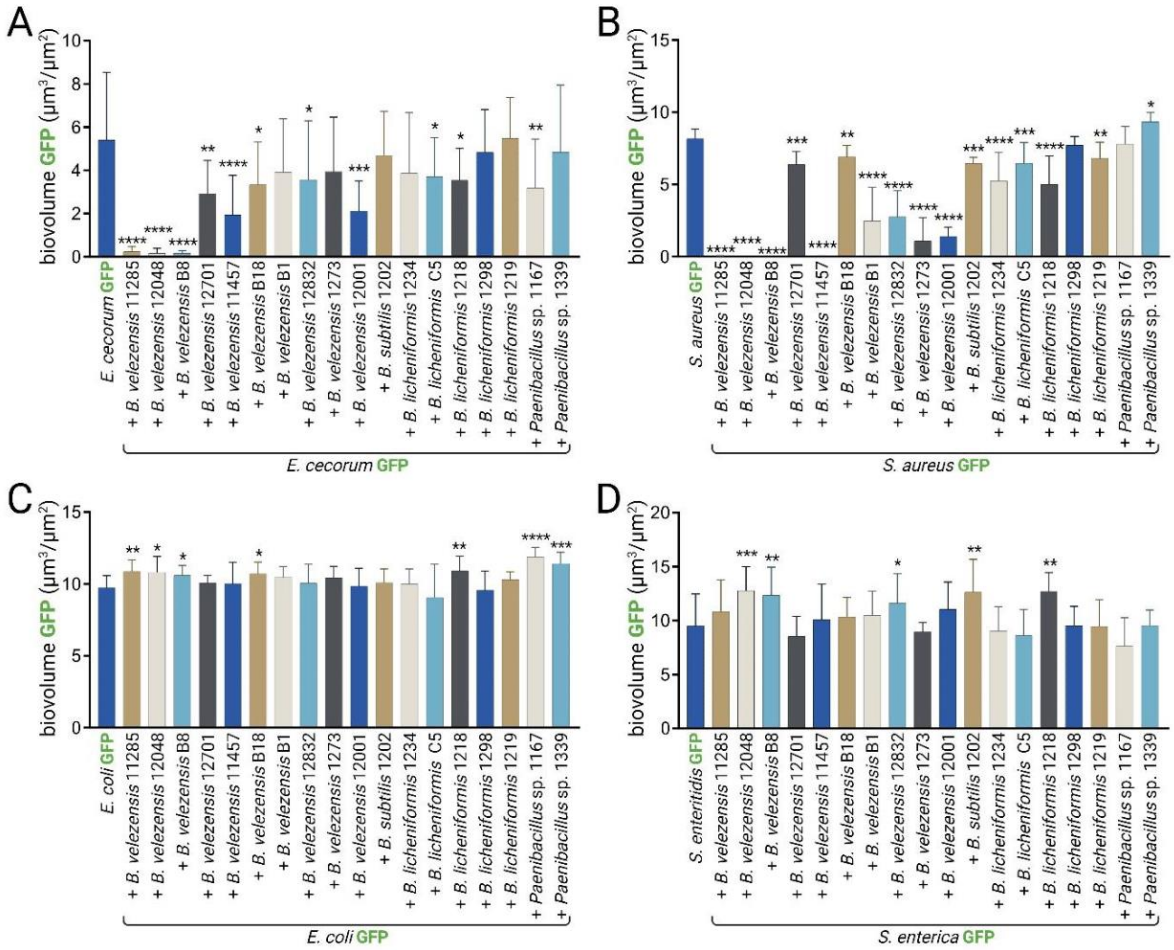

Supplementary data 5: GFP-labeled pathogen biovolume in the co-inoculation growth model co-cultured with *Bacillus* strains.

The results are shown for (A) GFP-labelled *E. cecorum*, (B) GFP-labelled *S. aureus*, (C) GFP-labelled *E. coli*, and (D) GFP-labelled *S. enterica*. 912 stacks of images were performed with 3 biological replicates. Error bars correspond to standard deviation.

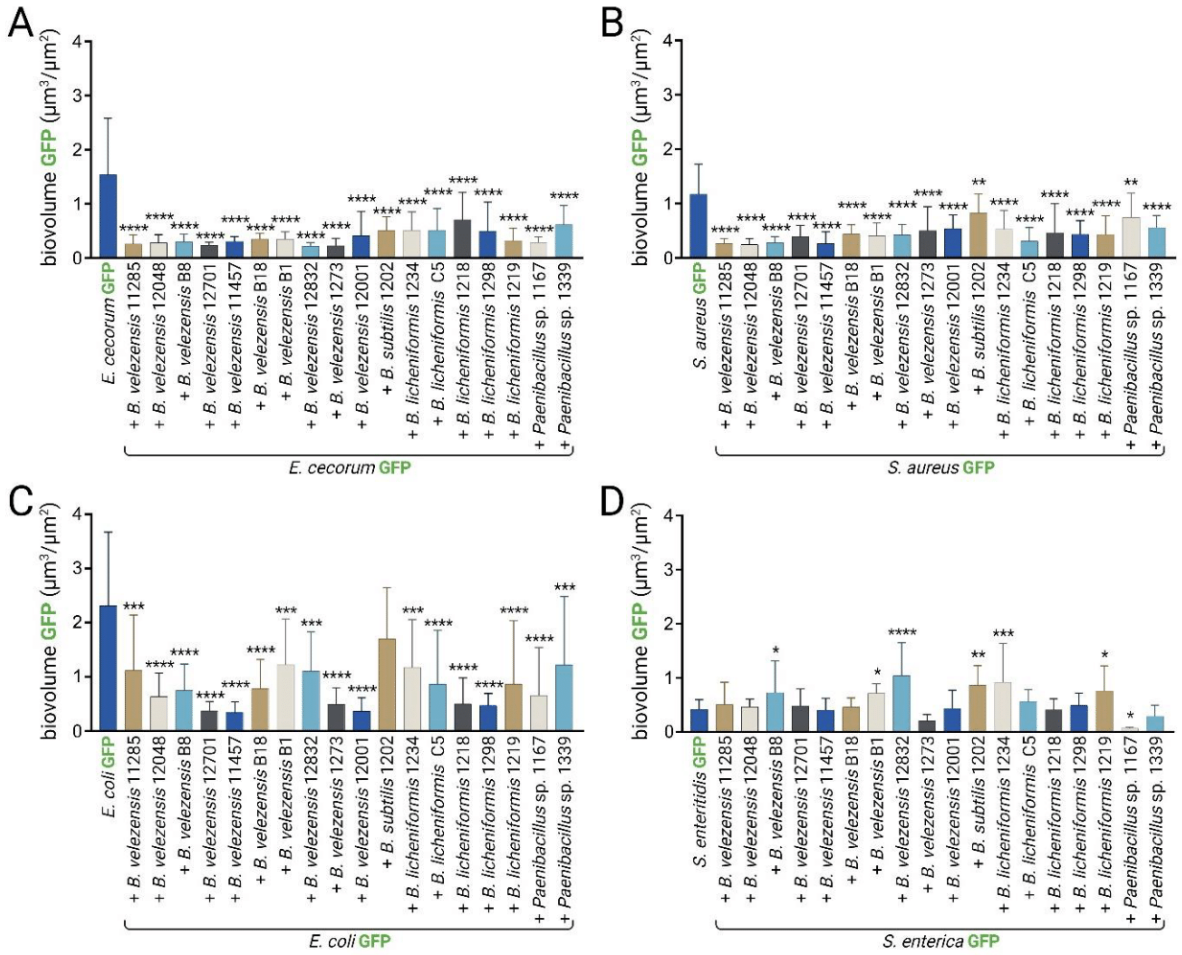

Supplementary data 6: GFP-labelled pathogen biovolume in the recruitment t=0 h growth model co-cultured with *Bacillus* strains.

The results are shown for (A) GFP-labelled *E. cecorum*, (B) GFP-labelled *S. aureus*, (C) GFP-labelled *E. coli*, and (D) GFP-labelled *S. enterica*. 912 stacks of images were performed with 3 biological replicates. Error bars correspond to standard deviation.

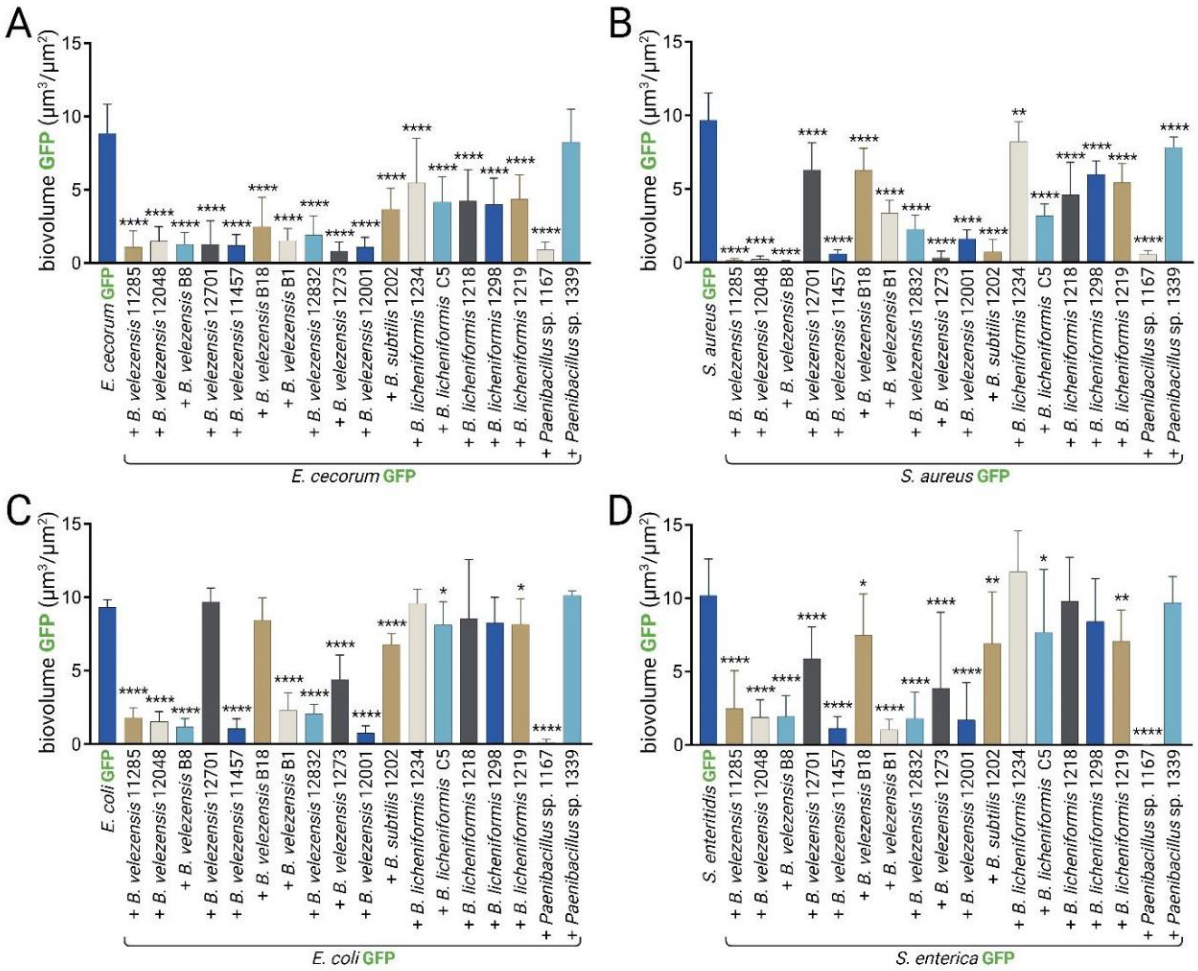

Supplementary data 7: GFP-labeled pathogen biovolume in the recruitment t=24 h growth model co-cultured with *Bacillus* strains.

The results are shown for (A) GFP-labelled *E. cecorum*, (B) GFP-labelled *S. aureus*, (C) GFP-labelled *E. coli*, and (D) GFP-labelled *S. enterica*. 912 stacks of images were performed with 3 biological replicates. Error bars correspond to standard deviation.

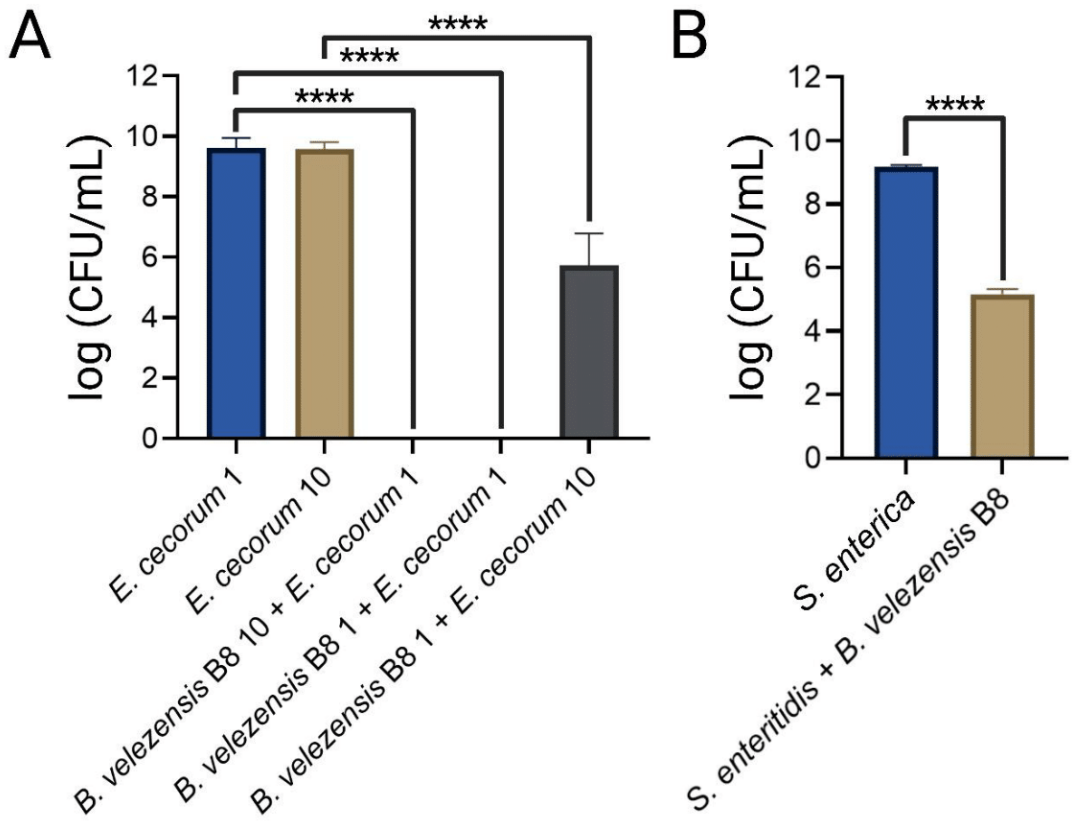

Supplementary data 8: Enumeration of pathogens after 24 hours of incubation in the presence or absence of *B. velezensis* B8.

(A) Results with *E. cecorum* using different ratios of the two partners at the start of the co-inoculation experiment. (A) Results with *S. enterica* in the recruitment model. Experiments were performed with 3 biological replicates. Error bars correspond to standard deviation.

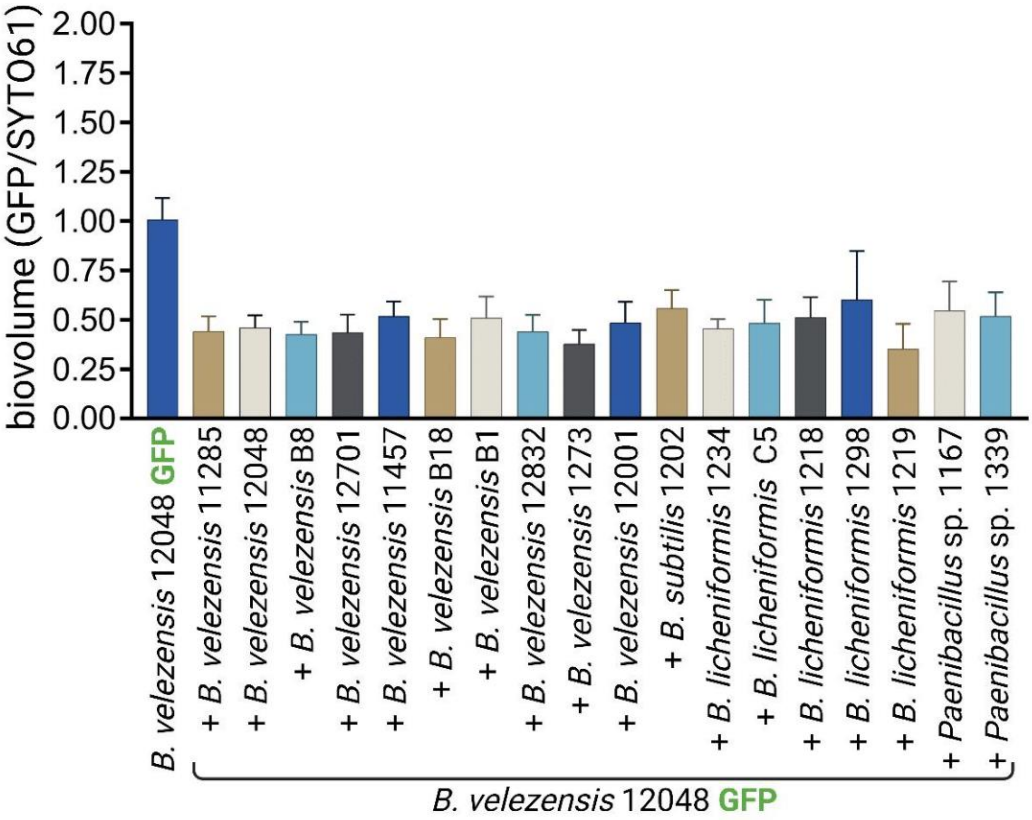

Supplementary data 9: Adhesion ratio of the 18 *Bacillus* strains and *B. velezensis* 12048 GFP in the co-inoculation growth model.

Volumes of non-labeled *Bacillus* strains overnight cultures were calibrated to achieve the same biovolume of pathogens and *Bacillus* strains adhered to the bottom of the wells. To accomplish this, *B. velezensis* 12048 was genetically marked with GFP, and the entire population was chemically labelled with SYTO61 after 1 h 30 min of adhesion. The GFP biovolume to SYTO61 biovolume ratio of 0.5 indicates an equal quantity of *B. velezensis* 12048 GFP and *Bacillus* strains. 228 stacks of images were performed with 3 biological replicates. Error bars correspond to standard deviation.

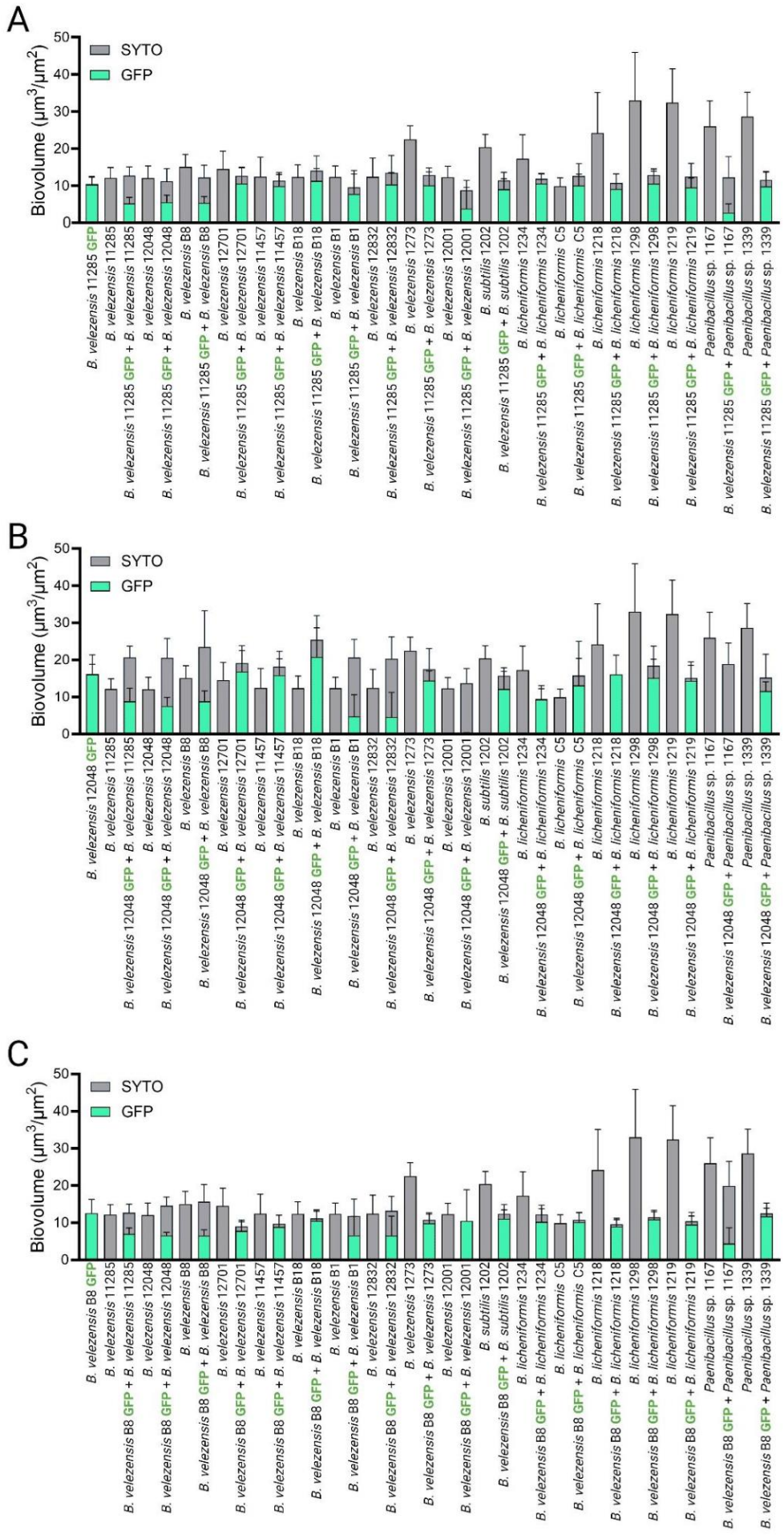
A
B
C
SYTO
GFP
Biovolume (µm³/µm²)
0
10
20
30
40
50
B. velezensis 11285 GFP
B. velezensis 11285
B. velezensis 11285 GFP + B. velezensis 11285
B. velezensis 12048
B. velezensis 12048 GFP + B. velezensis 12048
B. velezensis B8
B. velezensis 11285 GFP + B. velezensis B8
B. velezensis 12701
B. velezensis 12701 GFP + B. velezensis 12701
B. velezensis 11457
B. velezensis 11457 GFP + B. velezensis 11457
B. velezensis B18
B. velezensis 11285 GFP + B. velezensis B18
B. velezensis B1
B. velezensis 11285 GFP + B. velezensis B1
B. velezensis 12832
B. velezensis 11285 GFP + B. velezensis 12832
B. velezensis 1273
B. velezensis 11285 GFP + B. velezensis 1273
B. velezensis 12001
B. velezensis 11285 GFP + B. velezensis 12001
B. subtilis 1202
B. velezensis 11285 GFP + B. subtilis 1202
B. licheniformis 1234
B. velezensis 11285 GFP + B. licheniformis 1234
B. licheniformis C5
B. velezensis 11285 GFP + B. licheniformis C5
B. licheniformis 1218
B. velezensis 11285 GFP + B. licheniformis 1218
B. licheniformis 1298
B. velezensis 11285 GFP + B. licheniformis 1298
B. licheniformis 1219
B. velezensis 11285 GFP + B. licheniformis 1219
Paenibacillus sp. 1167
B. velezensis 11285 GFP + Paenibacillus sp. 1167
Paenibacillus sp. 1339
B. velezensis 11285 GFP + Paenibacillus sp. 1339
B. velezensis 12048 GFP
B. velezensis B8 GFP

Supplementary data 10: GFP-labelled *B. velezensis* biovolume in the co-inoculation growth model co-cultured with *Bacillus* strains.

The results are shown for (A) GFP-labelled *B. velezensis* 11285, (B) GFP-labelled *B. velezensis* 12048, and (C) GFP-labelled *B. velezensis* B8. 684 stacks of images were performed with 3 biological replicates. Error bars correspond to standard deviation.

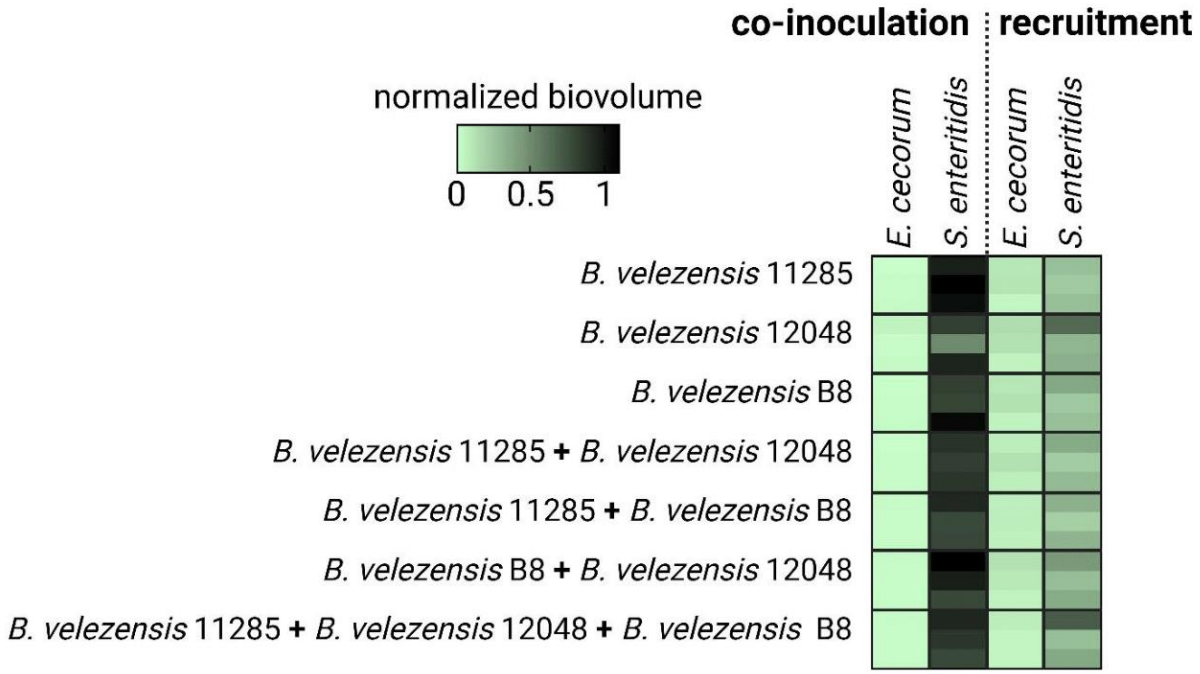

Supplementary data 11: Biovolume of the pathogens in the presence of *B. velezensis* normalised to the pathogen alone after interaction kinetics in the two co-incubation models.

This heat map represents the biovolume of the pathogen in interaction with *B. velezensis* normalised by the biovolume of the pathogen alone after 12 h of interaction. The co-inoculation model used the biovolume adhesion ratio of 1:1. Every square represents one interaction and displays the means of three biological replicates, which in turn are calculated using four technical replicates. The sum of *B. velezensis* or consortia scores against each pathogen in all models was calculated to total the antagonistic power of each strain. 384 stacks of images were analysed to produce this heat map.

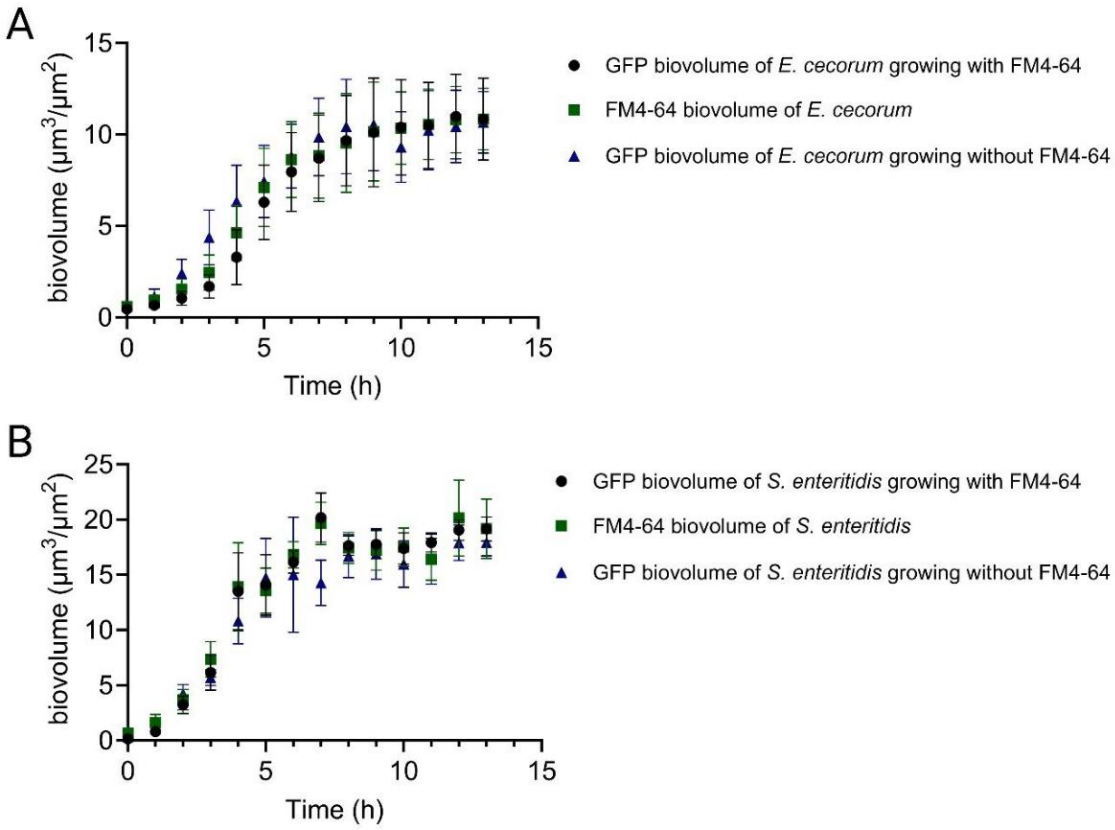

Supplementary data 12: Effect of the FM4-64 on the growth of pathogens.

(A) GFP or FM4-64 biofilm biovolumes of *E. cecorum* GFP growing with or without FM4-64 and (B) Same experiment with *S. enterica* GFP. 336 stacks of images were analysed to produce these curves.

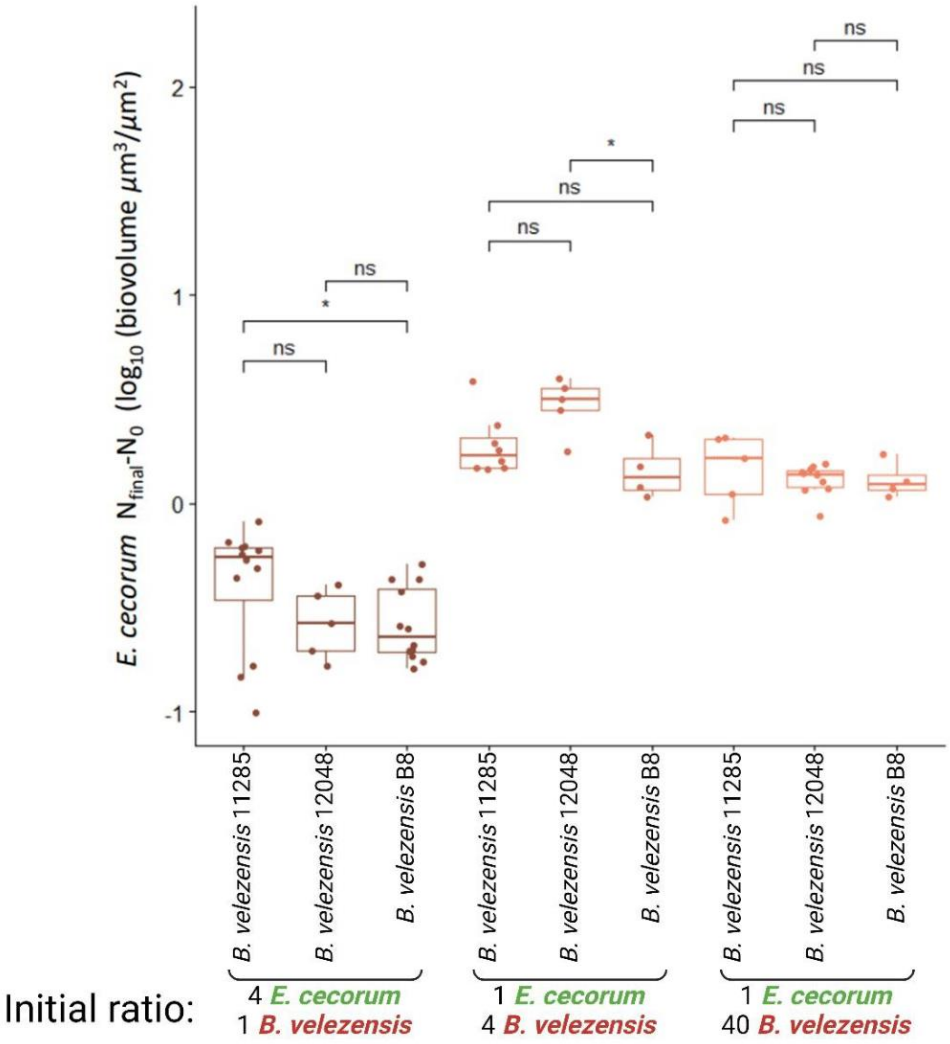

Supplementary data 13: Effect of *B. velezensis* strains on the difference between the final and the initial biovolumes of *E. cecorum* according to three co-inoculation ratios. Negative values indicate that a decrease of the biovolumes have been observed.

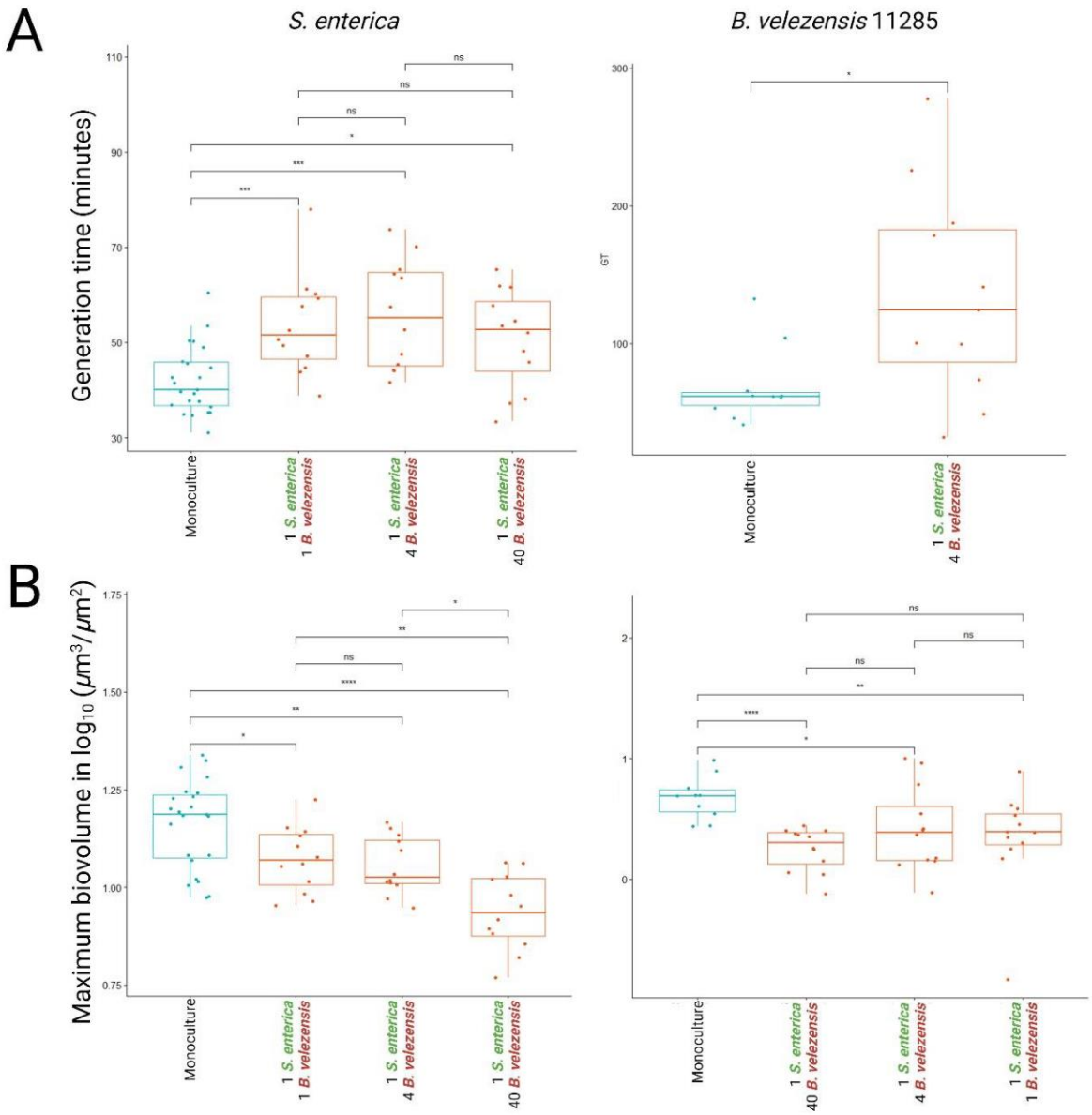

Supplementary data 14: Growth parameters of *S. enterica* and *B. velezensis* 11285 as representative examples, either alone or in interaction with each other at different initial adhesion ratios. (A) Determination of the generation time. (B) Determination of the maximum biovolume reached.

3.2.3 Article 8 : Intergenus associations in positive biofilms to bolster exclusion of bacterial pathogens

Virgile Guéneau, Cécile Berdous, Mathieu Castex, Romain Briandet.

En préparation.

Intergenus associations in positive biofilms to bolster exclusion of bacterial pathogens

Virgile Guéneau[a,b,#], Cécile Berdous[a,#], Mathieu Castex[b], and Romain Briandet[a*]

[a] Université Paris-Saclay, INRAE, AgroParisTech, Micalis Institute, 78350, Jouy-en-Josas, France

[b] Lallemand SAS, 31702, Blagnac, France

* Address correspondence to Romain Briandet, romain.briandet@inrae.fr

[#] These authors contributed equally

Keywords: Positive biofilms, *Bacillus velezensis*, *Pediococcus* spp., synergy, bacterial pathogens, synthetic microbial consortia

Abstract

Positive biofilms are increasingly employed as an innovative biosecurity measure in poultry farming. They play a crucial role in shaping the microbial ecology of surfaces, thereby reducing the presence of undesirable bacteria. However, the advantages of utilising consortia rather than individual strains in the development of commercial products remain unclear. This study aims to investigate the potential of intergenus consortia compared to single strains within the context of positive biofilms to mitigate the presence of undesirable bacteria on surfaces. To achieve this, we implemented a methodology combining Confocal Laser Scanning Microscopy (CLSM) and image analysis to investigate bacterial interactions within multi-species biofilms. Initially, we showed that *Bacillus velezensis* and *Pediococcus* spp., bacteria commonly used in biotechnological applications, can form stable consortia. We then compared the antagonistic activity of these consortia to that of individual strains when confronted to pathogens found in broiler farms, namely *Salmonella enterica* serovar Enteritidis and *Enterococcus cecorum,* in various multi-species biofilm scenarios. Our findings revealed that the consortia maintained the antagonistic activity against *E. cecorum,* even when compared to the already effective beneficial strains acting alone. Additionally, the consortia exhibited enhanced effects against *S. enterica* growth, occasionally demonstrating significant synergistic effects. These results provide a rational basis for considering the use of intergenus consortia in positive biofilm applications.

Introduction

Various methods with preventive or curative effects on animals, such as the use of vaccines or antibiotics, are employed to limit animal disease transmission in broiler farms. Additionaly, biosecurity procedures are applied in the animal environment to maintain farm hygiene and reduce disease transmission between two batches of animals. Within these protocols, surface cleaning and disinfection (C&D) protocols using biocides are established to reduce the microbial load, which can act as a reservoir of pathogens and therefore contribute to disease transmission. However, these procedures are not completely efficient due to biofilm formation [1]. Biofilms are complex three-dimensional microbial communities embedded within a self-produced matrix constituted by extracellular polymeric substances (EPS) [2,3]. Approximatively 40 to 80% of bacterial and archeal cells live in a biofilm lifestyle on earth, which can host various types of microorganisms (i.e. filamentous fungi, yeast, protist, virus) interacting with each other in cooperative or competitive ways [4]. The slimy EPS create a protective shield and diffusion barrier, conferring remarkable tolerance to environmental stress [5]. Hence, microorganisms residing in a biofilm, including microbial pathogens, demonstrated a typical tolerance to disinfectants that is 10 to 1000 times higher than that of their homologous planktonic counterparts [6].

Microbial biofilms can be beneficial and used by humans in various biotechnology applications [7,8]. Innovative alternative solutions for mitigating zoonotic diseases while reducing dependence on antibiotics are continuously being developed. In recent years, the implementation of positive biofilms has gained prominence as a biosecurity strategy aimed at managing the indigenous microbial ecosystem. This approach effectively minimises the settlement and proliferation of pathogens on surfaces that come into contact with animals [9]. However, there is currently a lack of scientific studies examining the utilisation of single microbial strains or synthetic consortia in this particular context, specifically exploring their potential advantages on colonisation or antagonist activity on pathogens over individual strains. In addition, it is essential that the strains chosen in the synthetic consortiums for their competitive characteristics can coexist without antagonistic interactions between them. The literature on this subject is sparse and somewhat controversial. One study outlined the broad-spectrum antibacterial activity of an intestinal isolate of *B. velezensis* against pathogens, but

also against many lactic acid bacteria [10]. Compatible consortia of two or three *B. velezensis* strains maintained antagonism compared with single strains without increasing it [11]. Moreover, another study has indicated than associations between *Bacillus subtilis* and specific strains of lactic acid bacteria exhibit improved antagonistic activity against *Staphylococcus aureus* in biofilm compared to individual strains [12].

In this study, we focused on exploring the compatibility of intergenus biofilm associations involving three strains of *B. velezensis* previously described as good candidates for positive biofilms [11] and two strains of lactic acid bacteria from the genus *Pediococcus* spp., commonly used in biotechnological applications. Our study employs a methodology that combines CLSM with image analysis techniques to track the formation of mixed biofilms [13]. Through our experiments, we have successfully demonstrated that all *B. velezensis* associations with *Pediococcus* spp. remain stable, with no exclusion of one partner by the other after 24 hours. We compared the antagonistic activity of consortia with individual strains on pathogen growth in various multi-species biofilm scenarios. For this purpose, *Enterococcus cecorum* and *Salmonella enterica* serovar Enteritidis (*S. enterica*) were selected as two major pathogens of broiler farms [14,15]. Our findings showed that the intergenus consortia exhibit superior antagonistic activity against pathogen growth compared to the single strains. These significant results provide valuable insights for rationalising the use of consortia rather than single strains in positive biofilm applications. By increasing our understanding of the dynamics and efficacy of mixed biofilm formation, our study paves the way for optimising the use of consortia to enhance positive biofilm applications.

Methods

Bacterial strains

The bacterial strains used in this study are described in the table below (**Table 1**). The experiments were all conducted using Tryptic Soy Broth (TSB) medium (BioMérieux, France) at a temperature of 30°C, without agitation. Plate and overnight cultures were supplemented with antibiotics (5 µg/mL erythromycin or 100 µg/mL ampicillin) where the strain carried the pCM11 plasmid. Plates were inoculated and incubated at 30°C for 3 days from a glycerol stock at -80 °C. Then, three representative clones were cultured in 10 mL TSB and incubated overnight. 2 mL of the overnight cultures were centrifuged at 5000 g for 5 minutes and the supernatants were replaced with fresh TSB without antibiotics (2 mL for GFP-labelled strains and 80 µL for *Pediococcus* spp.) before beginning the experiments.

Table 1: Bacterial strains used in this study.

Name	Origine and genotype	Reference
Bacillus velezensis 11285	Marine	Lallemand AQP
Bacillus velezensis 12048	Marine	Lallemand AQP
Bacillus velezensis B8	Surface of commercial broiler chicken house	[16]
Pediococcus acidilactici R1001	Plant	Lallemand AQP
Pediococcus pentosaceus R1094	Silage	Lallemand AQP
Bacillus velezensis 11285 GFP	*Bacillus velezensis* 11285, with pCM11-*gfp*	[11]
Bacillus velezensis 12048 GFP	*Bacillus velezensis* 12048, with pCM11-*gfp*	[11]
Bacillus velezensis B8 GFP	*Bacillus velezensis* B8, with pCM11-*gfp*	[11]
Enterococcus cecorum GFP	DSM20682 strain, isolated from chicken caecum, with pCM11-*gfp*	[11]
Salmonella enterica enterica serovar Enteritidis GFP	NCTC6676 strain, isolated from dead cow, with pCM11-*gfp*	[11]

Submerged multi-species biofilms

All biofilm structures were observed on polystyrene 96-well microtiter plates µclear® base (Greiner Bio-one, France) compatible with microscopy. The entire bacterial population of the biofilm (the GFP-strains alone or in combination with an unlabeled one) was visualised using SYTO61 (Invitrogen, Carlsbad, CA, USA), a cell-permeant red dye that labels nucleic acid.

The co-inoculation model

Our objective was to grow a multi-species biofilm using genetically labelled strains expression constitutively GFP protein (GFP-labelled pathogen, GFP-labelled *B. velezensis*) along with unlabelled *B. velezensis* strains or *Pediococcus* spp. strains (one or two species), starting with the an identical initial adhesion biovolume 0.50 +/- 0.25 between the GFP strain and the unlabeled strains. To determine the adhesion rates, we followed the protocol described by Guéneau et al. [13].

Concisely, submerged multi-species biofilms were cultivated utilising genetically labelled strains (GFP-labelled *B.velezensis* or GFP-labelled pathogens) in conjunction with unlabeled stains. Dilutions in one mL of TSB were carried out using overnight cultures to obtain a solution that would permit the adhesion of the correct quantity to the bottom of the microscopy plates (1:1 ratio in our case). 200 µL of these solutions were placed in 96-well plates. After 1h30 of adhesion, the supernatants were removed and replaced with fresh media containing 1 µg/mL of SYTO61 to remove non adhering planktonic cells. This time-point after adhesion step is considered as the beginning of the experiment. To determine the adhesion rates, the GFP biovolume was quantified, and the biovolume of the unlabeled strains was calculated by the subtraction of the GFP-labelled strains biovolume from the total biofilm biovolume.

After confirming the adhesion ratio, the same protocol was applied with the addition of 50 µL of a TSB solution containing SYTO61 at 2 µg/mL to the wells, precisely 24 hours of growth after the adhesion step.

The recruitment model

Biofilms using beneficial strains candidates were grown 24 hours after adhesion step at 30 °C following the procedure described above. Overnight cultures of the GFP-labeled pathogens were centrifuged for 10 min at 3500 g and then resuspended in fresh media to remove antibiotics. An adhesion step of 50 µL of pathogens suspension was carried out for 1h30 at 30°C in the wells containing the mature positive biofilms. The supernatant was gently replaced by 200 µL of fresh media containing 1 µg/mL of SYTO61 to perform microscopy acquisitions after adhesion phase (t = 0h recruitment model), or after 24 hours (t = 24h recruitment model) with the addition of 50 µL of SYTO61 at 2 µg/µL.

CLSM acquisitions

Acquisitions were performed using a Leica SP8 AOBS inverted high content screening confocal laser scanning microscope (HCS-CLSM, LEICA Microsystems, Germany) at the MIMA2 platform (https://doi.org/10.15454/1.5572348210007727E12). Images of the biofilm were captured using the 63x water objective lens with a numerical aperture of 1.2. The imaging was performed at a frequency of 600 Hz, with each image taken every micrometre to ensure the complete height coverage of the biofilm. The captured images had a resolution of 512 × 512 pixels, corresponding to a physical area of 147.62 × 147.62 µm, and a pixel size of 0.361 µm. The GFP were excited with an argon laser set at 488 nm, and the emitted fluorescence was collected with a hybrid detector (HyD LEICA Microsystems, Germany) in the range of 500-550 nm. SYTO 61 was excited with the helium-neon laser at 633 nm, and the emitted fluorescence was collected with a hybrid detector in the range of 650-750 nm. For each experiment, two stacks of images per well, with two wells as technical replicates, were acquired for each one of the 3 biological replicates made (12 biofilms analysed per condition).

CLSM image analysis

To visualise biofilm structures, IMARIS 9.3.1 software (Bitplane, AG-Zurich, Switzerland) was used. Images in blend mode were employed to generate a three-dimensional reconstruction of the biofilms, incorporating an artificial shadow for relief (cross section of the z, x axis). For quantitative analysis, the BiofilmQ software [17] was employed. Channels were analysed separately using the OTSU threshold method. The "global biofilm properties" and "substrate area" modules were chosen for calculation, enabling the extraction of biovolume and substrate area of binarised images.

To determine the antagonism score, we followed the protocol described by Guéneau et al. [11]. The average biovolume of each condition per replicate was deduced from the average biovolume of the pathogen, in order to compare the antagonistic effect of individual beneficial strains with that of the consortium. The percentage of antagonist activity was then calculated using the obtained delta values.

To assess the anti-pathogenic activity, the biovolumes ($\mu m^3/\mu m^2$) of the GFP channel of submerged mixed biofilms was measured and normalised against the biovolume of mono-

species GFP pathogen biofilms. We invert the value (1-x), where x represents the normalised GFP biovolume values, to assign a positive score to each condition. The aim was to give high scores to strains with strong anti-pathogenic activity and low scores to non-competitive strains. To standardise the scores, we centre-reduced the values between 0 and 1, where 1 represents the highest score and 0 the lowest. This approach allowed us to compare with a simple score between 0 and 1 the anti-pathogenic activity of different *Bacillus* strains and to identify those with the most promising potential against GFP pathogen biofilms.

Statistical analysis

Results are represented by mean and standard deviation for error bars. A one-way variance analysis (ANOVA) using the uncorrected Fisher's least was performed with the PRISM software (GraphPad, USA, California). Statistical significance was determined when the *p*-value associated with the Fisher test was less than 0.05.

Results

B. velezensis and *Pediococcus* spp. establish stable intergenus biofilms

Adhesion ratios were meticulously controlled to ensure an equal initial adhesive biovolume of *B. velezensis* GFP and *Pediococcus* spp. to the bottom of the wells at the start of the experiment (**Fig. S1**). After a 24 h incubation period, biofilms were imaged with CLSM (**Fig. 1A**). The biofilms formed by *B. velezensis* exhibited a structured and extensive morphology, in contrast the flatter, denser and thinner biofilms formed by *Pediococcus* spp. Within consortia, clusters of *B. velezensis* were surrounded by *Pediococcus* spp., effectively covering the unoccupied surface. Notably, the consortia displayed a SYTO61 biovolume comparable to that of *B. velezensis*, yet with a significant decrease in the proportion of *B. velezensis* GFP within the mixtures compared to when *B. velezensis* was alone ($p < 0.05$)(**Fig. 1B**). Furthermore, the biovolumes of SYTO61 in consortia were significantly higher than those of *Pediococcus* spp. ($p < 0.05$). Subtracting the GFP signal from SYTO61 in consortia gives access to the biovolume of *Pediococcus* spp. The amount of *P. pentosaceus* R1094 is significantly higher in the presence of *B. velezensis* 12048 and B8 compared to the control *P. pentosaceus* alone ($p < 0.05$). Conversely,

when quantified with the SYTO61, the area covered by the biofilm displayed a higher value for *Pediococcus* spp. compared with *B. velezensis* ($p < 0.0001$), a trend maintained by the consortia (**Fig. 1C**). In particular, all *B. velezensis* strains covered less surface area than the consortia ($p < 0.01$).

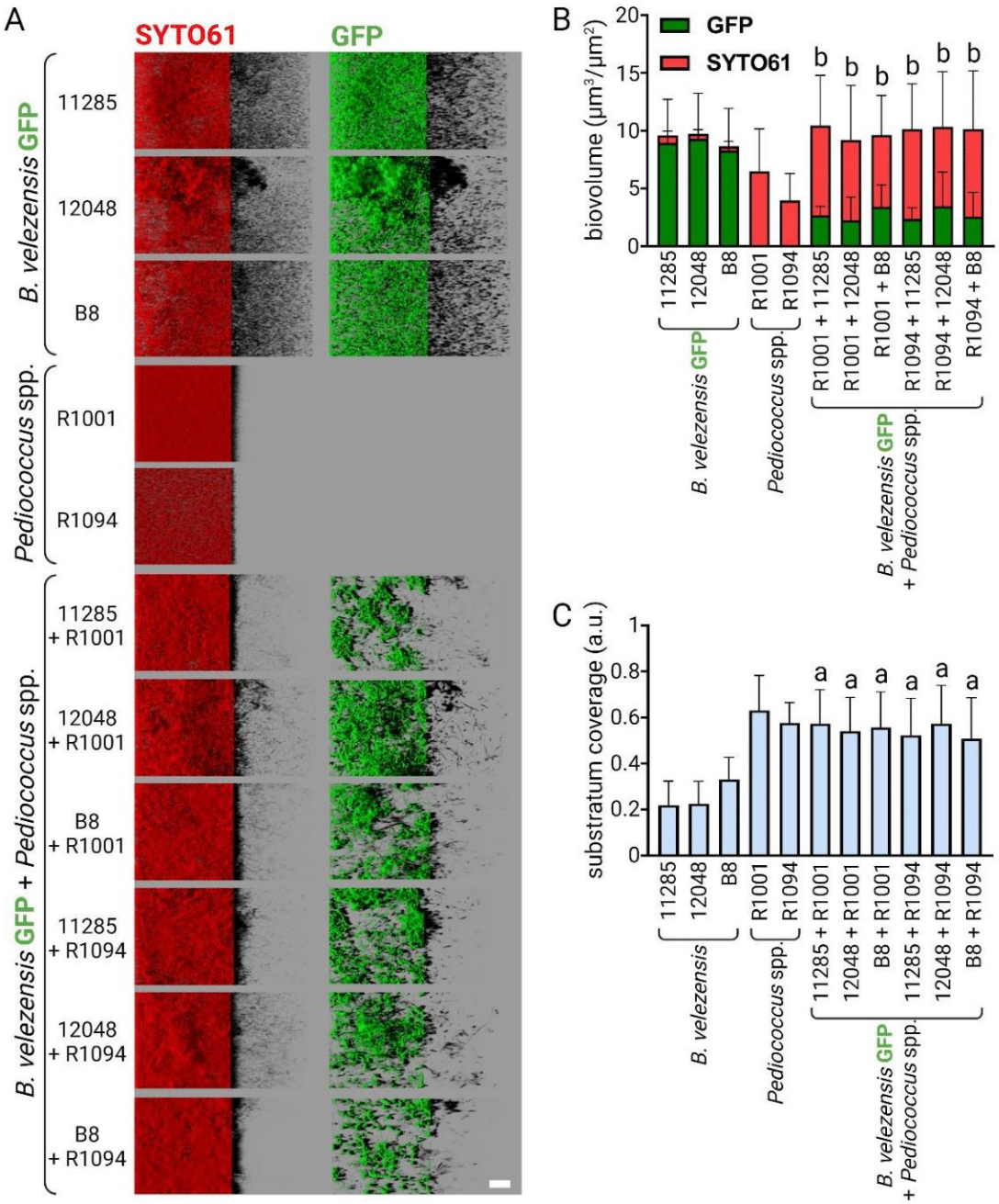

Figure 1: Interaction between *B. velezensis* GFP and *Pediococcus* spp. in a co-inoculation model. (A) Biofilm images from CLSM of *B. velezensis* GFP, *Pediococcus* spp. or consortia. Scale bar = 40 µm. (B) Quantification of GFP and SYTO61 biovolumes. a indicates that the consortium value is significantly different from that of *B. velezensis*. (C) Substratum coverage of the total biofilm determined with the SYTO61 channel. b indicates that the consortium value is significantly different from that of *Pediococcus* spp. Error bars = standard deviation.

Consortia exhibited enhanced antagonistic activity against *S. enterica* compared to individual strains

The impact of beneficial strains, either alone or in combination, was assessed on the growth of *E. cecorum* GFP. In the co-inoculation model, experiments commenced with calibrating adhesion ratios to obtain an equal amount of *E. cecorum* GFP with the candidate beneficial strains alone or with beneficial consortia (**Fig. S2**). After validating this ratio, mixed biofilms with *E. cecorum* GFP were observed after 24 h of incubation (**Fig. 2A**), consistenly demonstrating a significant decrease in GFP biovolume in all conditions compared to the control (**Fig. S3A**). The percentage reduction in the biovolume of *E. cecorum* GFP compared to the control was calculated in order to compare the performance of single strains and combinations (**Fig. 2D**). The effects of *B. velezensis* were sustained when in combination and surpassed those of *Pediococcus* spp.

Observations from the recruitment model after the adhesion of the GFP-labeled pathogen on a 24 h beneficial biofilm (t= 0h) are depicted in **Fig. 2B**. In this model at t= 0h, a consistent and significant decrease in pathogen biovolume was observed (**Fig. S3B**), with no significant change in GFP biovolume in the association compared to the single strains (**Fig. 2E**). In the recruitment model at t= 24h (i.e. after 24 hours of pathogen growth on the already installed positive biofilm)(**Fig. 2C**), a notable reduction in *E. cecorum* GFP was observed in all conditions (**Fig. S3C**), with no difference between associations and single strains (**Fig. 2F**).

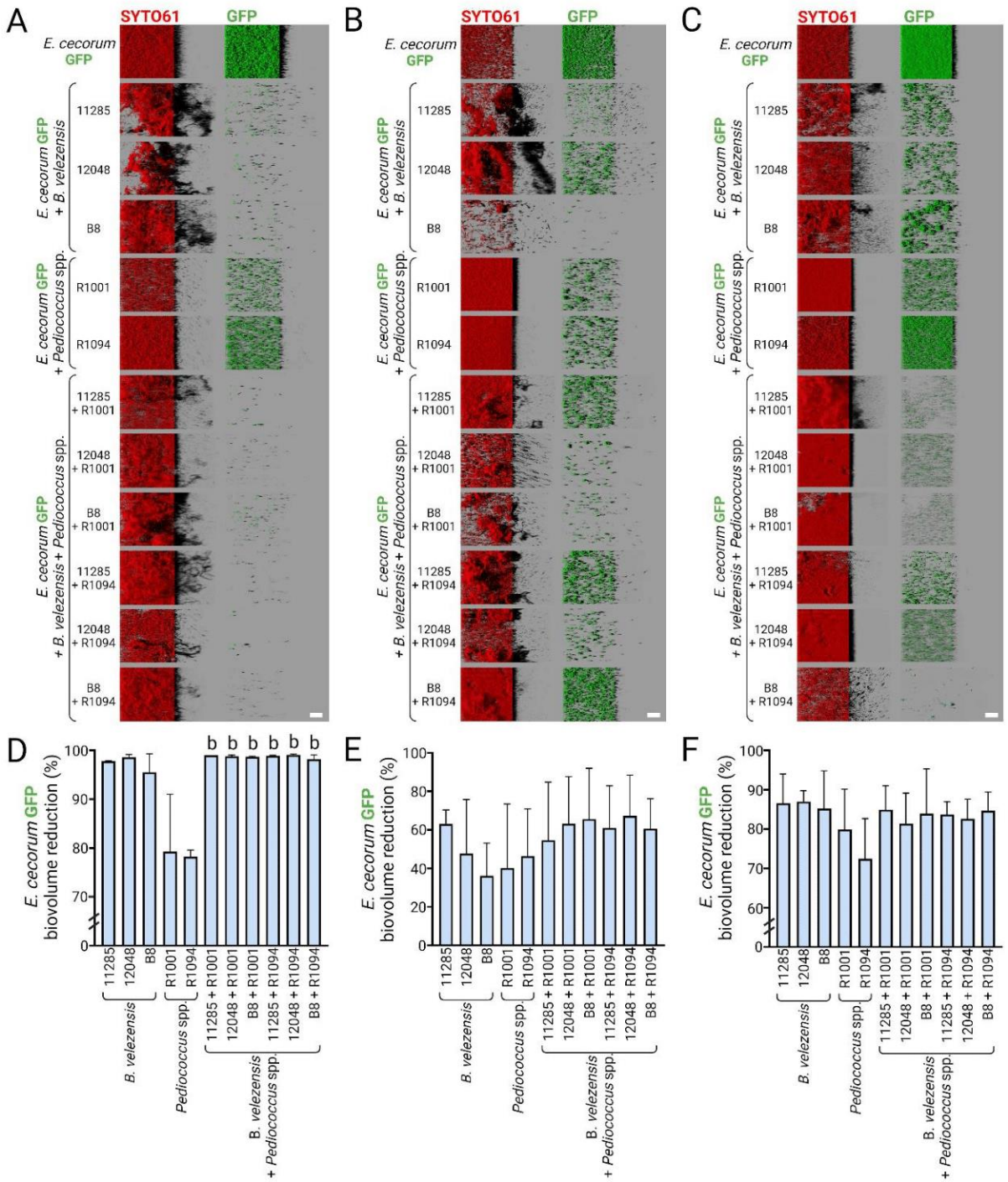

Figure 2: Antagonist activity of the positive biofilms on *E. cecorum* GFP. (A) Biofilm images from CLSM in the co-inoculation model with *E. cecorum* GFP alone, *Pediococcus* spp., *B. velezensis* or the beneficial consortia with the pathogen GFP. Scale bar = 40 µm. (B) Same experiment in the recruitment model at t=0 h. (C) Same experiment in the recruitment model at t=24 h. (D) Biovolume réduction of *E. cecorum* GFP interacting with *Pediococcus* spp., *B. velezensis* or the beneficial consortia. (E) Same experiment in the recruitment model at t=0 h. (F) Same experiment in the recruitment model at t=24 h. Error bar = standard deviations.

As explained above, the antagonist potential against *S. enterica* GFP growth was evaluated in the presence of the beneficial strains alone or in association. Adhesion ratios were meticulously verified in the co-inoculation model (**Fig. S4**), preceding the visualisation of 24h biofilms (**Fig. 3A**). Notably, a significant reduction in the biovolume of *S. enterica* GFP was observed in the presence of *Pediococcus* spp. and their respective associations, except for R1094 associated with 12048 or B8 (**Fig. S5A**). Particularly, the R1001+B8 and 1094+11285 associations excluded significantly more *S. enterica* GFP in the co-inoculation model than their strains alone (**Fig. 3D**).

Results of the recruitment model t =0h showed lesser adhesion of *S. enterica* GFP on the *Pediococcus* spp. biofilm (**Fig. 3B**), a significance observed only under these conditions (**Fig. S5B**). No combinations were more effective in this model than *Pediococcus* spp. alone (**Fig. 3E**). However, the two associations combining R1001 with 11285 or B8 showed less activity than R1001 alone ($p < 0.05$), presenting more variability in results for combinations compared to individual strains. In the recruitment model at t= 24h, observation showed a decrease in the density of planktonic *S. enterica* GFP biofilm cells in the presence of *B. velezensis* (**Fig. 3C**). *S. enterica* GFP biofilms were dense and localised at the bottom of the well, with no planktonic cells present in the presence of *Pediococcus* spp. The associations showed a combined effect of the two individual strains, resulting in a reduction in biofilm density of *S. enterica* GFP and a decrease in planktonic cells. A significant reduction in *S. enterica* GFP biovolume was observed in all conditions (**Fig. S5C**). Strikingly, all the combinations showed stronger antagonistic activity against *S. enterica* than the individual strains (**Fig. 3F**).

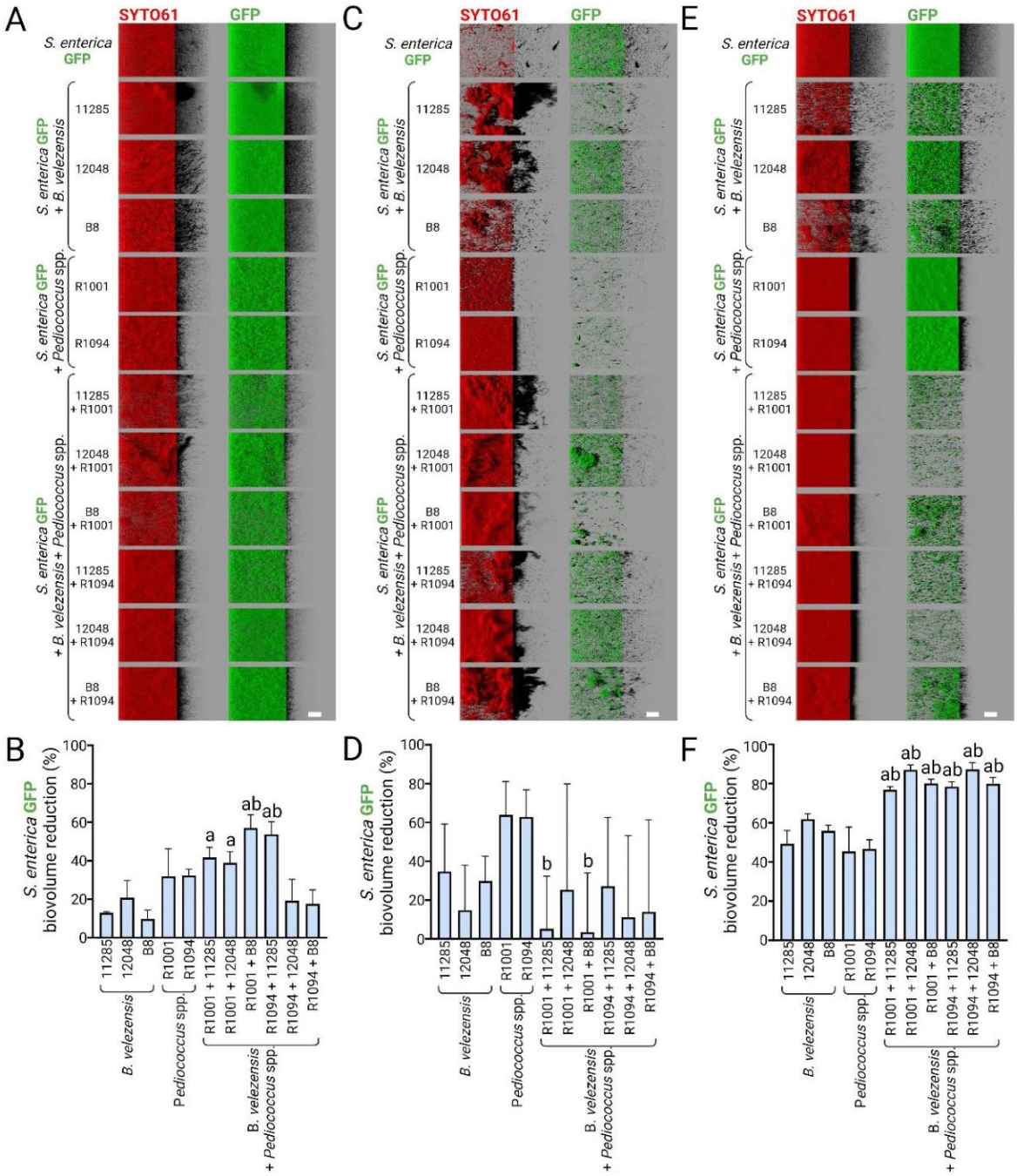

Figure 3: Antagonist activity of the positive biofilms on *S. enterica* GFP. (A) Biofilm images from CLSM in the co-inoculation model with *S. enterica* GFP alone, *Pediococcus* spp., *B. velezensis* or the beneficial consortia with the pathogen GFP. Scale bar = 40 µm. (B) Same experiment in the recruitment model at t=0 h. (C) Same experiment in the recruitment model at t=24 h. (D) Biovolume réduction of *S. enterica* GFP interacting with *Pediococcus* spp., *B. velezensis* or the beneficial consortia. Error bar = standard deviation. (E) Same experiment in the recruitment model at t=0 h. (F) Same experiment in the recruitment model at t=24 h. Error bar = standard deviations.

An antagonism score was calculated from the quantified GFP biovolume quantifications in the presence of candidate strains alone, or in associations. The heatmap in **figure 4** summarised

all antagonism scores. The findings highlight an increased efficacy of beneficial strains against *E. cecorum*, particularly in the co-inoculation model where *S. enterica* is only marginally excluded by the beneficial candidates. The overall efficacy of a candidate bacterium or consortium against pathogens is determined by the sum of their antagonism scores across all conditions. The cumulative scores illustrate that all consortia demonstrate a superior efficiency compared to individual strains, primarily due to their increased efficiency in the 24h recruitment model. The consortia with the most promising scores are *B. velezensis* B8+*P. acidilactici* R1001 and *B. velezensis* 11285+*P. pentosaceus* R1094.

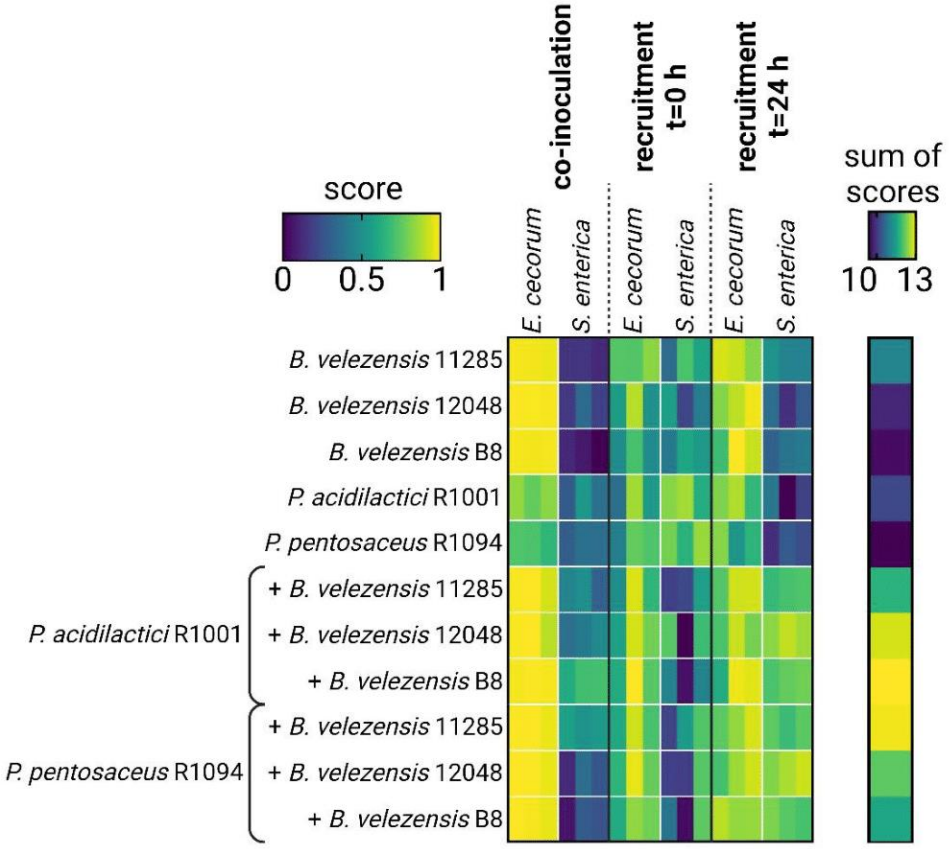

Figure 4: Antagonism score of the positive biofilms against pathogens in the 2 co-incubation models. Pathogens are grouped by models in the heat map. In this heat map, yellow represents the highest antagonist score and dark blue the lowest. Every square represents one interaction and displays the means of three biological replicates, which in turn are calculated using four technical replicates. The sum of scores by condition (every line in the heat map) were calculated to globalise the antagonistic power of each condition.

Discussion

Our study shed light on the synergistic effects of intergenus consortia of *B. velezensis* and *Pediococcus* spp. within the biofilm lifestyle in combating pathogens. We initiated our

investigation by examining the compatibility of *B. velezensis* and *Pediococcus* spp. to form a stable mixed biofilm without one species excluding the other, using a co-inoculation model. This step is crucial to cover the majority of the surface with a positive biofilm, as competition between beneficial strains could lead to territories and empty spaces susceptible to undesirable bacteria colonisation [18]. Establishing a controlled initial ratio for the adhered partners was imperative, given that adhesion can vary between strains [11]. This model affirmed the compatibility between *B. velezensis* and *Pediococcus* spp., demonstrating their ability to establish stable and reproducible multi-species biofilm after 24 h. Consortia maintain the highest biovolume and surface cover values compared to individual strains. However, a decrease in the biovolume of *B. velezensis* was observed in the presence of *Pediococcus* spp., potentially due to spatial and nutritional competition, considering the limited nutrients availability in the sample. Another hypothesis relate to media acidification by *Pediococcus* spp. potentially influencing *B. velezensis* biofilm formation [19,20]. To understand these observations better, it is essanetial to mesure pH and investigate biofilm formation of *B. velezensis* strains with *Pediococcus* spp. supernatant or artificial acidification with organic acids to determine the impact of *Pediococcus* spp. secretions on the structure of *B. velezensis* biofilms and their overall antagonist activity on pathogens [21].

Our results revealed a strong antagonist effect of *B. velezensis* towards *E. cecorum* compared to *Pediococcus* spp., an effect conserved in consortia. This suggests that the mechanisms involved with *B. velezensis* are maintained when associated with *Pediococcus* spp. Notably, in the co-inoculation model, significant effects were observed with some consortia, with a formal synergistic effect (greater than the sum of the two partners) on *S. enterica* growth compared to individual strains. Further research into the mechanisms involved is needed to understand the differences between associations in this context. The recruitment model mimics the situation where beneficial bacteria are applied on livestock building surfaces to form a positive biofilm before the potential arrival of pathogens by the entrance of animals. With *S. enterica*, recruitment on *Pediococcus* spp. lead to the best reduction of the pathogen biovolume. *S. enterica* may have less affinity for the matrix secreted by *Pediococcus* spp. compared with *B. velezensis*. Since pathogens are incorporated into the supernatant of a mature positive biofilm, the secreted molecules present in the supernatant may have an effect on pathogen adhesion or mortality. Indeed, *Pediococcus* spp. Is well described to produce interferent molecules

[22,23]. The results after 24 hours of growth indicate an increased antagonistic effect against *S. enterica* when a biofilm is already established for all consortia compared to individual strains. Further investigations are needed to decipher the contribution of each partner, determining if one enhances the effect of the other, or if a new mechanism is at play.

We have successfully identified strains that individually or in combination exhibit a significant reduction in pathogen level across different laboratory models. However, the underlying mechanisms responsible for the antagonism against pathogens or the synergy between beneficial strains remain to be determined. To shed light on this aspect, live-cell imaging coupled with image analysis may be employed to assess kinetics of biofilm formation. By studying the growth dynamics of each partner in multi-species biofilm, the could identify the primary categories of interaction involved [11], which might include spatial competition, nutritional competition, or interference [9].

While this study was performed under controlled laboratory conditions allowing high throughput analyses, future investigation should replicate these trials under physico-chemical conditions that closely mimic real-world field conditions, for example by using chemically controlled culture media. Additionally, exploring the impact of these associations on the modulation of native microbiota in animal environments, as well as on animal performance and disease transmission dynamics, will be vital for a comprehensive understanding.

Conclusion

Our study highlights the potential of *B. velezensis* and *Pediococcus* spp. intergenus consortia in positive biofilm applications. Prior to assessing their antagonist effect on pathogen growth, we rigorously characterized the compatibility of these strains, confirming their ability to form stable mixed consortia. We have demonstrated that positive biofilm formed by these intergenus consortia exhibits superior antagonistic activity against *S. enterica* than the individual strains. In order to gain a comprehensive understanding of the interactions and enhance the performance of the associations, it is imperative to identify the underlying mechanisms. This deeper insight will enable us to delve into the intricacies of these interactions and facilitate the testing of novel associations, ultimately leading to improved performance. These new associations must now be tested to assess their impact on pathogen exclusion under field conditions and animal performance.

Data availability

The original contributions presented in the study are included in the article. Further inquiries can be directed to the corresponding author.

Funding

This research was funded by INRAE, LALLEMAND SAS, and ANRT "Association Nationale de la Recherche et de la Technologie" (contract 2020/0548).

Conflict of interest

The authors declare that the research was conducted in the absence of any commercial or financial relationships that could be construed as a potential conflict of interest.

Acknowledgments

We thank the MIMA2 platform (Microscopie et Imagerie des Microorganismes, Animaux et Aliments, https://doi.org/10.15454/1.5572348210007727E12) for the Leica SP8-HCS microscopy observations.

Contributions

VG, MC and RB: conceptualization and methodology. MC and RB: validation and supervision. VG, CB: formal analysis and data curation. VG, CB, MC, and RB: investigation. MC and RB: resources, project administration, and funding acquisition. VG, CB: writing the original draft preparation. MC and RB: reviewing, and editing. All authors have read and agreed to the published version of the manuscript.

References

[1] Luyckx KY, Van Weyenberg S, Dewulf J, Herman L, Zoons J, Vervaet E, et al. On-farm comparisons of different cleaning protocols in broiler houses. Poultry Science 2015;94:1986–93. https://doi.org/10.3382/ps/pev143.

[2] Sauer K, Stoodley P, Goeres DM, Hall-Stoodley L, Burmølle M, Stewart PS, et al. The biofilm life cycle: expanding the conceptual model of biofilm formation. Nat Rev Microbiol 2022;20:608–20. https://doi.org/10.1038/s41579-022-00767-0.
[3] Flemming H-C, Wingender J. The biofilm matrix. Nat Rev Microbiol 2010;8:623–33. https://doi.org/10.1038/nrmicro2415.
[4] Flemming H-C, Wuertz S. Bacteria and archaea on Earth and their abundance in biofilms. Nat Rev Microbiol 2019;17:247–60. https://doi.org/10.1038/s41579-019-0158-9.
[5] Flemming H-C, Wingender J, Szewzyk U, Steinberg P, Rice SA, Kjelleberg S. Biofilms: an emergent form of bacterial life. Nat Rev Microbiol 2016;14:563–75. https://doi.org/10.1038/nrmicro.2016.94.
[6] Bridier A, Briandet R, Thomas V, Dubois-Brissonnet F. Resistance of bacterial biofilms to disinfectants: a review. Biofouling 2011;27:1017–32. https://doi.org/10.1080/08927014.2011.626899.
[7] Habimana O, Guillier L, Kulakauskas S, Briandet R. Spatial competition with Lactococcus lactis in mixed-species continuous-flow biofilms inhibits Listeria monocytogenes growth. Biofouling 2011;27:1065–72. https://doi.org/10.1080/08927014.2011.626124.
[8] Fira D, Dimkić I, Berić T, Lozo J, Stanković S. Biological control of plant pathogens by Bacillus species. J Biotechnol 2018;285:44–55. https://doi.org/10.1016/j.jbiotec.2018.07.044.
[9] Guéneau V, Plateau-Gonthier J, Arnaud L, Piard J-C, Castex M, Briandet R. Positive biofilms to guide surface microbial ecology in livestock buildings. Biofilm 2022;4:100075. https://doi.org/10.1016/j.bioflm.2022.100075.
[10] Byun H, Brockett MR, Pu Q, Hrycko AJ, Beld J, Zhu J. An Intestinal Bacillus velezensis Isolate Displays Broad-Spectrum Antibacterial Activity and Prevents Infection of Both Gram-Positive and Gram-Negative Pathogens In Vivo. J Bacteriol 2023;205:e0013323. https://doi.org/10.1128/jb.00133-23.
[11] Guéneau V, Guillier L, Jiménez G, Plateau-Gonthier J, Noirot-Gros M-F, Serror P, et al. Guided assembly of positive biofilms targeting pathogenic bacteria using live-cell imaging. In Preparation n.d.
[12] Kimelman H, Shemesh M. Probiotic Bifunctionality of Bacillus subtilis-Rescuing Lactic Acid Bacteria from Desiccation and Antagonizing Pathogenic Staphylococcus aureus. Microorganisms 2019;7:407. https://doi.org/10.3390/microorganisms7100407.
[13] Guéneau V, Charron R, Costache V, Bridier A, Briandet R. Chapter 9 - Spatial analysis of multispecies bacterial biofilms. In: Gurtler V, Patrauchan M, editors. Methods in Microbiology, vol. 53, Academic Press; 2023, p. 275–307. https://doi.org/10.1016/bs.mim.2023.03.002.
[14] Souillard R, Laurentie J, Kempf I, Le Caër V, Le Bouquin S, Serror P, et al. Increasing incidence of Enterococcus-associated diseases in poultry in France over the past 15 years. Vet Microbiol 2022;269:109426. https://doi.org/10.1016/j.vetmic.2022.109426.
[15] Jajere SM. A review of Salmonella enterica with particular focus on the pathogenicity and virulence factors, host specificity and antimicrobial resistance including multidrug resistance. Vet World 2019;12:504–21. https://doi.org/10.14202/vetworld.2019.504-521.
[16] Guéneau V, Jiménez G, Castex M, Briandet R. Insights into the genomic and phenotypic characteristics of Bacillus spp. strains isolated from biofilms in broiler farms. In Preparation n.d.

[17] Hartmann R, Jeckel H, Jelli E, Singh PK, Vaidya S, Bayer M, et al. Quantitative image analysis of microbial communities with BiofilmQ. Nat Microbiol 2021;6:151–6. https://doi.org/10.1038/s41564-020-00817-4.
[18] Kraigher B, Butolen M, Stefanic P, Mandic Mulec I. Kin discrimination drives territorial exclusion during Bacillus subtilis swarming and restrains exploitation of surfactin. ISME J 2022;16:833–41. https://doi.org/10.1038/s41396-021-01124-4.
[19] Sun R, Vermeulen A, Devlieghere F. Modeling the combined effect of temperature, pH, acetic and lactic acid concentrations on the growth/no growth interface of acid-tolerant Bacillus spores. Int J Food Microbiol 2021;360:109419. https://doi.org/10.1016/j.ijfoodmicro.2021.109419.
[20] Saint Martin C, Darsonval M, Grégoire M, Caccia N, Midoux L, Berland S, et al. Spatial organisation of Listeria monocytogenes and Escherichia coli O157:H7 cultivated in gel matrices. Food Microbiol 2022;103:103965. https://doi.org/10.1016/j.fm.2021.103965.
[21] Kundukad B, Udayakumar G, Grela E, Kaur D, Rice SA, Kjelleberg S, et al. Weak acids as an alternative anti-microbial therapy. Biofilm 2020;2:100019. https://doi.org/10.1016/j.bioflm.2020.100019.
[22] Millette M, Dupont C, Shareck F, Ruiz MT, Archambault D, Lacroix M. Purification and identification of the pediocin produced by Pediococcus acidilactici MM33, a new human intestinal strain. J Appl Microbiol 2008;104:269–75. https://doi.org/10.1111/j.1365-2672.2007.03583.x.
[23] Papagianni M, Anastasiadou S. Pediocins: The bacteriocins of Pediococci. Sources, production, properties and applications. Microb Cell Fact 2009;8:3. https://doi.org/10.1186/1475-2859-8-3.

Supplementary

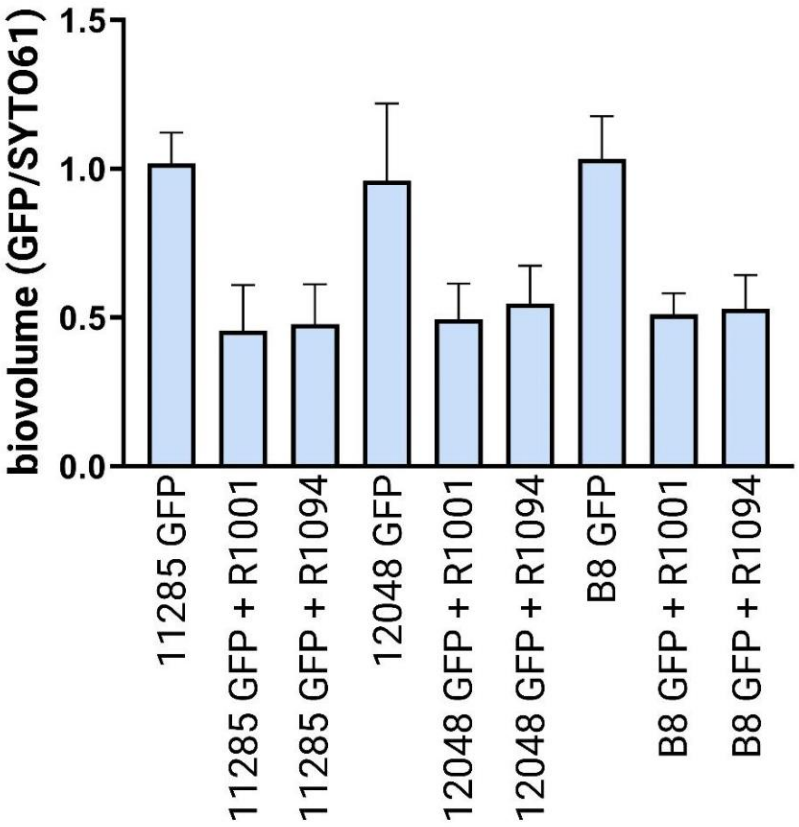

Supplementary data 1: Adhesion ratio of *B. velezensis* GFP. and *Pediococcus* spp. in the co-inoculation growth model.

Volumes of non-labeled *Pediococcus* spp. overnight cultures were calibrated to achieve the same biovolume of *B. velezensis* that constitutively express GFP adhered to the bottom of the wells. To accomplish this, the *B. velezensis* were genetically marked with GFP, and the entire population was chemically labelled with SYTO61 after 1 h 30 min of adhesion. The GFP biovolume to SYTO61 biovolume ratio of 0.5 indicates an equal quantity of *B. velezensis* and *Pediococcus* spp. Error bars correspond to standard deviation.

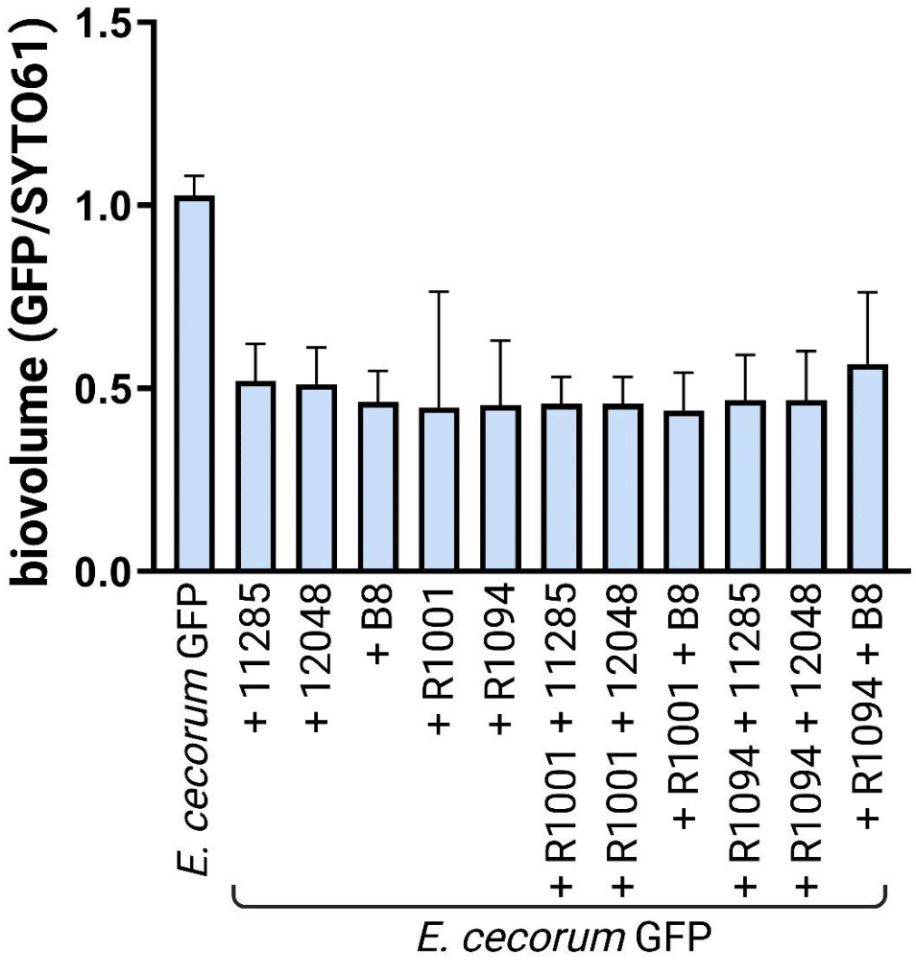

Supplementary data 2: Adhesion ratio of *B. velezensis*, *Pediococcus* spp. and *E. cecorum* GFP in the co-inoculation growth model.

Volumes of non-labeled *B. velezensis* and *Pediococcus* spp. overnight cultures were calibrated to achieve the same biovolume of pathogens and *B. velezensis*, *Pediococcus* spp. or consortia adhered to the bottom of the wells. To accomplish this, the pathogen was genetically marked with GFP, and the entire population was chemically labelled with SYTO61 after 1 h 30 min of adhesion. The GFP biovolume to SYTO61 biovolume ratio of 0.5 indicates an equal quantity of pathogens and *B. velezensis*, *Pediococcus* spp. or consortia. Error bars correspond to standard deviation.

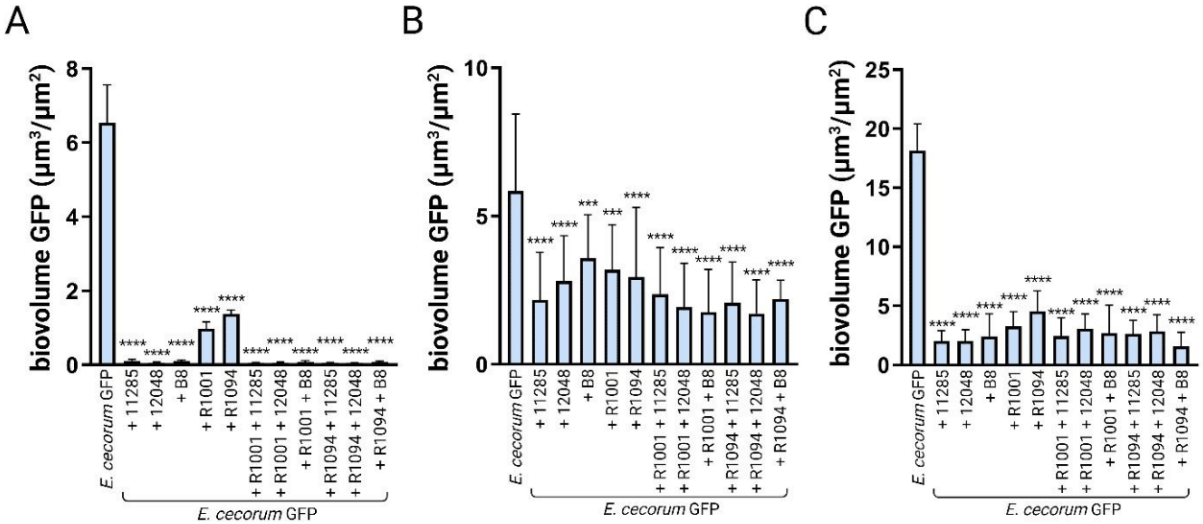

Supplementary data 3: *E. cecorum* GFP biovolume in the different growth model co-cultured with *B. velezensis*, *Pediococcus* spp. or consortia.

The results are shown for (A) the co-inoculation model, (B) the recruitment t=0 h model and (C) the recruitment t=24 h model. Error bars correspond to standard deviation.

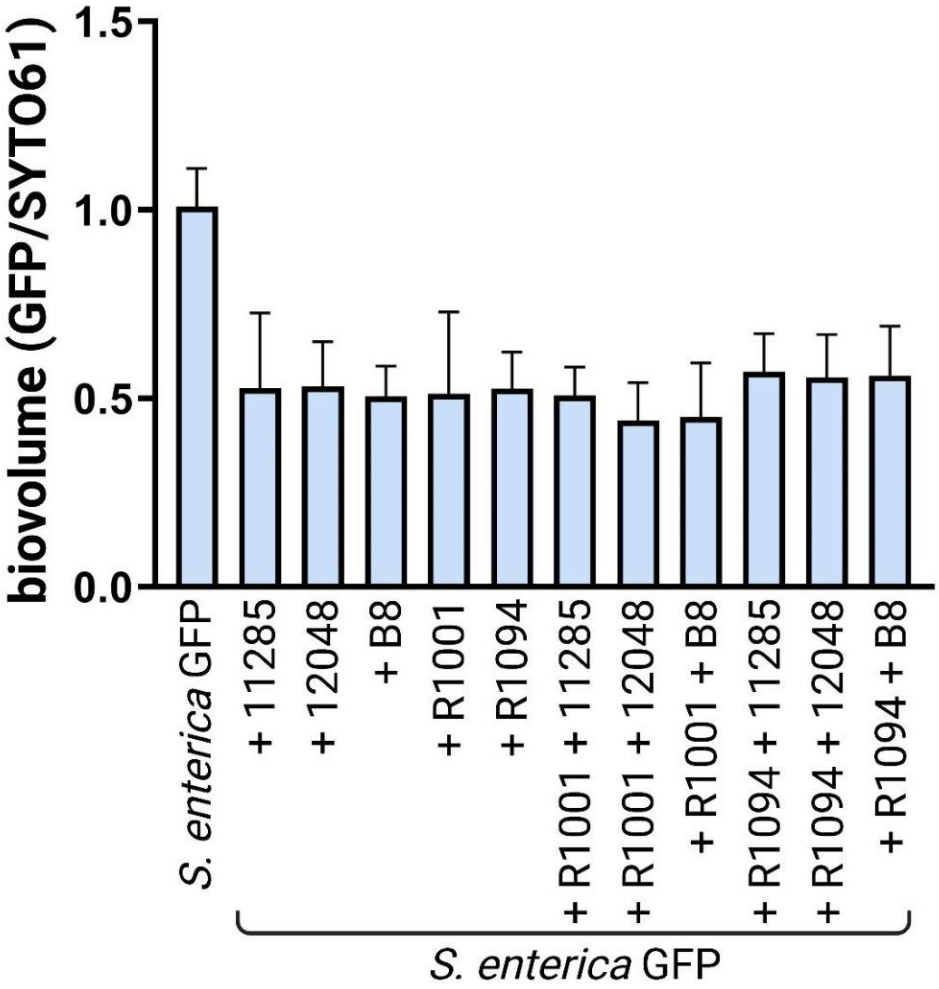

Supplementary data 4: Adhesion ratio of *B. velezensis*, *Pediococcus* spp. and *S. enterica* GFP in the co-inoculation growth model.

Volumes of non-labeled *B. velezensis* and *Pediococcus* spp. overnight cultures were calibrated to achieve the same biovolume of pathogens and *B. velezensis*, *Pediococcus* spp. or consortia adhered to the bottom of the wells. To accomplish this, the pathogen was genetically marked with GFP, and the entire population was chemically labeled with SYTO61 after 1 h 30 min of adhesion. The GFP biovolume to SYTO61 biovolume ratio of 0.5 indicates an equal quantity of pathogens and *B. velezensis*, *Pediococcus* spp. or consortia.

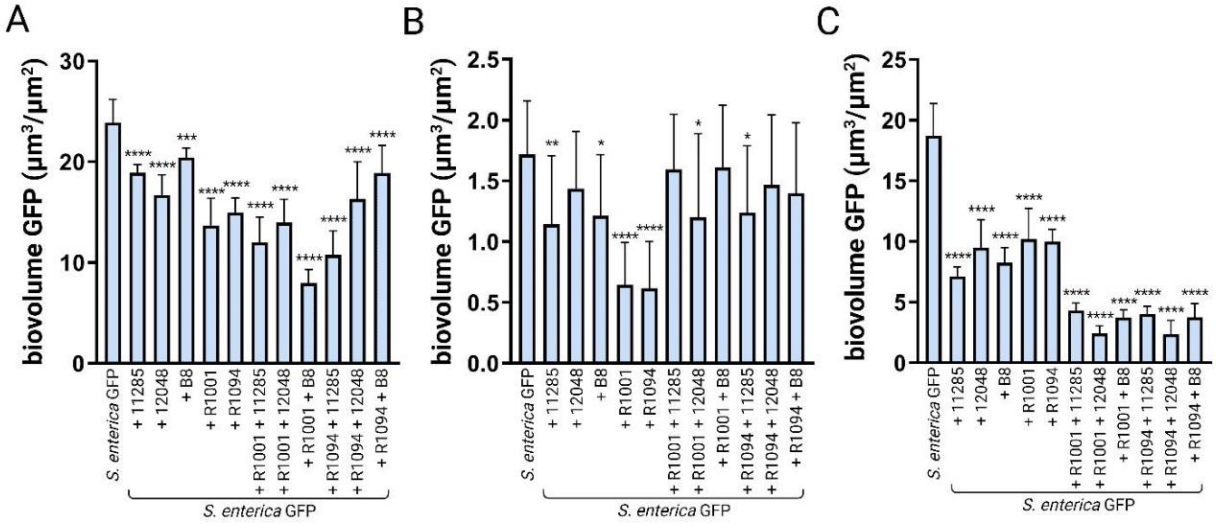

Supplementary data 5: *S. enterica* GFP biovolume in the different growth model co-cultured with *B. velezensis*, *Pediococcus* spp. or consortia.

The results are shown for (A) the co-inoculation model, (B) the recruitment t=0 h model and (C) the recruitment t=24 h model. Error bars correspond to standard deviation.

3.2.4 Exploration des biofilms en macro-colonies : étude des interactions pour une sélection de souches à fort potentiel anti-pathogène

3.2.4.1 Contexte et plan d'expérience

Les bactéries démontrent une remarquable capacité d'adaptation à leur environnement, ce qui les conduit à s'organiser en communautés dotées de structures distinctes en fonction de leur habitat. Ce phénomène est très bien documenté, et s'applique largement au monde bactérien [21,22]. En laboratoire, il est possible de moduler les paramètres physico-chimiques de croissance et de se focaliser sur des zones spécifiques d'un l'échantillon afin d'étudier les différentes formes de biofilms formés et leur structures particulières. Par exemple, dans un échantillon liquide, un biofilm immergé se forme à l'interface entre la surface de l'échantillon et le liquide, tandis qu'une pellicule peut se développer à l'interface entre le liquide et l'air [46]. Il est important de souligner que des bactéries planctoniques sont présentes dans l'ensemble de l'échantillon. Dans un modèle impliquant une interface entre une surface molle et l'air, les bactéries s'organisent en communauté exhibant les caractéristiques requises pour coloniser la surface, et former une colonie à la structure spatiale hautement organisée [47,48].

La MCBL a été utilisée tout au long du projet afin de quantifier finement les effets de bactéries candidates (*Bacillus* spp. et bactéries lactiques) sur la croissance des pathogènes, et d'identifier des consortiums stables capables de former des biofilms mixtes dans un modèle de biofilm immergé. Cependant, l'utilisation de la MCBL pour étudier les biofilms immergés présente des inconvénients, tels que sa complexité, le temps à y consacrer, la nécessité de compétences en analyse d'image ainsi que son coût élevé. L'un des avantages du modèle en macro-colonie réside dans sa simplicité de mise en place, permettant de cribler un grand nombre de souches. En effet, il suffit de déposer une goutte d'une culture bactérienne sur une boîte de Pétri contenant un milieu gélosé, sans nécessiter d'autres étapes de préparation. La boîte est ensuite incubée, et l'échantillon peut être observé macroscopiquement au fil du temps. Ce modèle s'avère particulièrement utile pour étudier un grand nombre d'interactions entre deux souches et pour identifier des phénomènes d'antagonisme ou de compatibilité [49–51]. En effet, la distance entre

deux colonies peut constituer un facteur majeur sur l'interaction sociale. La discrimination *kin*, ou discrimination de parenté, où des souches phylogénétiquement proches sont capables de coexister en biofilm mixte, est classiquement réalisée à l'aide du modèle de swarming [45]. Les protocoles en macro-colonie sont également utilisés pour explorer ce type d'interaction [52].

Dans le cadre des expériences présentées, notre objectif était d'explorer les avantages du modèle de biofilm en macro-colonie pour étudier des interactions bactériennes. Par conséquent, des compétitions ont été réalisées entre différentes bactéries candidates afin d'analyser leurs relations de compatibilité *kin*, ou d'antagonisme vis-à-vis des pathogènes. Une comparaison des résultats en macro-colonie au modèle en biofilm immergé, obtenu avec le MCBL, pour 18 souches de *Bacillus* spp. sera effectuée dans la section de discussion. De plus, l'utilisation du modèle en macro-colonie semble se rapprocher davantage des conditions réelles, en envisageant l'utilisation de biofilm positifs sur les surfaces de bâtiments d'élevage hors-sol (interface solide - air).

Enfin, dans le but d'améliorer la composition d'un produit de nouvelle génération, nous avons examiné l'impact de l'ajout de différents sucres dans le milieu sur les interactions entre les trois souches de *B. velezensis* (11285, 12048 et B8) et deux souches de *Pediococcus* spp. (*P. acidilactici* R1001 et *P. pentosaceus* R1094) en présence de pathogènes. En effet, il a récemment été démontré que la souche *Lacticaseibacillus rhamnosus* GG présentait un effet antagoniste contre *S. typhimurium* lorsque le milieu était enrichi en glucose en macro-colonie [53].

3.2.4.2 Méthode

Toutes les expériences ont été amorcées par des cultures de 5 ml dans un milieu trypticase soja (TSB ; Biomérieux, France) préparé à partir de cryotubes stockés à -80°C de cultures bactériennes en glycérol, placé à 30°C pendant une nuit sans agitation. Après 5 secondes de vortex pour homogénéiser les cultures, 3 µL de deux cultures ont été prélevés et déposés dans un puits contenant 4 ml d'agar TSA 1,5% d'une plaque à six puits (35 mm de diamètre). Préalablement, la plaque avait été séchée sous une hotte pendant 1h30. La surface sèche de l'agar permet plus

facilement de maintenir une distance d'environ 2 mm entre les bords des deux gouttes. Les échantillons ont été séchés pendant 10 minutes sous une hotte, puis incubés à 30°C pendant 4 jours.

Les mêmes procédures ont été effectuées en préparant des solutions de sucre à 1% final dans du TSA à partir de poudre. Les sucres utilisés étaient le D-glucose (Sigma, Réf. G8270), le sucrose (Euromedex, Réf. 6868), le lactose (VWR/Merck, Réf. 1.04062), le dextrose anhydre (D-glucose, conditionnement Lallemand) et la maltodextrine (conditionnement Lallemand).

Les interactions ont été réalisées avec 3 réplicats biologiques provenant de cultures de nuits différentes Pour chaque réplicats biologiques, 2 réplicats techniques ont été réalisés provenant des mêmes cultures liquides, dans deux boîtes différentes. Des images représentatives ont été sélectionnées pour illustrer les résultats obtenus.

3.2.4.3 Résultats

3.2.4.3.1 Discrimination kin dans un modèle de macro-colonie avec des isolats environnementaux de souches de Bacillus spp.

Le caractère *kin* compatible des 18 souches de *Bacillus* spp. a été évalué en réalisant des interactions deux à deux avec le modèle en macro-colonie (**figure 4**). Pour présenter les résultats de manière concise, une *heatmap* illustrant les 324 interactions (18 x 18) a été générée.

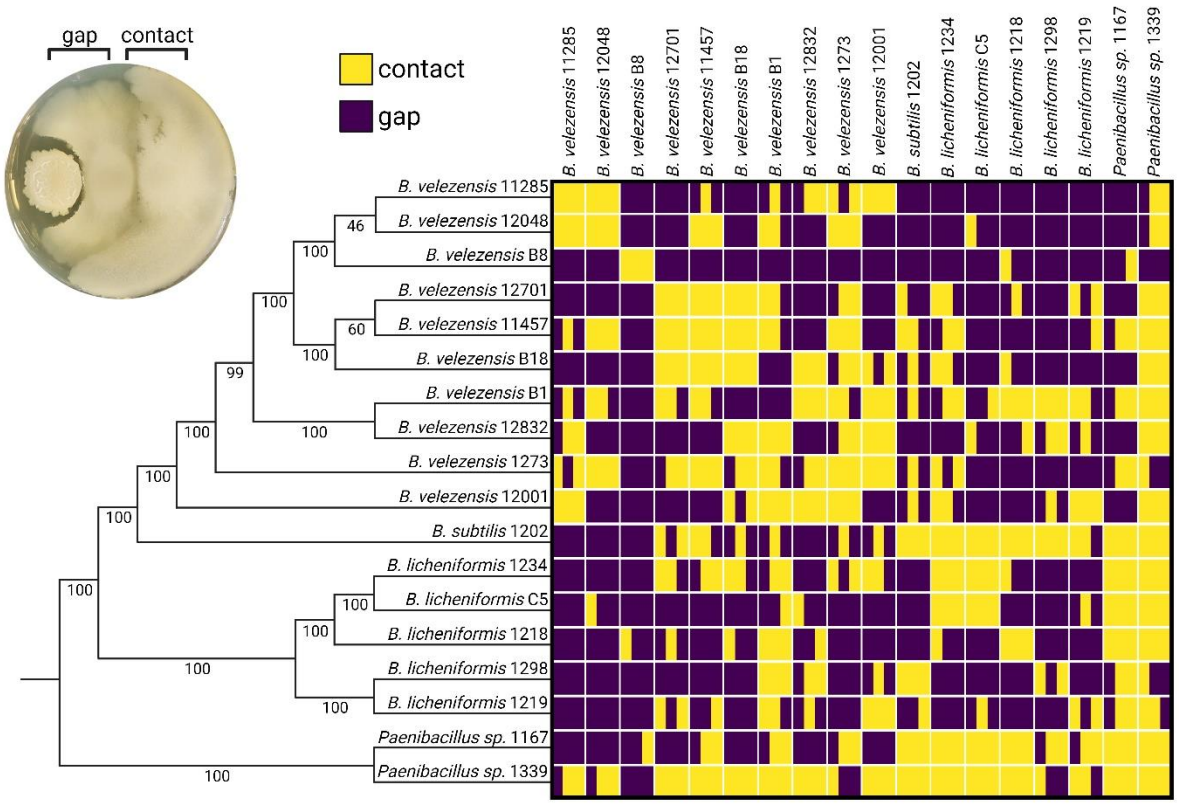

Figure 4: *Kin* discrimination dans un modèle de macro-colonie avec 18 souches de *Bacillus* spp. Un contact entre deux colonies est synonyme d'une interaction kin positive, et un espace comme une interaction *kin* négative. L'arbre phylogénétique est celui obtenu dans l'article 7.

Deux phénotypes d'interaction entre macro-colonies ont été observés selon la présence de contact physique entre les macro-colonies (représenté en jaune), ou la persistance d'un espace de séparation (représenté en violet). Dans ce contexte de macro-colonies, lorsque deux colonies de *Bacillus* spp. établissent un contact physique, elles sont considérées comme "*kin* positives". Il est intéressant de noter qu'aucune relation évidente n'a été observée entre la phylogénie des souches et les phénotypes de contact. Certaines souches regroupées au sein de l'arbre phylogénétique, telles que *B. velezensis* 12701, *B. velezensis* 11457 et *B. velezensis* B18, son capables d'établir un contact physiques entre leurs macro-colonies. Cependant, cette caractéristique n'est pas systématique, même pour les interactions impliquant deux colonies de la même souche provenant de deux cultures de nuit différentes, comme par exemple *B. velezensis* B1, *B. velezensis* 12832 ou *B. velezensis* 12001. A l'opposé, la souche *B. velezensis* B8 s'est avérée la

seule souche à ne pas former de contact physique avec aucune autre. Quant à la souche *Paenibacillus* sp. 1339, elle a principalement manifesté un phénotype kin positif avec chacune des 18 souches de Bacillus testées, sauf dans les interactions avec *B. velezensis* B8, *B. velezensis* 1273 et *B. licheniformis* 1298.

3.2.4.3.2 Détection d'activité antagoniste des souches de Bacillus spp. contre les agents pathogènes

Le modèle en macro-colonie a été adapté pour examiner le caractère antagoniste des *Bacillus* spp. vis-à-vis de quatre pathogènes distincts (*E. cecorum*, *S. aureus*, *E. coli*, *S. enterica* serovar Enteritidis), les mêmes que précédemment étudiés avec la MCBL. Les résultats sont présentés sous forme d'une *heatmap* dans la **figure 5**.

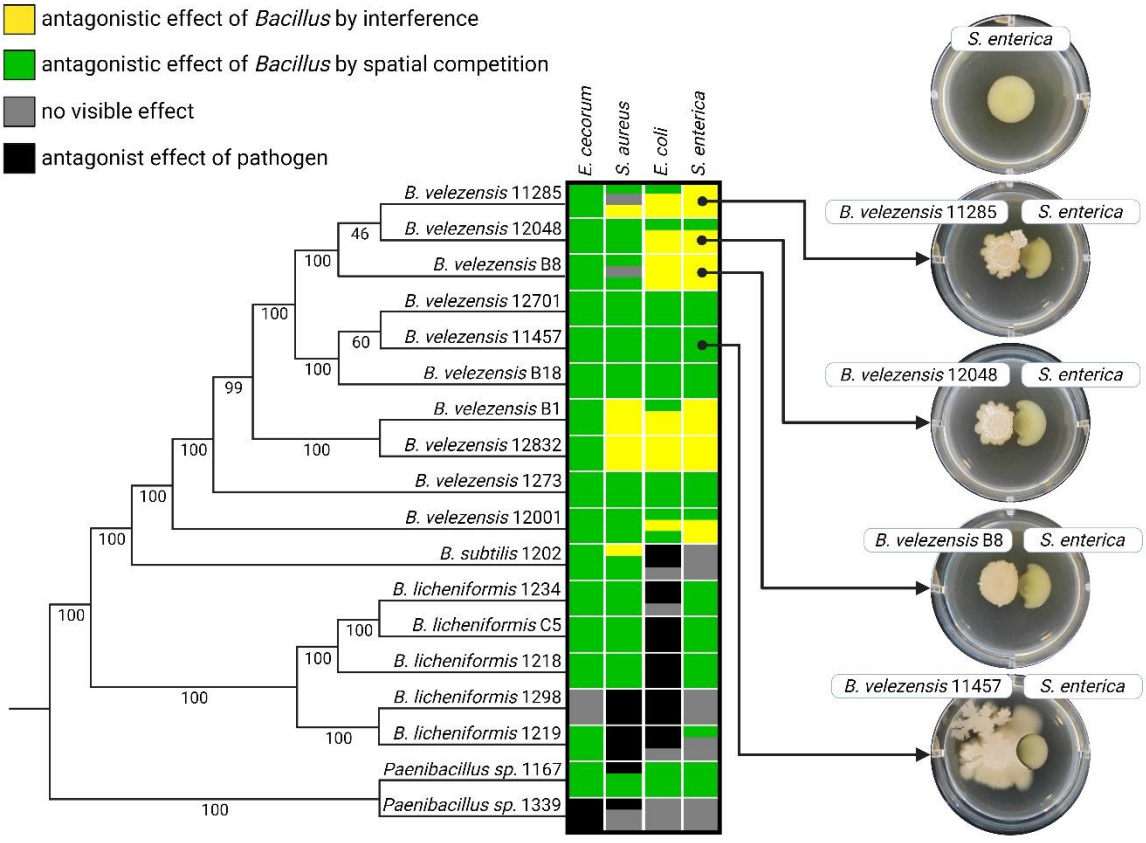

Figure 5: Heatmap des interactions entre deux macro-colonies de *Bacillus* spp. et de pathogènes. L'arbre phylogénétique est celui obtenu dans l'article 7. Des exemples représentatifs illustrent les différentes interactions observées.

Dans cette configuration expérimentale, une colonie de *Bacillus* spp. et une colonie de pathogènes sont formées à proximité l'une de l'autre, à partir d'un

dépôt de culture de nuit. Les situations où deux colonies entrent en contact sans qu'aucune ne prenne le dessus sur l'autre (interaction négative ou positive non décryptable), ou lorsque le pathogène manifeste une activité antagoniste le *Bacillus* spp. sont rares. En effet, la majorité des interactions testées révèlent une activité antagoniste des *Bacillus* spp. contre les pathogènes.

L'activité antagoniste entre macro-colonies se traduit par deux principaux phénotypes, la persistance d'un espace séparant les deux colonies ou que la macro-colonie du *Bacillus* spp. recouvre le pathogène entravant ainsi sa croissance. L'absence de contact entre les deux colonies illustre une compétition par interférence. Le recouvrement ou l'absorption d'une microcolonie par l'autre résulte d'une activité de type spatiale. La libération de molécules par les *Bacillus* spp. qui inhibent la croissance du pathogène est probablement à l'origine de l'espacement entre les deux colonies. Il convient de noter que les phénotypes d'interactions peuvent être différents pour un même *Bacillus* spp. en présence de différents pathogènes. Par exemple, la souche *B. velezensis* 12832 recouvre la colonie d'*E. cecorum* tandis qu'une interférence est observée avec *S. aureus*, *E. coli* et *S. enterica*.

3.2.4.3.3 Impact des sucres sur les phénotypes d'interaction

L'effet de sucres solubilisés dans la gélose a été examiné en ce qui concerne la morphologie des macro-colonies de *B. velezensis*, *Pediococcus* spp. et des pathogènes (*E. cecorum*, et *S. enterica*) (**Figure 6**).

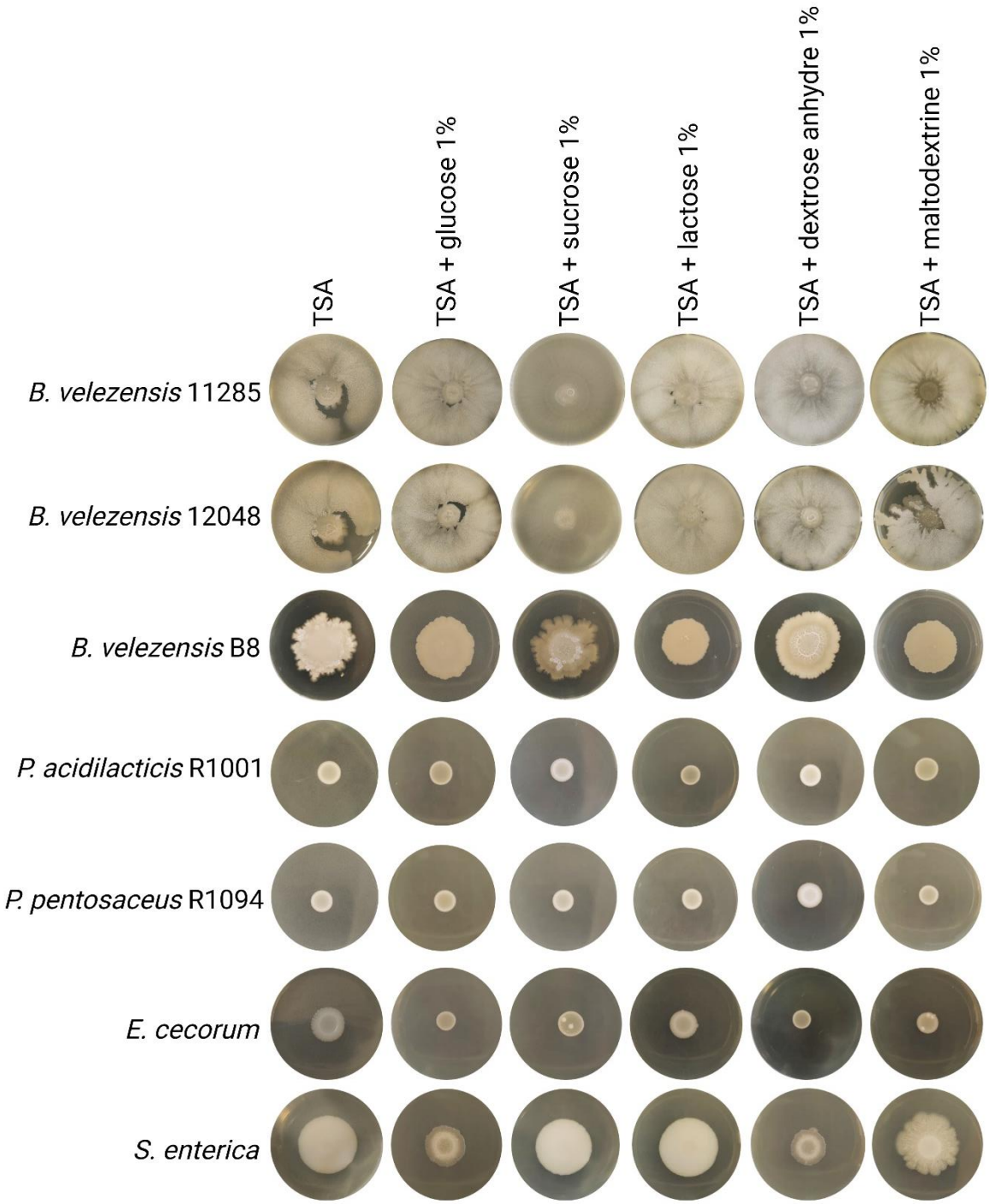

Figure 6: Formation des macro-colonies de souches candidates et de pathogènes en fonction de l'incorporation ou non de sucres dans le milieu gélosé. Les photos ont été prises après 4 jours d'incubation. Des images représentatives des réplicats sont montrées (N = 3).

En présence de sucrose, les colonies de *B. velezensis* affichent une structure moins organisée que les témoins sans sucre, notamment pour les souches *B. velezensis* 11285 et *B. velezensis* 12048 qui recouvrent entièrement la surface. Lorsque de la

maltodextrine est ajoutée, la souche *B. velezensis* B8 forme une macro-colonie au centre doté d'une morphologie intensément ridée, contrairement au contrôle sans sucre. De manière intéressante, la morphologie des colonies de *Pediococcus* spp. ne semble pas être influencée par l'ajout de sucre. *E. cecorum* forme une macro-colonie identique au contrôle sans sucre lorsque du lactose est supplémenté au TSA, tandis que les autres conditions entraînent une diminution de la croissance. *S. enterica,* en présence de glucose et de maltodextrine, forme une colonie moins étendue mais plus structurée que sur TSA sans sucre. En particulier, des structures dendritiques sont observées en présence de maltodextrine.

Les mêmes expériences d'interactions mentionnées précédemment ont été reproduites entre les souches bénéfiques et *E. cecorum* et *S. enterica* sur du TSA supplémenté ou non avec les différents sucres . Les résultats sont présentés sous la forme d'une *heatmap* (**Figure 7)**.

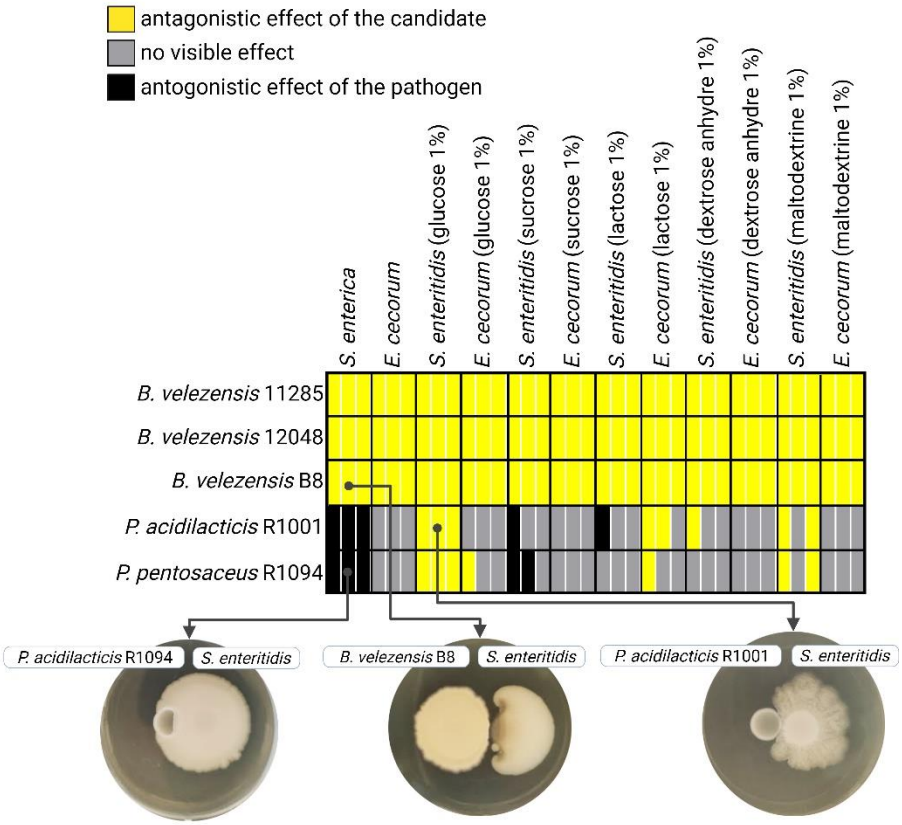

Figure 7: Influence des interactions en présence de sucres entre souches candidates et pathogènes dans un modèle de macro-colonie. Les photos ont été prises après 4 jours d'incubation. Des images représentatives des réplicats sont montrées (N = 3).

Bien que la morphologie des colonies de *B. velezensis* puisse varier en fonction de la nature du sucres, les interactions demeurent constantes, qu'il y ait ou non ajout de sucre dans le TSA. Contrairement aux *B. velezensis*, les interactions entre les pathogènes et les *Pediococcus* spp. sont modifiées par la présence de sucres. Les deux pathogènes manifestent une activité antagoniste envers la croissance des *Pediococcus* spp. sur TSA. Cependant, en présence de sucre, les deux colonies entrent en contact sans effet significatif observable. *Pediococcus* spp. présente une activité antagoniste contre la croissance des pathogènes. Cette observation est particulièrement remarquable en présence de glucose, de manière reproductible, et dans une moindre mesure en présence de lactose, de dextrose anhydre (uniquement pour la souche *P. acidilactici* R1001 contre *S. enterica*) et de maltodextrine.

3.2.4.4 Discussion et conclusion

Les études réalisées dans ce projet ont démontré la faisabilité d'utiliser le modèle en macro-colonie pour analyser les interactions entre diverses bactéries. Ce modèle se révèle une méthode simple pour la sélection de souches candidates bénéfiques, notamment *Bacillus* spp. et *Pediococcus* spp., qui possèdent un effet antagoniste contre des pathogènes ciblés. Les principales familles d'interaction sont discernables grâce à ce modèle. L'existence d'un espace entre deux colonies signale la présence de molécules sécrétées par un partenaire qui influe sur la croissance de l'autre, caractéristique d'un mode de compétition par interférence. Le recouvrement d'une colonie par une autre inhibe sa croissance en entravant son accès aux nutriments, témoignant d'une compétition spatiale pouvant se traduire par une compétition nutritionnelle. Cependant, dans le cas où les deux mécanismes sont présents et donc peu discriminables, l'interprétation du mode de compétition et plus compliqué, s'avère subjective subjectif car seulement basé sur l'observation, et donc expérimentateur dépendant.

A la différence du modèle de biofilm immergé étudié au MCBL pendant ce projet de thèse, les interactions entre bactéries ne se produisent consécutivement à la formation des biofilms. En conséquence, les mécanismes d'interactions au sein

des communautés déja établies en biofilm doivent différer de ceux qui s'établissent au sein de biofilms formés à partir d'un mélange de souches à l'état planctonique [54]. Par rapport à la MCBL, les phénotypes d'interactions entre *Bacillus* spp. et les pathogènes sont corrélés. Les modes d'interaction de *B. velezensis* contre les pathogènes dans le modèle de macro-colonie semblent plus se rapprocher du modèle de recrutement à T=24h, à l'exception des souches *B. velezensis* 12701 et *B. velezensis* B18, où l'effet est plus prononcé contre *S. aureus*, *E. coli* et *S. enterica* en macro-colonie (voir l'**article 7**). Cependant, la quantification des interactions en macro-colonie s'avère moins aisée en comparaison des expériences menées au MCBL. L'évaluation de la superficie des colonies en interaction comparée à celles se développant seules (contrôle) pourrait constituer une méthode de quantification.

Dans le contexte des expériences présentées, le modèle en MCBL macro-colonie présente le désavantage de devoir nécessiter qu'au moins l'un des partenaires expriment un fluorophore. En effet, les souches environnementales ne sont en général pas ou difficilement transformables. Ainsi, alors que seules trois souches partenaires ont été examinées au MCBL pour leurs interactions avec les 18 autres souches de *Bacillus* spp., le modèle en macro-colonie a permis d'explorer toutes les combinaisons d'interactions possibles (18x18). Cependant, le modèle n'a pas pris en compte les biofilms mixtes où deux souches différentes se développent ensemble. Pour les distinguer dans le même biofilm, une méthode de marquage similaire à celle utilisée dans le cadre des expériences de MCBL serait requise. Il faudrait avoir recours à la même approche dans le cas où les macro-colonies de deux souches se mélangent.

L'utilisation du modèle en macro-colonie pourrait être une première étape dans la sélection de souches pour des applications en biotechnologie, en permettant de cribler rapidement un grand nombre de candidats avant d'effectuer une caractérisation plus approfondie des interactions au moyen de la MCBL avec les meilleurs candidats. En effet, la MCBL permet non seulement de quantifier chacun des partenaires au cours du temps dans le biofilm, mais aussi d'étudier la spatialisation de ceux-ci dans la communauté.

4 DISCUSSION GENERALE ET PERSPECTIVES

Les travaux réalisés au cours de cette thèse ont permis de répondre aux objectifs scientifiques et industriels initialement définis. (1) Une démarche expérimentale basée sur un rationnel scientifique explicite a été développée pour améliorer le processus de sélection de souches en vue du développement de produits commerciaux de deuxième génération. Une méthode d'assemblage de souches basée sur leurs compatibilités en biofilm a permis d'identifier des consortiums avec des effets améliorés par rapport aux souches seules. Cette démarche constitue une réelle avancée pour l'industrie qui formule régulièrement des produits composés de plusieurs souches sélectionnées individuellement, sans nécessairement vérifier la compatibilité des souches entre elles ou la réelle plus-value de l'association. (2) Une méthode de prélèvement des communautés microbiennes associées aux surfaces des bâtiments d'élevages hors-sol a également été mise au point dans le contexte d'élevages industriels, permettant l'étude de la structure des biofilms capturés. Les communautés autochtones des surfaces des bâtiments d'élevage jusqu'alors peu documentées ont été étudiées ainsi que l'effet d'un produit commercial sur leur modulation.

Les résultats de ce volet de mes travaux de thèse sont encore en cours de valorisation avec plusieurs articles scientifiques publiés ou en en préparation, ainsi qu'une licence d'exploitation en copropriété INRAE/Lallemand d'une souche isolée et caractérisée dans le cadre du projet.

Cette section clôture le manuscrit en abordant les perspectives découlant de cette étude, tant du point de vue scientifique que de l'industrie. Elle met en lumière les réalisations accomplies et les connaissances acquises. De surcroît, elle explore les défis technologiques et industriels, tout en traçant les pistes à suivre pour les futures recherches dans ce domaine. Elle identifie également des opportunités d'amélioration pour les biofilms positifs à visée commerciale.

Vers une compréhension des mécanismes impliqués dans l'effet antagoniste des biofilms positifs sur les bactéries indésirables

Toutes les études d'interactions menées dans ce projet ont été réalisées sous forme de biofilms. Elles reflètent ainsi le mode de vie microbien le plus courant sur Terre, et celui présent sur les surfaces des bâtiments d'élevage [11,55]. Les principales familles d'interactions telles que l'interférence et la compétition spatiale/nutritionnelle ont été détectées dans nos systèmes. Cependant, une analyse approfondie des mécanismes impliqués reste à effectuer. Par exemple, dans le cas des interactions entre *B. velezensis* et *E. cecorum* dans le modèle de co-inoculation, une croissance suivie d'un déclin jusqu'à la disparition totale du pathogène n'est observée que lorsque *E. cecorum* est avantagé (article 7). Un modèle proie-prédateur Lotka-Volterra décrit alors cette interaction et suggère qu'une molécule active (ou un ensemble de molécules) sécrétée par *B. velezensis* pourrait impacter la viabilité d'*E. cecorum*. Dans toutes les autres conditions, une interaction décrite par le modèle de Jameson avec une diminution du temps de génération sans décroissance du pathogène est observée, ce qui suggère qu'une certaine quantité de *E. cecorum* peut être détectée par *B. velezensis* et induire alors la sécrétion de molécules bactéricides. Ces composés n'ont pas été identifiés à ce stade. Avec le génome des souches candidates à notre disposition, l'étude ciblée des gènes codant pour des molécules antimicrobiennes pourrait être entreprise afin d'identifier des candidats, en utilisant par exemple l'outil de recherche antiSMASH [56]. L'exploration des molécules sécrétées dans les surnageants des biofilms positifs pourrait également être réalisée afin d'identifier des gènes candidats déjà documentés pour leur activité antibactérienne, et ainsi améliorer le processus de sélection de souches à l'avenir. Une telle étude peut être envisagée en prélevant le surnageant de biofilms positifs matures, suivie d'une analyse biochimique des composés présents, par exemple en utilisant des méthodes telles que la spectrométrie de masse ou la résonance magnétique nucléaire [57].

L'identification des mécanismes exige une analyse minutieuse de la formation des biofilms sur une période étendue, en prenant en compte un grand nombre de

points temporels afin de permettre une modélisation précise des interactions. De plus, l'utilisation de différentes proportions initiales (définis par le ratio d'adhésion dans notre étude) des deux partenaires nécessite une multiplication des expériences. Cependant, la variation de ces ratios initiaux est essentielle et doit être rigoureusement mise en place pour étudier les mécanismes. La variation des ratios a permis, par exemple, de démontrer que l'exclusion d'*E. cecorum* se produisait de deux manières distinctes en fonction de sa quantité initiale relative par rapport à *B. velezenis*. Enfin, nous avons également prouvé que *S. enterica* était exclu par un biofilm préexistant de *B. velezensis*, en utilisant deux modèles d'étude expérimentaux distincts (co-inoculation et recrutement décrit dans l'article 7). Toutes ces expériences requièrent i) un espace de stockage numérique conséquent pour les données, ii) des capacités de calcul pour le traitement des images en microscopie, iii) la possibilité de suivre le devenir des partenaires distinctement dans l'échantillon, iv) ainsi que du temps, ce qui limite considérablement le nombre d'expérimentations possibles.

Les études réalisées au MCBL ont permis de quantifier les interactions en mesurant le biovolume des deux partenaires au sein du biofilm mixte. Cette approche microscopique permet également une étude structurale plus fine des biofilms, peu exploitée lors du projet. Des variables quantitatives permettant de décrire la structuration du biofilm sont disponibles dans les boîtes à outils de statistiques spatiales (BiofilmQ, IMARIS, http://spatstat.org/) [58,59]. Par exemple, avec nos données, nous avons observé dans le modèle de recrutement à T=24h que certains pathogènes se développent sous forme de clusters de différentes tailles sur le biofilm de *Bacillus* spp. Dans le contexte d'une application en biofilm positif, il serait plus judicieux de privilégier les *Bacillus* spp. permettant la formation de clusters de pathogènes de taille réduite. En effet, à mesure que les pathogènes forment des clusters de plus grand diamètre, les gradients deviennent plus prononcés et limitent la propagation des molécules au cœur du biofilm, réduisant l'efficacité des biocides appliqués lors des procédures de nettoyage et de désinfection [8]. Dans cette optique, il est envisagé d'améliorer le processus de sélection en accordant une plus grande importance aux statistiques spatiales de

ces systèmes multi-espèces.

Nouvelles règles raisonnées d'assemblage de communautés

Des produits utilisant des cocktails de microorganismes sont disponibles sur le marché pour des applications en biotechnologie. Cependant, le rationnel de l'association des souches n'est souvent pas démontré. Dans notre étude, différentes souches candidates ont été sélectionnées individuellement pour leur fort effet antagoniste sur la croissance de bactéries spécifiques. Or, des interactions antagonistes entre les souches du produits pourraient exister et être causées par des mécanismes tels que l'acidification du milieu ou la sécrétion de molécules antimicrobiennes à large spectre [60,61], diminuant ainsi ces performances. Dans le cadre du projet, la capacité des souches candidates à former un biofilm mixte stable sans exclusion de partenaires a été évaluée dans le but d'identifier des consortiums compatibles. A notre connaissance, c'est la première fois qu'une telle vérification est entreprise pour des applications en biofilm positif. Une fois ces consortiums identifiés, les propriétés émergentes inhérentes aux associations ont été étudiées, telles qu'une meilleure capacité de colonisation des surfaces et une activité antagoniste plus prononcée sur la croissance des pathogènes par rapport aux souches individuelles.

Quel est le rationnel de l'utilisation de consortiums par rapport à des souches pures? Nous avons observé que les associations entre différentes souches du genre *Bacillus* spp. sont hautement spécifiques. Ainsi, seulement 16,7% des associations obtenue par MCBL se sont avérée compatible (i.e. sans l'exclusion d'un partenaire) dans des biofilms 2 souches. Nous avons démontré que des consortiums 3 souches de *B. velezensis kin* compatibles forment un biofilm mixte stable couvrant mieux les surfaces en comparaison des souches seules et aux consortiums 2 souches. De plus, l'association de *B. velezensis* avec *Pediococcus* spp. permet un recouvrement de surface et un biovolume optimal et démontre un antagoniste significativement supérieur par rapport aux souches uniques, parfois synergiques, contre *S. enterica*. Intuitivement, l'idée de regrouper plusieurs

souches ayant individuellement des effets bénéfiques, sans nécessairement les amplifier en cocktail par rapport à une souche unique, pourrait être justifiée en considérant qu'au moins l'une d'entre elles serait capable de prospérer dans une niche spécifique. C'est pourquoi il serait intéressant d'étudier le pouvoir de colonisation dans différentes conditions physico-chimiques (exemple : gradient de température, pH, sels) de chaque souche afin d'identifier les éventuelles zones de recouvrement où une souche pourrait se développer tandis que les autres ne le peuvent pas.

Des études récentes ont démontré que des souches de *Bacillus* spp., *kin* positives dans un modèle de swarming, et proche phylogénétiquement, étaient capables de former des biofilms mixtes dans des modèles de swarming et de pellicule [62]. Or, dans nos expériences, la discrimination *kin* effectuée dans un modèle de macro-colonie ne corrèle pas strictement avec la capacité des souches à former des biofilms immergés mixtes. En effet, bien que la souche *B. velezensis* B8 soit capable de former un biofilm mixte immergé avec les souches *B. velezensis* 12048 et *B. velezensis* 11285, qui lui sont phylogénétiquement proche, une exclusion est observée lorsque *B. velezensis* B8 interagit avec les deux autres souches dans un modèle de macro-colonie. Ces deux modèles présentent des différences car, dans un modèle de macro-colonie, les interactions entre les deux partenaires se produisent lorsque les biofilms ont déjà atteint une certaine maturité. En revanche, dans un biofilm immergé, les deux partenaires sont sous forme de cellules isolées au début des interactions. Il est donc difficile de réaliser des corrélations entre une discrimination *kin* évaluée sur un milieu gélosé et une compatibilité entre souche en biofilm immergé. Il est donc préférable de rester dans le même modèle d'étude pour réaliser ce type de corrélations.

Les mécanismes moléculaires impliqués dans la compatibilité des souches bénéfiques à former des biofilms mixtes stables n'ont pas encore été étudiés. En effet, la compatibilité entre les souches est basée uniquement sur leur capacité à former des biofilms mixtes, et donc sur les biovolumes respectifs des deux partenaires après 24h d'incubation. Le mutualisme (+/+), le commensalisme (+/0), le neutralisme (0/0), ou même l'exploitation (+/-) d'un partenaire par l'autre sans

une exclusion totale pourraient expliquer la persistance des deux partenaires dans le biofilm, sans qu'aucune souche ne soit complètement exclue [63]. Des cinétiques permettant l'observation de la formation de biofilm mixte, comme effectuées dans le cadre du projet entre les *B. velezensis* et des pathogènes GFP, pourraient être réalisés pour identifier les grandes familles d'interactions entre les souches bénéfiques du consortium. Une étude métatranscriptomique permettrait d'analyser les variations d'expression génique en présence d'un partenaire. Cette approche permettrait par exemple d'identifier des gènes candidats impliqués dans l'interaction et de décrypter les voies potentielles de co-métabolisme [64,65]. Parallèlement, une étude métabolomique des surnageants des partenaires, qu'ils soient seuls ou en mélange, pourrait compléter ces résultats [57]. Il serait intéressant d'identifier les gènes liés à la capacité des souches à former des biofilms mixtes, afin d'effectuer une première étape de sélection des souches sur la base des génomes. Par exemple, un récent article met en évidence l'influence de la flagelline sur la discrimination *kin* chez *B. velezensis,* nous permettant ainsi l'identification de gènes candidats impliqués dans la formation de consortiums [66].

Dans notre étude, seuls la formation des biofilms et le potentiel antagoniste des consortiums ont été étudiés et comparés par rapport aux souches individuelles. Il est envisageable d'explorer d'autres propriétés émergentes de ces associations. Les *Bacillus* spp. étant capables de se déplacer sur différentes surfaces par leur capacité à swarmer, contrairement au *Pediococcus* spp. non motile, il serait intéressant d'étudier le transport des *Pediococcus* spp. par les *Bacillus* spp. Le "*hitchhiking*", est un sujet émergeant dans la communauté scientifique décrivant le transport d'un microorganisme non-motile par un organisme motile. Ce phénomène peut jouer un rôle important dans la dispersion des organismes microscopiques, leur permettant de coloniser de nouveaux habitats ou bien d'interagir avec d'autres espèces [67]. Par exemple, il été décrit que les spores de *Streptomyces coelicolor* sont transportées par *B. subtilis* via une interaction entre les flagelles de ce dernier et une protéine présente à la surface des spores de *S. coelicolor* [68]. Il serait intéressant de tester le transport de bactéries lactiques par

des *Bacillus* spp. avec des souches préalablement sélectionnées pour leurs effets bénéfiques en biofilm positif afin de rendre plus homogène la colonisation des surfaces.

Enfin, il est important de prendre en considération que tous les individus ne participent pas de façon équivalente au fonctionnement de la communauté [69]. Ainsi, il serait intéressant de faire varier les ratios des différents candidats bénéfiques pour analyser l'activité antagoniste contre les pathogènes et évaluer la formation du biofilm positif en consortiums.

Plusieurs défis technologiques entravent encore l'optimisation de l'assemblage de consortiums. Comme évoqué précédemment, la mise en place d'expériences de microscopie reste une tâche complexe. Par ailleurs, nous n'avons pas encore examiné les cinétiques de formation des consortiums bénéfiques. Comprendre l'impact de chaque membre du consortium sur la formation du biofilm positif et sur la compétition vis-a-vis de bactéries indésirables pourrait permettre d'optimiser ces associations. Il serait donc nécessaire, pour chaque combinaison, d'effectuer des expériences avec différents ratios initiaux des deux partenaires. Actuellement, réaliser ces études à haut débit de souches semble peu envisageable. Une approche prometteuse pourrait être l'utilisation de l'intelligence artificielle (IA) pour prédire le comportement des souches au sein du consortium en se basant par exemple sur leur croissance individuelle et leur génome, réduisant ainsi le nombre d'expériences nécessaires [70]. Dans le cas des consortiums, la visualisation de tous les membres du biofilm au fil du temps devient complexe lorsque le nombre de souches dépasse trois. Cela est dû à la nécessité d'éviter les chevauchements spectraux des fluorophores utilisés, afin d'éviter tout biais potentiel. Pour ces études, il est également essentiel d'utiliser des souches exprimant des protéines fluorescentes, mais il est souvent difficile de réaliser de telles manipulations génétiques dans le cas de souches sauvages.

Perspectives d'amélioration du pipeline de sélection de souche

Dans ce projet de recherche, une méthode innovante de sélection et d'association de souches a été développée dans le but de proposer des produits commerciaux de nouvelle génération. Les études mécanistiques telles qu'elles ont été exposées dans ce travail de thèse ne sont pas réalisables directement sur le terrain. Bien que des allers-retours soient effectués entre l'échelle du laboratoire et les études sur le terrain pour tester le produit, il serait judicieux d'incorporer des étapes intermédiaires visant à caractériser le plus fidèlement possible les interactions en conditions réelles. Il est possible que les interactions observées et quantifiées au laboratoire (utilisation de milieux de culture riches, petits volumes, biofilm immergé) ne soient pas identiques à celles présentes sur le terrain. L'utilisation de modèles qui imitent fidèlement les conditions sur le terrain permettrait d'étudier les interactions de manière plus réaliste, même si cela génère des débits de données plus faibles en raison de la complexité accrue des expériences à mettre en place. Ainsi, il serait intéressant de moduler des paramètres tels que la température, l'humidité, le pH, le milieu de culture ou les propriétés du substrat sur lequel le biofilm se développe. En effet, il est connu que la surface du matériau peut influencer les interactions [71] et ce, aussi dans le contexte d'élevage où nous avons observé des biofilms différents sur l'acier galvanisé et sur le PVC (article 3). Un milieu de culture spécifique de l'élevage étudié pourrait aussi être utilisé. Étant donné que les surfaces des coupons étaient principalement recouvertes de fèces d'animaux, il serait pertinent d'utiliser un milieu de culture qui imite leur composition. Il pourrait être intéressant d'utiliser un modèle de biofilm à l'interface entre une surface humide et l'air, car il serait plus représentatif de l'application réelle, contrairement à un modèle en biofilm immergé.

Les interactions caractérisées dans nos études au laboratoire ne prennent pas non plus en compte l'influence du microbiote naturellement présent sur les surfaces d'un bâtiment d'élevage. Il serait pertinent de concevoir un consortium simplifié représentatif du microbiote autochtone de l'élevage, possédant une composition

définie, stable et reproductible dans le temps. Ainsi, l'étude de son influence sur les interactions entre biofilm positif et pathogène et entre les différentes souches du biofilm positif dans différents modèles de laboratoire pourrait être effectuée.

La segmentation des images de microscopie de fluorescence pour extraire des valeurs quantitatives descriptives des biofilms représente une étape critique et délicate lors du traitement d'images. Il est fréquent d'observer des erreurs qui nécessitent une surveillance régulière des analyses et des ajustements des paramètres de segmentation afin de les minimiser. Ces erreurs sont particulièrement présentes lors de traitement de cinétique où l'intensité de fluorescence varie grandement au cours du temps. Ainsi, un biais de l'analyse est causé par l'expérimentateur qui choisit lui-même les paramètres de segmentation. Un temps non négligeable est ainsi ajouté à l'analyse. L'intégration de l'IA et plus particulièrement de l'apprentissage profond (deep learning) pour segmenter les images, constitue une alternative prometteuse afin de réduire considérablement le temps d'analyse et de corriger un grand nombre de biais. Grâce à ces nouveaux outils, les paramètres de segmentation peuvent être identifiés et appliqués automatiquement, même si le niveau de fluorescence varie au cours du temps. Cependant, il est essentiel de disposer d'un vaste ensemble de données préalables pour entraîner efficacement le modèle [72]. L'utilisation de l'IA pourrait aussi permettre de faire des liens entre les génotypes, la morphologie des biofilms, et l'activité antagoniste pour permettre d'identifier des marqueurs prédictifs des interactions en vue d'aide à la décision pour effectuer la sélection de souches. Par exemple, il a été montré récemment que les interactions entre des bactéries cultivables peuvent être décrites par la croissance des souches individuels des mélanges [70]. Le même principe pourrait être appliqué à notre ensemble de données afin de simuler des interactions sous forme de biofilm entre des souches bénéfiques et indésirables ou entre différentes souches bénéfiques. L'utilisation de ces approches nous permettrait de sélectionner des mélanges d'intérêt en fonction des marqueurs identifiés (gènes, paramètres structuraux des biofilms), évitant ainsi l'examen systématique de toutes les combinaisons par expérimentation, ce qui se traduirait par une économie de temps considérable [73].

La culturomique ciblée représente une méthode prometteuse qui pourrait être utilisée pour isoler à haut débit des microorganismes d'intérêt (genres ou espèces pré définis) de communautés complexes [74]. Cette approche pourrait être réalisée à partir du microbiote isolé de surfaces des bâtiments d'élevage. En effet, étant donné que ces souches seront isolées de ces surfaces, il est probable qu'une fois amplifiées industriellement et appliquées artificiellement, elles se révèlent suffisamment compétitrices dans ce biotope pour les coloniser à nouveau.

Enfin, il pourrait être envisagé de réaliser des expériences préliminaires de compétition pour un screening rapide avant de recourir à la MCBL. Des expérimentations d'interaction en macro-colonies [49,51,52,75] ou en croissance planctonique [76] pourraient être utilisées. Ces approches sont plus faciles à mettre en place, moins coûteuses et moins chronophages que la MCBL.

Validation des critères d'industrialisation des candidats bactériens

Avant d'initier les phases de développement d'un produit de nouvelle génération, il est essentiel de réaliser un certain nombre de vérifications afin d'évaluer la faisabilité industrielle. Parmi les vérifications, (1) des tests de faisabilité de production des souches candidates sont essentiels, ainsi (2) qu'une analyse des génomes dans le but d'identifier de potentiels gènes de virulence et de résistance aux antibiotiques doit être effectuée, tout comme nous l'avons fait pour les souches isolées de la surface des bâtiments d'élevage avicole (article 6).

(1) Les expérimentations effectuées au laboratoire dans le cadre de cette thèse ont été conduites dans de petits volumes (<10 mL, souvent dans 200 µL), à moyen/haut débit. Ainsi la croissance des souches candidates n'ont pas été réalisées dans des conditions mimant les conditions industrielles en bioréacteurs. Or, la croissance des microorganismes ne se comporte pas forcément de la même manière à une échelle laboratoire et industrielle. C'est pourquoi la production de ces souches dans des fermenteurs mimant les conditions de production industrielle doit être réalisée dans le but d'étudier la faisabilité d'un

développement et d'un transfert industriel. Cette étape de faisabilité intègre généralement une première estimation des coûts de production envisagés (Lallemand, communication). En effet, diverses difficultés techniques peuvent être rencontrées lors de cette étape. Par exemple, il est possible que les souches forment trop d'agrégats rendant difficile leur récolte et leur séchage. La résistance des cellules au séchage est un autre critère essentiel qui peut orienter les choix industriels. Dans le cas des *Bacillus* spp., la présence de bactériophages endogènes est également une entrave récurrente à la génération de biomasse en fermenteur. Enfin, les conditions de production des souches peuvent aussi impacter, non seulement les rendements et les coûts de production, mais aussi les phénotypes des souches en application [77].

(2) Dans les cas des gènes de résistance aux antibiotiques une attention particulière doit être portée au caractère intrinsèque ou acquis de la résistance, tant au niveau génotypique que phénotypique. Ainsi cette vérification doit être couplée à des tests phénotypiques de résistance aux antibiotiques d'intérêt clinique en suivant par exemple les recommandations de l'EFSA (European Food Safety Authority) ou de l'EFFCA[1] (European Food and Fermentation Cultures Association) pour la caractérisation de la sécurite d'utilisation des microorganismes en alimentation animale et humaine [78].

Optimisation de la formulation d'un produit de nouvelle génération par ajout de composés fonctionnels

Une étape d'optimisation de la formulation est nécessaire en vue de l'industrialisation d'un produit commercial de nouvelle génération. L'ajout de composés permettant l'amélioration des propriétés des biofilms positifs peut être envisagé. La plupart des surfaces de bâtiment d'élevage étant verticales, comme

[1] Industry guidance for quality, safety, effectiveness, and labelling of food cultures (preparations) are under development by EFFCA members.

les murs, un lessivage du produit est possible, limitant ainsi l'implantation d'un biofilm positif. Il est envisagé d'ajouter des composés tels que des gommes végétales pour rendre le produit plus visqueux et favoriser l'adhésion du produit aux surfaces [79]. Chez *B. amyloliquefaciens*, le sucrose a été décrit comme stimulant la production de d'acide poly-γ-glutamic, un biopolymère impliqué dans la structuration du biofilm [80]. Ce sucre promeut aussi la motilité de surface de *B. subtilis*, permettant par exemple une meilleure colonisation des racines [81] et la croissance et production de lactate accrue chez *P. pentosaceus* [82]. Il a été montré récemment que l'ajout de sucre fermentescibles dans le milieu permettait l'amélioration de l'activité antagoniste de *Lacticaseibacillus rhamnosus* GG par la sécrétion de métabolites et protéines ciblant *S. enterica serovar typhimurium* et *E. faecalis* [53]. L'ajout de sucre pour faciliter la croissance du biofilm positif peut être envisagé, cependant, il est nécessaire de s'assurer que ces sucres ne favorisent pas la croissance des bactéries indésirables. De la même manière, l'ajout de post/pré-biotiques peuvent être envisagés afin d'augmenter l'effet de compétition ou stimuler la croissance du biofilm positif [83].

Des biofilms résiduels sont présents après l'application des procédures de N&D, entre deux lots d'animaux. Ce microbiote de surface va donc entrer en compétition avec le biofilm positif. L'utilisation d'enzymes permettant de dégrader la matrice de ces biofilms résiduels, pouvant contenir des microorganismes indésirables, est une solution innovante dans ce domaine et complémentaire aux processus de N&D [84]. Nous avons montré que la structure des biofilms formés par certaines souches de *B. licheniformis* était dépendante de la présence de l'ADNe dans la matrice. La formation de biofilms par ces souches peut être fortement réduite par application de DNAse sur les surfaces. L'ajout de certaines enzymes ou de cocktails d'enzymes à spectres plus larges qui n'affecteraient pas la formation de biofilms par les souches qui composent le produit est une piste d'évolution de la formulation.

Enfin, les bactéries sont généralement produites à l'échelle industrielle dans des réacteurs où elles croissent sous forme planctonique dans des conditions physico-chimiques permettant d'obtenir une biomasse optimale. Une piste d'amélioration serait de les produire sous forme de biofilm à échelle industrielle, puis de les

lyophiliser avant application sur des surfaces de bâtiment d'élevage. En effet, il a été démontré qu'une pré-croissance de souches probiotiques en microcolonies dans des billes de pectine de calcium augmente l'effet probiotique chez la souris comparé aux mêmes souches cultivées sous forme planctonique [24]. De plus, ce type de formulation sous forme de biofilm pourrait permettre une résistance accrue à différents stress lors de la production et de l'utilisation du produit.

Mise en place d'une méthode de capture des biofilms environnementaux des bâtiments d'élevage

Le projet de thèse a abouti à l'élaboration d'une méthode novatrice pour l'étude des biofilms environnementaux présents dans les bâtiments d'élevage. L'objectif de cette méthode est d'évaluer l'impact des biofilms positifs commerciaux sur la structure du microbiote de surface des installations d'élevage, tout en examinant les communautés microbiennes naturellement présentes. La force de cette approche est sa capacité à fournir une représentation en trois dimensions des biofilms, contrairement aux méthodes conventionnelles telles que les écouvillonnages ou les prélèvements en boîte, qui ne prennent pas en compte la morphologie des biofilms. Cette morphologie revêt une importance cruciale en raison de son rôle dans la résistance de ces biofilms.

La faisabilité de la méthodologie de prélèvement *in-situ* et d'analyse *ex-situ* au laboratoire des communautés microbiennes attachées aux surfaces a été mise en pratique dans deux systèmes d'élevage, à savoir les élevages avicoles et porcins. Dans les deux cas, la caractérisation des communautés de surface a été possible. Le système d'élevage avicole présente plusieurs avantages par rapport à l'élevage porcin, notamment en ce qui concerne la fixation des coupons sur site et leur analyse au laboratoire. En effet, malgré une fixation appropriée des échantillons sur les murs en contact avec les animaux, un nombre plus important de coupons se sont détachés dans le cas de l'élevage porcin. Le contact plus étroit entre les porcs et les coupons positionnés sur les murs explique le détachement accidentel de ces coupons par frottement contre les parois où ils sont positionnés. De plus, les biofilms présents sur les coupons prélevés dans les élevages porcins

présentaient une forte charge en matière fécale, répartie de manière hétérogène sur la surface des coupons. En revanche, les coupons prélevés d'élevage avicole étaient quant à eux plus homogènes, rendant l'étude au MCBL plus aisée. Par conséquent, le reste du projet s'est concentré sur l'étude de ce système avicole.

Les études de structures de communautés microbiennes de surfaces de bâtiments d'élevages avicoles et porcins, telles que présentées dans ce manuscrit, font partie des premières du genre, en particulier en ce qui concerne la caractérisation de la morphologie des biofilms au MCBL. Ces résultats mettent en évidence une forte activité métabolique au sein de ces communautés microbiennes. Une perspective intéressante serait d'étudier l'interaction entre le microbiote intestinal des animaux et la structure et la composition du microbiote de surface des bâtiments d'élevage. Cela pourrait être réalisé en prélevant des échantillons de microbiotes intestinaux et en les analysant simultanément aux coupons prélevés sur les surfaces.

La méthodologie a été employée avec succès pour étudier l'effet de l'application d'un produit commercial, composé de bactéries formant des biofilms positifs, sur le microbiote de surface des bâtiments d'élevages avicoles. Les résultats ont démontré que cette intervention pouvait moduler la structure tridimensionnelle des biofilms, le nombre de bactéries viables et cultivables, ainsi que la diversité des populations présentes. Un point essentiel de notre étude réside dans la démonstration d'une modulation du microbiote environnemental exclusivement au cours des premières semaines de l'élevage. Cette observation ouvre des perspectives pour rechercher des solutions susceptibles d'avoir un impact durable. Cette conclusion constitue une piste de recherche concrète résultant de notre travail. Cependant, cette méthode présente souvent des limitations en ce qui concerne la quantification des effets des biofilms positifs à une échelle plus fine, principalement en raison de la résolution limitée de l'analyse des séquences du gène codant l'ARNr 16S. L'utilisation de la métagénomique, bien que plus coûteuse et nécessitant une analyse plus complexe, permettrait l'analyse de la diversité et des fonctions présentes au sein de la communauté [85]. Une amélioration possible de l'analyse serait de pouvoir suivre les différentes souches

présentes dans le produit sur les surfaces en développant une qPCR (PCR quantitative) pour quantifier la présence de gènes spécifiques des souches constituant les biofilms positifs. Toutefois, il serait important de s'assurer au préalable que ces gènes soient bien spécifiques de la souche et absents dans la communauté microbienne autochtone de l'élevage.

Les études réalisées n'ont pas permis d'analyser précisément les effets d'un biofilm positif sur des bactéries pathogènes présentes dans l'environnement d'élevages. Pour aborder cette question, il serait nécessaire de travailler avec des pathogènes préexistants sur les surfaces des bâtiments, ce qui est difficile à réaliser en pratique. De plus, les techniques de metabarcoding utilisées actuellement ne sont pas assez précises pour détecter et quantifier ces pathogènes. Il faudrait avoir recours à des qPCR ciblant un ou des gène(s) spécifique(s) de ces pathogènes [86,87].

Les études présentées se focalisent sur les communautés microbiennes attachées aux surfaces. Cependant, l'impact de l'application de souches bénéfiques sur l'holobionte, englobant à la fois l'hôte et sa communauté microbienne n'a pas été étudié [88]. Le principal objectif de l'utilisation de biofilms positifs est de limiter la transmission de bactéries indésirables à l'animal en réduisant leur apparition ou développement sur les surfaces. En perspective, il est également envisagé d'ajouter à l'analyse des données relatives aux performances globales des animaux (par exemple : qualité des fèces, poids, aspect, maladies), le taux de mortalité en présence ou non de biofilm positif ainsi que l'influence du traitement sur la modulation du microbiote intestinal.

Quel avenir pour les biofilms positifs?

Les réglementations de plus en plus strictes visant à réduire l'utilisation d'intrants chimiques tels que les molécules biocides ou les antibiotiques incitent les producteurs à repenser leurs approches techniques. Cette évolution s'inscrit dans le contexte du concept "*One Health*", qui met l'accent sur l'amélioration de la qualité de vie des animaux, la réduction des zoonoses et de la transmission de

maladies au sein de l'élevage. Par conséquent, il est essentiel de trouver des alternatives aux traitements chimiques antimicrobiens. L'utilisation des biofilms positifs fait partie de ces solutions innovantes, utilisées en complément des processus de N&D. Cependant, même si certains produits sont disponibles sur le marché, les industriels sont encore réticents à investir dans de telles solutions en raison d'une réglementation floue et changeante encadrant ces nouvelles approches. De plus, il existe encore très peu d'études, les principales étant celles écrites lors de ce projet, décrivant de façon standardisée les effets de l'application de tels produits sur le microbiote de surface de bâtiment d'élevage et sur les bactéries indésirables. Il est donc nécessaire de continuer à investiguer les effets potentiels des biofilms positifs à différentes échelles pour convaincre la communauté de l'utilité de ce type d'approches [89].

Les travaux menés dans le cadre de ce projet de thèse ont utilisé le système d'élevage avicole comme modèle d'étude. Des preuves de concept ont pu être validées avec un rationnel scientifique fort, ouvrant maintenant la porte à d'autres systèmes d'élevage. Ainsi, la méthodologie d'analyse des microbiotes de surface de bâtiment d'élevage, et de sélection de souche basée sur l'étude des interactions microbiennes au sein de biofilm mixte au laboratoire pourront être réalisées dans d'autres contextes. Par exemple, les systèmes d'élevage hors-sol, nécessitant d'effectuer des processus de N&D entre deux lots successifs d'animaux peuvent-être couverts par ce type d'approche pour implanter un consortium positif avant que les animaux entrent dans le bâtiment. C'est notamment le cas des élevages porcins, aux différents stades de croissance des animaux. Les systèmes d'aquaculture en bassins (par exemple : crevettes, bar commun, dorade royale, truite arc-en-ciel, toutes écloseries et nurseries pour coquillages, poissons et crustacés) peuvent également bénéficier de l'utilisation de biofilms positifs. En effet, les mêmes procédures de N&D sont appliquées entre différents lots d'animaux. Cette approche pourrait être particulièrement pertinente dans le cadre des écloseries, où les animaux se développent au cours de leurs premiers stades de vie et sont particulièrement sensibles à la contamination externe, pouvant être causée par la présence de biofilms indésirables résiduels sur les surfaces. L'étude

des biofilms immergés par MCBL dans nos modèles de laboratoire est particulièrement adaptée à une application dans des milieux aquatiques tels que les bassins d'aquaculture. Les modèles d'étude au laboratoire devront être adaptés au système d'étude ciblé, avec des conditions physico-chimiques, des bactéries bénéfiques candidates et des bactéries indésirables ciblées différentes.

Bien qu'il existe un grand nombre d'études qui établissent des corrélations ou mettent en évidence des tendances sur le terrain après l'ajout de consortiums complexes, contrôlés ou de souches uniques, il est nécessaire d'approfondir notre compréhension des mécanismes sous-jacents aux interactions dans le but d'améliorer dans le but d'améliorer l'utilisation de ces consortiums. Les connaissances sur l'utilisation des biofilms positifs sont actuellement limitées et il est encore difficile d'étudier de manière approfondie les mécanismes impliqués dans leurs effets bénéfiques sur l'hôte. Le nombre modeste d'échantillons étudiés, les biais expérimentaux, la complexité des interactions mises en place entre les différents représentants de la communauté ou la sensibilité parfois insuffisante des techniques utilisées (approches omiques) peuvent rendre l'interprétation des résultats difficile [90]. Il est donc nécessaire de mettre en place au laboratoire, dans des conditions physico-chimiques contrôlées, des modèles d'études mimant un maximum la réalité du système étudié afin d'étudier plus finement des relations entre moins de partenaires de la communauté.

L'intervention humaine visant à façonner les communautés microbiennes naturellement présentes dans un biotope est observée dans de nombreux domaines. Il existe de nombreux exemple d'utilisation de souches uniques [91–93], de consortium contrôlés [94,95] ou encore de consortium complexes [90,96] pour des applications en biotechnologie ou en santé. Il n'existe pas de réponses universelles privilégiant une utilisation spécifique, ce qui suscite un débat au sein de la communauté scientifique. Certaines études récentes démontrent que les interactions microbiennes sont plutôt négatives [63,97], alors que d'autres décrivent le contraire et promeuvent l'utilisation de consortium [76,98]. Dans le contexte des biofilms positifs, nous avons essayé de rationaliser l'utilisation de souches uniques ou de consortiums simplifiés.

Une autre option serait d'utiliser le principe de coalescence en intégrant délibérément une communauté microbiologique dans une autre déjà établie dans son environnement naturel [99]. Pour ce faire, des microbiotes de surfaces provenant d'un environnement sain (obtenu par un élevage sans problèmes de maladies spécifiques) peuvent être prélevés, amplifiés, puis les réimplanter après N&D des surfaces. La notion d'environnement sain est complexe et difficile à définir car elle prend en compte plusieurs variables telles que la présence de virus, toxines, l'étude du pathobiome et autres bactéries indésirables pouvant être en état de dormance ou métaboliquement peu actives rendant difficile leur détection. L'avantage est l'utilisation de communautés isolées de surfaces dans ces biotopes et donc capables de s'implanter et coloniser à nouveau la niche écologique. Ce principe est utilisé en santé humaine et animale avec la transplantation fécale. Cette technique a démontré une très bonne efficacité sur la diminution de l'infection chronique à *Clostridium difficile* chez l'Homme [100] ou de la présence Salmonelles [101] et de *Campylobacter jejuni* chez le poulet [96,102]. Le modelage des niches écologiques d'un écosystème pour favoriser l'implantation de populations d'intérêt semble peu adapté dans le contexte des systèmes d'élevage commerciaux [103]. En effet, les paramètres physico-chimiques appliqués dans ce type d'élevage sont spécifiquement déterminés pour optimiser la croissance des animaux. Une modification de ces paramètres pour le modelage pourrait entraîner une diminution de la croissance des animaux et, par conséquent, une baisse de la rentabilité de la ferme.

Enfin, les outils et approches développés dans ce travail de thèse pourraient également se révéler d'un grand intérêt pour l'étude des biofilms positifs dans d'autres contextes comme le biocontrôle des plantes, la biopréservation des aliments et la santé (modulation des écosystèmes digestifs par les probiotiques ou les transplants fécaux), domaines où la notion de biofilm demeure encore peu explorée.

5 REFERENCES BIBLIOGRAPHIQUES

[1] OECD, Food and Agriculture Organization of the United Nations. OECD-FAO Agricultural Outlook 2023-2032. OECD; 2023. https://doi.org/10.1787/08801ab7-en.
[2] Chlebicz A, Śliżewska K. Campylobacteriosis, Salmonellosis, Yersiniosis, and Listeriosis as Zoonotic Foodborne Diseases: A Review. Int J Environ Res Public Health 2018;15:863. https://doi.org/10.3390/ijerph15050863.
[3] Munita JM, Arias CA. Mechanisms of Antibiotic Resistance. Microbiol Spectr 2016;4. https://doi.org/10.1128/microbiolspec.VMBF-0016-2015.
[4] Larsson DGJ, Flach C-F. Antibiotic resistance in the environment. Nat Rev Microbiol 2022;20:257–69. https://doi.org/10.1038/s41579-021-00649-x.
[5] O'Neill J. Tackling drug-resistant infections globally: final report and recommendations. Government of the United Kingdom; 2016.
[6] WHO. Global action plan on antimicrobial resistance. 2015.
[7] Luyckx K, Millet S, Van Weyenberg S, Herman L, Heyndrickx M, Dewulf J, et al. A 10-day vacancy period after cleaning and disinfection has no effect on the bacterial load in pig nursery units. BMC Vet Res 2016;12:236. https://doi.org/10.1186/s12917-016-0850-1.
[8] Bridier A, Briandet R, Thomas V, Dubois-Brissonnet F. Resistance of bacterial biofilms to disinfectants: a review. Biofouling 2011;27:1017–32. https://doi.org/10.1080/08927014.2011.626899.
[9] O'Toole G, Kaplan HB, Kolter R. Biofilm formation as microbial development. Annu Rev Microbiol 2000;54:49–79. https://doi.org/10.1146/annurev.micro.54.1.49.
[10] Sauer K, Stoodley P, Goeres DM, Hall-Stoodley L, Burmølle M, Stewart PS, et al. The biofilm life cycle: expanding the conceptual model of biofilm formation. Nat Rev Microbiol 2022;20:608–20. https://doi.org/10.1038/s41579-022-00767-0.
[11] Flemming H-C, Wuertz S. Bacteria and archaea on Earth and their abundance in biofilms. Nat Rev Microbiol 2019;17:247–60. https://doi.org/10.1038/s41579-019-0158-9.
[12] Flemming H-C, van Hullebusch ED, Neu TR, Nielsen PH, Seviour T, Stoodley P, et al. The biofilm matrix: multitasking in a shared space. Nat Rev Microbiol 2023;21:70–86. https://doi.org/10.1038/s41579-022-00791-0.
[13] Flemming H-C, Wingender J, Szewzyk U, Steinberg P, Rice SA, Kjelleberg S. Biofilms: an emergent form of bacterial life. Nat Rev Microbiol 2016;14:563–75. https://doi.org/10.1038/nrmicro.2016.94.
[14] Maali Y, Journo C, Mahieux R, Dutartre H. Microbial Biofilms: Human T-cell Leukemia Virus Type 1 First in Line for Viral Biofilm but Far Behind Bacterial Biofilms. Front Microbiol 2020;11:2041. https://doi.org/10.3389/fmicb.2020.02041.
[15] Pereira R, Dos Santos Fontenelle RO, de Brito EHS, de Morais SM. Biofilm of Candida albicans: formation, regulation and resistance. J Appl Microbiol 2021;131:11–22. https://doi.org/10.1111/jam.14949.
[16] Ren Z, Jeckel H, Simon-Soro A, Xiang Z, Liu Y, Cavalcanti IM, et al. Interkingdom assemblages in human saliva display group-level surface mobility and disease-promoting emergent functions. Proc Natl Acad Sci U S A 2022;119:e2209699119. https://doi.org/10.1073/pnas.2209699119.
[17] Motaung TE, Peremore C, Wingfield B, Steenkamp E. Plant-associated fungal biofilms-knowns and unknowns. FEMS Microbiol Ecol 2020;96:fiaa224. https://doi.org/10.1093/femsec/fiaa224.
[18] Ugya AY, Chen H, Wang Q. Microalgae biofilm system as an efficient tool for wastewater remediation and potential bioresources for pharmaceutical product production: an overview. Int J Phytoremediation 2023:1–12.

https://doi.org/10.1080/15226514.2023.2229920.
[19] Fanesi A, Martin T, Breton C, Bernard O, Briandet R, Lopes F. The architecture and metabolic traits of monospecific photosynthetic biofilms studied in a custom flow-through system. Biotechnology and Bioengineering 2022;119:2459–70. https://doi.org/10.1002/bit.28147.
[20] Vivier B, Navon M, Dauvin J-C, Chasselin L, Deloor M, Orvain F, et al. Colonisation of artificial structures by primary producers: competition and photosynthetic behaviour. Biofouling 2022;38:493–506. https://doi.org/10.1080/08927014.2022.2088285.
[21] Arnaouteli S, Bamford NC, Stanley-Wall NR, Kovács ÁT. Bacillus subtilis biofilm formation and social interactions. Nat Rev Microbiol 2021;19:600–14. https://doi.org/10.1038/s41579-021-00540-9.
[22] Dergham Y, Coq DL, Nicolas P, Deschamps J, Huillet E, Sanchez-Vizuete P, et al. Multi-scale transcriptome unveils spatial organisation and temporal dynamics of Bacillus subtilis biofilms 2023:2023.01.06.522868. https://doi.org/10.1101/2023.01.06.522868.
[23] Chamignon C, Guéneau V, Medina S, Deschamps J, Gil-Izquierdo A, Briandet R, et al. Evaluation of the Probiotic Properties and the Capacity to Form Biofilms of Various Lactobacillus Strains. Microorganisms 2020;8:1053. https://doi.org/10.3390/microorganisms8071053.
[24] Heumann A, Assifaoui A, Da Silva Barreira D, Thomas C, Briandet R, Laurent J, et al. Intestinal release of biofilm-like microcolonies encased in calcium-pectinate beads increases probiotic properties of Lacticaseibacillus paracasei. NPJ Biofilms Microbiomes 2020;6:44. https://doi.org/10.1038/s41522-020-00159-3.
[25] Ciofu O, Moser C, Jensen PØ, Høiby N. Tolerance and resistance of microbial biofilms. Nat Rev Microbiol 2022;20:621–35. https://doi.org/10.1038/s41579-022-00682-4.
[26] Ch'ng J-H, Chong KKL, Lam LN, Wong JJ, Kline KA. Biofilm-associated infection by enterococci. Nat Rev Microbiol 2019;17:82–94. https://doi.org/10.1038/s41579-018-0107-z.
[27] Davies D. Understanding biofilm resistance to antibacterial agents. Nat Rev Drug Discov 2003;2:114–22. https://doi.org/10.1038/nrd1008.
[28] Notcovich S, DeNicolo G, Flint SH, Williamson NB, Gedye K, Grinberg A, et al. Biofilm-Forming Potential of Staphylococcus aureus Isolated from Clinical Mastitis Cases in New Zealand. Vet Sci 2018;5:8. https://doi.org/10.3390/vetsci5010008.
[29] Weber K, Baethmann A, Kempski O. Determinants of survival after forebrain ischemia in Mongolian gerbils. Metab Brain Dis 1988;3:247–55. https://doi.org/10.1007/BF00999534.
[30] Artini M, Cellini A, Papa R, Tilotta M, Scoarughi GL, Gazzola S, et al. Adhesive behaviour and virulence of coagulase negative staphylococci isolated from Italian cheeses. Int J Immunopathol Pharmacol 2015;28:341–50. https://doi.org/10.1177/0394632015593236.
[31] Xu D, Gu T, Lovley DR. Microbially mediated metal corrosion. Nat Rev Microbiol 2023. https://doi.org/10.1038/s41579-023-00920-3.
[32] Cámara M, Green W, MacPhee CE, Rakowska PD, Raval R, Richardson MC, et al. Economic significance of biofilms: a multidisciplinary and cross-sectoral challenge. NPJ Biofilms Microbiomes 2022;8:42. https://doi.org/10.1038/s41522-022-00306-y.
[33] Scatassa ML, Gaglio R, Macaluso G, Francesca N, Randazzo W, Cardamone C, et al. Transfer, composition and technological characterization of the lactic acid bacterial populations of the wooden vats used to produce traditional stretched cheeses. Food Microbiol 2015;52:31–41. https://doi.org/10.1016/j.fm.2015.06.008.
[34] Pandin C, Le Coq D, Canette A, Aymerich S, Briandet R. Should the biofilm mode of life be taken into consideration for microbial biocontrol agents? Microb Biotechnol 2017;10:719–

34. https://doi.org/10.1111/1751-7915.12693.
[35] Guéneau V, Plateau-Gonthier J, Arnaud L, Piard J-C, Castex M, Briandet R. Positive biofilms to guide surface microbial ecology in livestock buildings. Biofilm 2022;4:100075. https://doi.org/10.1016/j.bioflm.2022.100075.
[36] Koutsoumanis K, Allende A, Alvarez-Ordóñez A, Bolton D, Bover-Cid S, Chemaly M, et al. Microbial species as notified to EFSA 2020. https://doi.org/10.5281/zenodo.3607184.
[37] Grand I, Bellon-Fontaine M-N, Herry J-M, Hilaire D, Moriconi F-X, Naïtali M. Possible overestimation of surface disinfection efficiency by assessment methods based on liquid sampling procedures as demonstrated by in situ quantification of spore viability. Appl Environ Microbiol 2011;77:6208–14. https://doi.org/10.1128/AEM.00649-11.
[38] Guéneau V, Rodiles A, Frayssinet B, Piard J-C, Castex M, Plateau-Gonthier J, et al. Positive biofilms to control surface-associated microbial communities in a broiler chicken production system - a field study. Front Microbiol 2022;13:981747. https://doi.org/10.3389/fmicb.2022.981747.
[39] Heilbronner S, Krismer B, Brötz-Oesterhelt H, Peschel A. The microbiome-shaping roles of bacteriocins. Nat Rev Microbiol 2021;19:726–39. https://doi.org/10.1038/s41579-021-00569-w.
[40] Granato ET, Meiller-Legrand TA, Foster KR. The Evolution and Ecology of Bacterial Warfare. Curr Biol 2019;29:R521–37. https://doi.org/10.1016/j.cub.2019.04.024.
[41] Dedrick S, Warrier V, Lemon KP, Momeni B. When does a Lotka-Volterra model represent microbial interactions? Insights from in vitro nasal bacterial communities. mSystems 2023;8:e0075722. https://doi.org/10.1128/msystems.00757-22.
[42] Guillier L, Stahl V, Hezard B, Notz E, Briandet R. Modelling the competitive growth between Listeria monocytogenes and biofilm microflora of smear cheese wooden shelves. Int J Food Microbiol 2008;128:51–7. https://doi.org/10.1016/j.ijfoodmicro.2008.06.028.
[43] Habimana O, Guillier L, Kulakauskas S, Briandet R. Spatial competition with Lactococcus lactis in mixed-species continuous-flow biofilms inhibits Listeria monocytogenes growth. Biofouling 2011;27:1065–72. https://doi.org/10.1080/08927014.2011.626124.
[44] Strassmann JE, Gilbert OM, Queller DC. Kin discrimination and cooperation in microbes. Annu Rev Microbiol 2011;65:349–67. https://doi.org/10.1146/annurev.micro.112408.134109.
[45] Stefanic P, Kraigher B, Lyons NA, Kolter R, Mandic-Mulec I. Kin discrimination between sympatric Bacillus subtilis isolates. Proc Natl Acad Sci U S A 2015;112:14042–7. https://doi.org/10.1073/pnas.1512671112.
[46] Sanchez-Vizuete P, Dergham Y, Bridier A, Deschamps J, Dervyn E, Hamze K, et al. The coordinated population redistribution between Bacillus subtilis submerged biofilm and liquid-air pellicle. Biofilm 2022;4:100065. https://doi.org/10.1016/j.bioflm.2021.100065.
[47] Wadhwa N, Berg HC. Bacterial motility: machinery and mechanisms. Nat Rev Microbiol 2022;20:161–73. https://doi.org/10.1038/s41579-021-00626-4.
[48] Eigentler L, Davidson FA, Stanley-Wall NR. Mechanisms driving spatial distribution of residents in colony biofilms: an interdisciplinary perspective. Open Biol 2022;12:220194. https://doi.org/10.1098/rsob.220194.
[49] Hernandez-Valdes JA, Zhou L, de Vries MP, Kuipers OP. Impact of spatial proximity on territoriality among human skin bacteria. NPJ Biofilms Microbiomes 2020;6:30. https://doi.org/10.1038/s41522-020-00140-0.
[50] Maan H, Itkin M, Malitsky S, Friedman J, Kolodkin-Gal I. Resolving the conflict between antibiotic production and rapid growth by recognition of peptidoglycan of susceptible

competitors. Nat Commun 2022;13:431. https://doi.org/10.1038/s41467-021-27904-2.
[51] Amor DR, Montañez R, Duran-Nebreda S, Solé R. Spatial dynamics of synthetic microbial mutualists and their parasites. PLoS Comput Biol 2017;13:e1005689. https://doi.org/10.1371/journal.pcbi.1005689.
[52] Rendueles O, Zee PC, Dinkelacker I, Amherd M, Wielgoss S, Velicer GJ. Rapid and widespread de novo evolution of kin discrimination. Proc Natl Acad Sci U S A 2015;112:9076–81. https://doi.org/10.1073/pnas.1502251112.
[53] Suissa R, Olender T, Malitsky S, Golani O, Turjeman S, Koren O, et al. Metabolic rewiring of the probiotic bacterium Lacticaseibacillus rhamnosus GG contributes to cell-wall remodeling and antimicrobials production 2023:2023.01.03.522566. https://doi.org/10.1101/2023.01.03.522566.
[54] Estrela S, Libby E, Van Cleve J, Débarre F, Deforet M, Harcombe WR, et al. Environmentally Mediated Social Dilemmas. Trends Ecol Evol 2019;34:6–18. https://doi.org/10.1016/j.tree.2018.10.004.
[55] Henriksen NNSE, Hansen MF, Kiesewalter HT, Russel J, Nesme J, Foster KR, et al. Biofilm cultivation facilitates coexistence and adaptive evolution in an industrial bacterial community. NPJ Biofilms Microbiomes 2022;8:59. https://doi.org/10.1038/s41522-022-00323-x.
[56] Blin K, Shaw S, Augustijn HE, Reitz ZL, Biermann F, Alanjary M, et al. antiSMASH 7.0: new and improved predictions for detection, regulation, chemical structures and visualisation. Nucleic Acids Res 2023;51:W46–50. https://doi.org/10.1093/nar/gkad344.
[57] Mielko KA, Jabłoński SJ, Milczewska J, Sands D, Łukaszewicz M, Młynarz P. Metabolomic studies of Pseudomonas aeruginosa. World J Microbiol Biotechnol 2019;35:178. https://doi.org/10.1007/s11274-019-2739-1.
[58] Hartmann R, Jeckel H, Jelli E, Singh PK, Vaidya S, Bayer M, et al. Quantitative image analysis of microbial communities with BiofilmQ. Nat Microbiol 2021;6:151–6. https://doi.org/10.1038/s41564-020-00817-4.
[59] Azimi S, Lewin GR, Whiteley M. The biogeography of infection revisited. Nat Rev Microbiol 2022;20:579–92. https://doi.org/10.1038/s41579-022-00683-3.
[60] Özogul F, Hamed I. The importance of lactic acid bacteria for the prevention of bacterial growth and their biogenic amines formation: A review. Crit Rev Food Sci Nutr 2018;58:1660–70. https://doi.org/10.1080/10408398.2016.1277972.
[61] Byun H, Brockett MR, Pu Q, Hrycko AJ, Beld J, Zhu J. An Intestinal Bacillus velezensis Isolate Displays Broad-Spectrum Antibacterial Activity and Prevents Infection of Both Gram-Positive and Gram-Negative Pathogens In Vivo. J Bacteriol 2023;205:e0013323. https://doi.org/10.1128/jb.00133-23.
[62] Bolješić M, Kraigher B, Dogsa I, Jerič Kokelj B, Mandic-Mulec I. Kin Discrimination Modifies Strain Distribution, Spatial Segregation, and Incorporation of Extracellular Matrix Polysaccharide Mutants of Bacillus subtilis Strains into Mixed Floating Biofilms. Appl Environ Microbiol 2022;88:e0087122. https://doi.org/10.1128/aem.00871-22.
[63] Palmer JD, Foster KR. Bacterial species rarely work together. Science 2022;376:581–2. https://doi.org/10.1126/science.abn5093.
[64] Campana S, Riesgo A, Jongepier E, Fuss J, Muyzer G, de Goeij JM. Meta-transcriptomic comparison of two sponge holobionts feeding on coral- and macroalgal-dissolved organic matter. BMC Genomics 2022;23:674. https://doi.org/10.1186/s12864-022-08893-y.
[65] Schirmer M, Garner A, Vlamakis H, Xavier RJ. Microbial genes and pathways in inflammatory bowel disease. Nat Rev Microbiol 2019;17:497–511. https://doi.org/10.1038/s41579-019-

0213-6.
[66] Liu Y, Huang R, Chen Y, Miao Y, Štefanič P, Mandic-Mulec I, et al. Involvement of Flagellin in Kin Recognition between Bacillus velezensis Strains. mSystems 2022;7:e0077822. https://doi.org/10.1128/msystems.00778-22.
[67] Muok AR, Briegel A. Intermicrobial Hitchhiking: How Nonmotile Microbes Leverage Communal Motility. Trends Microbiol 2021;29:542–50. https://doi.org/10.1016/j.tim.2020.10.005.
[68] Muok AR, Claessen D, Briegel A. Microbial hitchhiking: how Streptomyces spores are transported by motile soil bacteria. ISME J 2021;15:2591–600. https://doi.org/10.1038/s41396-021-00952-8.
[69] Sun X, Xie J, Zheng D, Xia R, Wang W, Xun W, et al. Keystone species determine the productivity of synthetic microbial biofilm communities 2022:2022.01.23.477386. https://doi.org/10.1101/2022.01.23.477386.
[70] Nestor E, Toledano G, Friedman J. Interactions between Culturable Bacteria Are Predicted by Individual Species' Growth. mSystems 2023;8:e0083622. https://doi.org/10.1128/msystems.00836-22.
[71] Ly S, Bajoul Kakahi F, Mith H, Phat C, Fifani B, Kenne T, et al. Engineering Synthetic Microbial Communities through a Selective Biofilm Cultivation Device for the Production of Fermented Beverages. Microorganisms 2019;7:206. https://doi.org/10.3390/microorganisms7070206.
[72] Jelli E, Ohmura T, Netter N, Abt M, Jiménez-Siebert E, Neuhaus K, et al. Single-cell segmentation in bacterial biofilms with an optimized deep learning method enables tracking of cell lineages and measurements of growth rates. Mol Microbiol 2023;119:659–76. https://doi.org/10.1111/mmi.15064.
[73] Karlsen ST, Rau MH, Sánchez BJ, Jensen K, Zeidan AA. From genotype to phenotype: computational approaches for inferring microbial traits relevant to the food industry. FEMS Microbiol Rev 2023;47:fuad030. https://doi.org/10.1093/femsre/fuad030.
[74] Lagier J-C, Dubourg G, Million M, Cadoret F, Bilen M, Fenollar F, et al. Culturing the human microbiota and culturomics. Nat Rev Microbiol 2018;16:540–50. https://doi.org/10.1038/s41579-018-0041-0.
[75] Jeanson S, Floury J, Gagnaire V, Lortal S, Thierry A. Bacterial Colonies in Solid Media and Foods: A Review on Their Growth and Interactions with the Micro-Environment. Front Microbiol 2015;6:1284. https://doi.org/10.3389/fmicb.2015.01284.
[76] Kehe J, Ortiz A, Kulesa A, Gore J, Blainey PC, Friedman J. Positive interactions are common among culturable bacteria. Sci Adv 2021;7:eabi7159. https://doi.org/10.1126/sciadv.abi7159.
[77] Abuhena M, Al-Rashid J, Azim MF, Khan MNM, Kabir MG, Barman NC, et al. Optimization of industrial (3000 L) production of Bacillus subtilis CW-S and its novel application for minituber and industrial-grade potato cultivation. Sci Rep 2022;12:11153. https://doi.org/10.1038/s41598-022-15366-5.
[78] EFSA Panel on Additives and Products or Substances used in Animal Feed (FEEDAP), Rychen G, Aquilina G, Azimonti G, Bampidis V, Bastos M de L, et al. Guidance on the characterisation of microorganisms used as feed additives or as production organisms. EFSA Journal 2018;16:e05206. https://doi.org/10.2903/j.efsa.2018.5206.
[79] Fan Y, Yang J, Duan A, Li X. Pectin/sodium alginate/xanthan gum edible composite films as the fresh-cut package. Int J Biol Macromol 2021;181:1003–9. https://doi.org/10.1016/j.ijbiomac.2021.04.111.

[80] Feng J, Gu Y, Quan Y, Gao W, Dang Y, Cao M, et al. Construction of energy-conserving sucrose utilization pathways for improving poly-γ-glutamic acid production in Bacillus amyloliquefaciens. Microb Cell Fact 2017;16:98. https://doi.org/10.1186/s12934-017-0712-y.
[81] Tian T, Sun B, Shi H, Gao T, He Y, Li Y, et al. Sucrose triggers a novel signaling cascade promoting Bacillus subtilis rhizosphere colonization. ISME J 2021;15:2723–37. https://doi.org/10.1038/s41396-021-00966-2.
[82] de Souza de Azevedo PO, de Azevedo HF, Figueroa E, Converti A, Domínguez JM, de Souza Oliveira RP. Effects of pH and sugar supplements on bacteriocin-like inhibitory substance production by Pediococcus pentosaceus. Mol Biol Rep 2019;46:4883–91. https://doi.org/10.1007/s11033-019-04938-w.
[83] Liu Y, Wang J, Wu C. Modulation of Gut Microbiota and Immune System by Probiotics, Pre-biotics, and Post-biotics. Front Nutr 2021;8:634897. https://doi.org/10.3389/fnut.2021.634897.
[84] Thallinger B, Prasetyo EN, Nyanhongo GS, Guebitz GM. Antimicrobial enzymes: an emerging strategy to fight microbes and microbial biofilms. Biotechnol J 2013;8:97–109. https://doi.org/10.1002/biot.201200313.
[85] Byrd AL, Belkaid Y, Segre JA. The human skin microbiome. Nat Rev Microbiol 2018;16:143–55. https://doi.org/10.1038/nrmicro.2017.157.
[86] Postollec F, Falentin H, Pavan S, Combrisson J, Sohier D. Recent advances in quantitative PCR (qPCR) applications in food microbiology. Food Microbiol 2011;28:848–61. https://doi.org/10.1016/j.fm.2011.02.008.
[87] Sohail MN, Rathnamma D, Priya SC, Isloor S, Naryanaswamy HD, Ruban SW, et al. Salmonella from Farm to Table: Isolation, Characterization, and Antimicrobial Resistance of Salmonella from Commercial Broiler Supply Chain and Its Environment. Biomed Res Int 2021;2021:3987111. https://doi.org/10.1155/2021/3987111.
[88] Theis KR, Dheilly NM, Klassen JL, Brucker RM, Baines JF, Bosch TCG, et al. Getting the Hologenome Concept Right: an Eco-Evolutionary Framework for Hosts and Their Microbiomes. mSystems 2016;1:e00028-16. https://doi.org/10.1128/mSystems.00028-16.
[89] De Roy K, Marzorati M, Van den Abbeele P, Van de Wiele T, Boon N. Synthetic microbial ecosystems: an exciting tool to understand and apply microbial communities. Environ Microbiol 2014;16:1472–81. https://doi.org/10.1111/1462-2920.12343.
[90] Porcari S, Benech N, Valles-Colomer M, Segata N, Gasbarrini A, Cammarota G, et al. Key determinants of success in fecal microbiota transplantation: From microbiome to clinic. Cell Host Microbe 2023;31:712–33. https://doi.org/10.1016/j.chom.2023.03.020.
[91] Castex M, Leclercq E, Lemaire P, Chim L. Dietary Probiotic Pediococcus acidilactici MA18/5M Improves the Growth, Feed Performance and Antioxidant Status of Penaeid Shrimp Litopenaeus stylirostris: A Growth-Ration-Size Approach. Animals (Basel) 2021;11:3451. https://doi.org/10.3390/ani11123451.
[92] Pandin C, Le Coq D, Deschamps J, Védie R, Rousseau T, Aymerich S, et al. Complete genome sequence of Bacillus velezensis QST713: A biocontrol agent that protects Agaricus bisporus crops against the green mould disease. J Biotechnol 2018;278:10–9. https://doi.org/10.1016/j.jbiotec.2018.04.014.
[93] Torres-Maravilla E, Holowacz S, Delannoy J, Lenoir L, Jacouton E, Gervason S, et al. Serpin-positive Bifidobacterium breve CNCM I-5644 improves intestinal permeability in two models of irritable bowel syndrome. Sci Rep 2022;12:19776. https://doi.org/10.1038/s41598-022-21746-8.

[94] Louie T, Golan Y, Khanna S, Bobilev D, Erpelding N, Fratazzi C, et al. VE303, a Defined Bacterial Consortium, for Prevention of Recurrent Clostridioides difficile Infection: A Randomized Clinical Trial. JAMA 2023;329:1356–66. https://doi.org/10.1001/jama.2023.4314.
[95] Kurt F, Leventhal GE, Spalinger MR, Anthamatten L, Rogalla von Bieberstein P, Menzi C, et al. Co-cultivation is a powerful approach to produce a robust functionally designed synthetic consortium as a live biotherapeutic product (LBP). Gut Microbes 2023;15:2177486. https://doi.org/10.1080/19490976.2023.2177486.
[96] Kayal A, Stanley D, Radovanovic A, Horyanto D, Van TTH, Bajagai YS. Controlled Intestinal Microbiota Colonisation in Broilers under the Industrial Production System. Animals (Basel) 2022;12:3296. https://doi.org/10.3390/ani12233296.
[97] Chang C-Y, Bajic D, Vila J, Estrela S, Sanchez A. Emergent coexistence in multispecies microbial communities 2022:2022.05.20.492860. https://doi.org/10.1101/2022.05.20.492860.
[98] Liu X, Mei S, Salles JF. Inoculated microbial consortia perform better than single strains in living soil: A meta-analysis. Applied Soil Ecology 2023;190:105011. https://doi.org/10.1016/j.apsoil.2023.105011.
[99] Rillig MC, Antonovics J, Caruso T, Lehmann A, Powell JR, Veresoglou SD, et al. Interchange of entire communities: microbial community coalescence. Trends Ecol Evol 2015;30:470–6. https://doi.org/10.1016/j.tree.2015.06.004.
[100] Quraishi MN, Widlak M, Bhala N, Moore D, Price M, Sharma N, et al. Systematic review with meta-analysis: the efficacy of faecal microbiota transplantation for the treatment of recurrent and refractory Clostridium difficile infection. Aliment Pharmacol Ther 2017;46:479–93. https://doi.org/10.1111/apt.14201.
[101] Nakamura A, Ota Y, Mizukami A, Ito T, Ngwai YB, Adachi Y. Evaluation of aviguard, a commercial competitive exclusion product for efficacy and after-effect on the antibody response of chicks to Salmonella. Poult Sci 2002;81:1653–60. https://doi.org/10.1093/ps/81.11.1653.
[102] Heimesaat MM, Weschka D, Mousavi S, Bereswill S. Treatment with the Probiotic Product Aviguard® Alleviates Inflammatory Responses during Campylobacter jejuni-Induced Acute Enterocolitis in Mice. Int J Mol Sci 2021;22:6683. https://doi.org/10.3390/ijms22136683.
[103] Delattre H, Desmond-Le Quéméner E, Duquennoi C, Filali A, Bouchez T. Consistent microbial dynamics and functional community patterns derived from first principles. ISME J 2019;13:263–76. https://doi.org/10.1038/s41396-018-0272-0.
[104] Guéneau V, Rodiles A, Piard J-C, Frayssinet B, Castex M, Plateau-Gonthier J, et al. Capture and Ex-Situ Analysis of Environmental Biofilms in Livestock Buildings. Microorganisms 2021;10:2. https://doi.org/10.3390/microorganisms10010002.

6 ANNEXES

6.1 EXPERIMENTATION PRELEMINAIRE EN ELEVAGE DE POULET DE CHAIR

6.1.1 Contexte et plan d'expérience

Ce premier essai s'est déroulé dans un élevage expérimental de poulet de chair appartenant à Lallemand, proche de Toulouse. L'objectif principal était de se familiariser avec les expérimentations sur coupons de PolyChlorure de Vinyle (PVC) et d'acier inoxydable 316 (INOX), aussi bien sur le terrain qu'en laboratoire avant de changer d'échelle et de passer en élevage commercial.

Dans cette expérience, 16 coupons en PVC et 16 en INOX (L = 7.5cm, l = 2.5cm) provenant de chez BioSurface Technologies Corporation (Bozeman, Montana, USA) ont été utilisés. 1 coupon en INOX et 1 en PVC ont été placés dans une même case pour faire en sorte d'être le plus proche possible des animaux (**Figure 8**).

Figure 8: Différents points de vue de la ferme expérimentale de poulet de chair appartenant à la société Lallemand. Les coupons sont placés sous les abreuvoirs, au contact des animaux. Un scotch double face permet un maintien solide des coupons.

8 cases possédaient des coupons traités avec le produit commercial Lalfilm Pro, utilisé avec les recommandations de Lallemand à 0.2 g/m2 de surface au sol, et 8 autres cases étaient pourvues de coupons témoins, sans traitement. Dans la condition Lalfilm Pro, seuls les coupons sont traités (**Figure 9**). Les coupons ont tous été échantillonnés après 30 jours d'incubation au contact des animaux.

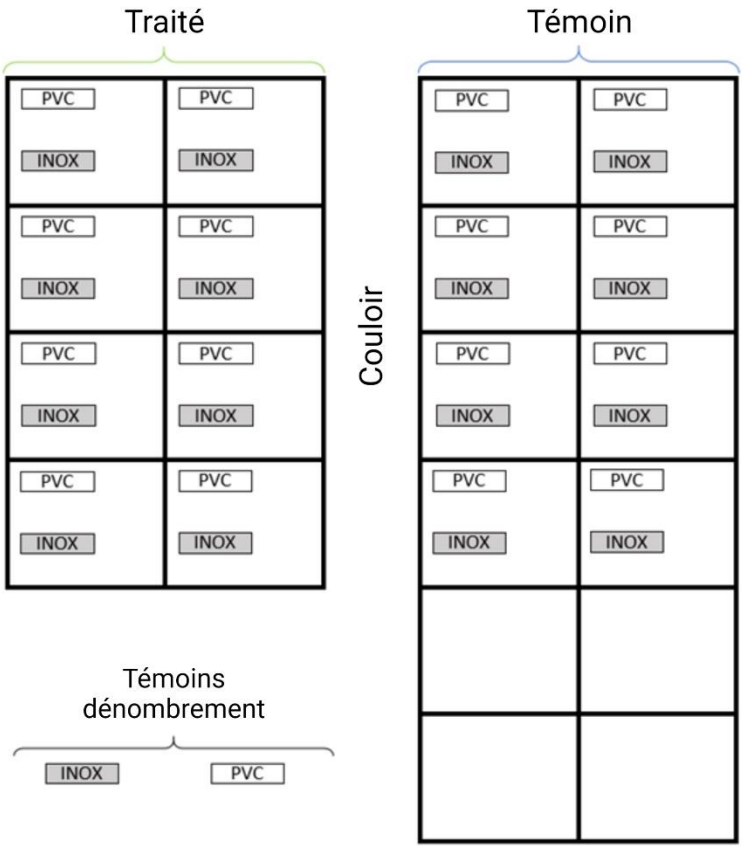

Figure 9: Disposition des coupons dans l'élevage. Seulement les coupons sont pulvérisés avec le produit commercial dans la condition traitée. Les témoins dénombrement n'ont pas été traités, ni disposés dans l'élevage.

Le jour de l'échantillonnage, les coupons sont prélevés avec des gants et disposés individuellement dans des boîtes de Pétri contenant une compresse saturée en eau stérile. Le scotch double face permet un bon maintien du coupon sur le fond de la boîte. Les boîtes sont ensuite scellées avec du parafilm. Ici les échantillons ont été transportés le jour du prélèvement et traités le lendemain au laboratoire (**figure 10**).

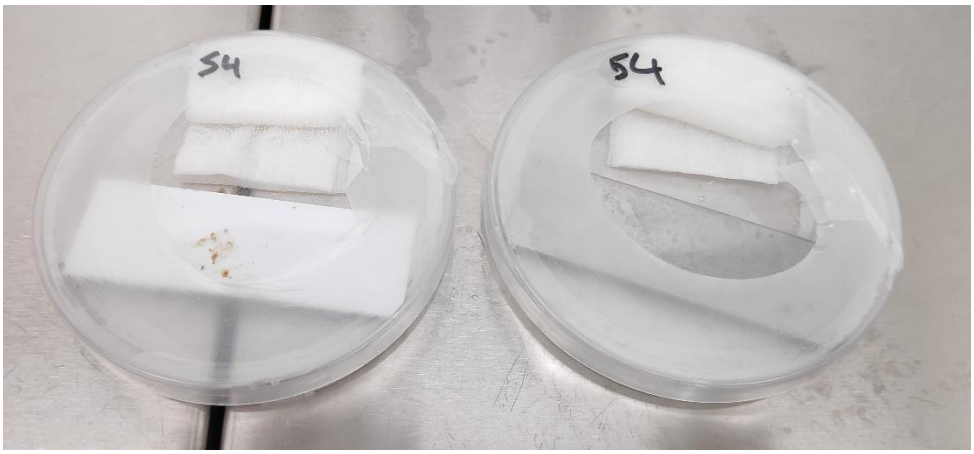

Figure 10: Conditionnement des coupons pour le transport après prélèvement dans la ferme. Une compresse en coton stérile imbibée d'eau est coincée par le couvercle de la boîte de Petri. Du parafilm scelle la boîte.

Après réception des coupons, deux expérimentations ont été réalisées. La première a eu comme objectif de quantifier le nombre total de bactéries à la surface des coupons. La seconde a permis l'observation de la structure 3D des biofilms. Dans cette expérience, un seul coupon de chaque matériau était disposé dans les cases. La moitié de la surface des coupons a donc servi à l'observation des biofilms par microscopie. L'autre moitié ayant servi aux expériences de quantification de la flore totale. Les protocoles utilisés sont décrits dans les articles 3 et 4 [38,104].

6.1.2 Dénombrement des microorganismes attachés sur les coupons

Le coupon est trempé une heure dans de l'eau physiologique (25 mL afin de recouvrir la moitié du coupon, soit 18.5 cm^2) (**figure 11**). A l'aide d'un cône et d'une P1000 les biofilms sur la partie immergée sont décrochés en grattant la surface et suspendus dans les 25 mL d'eau physiologique.

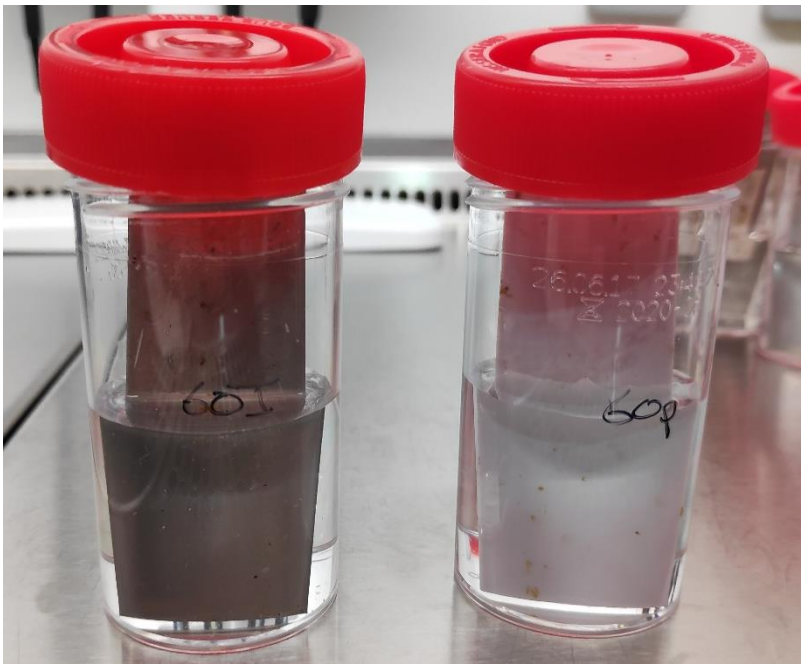

Figure 11: Incubation des coupons pour prélever les microorganismes sur la moitié de la surface. Un détachement mécaniques des biofilms de la surface immergé est effectué à l'aide d'un cône d'une pipette P1000, et pipetage successif.

Avec cette solution, des ensemencements en masses dans du milieu BHI (*Brain Heart Infusion*, Difco, réf. 237500) ont été réalisés. Cette expérience a pour but de quantifier le nombre de bactéries viables et cultivables présentes sur les coupons en fonction du matériau et du traitement.

Après avoir rapporté à la surface, la population bactérienne est comprise entre 5 et 6 Log UFC/cm^2 dans chaque condition (**Figure 12**). Aucune différence significative entre les dénombrements en fonction du traitement ou des matériaux n'a été observé. A noter que dans cette expérience, seuls les coupons ont été traités.

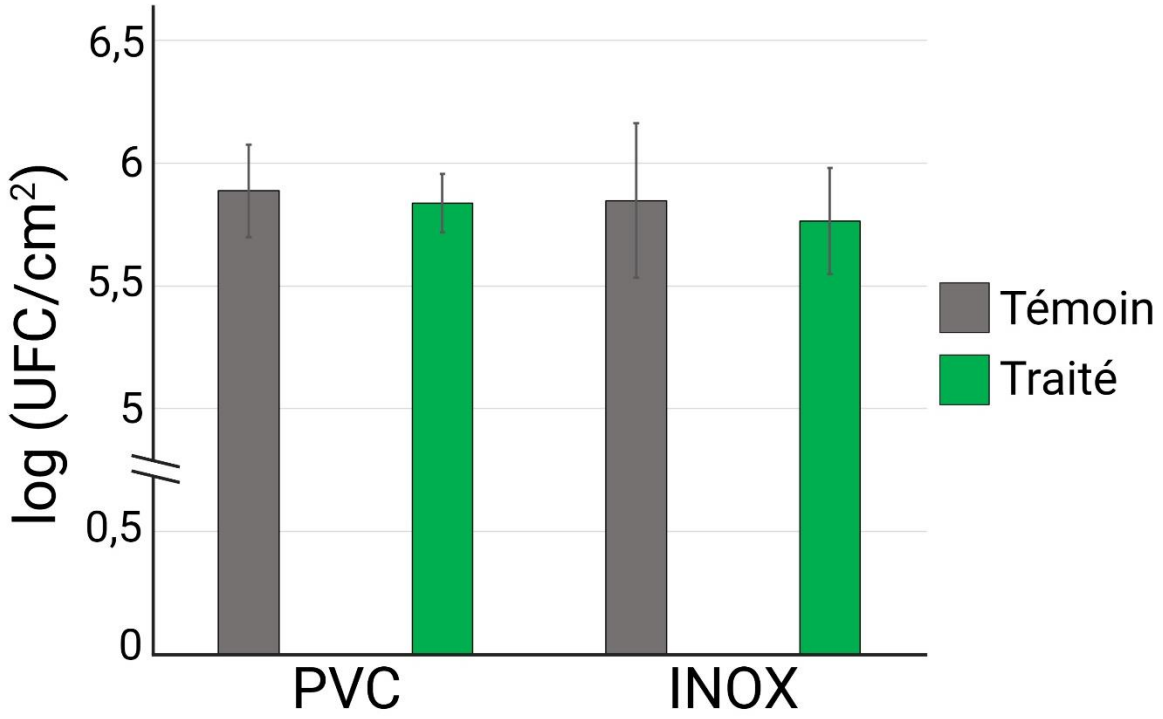

Figure 12: Bactéries totales prélevées sur les coupons après dénombrement sur un milieu riche (TS). Le dénombrement correspond à la quantité bactérienne de la moitié d'un coupon, soit 9.4 cm^2. Les barres d'erreurs correspondent aux écart-types standards.

6.1.3 Observation des biofilms au microscope confocal à balayage laser (MCBL)

Les coupons ont été marqués avec 25 µL une solution de SYTO61 à 3 µL/mL, marquant en rouge les acides nucléiques. Après dépôt du colorant, une lamelle de microscopie est placée sur le coupon. Celui-ci est retourné sur la platine afin d'être observé au MCBL (microscopie inversée). L'objectif utilisé est à immersion à eau x63. Le SYTO61 est excité avec un laser HeNe 633 nm. La collecte de la fluorescence se fait dans le rouge (z step : 1 µm, 600 Hz). La topographie de la surface est réalisée à l'aide de la réflexion laser (en gris). 3 champs par coupons sont capturés.

Les biofilms présents sur l'INOX et le PVC sont hétérogènes (**Figure 13**). Une grande diversité de structures sont observables. La présence de nombreuses bactéries et hyphes fongiques sont à noter. Toute la surface des coupons n'est pas recouverte par les biofilms, même lorsque celui-ci est traité.

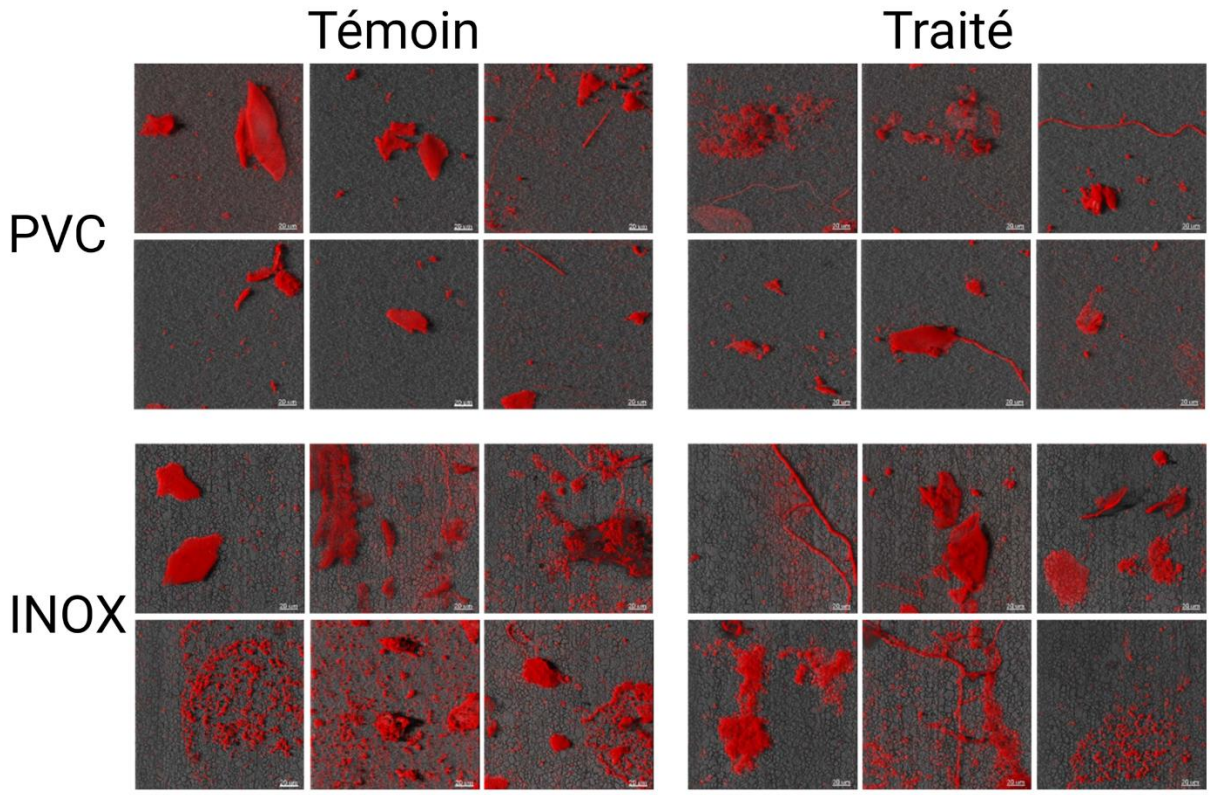

Figure 13: Exemples représentatifs de structures de biofilms observés au MCBL sur les coupons. La topographie de surface des coupons est visualisée en gris avec le mode reflection du MCBL, montrant une surface plus lisse des coupons en PVC comparé aux coupons en INOX. Le marquage des biofilms en rouge a été réalisé avec du SYTO61, un fluorophore capable de pénétrer dans les cellules et s'intercaler entre les bases de l'ADN. La barre d'échelle correspond à 20 µm.

Les images sont traitées avec le logiciel IMARIS v9.3.1 . Le biovolume est calculé à l'aide d'une fonction d'IMARIS permettant de quantifier le volume binarisé correspondant au signal rouge du SYTO61 (**Figure 14**).

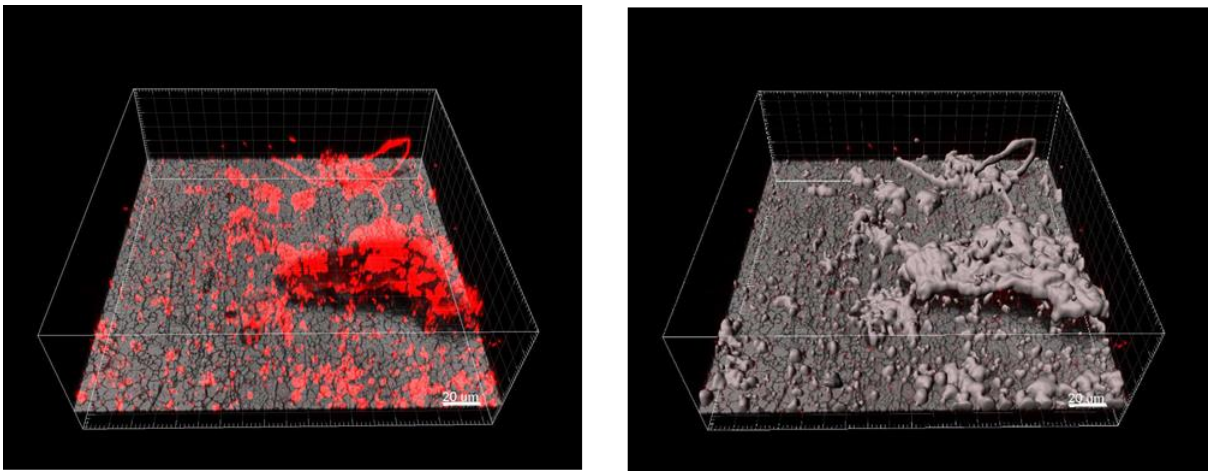

Figure 14: Binarisation du signal rouge de l'image avec le logiciel IMARIS. A gauche, l'image brute observée au MCBL. A droite, le signal rouge est binarisé (gris clair) pour déterminer le biovolume du biofilm. La barre d'échelle correspond à 20 µm.

Après traitement des images, les biovolumes sont déterminés (**Figure 15**). Un biovolume plus important (p < 0.05, One-Way ANOVA, Fisher's LSD test) est observé sur les coupons en INOX comparé aux coupons en PVC dans les deux conditions. Il n'y a pas de différences significatives entre les conditions témoins et traitées pour un matériau donné.

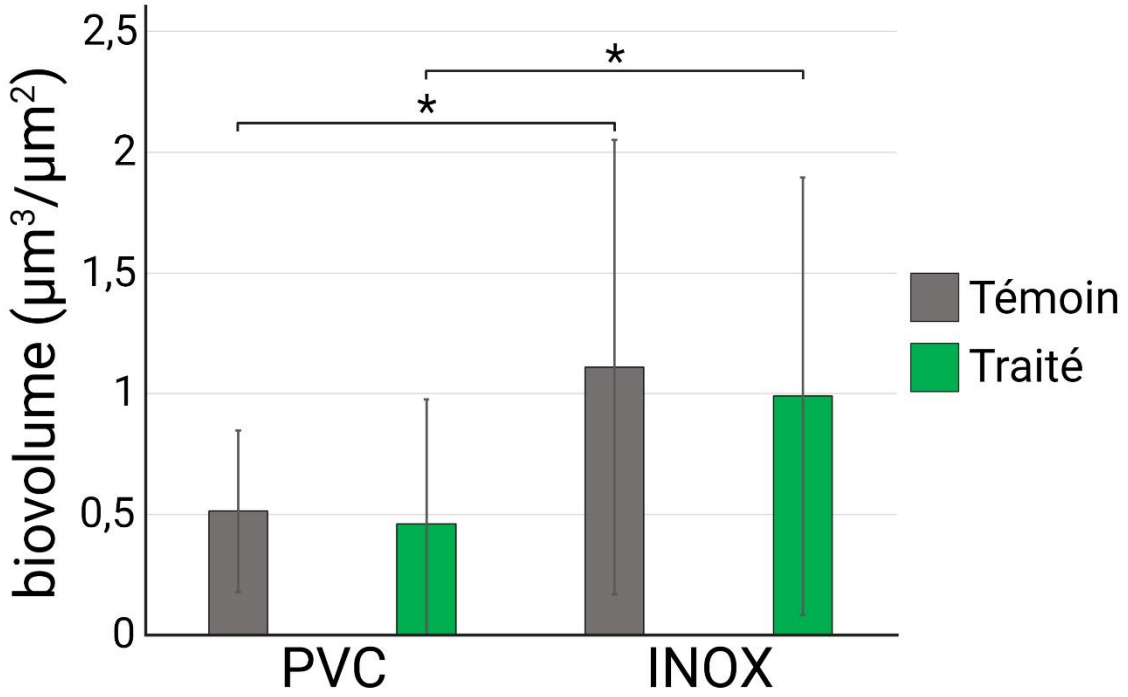

Figure 15: Biovolume des biofilms en fonction des surfaces et du traitement par Lalfilm Pro. Les barres d'erreurs correspondent aux écart-types standards (*p < 0.05).

Ces résultats sont différents de ceux observés lors du dénombrement de la flore totale dans du BHI. En effet, il ne semble pas y avoir de différences du nombre de bactéries en fonction des conditions, mais une différence de volume de biofilms, probablement dûe à des bactéries mortes marquées avec le SYTO61, ou à un marquage non spécifique de la matrice.

6.2 VALORISATIONS SCIENTIFIQUES ET INDUSTRIELLES

Publications scientifiques

Article 1 : Virgile Guéneau, Julia Plateau-Gonthier, Ludovic Arnaud, Jean-Christophe Piard, Mathieu Castex, Romain Briandet. Positive biofilms to guide surface microbial ecology in livestock buildings. Biofilm, 2022, 4, pp.100075. 10.1016/j.bioflm.2022.100075.

Article 2 : Virgile Guéneau, Raphaël Charron, Vlad Costache, Arnaud Bridier, Romain Briandet. Spatial analysis of multispecies bacterial biofilms. MIM 53: Biofilms, Elsevier, 2023, Methods in Microbiology, 10.1016/bs.mim.2023.03.002.

Article 3 : Virgile Guéneau, Ana Rodiles, Jean-Christophe Piard, Bastien Frayssinet, Mathieu Castex, Romain Briandet. Capture and Ex-Situ Analysis of Environmental Biofilms in Livestock Buildings. Microorganisms, 2022, 10 (1), pp.2. 10.3390/microorganisms10010002.

Article 4 : Virgile Guéneau, Jean-Christophe Piard, Bastien Frayssinet, Valentin Loux, Hélène Chiapello, Romain Briandet. Genome Sequence of Bacillus velezensis P1, a Strain Isolated from a Biofilm Captured on a Pig Farm Building. Microbiology Resource Announcements, 2022, 10.1128/mra.01219-21.

Article 5 : Virgile Guéneau, Ana Rodiles, Bastien Frayssinet, Jean-Christophe Piard, Mathieu Castex, Romain Briandet. Positive biofilms to control surface-associated microbial communities in a broiler chicken production system - a field study. Frontiers in Microbiology, 2022, 13, pp.981747. 10.3389/fmicb.2022.981747.

Article 6 : Virgile Guéneau, Guillermo Jiménez, Mathieu Castex, Romain Briandet. Insights into the genomic and phenotypic characteristics of *Bacillus* spp. strains isolated from biofilms in broiler farms. *En préparation*.

Article 7 : Virgile Guéneau, Laurent Guillier, Guillermo Jiménez, Julia Plateau-Gonthier, Marie-Françoise Noirot-Gros, Pascale Serror, Mathieu Castex, Romain Briandet. Guided assembly of positive biofilms targeting pathogenic bacteria using live-cell imaging. *En préparation*.

Article 8 : Virgile Guéneau, Cécile Berdous, Mathieu Castex, Romain Briandet. Intergenus associations in positive biofilms to bolster exclusion of bacterial pathogens. *En préparation*.

Licence d'exploitation de souche

Virgile Guéneau, Bastien Frayssinet, Mathieu Castex, Romain Briandet. Licence d'exploitation de la souche *Bacillus velezensis* B8 en tant que co-propriété INRAE/Lallemand. En préparation.

Communications orales

Romain Briandet, Yasmine Dergham, Cédric Saint Martin, **Virgile Guéneau**, Julien Deschamps, Jean Christophe Piard. Biofilms dans l'industrie : comment lutter contre ou les utiliser à bon escient ?, Clubster NSL (Nutrition Santé Longévité), avril 2021, Webinaire.

Virgile Guéneau, Julia Plateau-Gonthier, Jean-Christophe. Piard, Mathieu Castex, Romain Briandet. Towards the rational use of protective biofilms to fight against unwanted microorganisms in livestock buildings. Séminaire Micalis, décembre 2021, Jouy-en-Josas, France.

Romain Briandet, Yasmine Dergham, Dominique Le Coq, Julien Deschamps, **Virgile Guéneau**, Cédric Saint Martin, Pilar Sanchez-Vizuete. Actualité et perspectives sur les biofilms dans l'industrie pharmaceutique, Symposium Pharmaceutique BioMérieux 2021. 17 Juin 2021, Marcy L'Etoile.

Virgile Guéneau, Julia Plateau-Gonthier, Jean Christophe Piard, Mathieu Castex, Romain Briandet. 3D-fluorescent imaging to select positive biofilm forming bacteria to limit pathogen establishment on livestock building surfaces. Journées ABIES, avril 2022, Paris, France. 2e prix de la meilleure présentation orale.

Romain Briandet, **Virgile Guéneau**, Cédric Saint Martin, Caroline Pandin, D. Lecoq, A. Bridier. Positive biofilms to guide surface microbial ecology. International Association for Food Protection (IAFP), Mai 2022, Munich, Allemagne.

Virgile Guéneau, Julia Plateau-Gonthier, Mathieu Castex, Romain Briandet. Towards the rational use of positive biofilms to fight against unwanted microorganisms in livestock buildings, Séminaire RnD interne Lallemand, Juin 2022, La Grande-Motte, France.

Virgile Guéneau, Julia Plateau-Gonthier, Ana Rodiles, J.C. Piard, Mathieu Castex, Romain Briandet. Positive biofilms to guide surface microbial ecology in livestock buildings. ISME18, août 2022, Lausanne, Switzerland.

Virgile Guéneau, Julia Plateau-Gonthier, Mathieu Castex, Romain Briandet. High Content Screening Confocal Laser Scanning Microscopy (HCS-CLSM) to decipher the mechanisms of bacterial pathogens exclusion by positive biofilms. PhysChemCell2022, Octobre 2022, Saclay, France.

Virgile Guéneau, Julia Plateau-Gonthier, Mathieu Castex, Romain Briandet. Harnessing Positive Biofilms: An Innovative Method to Manage Unwanted Microorganisms on Livestock Building Surfaces. MEET THE EXPERT webinar, juin 2023, webinaire.

Virgile Guéneau, Julia Plateau-Gonthier, Mathieu Castex, Romain Briandet. Exploring the potential of synthetic microbial consortia for positive biofilms. Séminaire RnD interne Lallemand, Juillet 2023, webinaire.

Posters

Ana Rodiles, **Virgile Guéneau**, Bastien Frayssinet, Julia Plateau-Gonthier, J.C. Piard, Romain Briandet, Matthieu Castex. Assessment of a microbial external inoculation in a broiler chicken production building post disinfection and prior animal entrance on environmental biofilm using 16S rRNA analysis. Beneficial Microbes, 2021, Montréal, Canada.

Virgile Guéneau, Julia Plateau-Gonthier, Mathieu Castex, Romain Briandet. High Content Screening Confocal Laser Scanning Microscopy (HCS-CLSM) to decipher the mechanisms of bacterial pathogens exclusion by positive biofilms. EMBO Workshop Adherent microbial communities: Quantitative approaches from single cell to ecosystems, Octobre 2022, Cargèse, France.

Cécile Berdous, **Virgile Guéneau**, Ariane Deniset-Besseau, Romain Briandet. Emergent properties of a multi-species positive biofilm : structural and chemical analysis of the extracellular matrix. PhyChemCell2022, Octobre 2022, Saclay, France.

Virgile Guéneau, Cécile Berdous, Julia Plateau-Gonthier, Mathieu Castex, Romain Briandet. The concept of positive biofilm in the context of livestock building surfaces. Symposium "Environment and Host Microbiomes - Functional Interactions", Mai 2023, Saclay, France.

Virgile Guéneau, Mathieu Castex, Romain Briandet. Development of a strain selection pipeline for positive biofilm. Ferment'IA, Septembre 2023, Saclay, France.

Autres communications

Environmental Biofilms in Livestock Buildings: History. Encyclopedia. 2021. https://encyclopedia.pub/item/revision/dbf663d66f75e591facff3c4f60614c3

New publication helps sample and study biofilms in livestock buildings. Lallemand. Mars 2022.
https://www.lallemandanimalnutrition.com/en/europe/articles/new-publication-helps-sample-and-study-biofilms-in-livestock-buildings/

The potential of positive biofilms to complement on-farm biosecurity measures. Lallemand. Juin 2022.
https://www.lallemandanimalnutrition.com/en/europe/articles/the-potential-of-positive-biofilms-to-complement-on-farm-biosecurity-measures/

Positive biofilms to guide surface microbial ecology, Article poultry world, no. 6, 2022.
https://www.poultryworld.net/health-nutrition/health/positive-biofilms-to-guide-surface-microbial-ecology/

Expert talk. Réponses aux questions sur les biofilms positifs et leur importance dans les bâtiments agricoles.

https://www.linkedin.com/feed/update/urn:li:activity:7108074509965897728/

Encadrements

Virgile Guéneau, Romain Briandet, Marie-Françoise Noirot-Gros. Encadrement de 2 stagiaires lors des travaux pratiques du Master 2 microbiologie fondamentale de l'Université Paris-Saclay dédiés au swarming de *Bacillus* spp. 3 semaines, Septembre 2021.

Virgile Guéneau, Mathieu Castex, Romain Briandet. Stage de Master 1 de Cécile Berdous. Propriétés émergentes d'un biofilm positif multi-espèces : analyse structurale et chimique de la matrice extracellulaire. Avril-Juin 2022.

Virgile Guéneau. Stage d'observation de Chiara Boldrin Kervella (3e). Observation et vulgarisation du travail de recherche. 1 semaine, Janvier 2023.

Virgile Guéneau, Mathieu Castex, Romain Briandet. Stage de Master 2 de Cécile Berdous. Exploring the potential of mixed-species positive biofilms: enhanced antagonistic activity against *Salmonella enteritidis* and *Enterococcus cecorum* using *Bacillus velezensis* with *Pediococcus* spp. Janvier-Juillet 2023.

Bourses compétitrices

Participation à l'écriture de l'appel à projet BIOPROBE 2022 (Université Paris-Saclay) pour financer les 3 mois de stage de Master 1 de Cécile Berdous.

Participation à l'écriture de l'appel à projet BIOPROBE 2022 (Université Paris-Saclay) pour financer ma participation au congrès ISME18.